

*Analytische Chemie*

Dissertationsthema

**Capillary Electrophoretic Methods for the  
Separation of Polycyclic Aromatic Sulfur  
Heterocycles from Fossil Fuels**

Inaugural-Dissertation

zur Erlangung des Doktorgrades

der Naturwissenschaften im Fachbereich Chemie und Pharmazie

der Mathematisch-Naturwissenschaftlichen Fakultät

der Westfälischen Wilhelms-Universität Münster

vorgelegt von

*Thies Nolte*

aus *Dorsten*

- 2011 -

Dekanin/Dekan: Prof. Dr. A. Hensel

Erste Gutachterin/  
Erster Gutachter: Prof. Dr. J. T. Andersson

Zweite Gutachterin/  
Zweiter Gutachter: Prof. Dr. U. Karst

Tag der mündlichen  
Prüfung(en):.....

Tag der Promotion: .....

## **Prior printed publications of the dissertation**

Partial results of this work were published with permission of the Institute for Inorganic and Analytical Chemistry of the University of Münster/Germany represented by Prof. Jan T. Andersson in the following articles:

Nolte, T. and J. T. Andersson. 2009. Capillary electrophoretic separation of polycyclic aromatic sulfur heterocycles. *Anal. Bioanal. Chem.* 395:1843-1852.

Nolte, T. and J. T. Andersson. 2011. Capillary Electrophoretic Methods for the Separation of Polycyclic Aromatic Compounds. *Polycyclic Aromatic Compounds*, 31:287-338.

## Table of contents

Prior printed publications of the dissertation.....	III
Table of contents .....	IV
Table of figures.....	VI
1 Introduction.....	1
1.1 Origin of petroleum .....	2
1.2 Sulfur compounds in fossil fuels .....	2
1.3 The refining process .....	4
1.4 Hydrodesulfurization .....	5
1.5 Analytical methods for the identification of PASHs in fossil fuels.....	9
1.5.1 Gas chromatography .....	9
1.5.2 High performance liquid chromatography .....	10
1.5.3 High resolution mass spectrometry .....	11
2 Introduction to capillary electrophoretic methods.....	13
2.1 CE-MS .....	13
2.2 Micellar elctrokinetic chromatography.....	18
3 State-of-the-art: Capillary electrophoretic separation of PAHs.....	21
3.1 Introduction.....	21
3.2 Solvophobic association with tetraalkylammonium ions .....	22
3.3 Solvophobic/hydrophobic interaction with other ionic surfactants .....	25
3.4 Separation through charge-transfer complexation with planar organic cations ..	30
3.5 Separation through distribution into charged and uncharged cyclodextrins .....	32
3.6 Separation through distribution into resorcarenes and calixarenes .....	38
3.7 Conclusion .....	40
4 Scope of work.....	42
5 Experimental introduction .....	43
5.1 CE instrumentation .....	43
5.1.1 CE-UV and MEKC .....	43
5.1.2 CE-TOF MS .....	44
5.2 Procedures and conditions .....	44
5.2.1 CE-UV.....	44
5.2.2 MEKC-UV .....	44
5.2.3 CE-TOF MS .....	44
5.3 Chemicals and reagents .....	45
5.4 Ligand exchange chromatography.....	45
5.5 Derivatization of the PASHs .....	46
5.5.1 Methylation .....	47
5.5.2 Phenylation.....	48
6 Capillary electrophoretic separation of standard compounds.....	49
6.1 CE separation of fuel related PASHs in comparison to HPLC .....	49
6.2 Comparison between the derivatization methods .....	51
6.3 Cyclodextrin supported separation of derivatized standard compounds .....	56



6.3.1	Cyclodextrin supported enantiomeric separation of phenylated PASHs ...	56
6.3.2	Cyclodextrin supported separation of all monomethyl-BT isomers .....	57
6.4	Correlation of molecular volume and migration time in CE-UV .....	62
6.4.1	Calculation of the molecular volume .....	62
6.4.2	Correlation for PASHs with long alkyl chains .....	63
6.5	MEKC separation of standard compounds .....	69
6.5.1	Addition of organic modifier .....	70
6.5.2	Addition of cyclodextrin .....	73
6.5.3	Combination of organic modifier and cyclodextrins .....	75
6.6	CE-TOF MS separation of standard compounds .....	77
6.6.1	Aqueous CE-TOF MS .....	77
6.6.2	Non-aqueous CE-TOF MS .....	80
6.7	Discussion .....	82
7	CE separation of PASHs from real world samples .....	84
7.1	Danish diesel fuel .....	84
7.1.1	Comparison to HPLC .....	85
7.1.2	Addition of cyclodextrins .....	87
7.2	Desulfurized Syncrude light gas oils .....	88
7.2.1	Separation of the three derivatized LGO samples .....	88
7.2.2	Partly-aqueous and non-aqueous CE of the first stage sample .....	91
7.2.3	MEKC of the feedstock sample .....	92
7.3	Syncrude heavy gas oils at different desulfurization stages .....	94
7.4	Separation of different boiling fractions of Syncrude HGOs by CE-TOF MS ...	99
7.4.1	Aqueous CE-TOF MS .....	101
7.4.2	Nonaqueous CE-TOF MS .....	112
7.4.3	Comparison with GC-MS .....	121
7.4.4	Comparison to Orbitrap MS .....	128
7.5	Discussion .....	135
8	Summary and outlook .....	137
9	Literature .....	140
10	Appendix .....	151
10.1	Synthesis of 4,6-dipropyl-DBT .....	151
10.2	Synthesis of 4,6-dipentyl-DBT .....	151
10.3	Synthesis of 4,6-dioctyl-DBT .....	152
10.4	Synthesis of 4,6-didecyl-DBT .....	153
10.5	RP-HPLC parameters .....	153
10.6	GC-FID parameters .....	154
10.7	GC-MS parameters .....	154
10.8	List of chemicals .....	155
10.9	List of abbreviations .....	156
11	Curriculum Vitae .....	159

## Table of figures

Fig. 1: Peak oil scenario from the Association for the Study of Peak Oil and Gas [4]. ...	1
Fig. 2: Oil price per barrel for different crude oils [8]. .....	3
Fig. 3: Typical sulfur compounds from low boiling petroleum fractions .....	6
Fig. 4: Typical sulfur compounds from high boiling petroleum fractions .....	6
Fig. 5: Structures for dibenzothiophene and 4,6-dimethyldibenzothiophene.....	8
Fig. 6: Schematic layout of an Orbitrap cell.....	11
Fig. 7: Design of a coaxial sheath liquid interface. ....	15
Fig. 8: Design of a liquid junction interface.....	16
Fig. 9: Design of a sheathless interface. ....	17
Fig. 10: Schematic design of an ESI source with 90° angle between spray direction and MS entry. ....	17
Fig. 11: Schematic molecular composition of a SDS micelle in water. ....	20
Fig. 12: Illustration of the principles of MEKC. ....	20
Fig. 13: Electropherogram of sixteen non-ionic aromatic organic compounds separated by solvophobic association with tetraheptylammonium bromide. ....	24
Fig. 14: Dioctyl sulfosuccinate.....	26
Fig. 15: Separation of nonionic aromatic compounds by hydrophobic interaction with DOSS.....	26
Fig. 16: Sulfonated Brij-30 (Brij-S) .....	27
Fig. 17: Separation of PAHs by hydrophobic interaction with Brij-S. ....	27
Fig. 18: Sodium dodecyl sulfate (SDS), sodium tetradecyl sulfate (STS), sodium hexadecyl sulfate (SHS) .....	28
Fig. 19: Structures of SDBS and CPBr .....	29
Fig. 20: Electropherogram of PAHs separated by hydrophobic interaction and $\pi$ - $\pi$ -interactions with CPBr. ....	30
Fig. 21: Tropylium ion and triphenylpyrylium ion .....	31

Fig. 22: $\beta$ -Cyclodextrin (with R = H) with 7 glucopyranose units (carboxymethyl- $\beta$ -cyclodextrin: R = CH <sub>2</sub> COO <sup>-</sup> ).....	32
Fig. 23: CE separation of soil PAH mixture after Soxhlet extraction using a M- $\beta$ -CD/SB- $\beta$ -CD modified buffer. ....	34
Fig. 24: Electropherogram of a mixture of 16 EPA priority PAHs, using 35 mM sulfobutyl- $\beta$ -CD, 15 mM methyl- $\beta$ -CD.....	35
Fig. 25: Separation of the 16 PAHs using two pseudo-stationary phases, DOSS and sulfobutyl- $\beta$ -CD, in mixed-mode EKC. ....	36
Fig. 26: Separation of the Mars nine PAH standard by distribution into cyclodextrins. ....	39
Fig. 28: Separation of twelve PAHs with undecyl modified resorcarene. ....	39
Fig. 29: Structure of the carrier p-(carboxyethyl)calix[4]arene .....	40
Fig. 30: Schematic principle of Pd-mercaptopropano silica gel.....	46
Fig. 31: Methylation reaction for the formation of methyl thiophenium ions.....	47
Fig. 32: Phenylation reaction for the formation of phenyl-thiophenium ions. ....	48
Fig. 33: Separation of six fuel-related PASHs with a) CE b) RP-HPLC. ....	50
Fig. 34: Derivatization of four PASHs to the corresponding methyl- and phenyl-thiophenium ions. ....	52
Fig. 35: CE-separation of a mixture of a) four methyl-thiophenium ions and b) four phenyl-thiophenium ions. ....	53
Fig. 36: a) Migration time difference between S-methyl-DBT and S-phenyl-DBT and b) Migration time difference between all the methylated and phenylated products.....	55
Fig. 37: Formation of two enantiomeric structures during the derivatization reaction. .	57
Fig. 38: a) Enantiomeric separation of 2-methyl-SPDBT b) no enantiomeric separation four 4,6-dimethyl-SPDBT.....	59
Fig. 39: Capillary electrophoretic separations of a mixture containing seven S-methyl-benzothiophenium salts. ....	60
Fig. 40: Structures of the analytes a) and electropherogram for the separation of a mixture containing seven S-methyl-benzothiophenium salts.....	61
Fig. 41: Optimized structures for S-methyl-DBT and S-phenyl-DBT with the calculated molecular volume by the software PCModel. ....	63

Fig. 42: a) Capillary electrophoretic separation of a mixture containing 14 PASH-methyl thiophenium salts. b) Plot of calculated molecular volume vs. the migration time.....	64
Fig. 43: Plot of calculated molecular volume vs. the migration time for the separation of seven PASHs with five analytes containing alkylations in 4- and 6-positions. ....	65
Fig. 44: Plot of calculated molecular volume vs. the migration time for the separation of six PASHs with four analytes containing alkylations in 4-position. ....	66
Fig. 45: a) Structures of the analytes and b) plot of calculated molecular volume vs. the migration time for the separation of 13 PASHs with different alkylations in 4- and 6-positions.....	68
Fig. 46: MEKC-separation of four PASH standard compounds..	70
Fig. 47: MEKC-separation of four PASH standard compounds with addition of organic modifier..	72
Fig. 48: MEKC-separation of four PASH standard compounds with addition of cyclodextrins.....	74
Fig. 49: MEKC-separation of four PASH standard compounds with combined addition of organic modifier and cyclodextrins.....	76
Fig. 50: Derivatization of four standard PASHs for CE-TOF MS measurements. ....	78
Fig. 51: Electropherogram of the aqueous CE-TOF MS separation with extracted masses for the four analytes.....	79
Fig. 52: Electropherogram of the nonaqueous CE-TOF MS separation with extracted masses for the four analytes.....	81
Fig. 53: a) Capillary electrophoretic separation of the methylated PASH fraction of a desulfurized diesel fuel.....	84
Fig. 54: a) Capillary electrophoretic separation of the methylated PASH fraction of a desulfurized diesel fuel.....	86
Fig. 55: Separation of a real world sample (diesel fuel Denmark, 2001) with and without $\beta$ -CD.....	87
Fig. 56: Electropherogram of the separation of the feedstock LGO PASHs.....	89
Fig. 57: Electropherogram of the separation of the first-stage LGO PASHs.....	90
Fig. 58: Electropherogram for the separation of the first-stage LGO PASHs with nonaqueous CE and aqueous CE with addition of different isopropanol concentrations. (Different time scales on x-axis in the three electropherograms).....	92

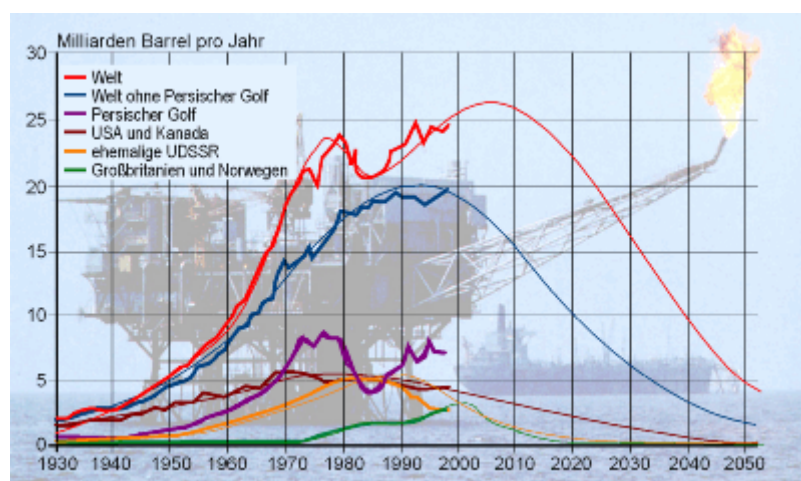
Fig. 59: MEKC separation of the LGO feedstock PASHs. ....	93
Fig. 60: GC-separation of LGO-feedstock and HGO-feedstock (red) PASHs with the identification through reference compounds. ....	95
Fig. 61: CE-separation of the HGO-feedstock PASHs.....	96
Fig. 62: GC-separation of desulfurized HGO PASHs after desulfurization at 385 °C and desulfurization at 370 °C and reference compounds. ....	97
Fig. 63: CE-separation of desulfurized HGO samples with desulfurization at 385 °C and desulfurization at 370 °C. ....	98
Fig. 64: Overlay of the electropherograms of desulfurized HGO samples with desulfurization at 385 °C and desulfurization at 370 °C. ....	99
Fig. 65: GC-separation of the desulfurized HGO with the corresponding low boiling fraction and high boiling fraction. ....	100
Fig. 66: GC-separation of the desulfurized HGO PASHs with the corresponding low boiling fraction PASHs and high boiling fraction PASHs. ....	101
Fig. 67: Aqueous CE-TOF MS electropherogram of the low boiling fraction.....	102
Fig. 68: Extracted ion electropherograms of the low boiling fraction PASHs from SMDBT to C3-SMDBT. ....	103
Fig. 69: Overlay of SMDBT to C7-SMDBT extracted ion electropherograms of the low boiling fraction. ....	104
Fig. 70: Formation of tetrahydrodibenzothiophenes by hydrogenation as competitive reaction to the hydrodesulfurization. ....	105
Fig. 71: Overlay of methylated C1-THDBT to C4-THDBT extracted ion electropherograms. ....	106
Fig. 72: Aqueous CE-TOF MS electropherogram of the higher boiling fraction. ....	106
Fig. 73: Extracted ion electropherograms of the higher boiling fraction PASHs from SMDBT to C3-SMDBT. ....	108
Fig. 74: Overlay of methylated DBT to C10-DBT extracted ion electropherograms of the higher boiling fraction. ....	109
Fig. 75: Extracted ion electropherograms for methylated C1 to C3-THDBTs of the higher boiling fraction. ....	109

Fig. 76: Extracted ion electropherograms for THBNTs and DHPTs from the parent HGO sample after separation with aqueous CE-TOF MS. ....	110
Fig. 77: Overlay of methylated DBT to C9-DBT extracted ion electropherograms of the parent HGO PASH fraction obtained with aqueous CE-TOF MS. ....	111
Fig. 78: Overlay of methylated THDBT to C7-THDBT extracted ion electropherograms of the parent HGO PASH fraction obtained with aqueous CE-TOF MS. ....	112
Fig. 79: Overlay of THBNTs and DHPTs extracted ion electropherograms of the parent HGO PASH fraction obtained with aqueous CE-TOF MS. ....	112
Fig. 80: Extracted ion electropherograms for methylated DBT to C3-DBTs for the low boiling HGO PASHs with nonaqueous CE. ....	114
Fig. 81: Overlay of methylated DBT to C7-DBT extracted ion electropherograms of the low boiling fraction PASHs. ....	115
Fig. 82: Overlay of methylated C1-THDBT to C5-THDBT extracted ion electropherograms of the low boiling HGO sample by nonaqueous CE-TOF MS. ....	115
Fig. 83: Extracted ion electropherograms of DBT to C8-DBT for the higher boiling HGO sample by nonaqueous CE-TOF MS. ....	116
Fig. 84: Overlay of methylated C1-THDBT to C6-THDBT extracted ion electropherograms of the higher boiling HGO sample by nonaqueous CE-TOF MS. ....	117
Fig. 85: Overlay of the extracted ion electropherograms of methylated THBNTs and DHPTs of the higher boiling HGO sample by nonaqueous CE-TOF MS. ....	117
Fig. 86: Extracted ion electropherograms for methylated DBT to C3-DBTs for the parent HGO PASHs with nonaqueous CE-TOF MS. ....	118
Fig. 87: Overlay of methylated DBT to C12-DBT extracted ion electropherograms of the parental HGO sample by nonaqueous CE-TOF MS. ....	119
Fig. 88: Overlay of methylated C1-THDBT to C6-THDBT extracted ion electropherograms of the parental HGO sample by nonaqueous CE-TOF MS. ....	120
Fig. 89: Overlay of extracted ion electropherograms of methylated THBNTs and DHPTs of the parental HGO sample by nonaqueous CE-TOF MS. ....	120
Fig. 90: GC-MS chromatogram of the low boiling sample PASHs with the extracted ion chromatograms for DBT to C3-DBTs. ....	122
Fig. 91: GC-MS chromatogram of the low boiling sample PASHs with identification of different compounds by fragmentation pattern. ....	123
Fig. 92: GC-MS chromatogram of the low boiling sample PASHs with the extracted ion chromatograms for C1-THDBTs to C4-THDBTs. ....	124

Fig. 93: GC-MS chromatogram of the higher boiling sample PASHs with the extracted ion chromatograms for DBT to C6-DBTs.....	125
Fig. 94: GC-MS chromatogram of the higher boiling sample PASHs with the extracted ion chromatograms for the homologous series of THBNTs and DHPTs.....	126
Fig. 95: GC-MS chromatogram of the parental sample PASHs with the extracted ion chromatograms for DBT to C6-DBTs.....	127
Fig. 96: GC-MS chromatogram of the parental sample PASHs with the extracted ion chromatograms for C1-THDBTs to C4-THDBTs.....	127
Fig. 97: GC-MS chromatogram of the parental sample PASHs with the extracted ion chromatograms for the homologous series of THBNTs and DHPTs.....	128
Fig. 98: Orbitrap MS spectrum of the low boiling HGO PASHs with alkylated DBTs marked in red.....	129
Fig. 99: Orbitrap MS spectrum of the low boiling HGO PASHs with demethylated DBT radical cations marked in red.....	131
Fig. 100: Orbitrap MS spectrum of methylated benzophenanthro[9,10- <i>d</i> ]thiophene. .	131
Fig. 101: Orbitrap MS spectrum of the low boiling HGO PASHs with alkylated THDBTs marked in blue. ....	132
Fig. 102: Orbitrap MS spectrum of the higher boiling HGO PASHs with alkylated DBTs marked in red. ....	133
Fig. 103: Orbitrap MS spectrum of the higher boiling HGO PASHs with alkylated THBNTs and DHPTs marked in green. ....	133
Fig. 104: Orbitrap MS spectrum of the parental HGO PASHs with alkylated DBTs marked in red, THBNTs and DHPTs marked in green and alkylated THDBTs marked in blue. ....	134

# 1 Introduction

Petroleum will remain the world's major energy supply in the coming decades. Especially after the disaster at the Fukushima nuclear power plant on March 11<sup>th</sup> many countries like Germany want to terminate the nuclear power supply due to security reasons and protests against this energy source [1]. The resulting energy gap can only be closed by using fossil fuels. Sustainable energy sources cannot be used to fill this gap yet, because a massive expansion of this energy supply would be needed and it would probably take decades to assure a constant supply. One major problem that occurs with the use of fossil fuels is that this energy source is limited. For petroleum, for example, many depletion scenarios exist [2]. The most important definition within these scenarios is the peak oil maximum. This point is defined as the time when the global maximum of petroleum extraction is reached. An example for a peak oil scenario from the Association for the Study of Peak Oil and Gas is presented in figure 1. Although several of these models predict the peak oil maximum to be close to the year 2000, this point has not been reached yet. This might be explained by the massive technological improvement in drilling and oil well technology in recent years. Oil fields that were unaccessible or too small for economic extraction years ago can nowadays be exploited. New technology in geophysical exploration, for example, led to the discovery of huge petroleum fields close to the coast of Norway in the last months [3]. Nevertheless, the peak oil maximum is sure to come and will mean a shortage of energy and massively increasing prices for crude oil and transportation fuels.



**Fig. 1: Peak oil scenario from the Association for the Study of Peak Oil and Gas [4].**



### 1.1 Origin of petroleum

The parent material for the formation of petroleum are plankton, algae and further microorganisms that accumulate on the submarine ground after dying off. Over millions of years this organic matter undergoes a series of complex geochemical transformation reactions. The first step during this transformation is that the layer of organic material is covered by sediments. Due to the high pressure and increased temperature in this area, the matter undergoes rock formation that is called diagenesis. During the diagenesis the material is compacted and dehydrated to kerogen, which is a geoorganic polymer without defined structure that makes up the organic matter in the sedimentary rocks. Under special conditions some types of kerogen can release crude oil and natural gas. This happens during a process that is called catagenesis. Within this process the kerogen undergoes a maturation that leads to increased aromatization and the formation of bitumen. With increasing temperature and pressure in deeper strata, a process occurs which is comparable to a pyrolytic cracking process. The long chains of the hydrocarbons are cracked to shorter ones on the one hand, while other parts of the hydrocarbons are further aromatized. This process, the so called metagenesis, leads to the formation of fossil gas and pyrobitumen and would finally end up with methane and graphite as the final products. The kerogenic products can migrate into the pores of the rocks, which can lead to accumulation of the products in special places, for example, under impermeable strata. These accumulations are the typical petroleum fields that can be exploited.

### 1.2 Sulfur compounds in fossil fuels

Typical commercially available crude oils have sulfur contents ranging from 0.1 % to 4 % although crudes with up to 14 % sulfur can be found [5]. To some extent the sulfur in petroleum can have its origin in sulfuric organic compounds, like the amino acids cysteine or methionine, occurring in the microorganisms that formed the organic matter for the petroleum formation. But as the sulfur content in the biosphere (plants and animals) is only 0.05 % to 0.2 %, this only explains a small part of the sulfur content in petroleum. Different approaches to find an explanation for this can be found. One of the most accepted versions is that the sulfur has its origin in sulfate ions of the sea water. Under anaerobic conditions some bacteria (*Desulfovibrio*, *Desulfobacter*) are able to reduce sulfate to hydrogen sulfide and further on oxidize them to elementary sulfur and polysulfides [6, 7].

These reduced sulfur species are able to react with isoprenic or terpenoic double bonds to form thiols and sulfides. Within the catagenetic process during petroleum formation these compounds can be converted to the typically abundant aromatic sulfur compounds in petroleum.

Following a traditional description, crude oils with less than 1 % of sulfur are called “sweet”, while crudes with sulfur exceeding 1 % are called “sour”. This description was originally connected to the concentration of  $H_2S$  in the petroleum as the  $H_2S$  made the petroleum sour. Over the years this description was adapted for the overall sulfur content. Sour crude oils usually have a lower market price. The most well-known example for low boiling low sulfur petroleum is the Brent crude. The price of this crude is used as a marker for more than two third of the worldwide traded crude oils. A comparison with the prices of other crudes with higher sulfur content and higher boiling range shows significant differences. The lower price for the higher boiling and sour crudes can be explained by the larger efforts needed to deal with this material. Laborious and expensive hydrodesulfurization and refining methods have to be performed to transform the crudes to commercially usable products that comply with legal standards. The difference in the prices depending on the boiling range can be seen in figure 2. The low boiling and sweet Brent is usually traded for higher prices than heavier and sour crudes like Arab Medium or Arab Heavy.

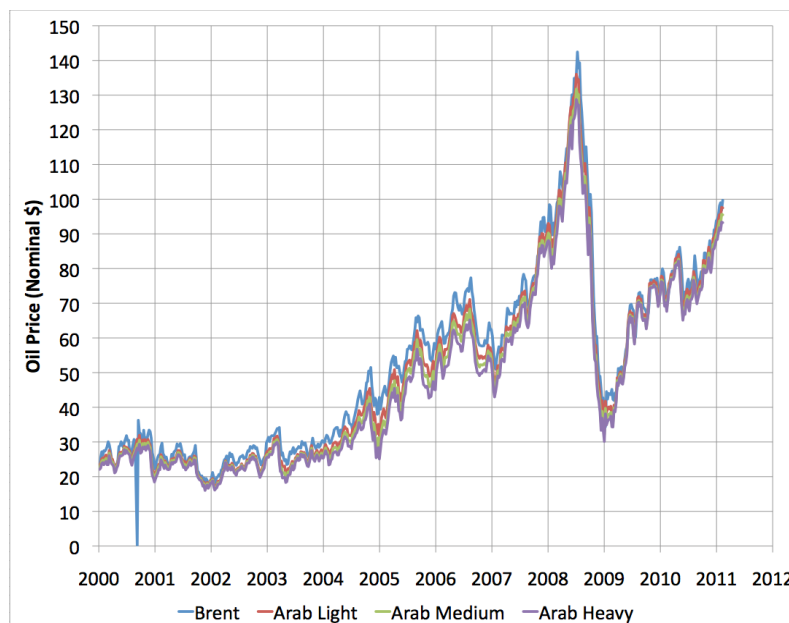


**Fig. 2: Oil price per barrel for different crude oils [8].**

As more and more oil deposits with sweet and low boiling crudes are depleted and the price for petroleum increases, the interest in sulfur rich petroleum expands. Petroleum deposits that were seen as non-economic some years ago can now be commercially exploited.

### 1.3 The refining process

Petroleum is a complex mixture of innumerable compounds with a composition that differs from source to source [9]. Typically the different compounds can be assigned to three major fractions, where the aliphatics make up the largest one. Within this class of compounds, homologous alkanes as well as cyclic and branched ones can be found. Sulfidic and disulfidic alkanes are present, depending on the sulfur content of the crude. The second main fraction of petroleum are the aromatic compounds. Polycyclic aromatic hydrocarbons (PAH) and their alkylated derivatives are among the most abundant ones, followed by polycyclic aromatic sulfur heterocycles (PASHs) and polycyclic aromatic oxygen heterocycles. Other heteroaromatic compounds containing nitrogen or oxygen are assigned (with some exceptions) to the third and so-called “polar” fraction.

The first step during the refining process to make crude oil commercially usable is the distillative separation by boiling range. The crude is heated under atmospheric pressure so that volatile compounds, like propane and butane, evaporate and ascend in a column of up to 50 m height. The temperature profile in the column declines with increasing height, so that the volatile compounds condense in the upper part of the column. Compounds with intermediate molecular weight condense in the middle part of the column and generate the main stock for naphtha, gasoline, kerosene and diesel fuel. Heavy boiling materials, like so-called gasoils, condense in the lower part of the column under atmospheric pressure. The remaining heavy bottom fraction that cannot be evaporated at atmospheric pressure is treated by vacuum distillation afterwards. The vacuum greatly lowers the boiling point of the compounds, so that distillation leads to products like lubricating oils, paraffin waxes and asphalt.

Because the demand for the products gained by the vacuum distillation is much lower than the supply, most of the very high boiling products are treated further in cracking processes to obtain higher yields of transportation fuel like gasoline and diesel. During this process the large hydrocarbons from the vacuum residue and other high boiling fractions are

cleaved into smaller pieces with a molecular weight that is typical for transportation fuels. The three mainly used cracking processes are the “fluid catalytic cracking”, the “hydrocracking” and the “delayed coking”. The fluid catalytic cracking is usually performed at increased temperatures on fluidized solid catalysts. The hydrocracking process is similar to the fluid catalytic cracking with the difference that pressurized hydrogen is added to the reaction. The products of the reaction are largely aromatic and alkene free, because unsaturated compounds are hydrogenated to the saturated homologous. The delayed coking is the most rigorous of the cracking processes. Vacuum residues of low quality are treated at temperatures of 500° C and pressures between 20 and 30 atmospheres to yield short chain hydrocarbons and coke, which can be used as combustible material in power plants or as additive in blast furnaces for steel production.

### 1.4 Hydrodesulfurization

The fractions obtained from the rectification of the crudes can usually be forwarded directly to the designated use without further treatment. However, in most cases legal standards have to be complied depending on the different designations. Legal limits can be found in most of the countries for the sulfur content in transportation fuels. The idea of setting such limits dates back to the 1980s when the massive Waldsterben was found to be caused by acidic rain that resulted from sulfur oxides from fossil fuel combustion. While the exhaust of fossil fuel burning power plants could easily be treated with calcium hydroxide or calcium carbonate to remove sulfur oxides as gypsum, this was impossible for cars and other vehicles. This made desulfurization of crudes compulsory during the refining process. The legal limits for the sulfur content in transportation fuels was stepwise decreased. In 2001 a legal limit of 150 ppm in transportation fuels was set, and this value was decreased to 50 ppm in the year 2005 [10]. Since 2003 fuels exceeding 10 ppm of sulfur were taxed 1.7 € cent per liter additionally, followed by decreasing the legal standard to 10 ppm in entire Europe on January 1<sup>st</sup> 2009.

Sulfur compounds can be found in all distilled fractions from crudes, while the sulfur content and the structural composition greatly varies with the boiling range. The low molecular fractions with a boiling range up to 150 °C mainly contain thiols, sulfides, disulfides, thianes and thiophenes in low concentrations (figure 3). Higher boiling fractions exceeding 250 °C come along with higher sulfur contents and mostly aromatic compounds.

The most common compounds are thiophene rings condensed to aromatic systems, like benzothiophenes (BTs), dibenzothiophenes (DBTs) and benzonaphthothiophenes (BNTs). A variety of aromatic sulfur compounds typically found in high boiling fractions is presented in figure 4.

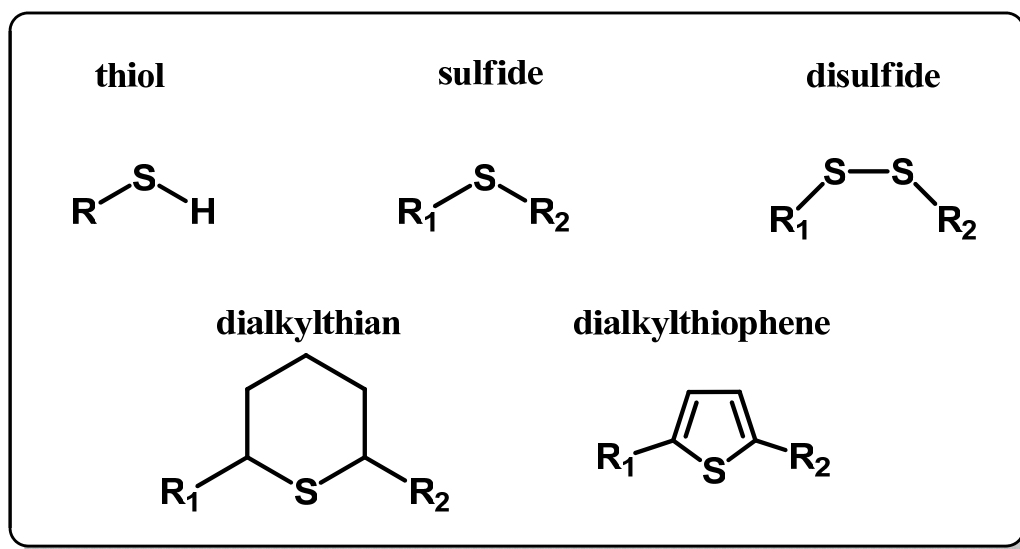


Fig. 3: Typical sulfur compounds from low boiling petroleum fractions

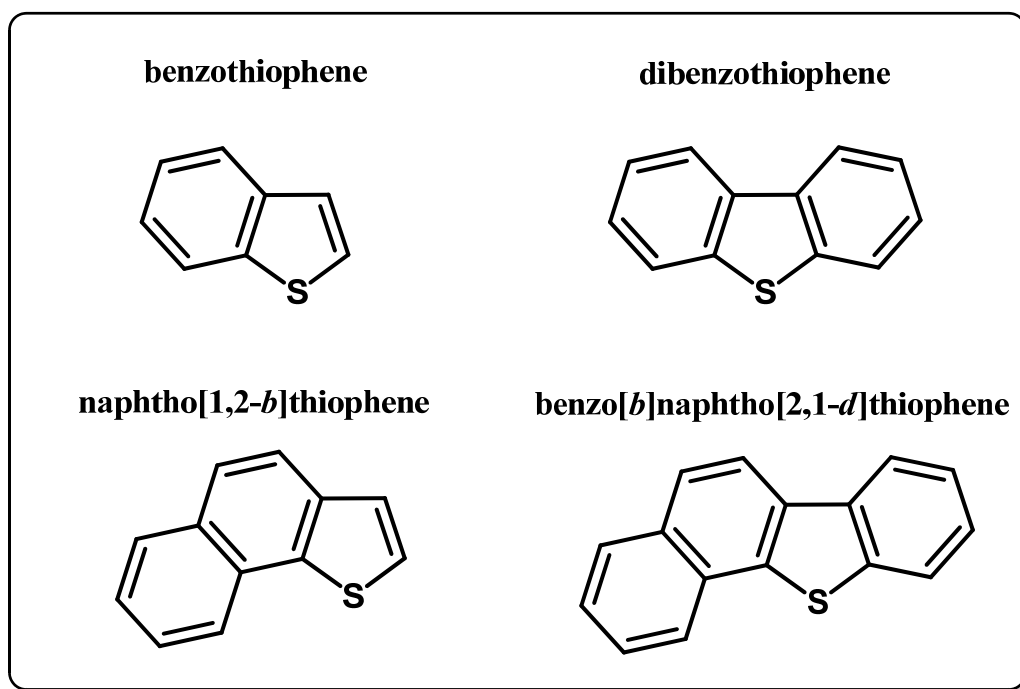


Fig. 4: Typical sulfur compounds from high boiling petroleum fractions

To comply with the legal standards, the crudes have to be treated by energy-intensive desulfurization processes. The most common among these processes is the hydrodesulfurization (HDS), which is based on the ability of some transition metals to hydrogenate sulfur from sulfur compounds and hence remove it in form of  $\text{H}_2\text{S}$  in the presence of pressurized hydrogen. The reaction is greatly affected by the hydrogen pressure, the temperature and catalyst used. Typical conditions for the HDS are temperatures of 300 to 340° C with 20 to 100 atm of pressurized hydrogen on Co-Mo/ $\text{Al}_2\text{O}_3$  or Ni-Mo/ $\text{Al}_2\text{O}_3$  catalysts.

The reactivity of the different sulfur compounds during HDS varies greatly depending on the structure and aromaticity of the species. While nonaromatic, saturated compounds like thiols, sulfides and disulfides can easily be desulfurized, this reaction is much slower for aromatic compounds. This can easily be explained by the higher stability of the compounds, when sulfur is incorporated in the aromatic system. Varieties in reactivity for the different aromatic compounds can be observed as well, [11] with thiophene having the highest reactivity, followed by BT and BNT. Tetrahydrobenzonaphthothiophenes and DBTs showed the lowest reactivity to HDS.

The typical course of reactions during HDS of aromatic compounds begins with the adsorption to the catalyst. For most of the compounds a direct desulfurization (DDS), which is also called hydrogenolysis, occurs. The carbon-sulfur bond is cleaved and the sulfur released as hydrogen sulfide while phenylic and biphenylic compounds are formed as desulfurized products [12]. Within the different classes of aromatic compounds the substitution pattern of alkyl groups influences the hydrodesulfurization, because the accessibility of the sulfur atom to the HDS catalyst might be reduced. The sulfur atom in dibenzothiophene for example can easily approach the catalyst surface, while the sulfur in 4,6-dimethyldibenzothiophene (structures shown in figure 5) is shielded by the two flanking methyl groups. When the direct approach of the sulfur to the catalyst is inhibited, no coordinative bonding can be formed and the sulfur cannot directly be released as hydrogen sulfide. For these recalcitrant compounds a different reaction pathway via intermediates usually occurs: the  $\pi$ -electron system of the aromatic compound coordinates to the catalyst surface in form of a  $\pi$ -complex bonding (side-on-adsorption) which leads to a hydrogenation of the aromatic ring. The partly reduced compound can be desulfurized by the common DDS reaction afterwards. Due to the detour that occurs when aromatic

compounds with alkyl groups flanking the sulfur atom are desulfurized, the HDS for these compounds is much slower. This leads to the fact that a variety of these recalcitrant compounds can still be found in modern desulfurized transportation fuels [13].

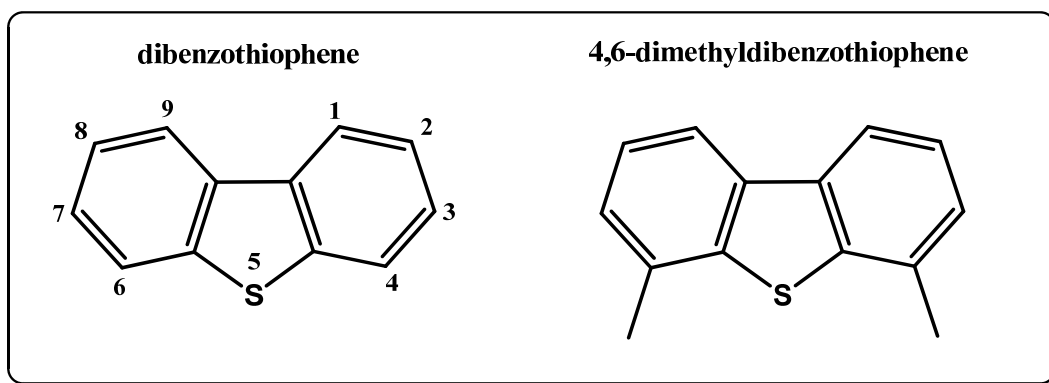


**Fig. 5: Structures for dibenzothiophene and 4,6-dimethyldibenzothiophene**

In addition to the traditionally used desulfurization methods, an increasing interest in biodesulfurization with the help of microorganisms can be observed. Nevertheless all of these approaches are still in an experimental state, because the traditional HDS is still the more economic and quantitative method. Some bacteria, like *Rhodococcus erythropolis*, can remove sulfur directly from aromatic sulfur compounds in an oxidative C-S cleavage [14]. Typically the sulfur atom is oxidized to the corresponding sulfoxide and subsequently to the sulfone by the bacteria. In the following step, the carbon-sulfur bond is cleaved by a monooxygenase and the sulfur released as  $\text{SO}_2$ . The desulfurized species can be compared to the products from the HDS with the difference that during the oxidative cleavage, a hydroxy group is attached in the place where the carbon-sulfur bond was cleaved, so that the resulting desulfurized species is a 2-hydroxybiphenyl [15]. Another approach to biodesulfurization uses the reductive C-S cleavage by bacteria. This method comes with the drawback that a reducing agent has to be added to the reaction mixture. With help of this reducing agent, the bacteria can release the sulfur as hydrogen sulfide leading to the same desulfurized species occurring in the common HDS [16] except for compounds with hydrogenated aromatic rings.

### 1.5 Analytical methods for the identification of PASHs in fossil fuels

PASHs are an important compound class in fossil fuels. The interest in analytics of these compounds dates back to the 1980s, when the massive Waldsterben was related to the combustion of sulfur compounds in fossil fuels, as mentioned before. After legal limits for the sulfur content in transportation fuels were set, the environmental problems decreased. Nevertheless PASHs stayed in the focus of research as other problems arose: Modern car catalytic converters are very susceptible to even low concentrations of PASHs as found in desulfurized transportation fuels. The increasing complexity of the catalysts comes along with higher vulnerability for poisoning. Several studies demonstrated that even low concentrations of sulfur in the fuel can drastically decrease the efficiency of the catalysts in the converters [17].

One of the main problems that occur when dealing with the analytics of sulfur compounds in fossil fuels is the fact that these compounds are present in very low concentrations in the matrix. This makes the direct analysis of single compounds difficult as the signal for the hydrocarbon matrix usually massively exceeds the signals for the target compounds.

Both high performance liquid chromatography (HPLC) and gas chromatography (GC) are the most commonly used chromatographic methods for the analysis of PASHs. HPLC can be used for a group type separation of the different compounds in fuels, which drastically simplifies the chromatograms. The interest in high resolution mass spectrometry as a spectrometric method for the analysis of PASHs is strongly increasing, because this method can help to identify compounds by allowing the molecular composition to be calculated from the accurate masses.

#### 1.5.1 Gas chromatography

GC analysis is usually the method of choice when the analytes are thermally stable and have a sufficient volatility as it is the case for the PASHs from low boiling or middle boiling fractions. A variety of detectors can be coupled to the GC, with the flame ionization detector (FID) the most commonly used one. One drawback of this detector is that it detects all carbon-containing analytes and has no sulfur selectivity, so that the signals for the sulfur compounds are hidden covered by the more intense signals of the hydrocarbon matrix.



Another commonly used detection technique coupled to the GC is the mass spectrometric (MS) detection, where the GC is used to separate the sample and the MS to identify the compounds by mass or by fragmentation pattern. This technique can only be used for compounds up to masses of ca. 500 u. PASHs from high boiling fractions or vacuum residues are hence difficult to analyze by GC because sufficient volatility cannot be assured.

Detectors like the flame photometric detector, the sulfur-chemoluminescence detector or the atomic emission detector (AED) can be coupled to GC to detect sulfur compounds selectively. All of these three detectors create species that emit light of a specific wavelength. The sulfur species can be analyzed by detecting the signal at this particular wavelength. Additionally, the signals for all carbon containing compounds can be detected at the same time through use of parallel detection so that an overlay of both chromatograms reveals the composition of the sample.

### **1.5.2 High performance liquid chromatography**

HPLC is the method of choice when dealing with samples that are not volatile enough for GC analysis, or to achieve a group type separation of the different compound classes from fuels to decrease the complexity of the sample. Especially for the analysis of PASHs, the group type separation is of major interest. The PASHs can be isolated from fossil fuels by the use of ligand exchange chromatography (LEC) and can then be analyzed with offline mass spectrometric methods or further separated using other HPLC methods [18]. LEC is based on a complexation interaction of the stationary phase and the target compounds. Heteroatoms in the target molecules coordinate to transition metal cations of the stationary phase by means of a donor-acceptor interaction. In case of PASHs, a typically used stationary phase contains palladium(II) cations. The sulfur atoms of the PASHs donate their lone electron pairs to the metal cations, so that a complex bonding occurs and the PASHs adsorb to the column. Compounds without sulfur can easily be released from the column by choosing an adequate solvent. The PASH compounds can then be released from the stationary phase by adding a competitive ligand to the solvent. The isolated PASH fraction can be further separated and simplified according to the number of  $\pi$ -electrons in the aromatic system on a silver(I) phase as presented by NOCUN [19].

### 1.5.3 High resolution mass spectrometry

Nowadays two ultrahigh resolution mass spectrometric methods, Orbitrap mass spectrometry and Fourier transform ion cyclotron resonance mass spectrometry (FT-ICR MS), are used to characterize very complex or high boiling petroleum samples without a prior separation [20, 21]. Both of the techniques measure the masses by detecting the harmonic oscillations of the ions. The Orbitrap MS consists of two electrodes with the outer one in shape of a barrel and the inner one spindle shaped (figure 6). When ions are released into the space between both electrodes they start to oscillate around the inner electrode and are hence trapped, because the centrifugal forces are balanced by the electrostatic attraction to the inner electrode. Additionally, the ions move forth and back along the central axis of the chamber. Therefore ions of a specific mass begin to oscillate at a certain frequency along the central axis. The oscillating ions induce an image current that can be measured and transformed by Fourier transformation to an overlay of different frequencies. Each frequency can hence be related to a certain mass.

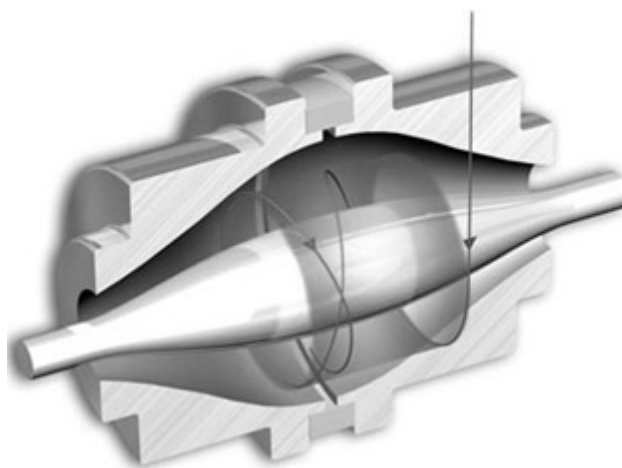


**Fig. 6: Schematic layout of an Orbitrap cell**

The principle of FT-ICR MS is very similar to Orbitrap MS, the differences can mostly be found in the instrumental setup [22]. The ions are not released into the space between two electrodes but into a magnetic field created by superconducting electromagnets. By applying an oscillating electric field, perpendicular to the static magnetic field, the ions

start to oscillate in the magnetic field. As described for Orbitrap MS, the ions induce an image current that is measured. The resulting free induction decay can be transformed by Fourier transformation to an overlay of frequencies which can be related to the masses.

Both of the ultra high resolution mass spectrometric methods have the big advantage that they measure the ions without destroying them. The analytes do not hit a detector plate such as an electronic multiplier but are measured by passing by the detector while oscillating. Hence, the ions are not only measured once but every time they pass the detector. This leads to the superb mass resolution that is observed for both methods.

## 2 Introduction to capillary electrophoretic methods

As capillary electrophoresis is a commonly used technique in analytical chemistry, the basic principles of this method shall not be presented in this work. An overview explaining this analytical method was given in earlier studies [23] or can be found in various books [24, 25]. Within the next chapter, the coupling of CE to MS will be explained as this method is not commonly used yet and plays an important role in this work. In addition the principles of micellar electrokinetic chromatography (MEKC) will be explained as this technique differs dramatically from the regular CE and was used as a second separation method in this work.

### 2.1 CE-MS

The typically used detection methods for CE are UV and fluorescence detection. One disadvantage is obvious for both of these methods: a chromo- or a fluorophor is needed in the target analyte. Since this is not always the case, mass spectrometric detection may be the method of choice. Further advantages, like low limits of detection and the possibility to separate comigrating analytes by the difference in the mass to charge ratio, come along with MS detection. Additionally, structural properties of the analytes can be elucidated by the fragmentation pattern if ion trap MS is used for detection.

For the coupling of CE to MS a variety of interfaces exist, because a direct coupling is technically not feasible [26]. These interfaces are typically based on HPLC electrospray ionization (ESI) MS interfaces but have to be adapted to CE because two major problems arise: Both the CE and the MS units can be seen as individual electric cells, so a decoupling of the voltage regulation is necessary but difficult to realize. The other problem can be found in the significantly different flow rates of HPLC and CE. While for HPLC flow rates of 1 to 2 mL/min are commonly used, the flow rate for CE depends on the electroosmotic flow and ranges between zero and 250 nL/min [27]. For the traditionally used HPLC-ESI-MS interfaces, it is technically not feasible to create a constant electrospray with such low flow rates. For this reason so-called sheath liquid interfaces were developed, originally described by SMITH in 1988 [28]. These interfaces provide a supporting flow (sheath flow) of liquid (sheath liquid) in addition to the flow coming from the CE capillary. Though the analytes leaving the capillary are diluted, a stable electrospray can be obtained. The sheath liquid fulfils a further technical function in the

interface, as it establishes an electric connection between the analyte solution in the capillary and the electrode of the interface. Because the silica capillary is not electrically conducting, the electric circuit in the interface needs to be closed via the sheath liquid.

Differences in the instrumental setup between CE-UV and CE-MS are mostly of a technical nature, as both devices (the CE and the MS) are individual instruments. This implies that the capillary needs to be at least long enough that a connection between the CE and the MS is possible. Usually a minimal length of 50 cm is necessary to couple both instruments [29]. Sometimes this makes adaption of CE-UV methods to CE-MS difficult, because most of the CE-UV methods are performed with capillaries shorter than 50 cm. Longer capillaries mean a lower field strength in the capillary so that longer migration times and hence broader signals result. This problem can be solved by increasing the applied voltage to the capillary when CE-MS is used. However, this provides new problems, like increased Joule heating and larger longitudinal diffusion of the analytes, which again results in a broadening of the signals. Nonconstant temperature conditions also follow from the fact that the capillary cannot be cooled. In the space between the two instruments the capillary is exposed to room temperature so that migration times vary with changing room temperature. A positive effect that occurs with the CE-MS instrumental setup is that there is no difference between the total length and the effective length of the capillaries because the analytes are measured when they leave the capillary and not on-capillary, as is done in UV and fluorescence detection.

Because the sheath liquid is used to establish an electric connection between the analyte solution in the capillary and the electrode of the interface, an electrolyte solution is needed. Purely organic media like methanol or isopropanol are not useable because the conductivity of these is too low. In many cases a mixture of water, isopropanol and acetic acid is used. The addition of isopropanol increases the volatility of the sheath liquid and this increases the ionization efficiency.

The most commonly used sheath liquid interface is the “coaxial sheath liquid interface” presented in figure 7 [26].

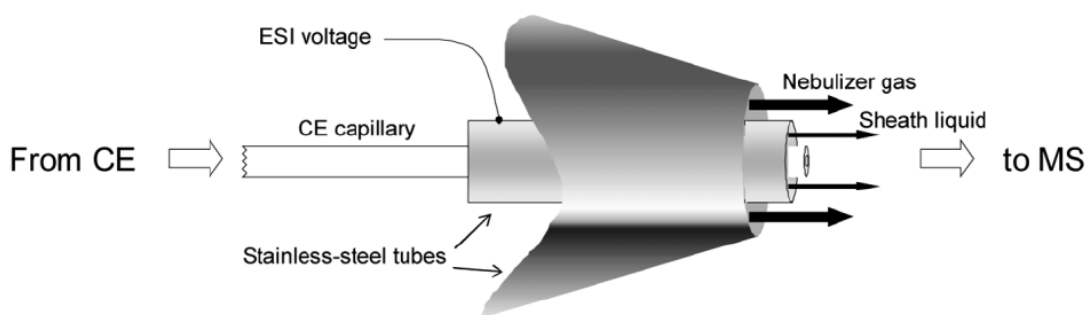


**Fig. 7: Design of a coaxial sheath liquid interface [26] (reprinted with permission of Wiley-VCH)**

The central unit of this interface is the CE capillary, which is surrounded by a steel tube, which at the same time is the ESI electrode. The space in between the capillary and the ESI electrode is used to feed the sheath liquid. Both the capillary and the ESI electrode are surrounded by a larger diameter tube which is used for the supply of a sheath gas flow. This gas flow is used to nebulize the mixture of analytes and sheath liquid that is leaving the interface. Due to the dilution of the analytes by the sheath liquid at the end of the capillary, a slight broadening of the signals occurs [30]. Additionally, problems can occur when the cone end of the capillary is not completely flat. After cutting a capillary, the cone end always has to be checked for accurate cutting because irregularities can greatly influence the electrospray behavior and hence the ionization efficiency. Nevertheless, the coaxial sheath liquid interface is the most robust one.

A further type of sheath liquid interface is the “liquid junction interface” (figure 8). Here, the sheath liquid is applied over a T-fitting [31, 32]. The end of the CE capillary is mounted in the left part of the T-fitting and the analytes leaving the capillary are dissolved by the sheath liquid, that is fed through the lower part of the T-fitting. The mixture of analytes and supporting sheath liquid leaves the T-fitting through a mounted transfer capillary and is subsequently nebulized with the help of a sheath gas flow at the end of the capillary. The ESI voltage is directly applied via the sheath liquid. This setup comes with the disadvantage that the analytes and sheath liquid are mixed before the end of the capillary. A broadening of the signals has to be accepted due to dilution effects and because the flow in the transfer capillary is laminar and not plug-like as it is known from

CE [33]. The main advantage can be seen in the electrical and physical decoupling of both CE and ESI.

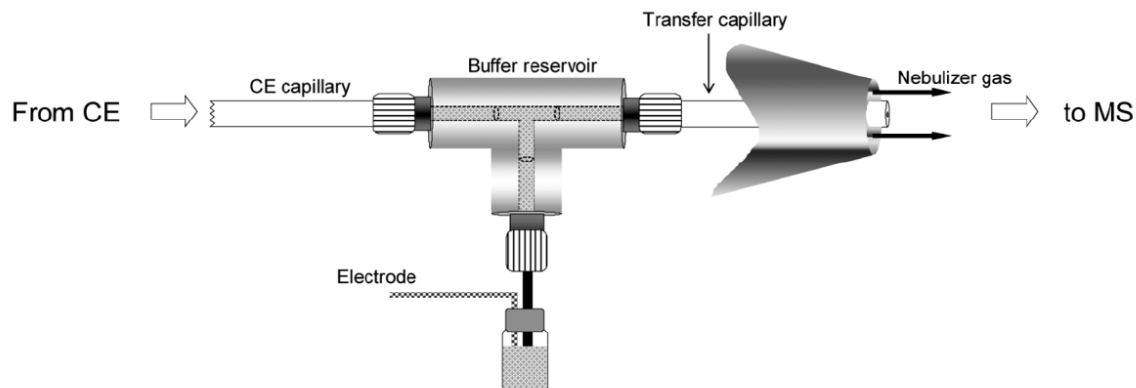


**Fig. 8: Design of a liquid junction interface [26] (reprinted with permission of Wiley VCH).**

In addition to the sheath liquid interfaces, so-called “sheathless interfaces” exist [34]. These setups work without supporting the flow of the capillary by an auxiliary liquid. For this reason the setup can only be applied when a CE method with a high EOF is used to provide a sufficient flow from the capillary. Because no supporting liquid is used, the ESI voltage cannot be applied via the sheath liquid, but needs to be applied over a conductive coating on the spray capillary [35]. The flow directly from the capillary is nebulized by a sheath gas flow and results in a nanospray. The main advantage of the setup is that the loss of efficiency is quite low because no dilution effects through the sheath liquid occur. The nanospray additionally increases the ionization efficiency during the ESI process. The main disadvantage of the setup is the lack of robustness [36, 37]. The extremely low flow from the capillary has to be focussed to produce an ESI spray. This is usually done by using reduced cone ends, but they tend to clog. In addition it is usually time consuming to position the small diameter nanospray in front of the entry of the MS.

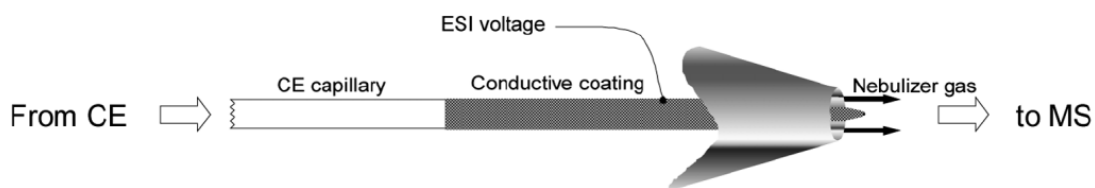


**Fig. 9: Design of a sheathless interface [26]. (Reprinted with permission of Wiley VCH)**

For all of the introduced interfaces different methods to guide the ions into the MS can be found. While some time ago it was still routine to direct the ESI spray straight onto the entrance of the MS, this is not common anymore. As presented in figure 10, nowadays an angle of  $90^\circ$  between the direction of the spray and the entry of the MS is common. This construction has the large advantage, that the MS is not contaminated by matrix compounds. Only the ionized compounds are carried through the electric field to the entry of the MS while non-ionized compounds miss the entry. This method can be improved by using a “z-cell”, where the ions have to move through a z-shaped cell to enter the MS, which leads to superb isolation of the ions.

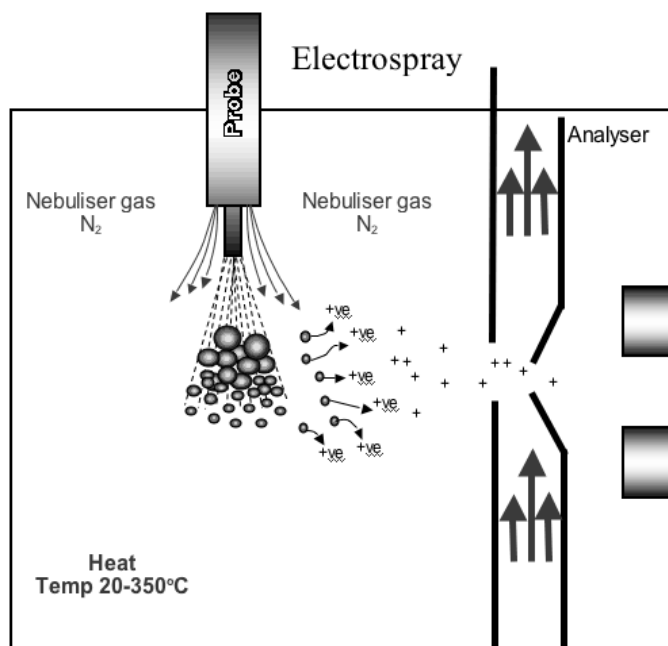


**Fig. 10: Schematic design of an ESI source with  $90^\circ$  angle between spray direction and MS entry [38].**



## **2.2 Micellar electrokinetic chromatography**

Micellar electrokinetic chromatography (MEKC) is a special form of capillary electrophoresis where surfactants are added to the buffer solution. The concentration of the surfactants has to be above the critical micelle concentration (CMC) [39, 40] so that colloidal-sized aggregates, the micelles, are formed. The surfactants usually possess a hydrophilic head group and a hydrophobic hydrocarbon tail. The hydrophilic headgroup is usually anionic [41], but cationic [42, 43] or even zwitterionic [44, 45] surfactants are used as well. Simplified, micelles can be seen as spherical aggregates whose hydrophilic head-groups are directed towards the aqueous phase and the hydrophobic tails are directed to the centre of the micelle. Monomers from the micelles can leave the aggregates into the aqueous phase on the one hand, while dissolved monomeric surfactants from the aqueous phase can be incorporated in the micelle on the other hand. This leads to a dynamic equilibrium state. A schematic illustration of a sodium dodecylsulfate (SDS) micelle (SDS is the most commonly used detergent in MEKC) is presented in figure 11.

The largest advantage that comes with MEKC in comparison to CE is the possibility to separate neutral analytes. Neutral molecules partition between the aqueous phase and the strongly hydrophobic center of the micelles. The partitioning of the analytes occurs depending on their polarity. This means that highly polar analytes will rather stay in the aqueous phase, while non-polar compounds will partition into the hydrophobic centre of the micelle. A partitioning equilibrium is established for every analyte and depends on the aqueous phase and micelle. Therefore the micelles can be seen as a kind of stationary phase in the chromatographic sense. But as the stationary phase itself is moving when a high voltage is applied, it is called a “pseudostationary phase” (PSP) [39, 40]. The separation of the analytes is based on the principle that the electroosmotically driven aqueous phase moves with a different speed than the electrophoretically driven micellar PSP. As an example, the separation of analytes in an SDS-MEKC method shall be described in the following and illustrated in figure 12.

The SDS micelles are negatively charged and hence migrate in the direction of the anode with a mobility of  $\mu_m$ . The electroosmotic flow ( $\mu_{EOF}$ ) is directed to the cathode and exceeds the mobility of the micelles. Thus, the effective mobility of the micelles is designated by the sum of the two vectorial mobilities ( $\mu_m + \mu_{EOF}$ ) and results in the

effective mobility ( $\mu_{\text{net}}$ ) of the micelles into direction of the cathode where the detector is placed. During this process, the analytes distribute themselves between the micellar and the aqueous phase according to their polarity. Very polar analytes will stay in the aqueous phase and hence move with the speed of the electroosmotic flow  $\mu_{\text{EOF}}$ . These analytes reach the detector first. The time when these compounds, driven by the EOF, reach the detector is referred to as  $t_{\text{EOF}}$ . Very nonpolar compounds will mainly remain in the micelles and move with an effective mobility of  $\mu_{\text{net}}$  in the direction of the detector. These compounds will reach the detector last, at a time referred to as  $t_{\text{m}}$ . All the other analytes with intermediate polarity partition in a dynamic equilibrium into the micelles as well as the aqueous phase. Thus, all these analytes migrate in between  $t_{\text{EOF}}$  and  $t_{\text{m}}$ . This time period in which the analytes can arrive at the detector is called the “micellar window”.

The partitioning of the analytes resembles the partitioning between two different phases as seen in chromatography. The movement on the micellar PSP is mainly based on electrophoretic principles, so that MEKC in the whole can be seen as a hybrid technique of both methods. The major advantage of this method is that several factors can be adjusted, so that this method can be used for a broad line-up of neutral analytes. Changing the surfactant results in different polarities of the micelle interior or even in a reverse of  $\mu_{\text{m}}$  in case that cationic surfactants are used [43]. The electroosmotic flow  $\mu_{\text{EOF}}$  can be influenced by the pH of the aqueous phase and by the chosen buffer system. The addition of organic media like methanol or acetonitrile results in different partition coefficients for the analytes as well as an increase of the micellar window.

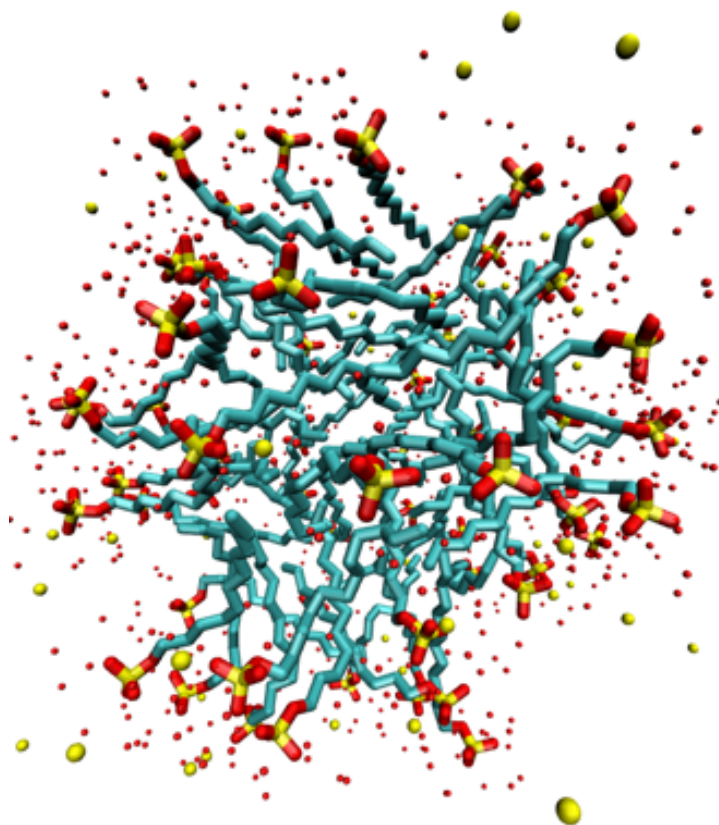


Fig. 11: Schematic molecular composition of a SDS micelle in water [46].

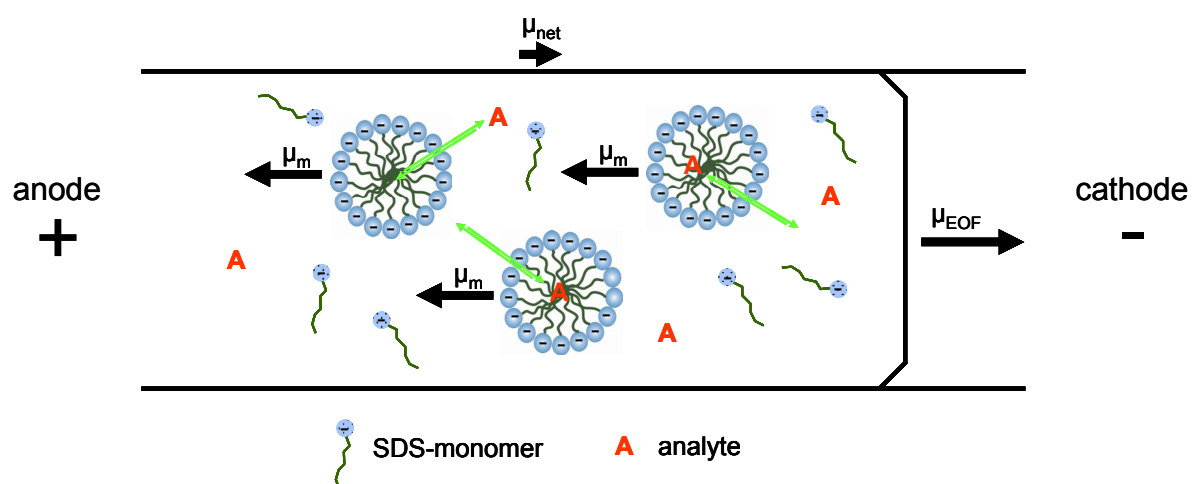


Fig. 12: Illustration of the principles of MEKC

### 3 State-of-the-art: Capillary electrophoretic separation of PAHs

Because hardly any studies have been done separating PAHs by electrophoresis, the literature overview will mainly focus on other classes of compounds also belonging to the polycyclic aromatic compounds (PACs). Because the micellar electrokinetic chromatography (MEKC) will not be a main issue in this work, the separation of PAHs with this method is not further discussed here but is described in a variety of publications [47-65]. As capillary electrochromatography (CEC) was not used during this work either, this electrophoretic technique will be left out in the following chapter. Further information concerning the separation of PAHs with this method are widely published [66-80].

Because PAHs cannot be protonated or deprotonated for capillary electrophoretic separations, all of the methods are performed by using charged buffer additives. This section of separations will be discussed in the following [81].

#### 3.1 Introduction

The toxicity, mutagenicity and carcinogenicity of many representatives of the polycyclic aromatic compounds (PAC) have led to this class of compounds being one of the most intensely investigated ones. The basis for all such studies is formed by reliable analytical measurements which largely are based on either HPLC or GC. These have reached a considerable degree of sophistication due to their high separation efficiency and the availability of a wide variety of detectors. Many kinds of sample preparation and preconcentration techniques have been introduced to deal with even the lowest PAC concentrations in highly varying matrices.

Despite their sophistication, both HPLC and GC are associated with several drawbacks. One limiting problem in GC is the volatility of the analytes. While the PACs of largest concern (e.g. the EPA PAHs) can be well separated, compounds of higher molecular weight – like those in asphaltenes, of interest in the petroleum industry – possess too low a volatility to be readily analyzed by GC. In case of polar substituted compounds such as hydroxy-PAHs or sulfonated PAHs, a derivatization of the analytes prior to GC separation is usually necessary and therefore these compounds are often analyzed in the condensed phase by HPLC. The major drawback of this technique, however, is the insufficient

resolution of such complex samples as found in petroleum and related matrixes.

Efforts to circumvent these problems can be found in the field of electrophoretic separations. The volatility of the analytes is not an issue since they are dissolved in a solvent, and the high resolution of electrophoretic separations can be utilized to great advantage. But electrophoretic methods do not come without their own problems, such as the lack of charge of unsubstituted PAHs. They are not ionogenic so that simple proton addition or removal to generate ions is out of the question and therefore a direct capillary electrophoretic separation is impossible.

Basically CE offers the analytes nothing more than an open capillary filled with a liquid that moves in an electric field due to the electroosmotic flow (EOF). Neutral compounds thus experience only this moving force and are not separated since the flow is identical to all analytes. If they can interact with an added ionic species, then they will move along the capillary as soon as they interact with the ion, at a different rate than the EOF. If the strength of this interaction is different for the analytes, then this strength will determine how fast each species moves – a stronger interaction will mean a higher mobility towards the detector (if the ionic charge is opposite to that of the electrode at the detector end, otherwise a stronger interaction will mean a slower transport toward the detector). Analytical chemists have shown much imagination in devising such interactions of PACs with ions.

### 3.2 Solvophobic association with tetraalkylammonium ions

The first time the solvophobic association of PACs with tetraalkylammonium ions was used for electrophoretic separation was in 1986 when CE was still in an early stage of development. A major aim was to extend the capillary electrophoresis to separations in nonaqueous media and mixed aqueous/organic media to broaden the range of potential analytes. Tetrahexylammonium perchlorate (THAP),  $(C_6H_{13})_4N^+ClO_4^-$ , as buffer additive enters into solvophobic interactions with the neutral PAHs and this induces electrophoretic mobility to the PAH/THA<sup>+</sup> entity [82]. The separation of benzo[ghi]perylene, perylene, pyrene, methylanthracene and naphthalene was performed in aqueous acetonitrile. The larger and less polar analytes exhibit stronger interaction with the THA<sup>+</sup> so that they move

faster than smaller and less hydrophobic ones.

Solvophobic interaction with tetraalkylammonium ions was adopted in an effort to decrease the detection limits by using UV-laser excited fluorescence [83]. The four PACs perylene, benz[*a*]anthracene, pyrene and anthracene were separated with detection limits as low as  $(3-15) \times 10^{-20}$  mol. Despite about 200,000 theoretical plates/m being reached, isomers like anthracene and phenanthrene coeluted.

The use of tetraalkylammonium salts for imparting electrophoretic mobility to neutral compounds was studied in more depth [84], showing that both the type and the concentration of the quaternary ammonium salts play a role. While tetrabutyl- and tetrapentylammonium ions were unable to separate the analytes, tetrahexyl- and tetraheptylammonium ions showed very good properties. The results were used to optimize the separation conditions for various types of neutral analytes, including six PACs. 16 neutral aromatic compounds including the six PACs were separated in 20 minutes (figure 13). A reduction of the pH or a decrease of the acetonitrile concentration led to even better separations but came along with increased migration times.

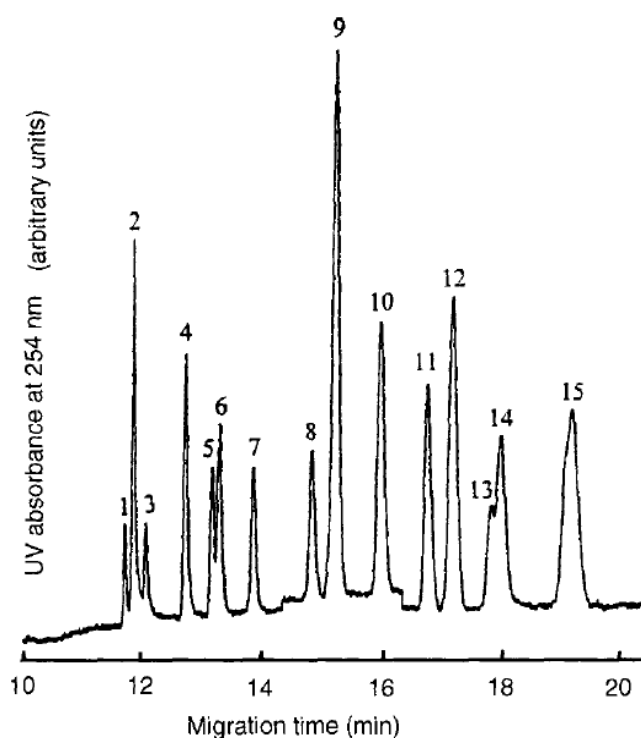


**Fig. 13: Electropherogram of sixteen non-ionic aromatic organic compounds separated by solvophobic association with tetraheptylammonium bromide.** Electrolyte: 50 mM tetraheptylammonium bromide, 8 mM borate, 42 % acetonitrile, pH 9.4; applied potential 12 kV; injection time 30 s. Peak identification: 1: coronene; 2: benzo[ghi]perylene; 3: perylene; 4: pyrene; 5: anthracene; 6: 1-pyrenecarboxaldehyde; 7: 9-anthraldehyde; 8: naphthalene; 9: benzophenone; 10: 1-bromo-4-nitrobenzene; 11: 5,6-dinitroquinoline; 12: nitrobenzene; 13: 3-nitroacetophenone; 14: 4-nitroacetophenone; 15: acetophenone and benzaldehyde ([84] Reproduced with permission of Wiley VCH)

The observation that long alkyl chains in the quarternary ammonium ions led to better separations made it desirable to investigate even longer chain surfactants, namely tetraoctylammonium ( $\text{TOA}^+$ ) and tetradecylammonium ( $\text{TDA}^+$ ) [85]. Six neutral hydrophobic analytes, including five PACs, were separated in aqueous acetonitrile containing tetraoctylammonium bromide. As expected, the more hydrophobic compounds showed the shortest migration time due to the stronger association with the surfactant. Because  $\text{TOA}^+$  and  $\text{TDA}^+$  show micellar aggregation in organic media, a dynamic coating of the capillary wall occurs when the acetonitrile concentration of the electrolyte is increased to 60 %. This leads to a reversed electroosmotic flow (EOF) so that the polarity of the electrophoresis system must be reversed. The resolution of the separation was improved to the point where four-ring PAHs like pyrene and chrysene were separated.

Later it was demonstrated that the separation through association with tetraalkylammonium ions can be performed even in completely organic media [86]. All tetraalkylammonium ions from one to eight carbons in the alkyl chain were tested with PAHs and, as in the aqueous system, the resolution increased with the chain length of the alkyl groups. Tetraoctylammonium ions show limited solubility in pure methanol so that tetrahexylammonium ( $\text{THA}^+$ ) bromide was favored in that medium. A standard mixture of 13 PAHs was separated using  $\text{THA}^+$  in pure methanol. This solvent was used not only to increase the solubility of the analytes but also to couple solid phase microextraction (SPME) to CE. The successful separation of a PAH mixture in water extracted via SPME and followed by the tetraalkylammonium ion aided CE separation demonstrate the power of the method.

Cetyltrimethylammonium bromide (CTAB, cetyl = hexadecyl) was employed in the dual function as detergent and for the solvophobic association with the analytes [87] in a medium of high acetonitrile concentration (40 %) to prevent the formation of micelles. This composition led to a dynamic coating of the capillary wall with a reversed EOF so that a negative voltage had to be applied for the analysis of the PAHs from cooked soybeans.

### **3.3 Solvophobic/hydrophobic interaction with other ionic surfactants**

Ionic surfactants for the separation of nonionic organic compounds were introduced in 1995 [88] with dioctyl sulfosuccinate (DOSS, figure 14) as detergent. DOSS is a more suitable detergent for the separation of neutral molecules than quarternary ammonium ions due to a larger separation window and less interaction with the capillary wall [88]. Again, the separation is assumed to be due to the electrophoretic mobility of analyte/detergent associates. A buffer of optimized DOSS, borate and acetonitrile concentrations allowed the separation of 23 neutral organic compounds, most of them PAHs, within 22 minutes. (figure 15) Since an anion was used, the migration order of the analytes was opposite to that obtained with positively charged tetraheptylammonium ions.



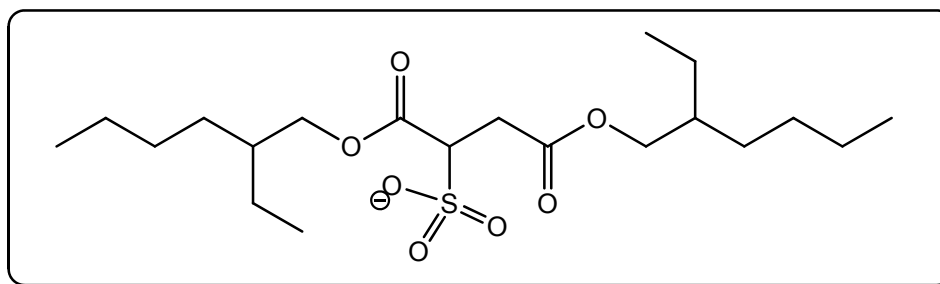
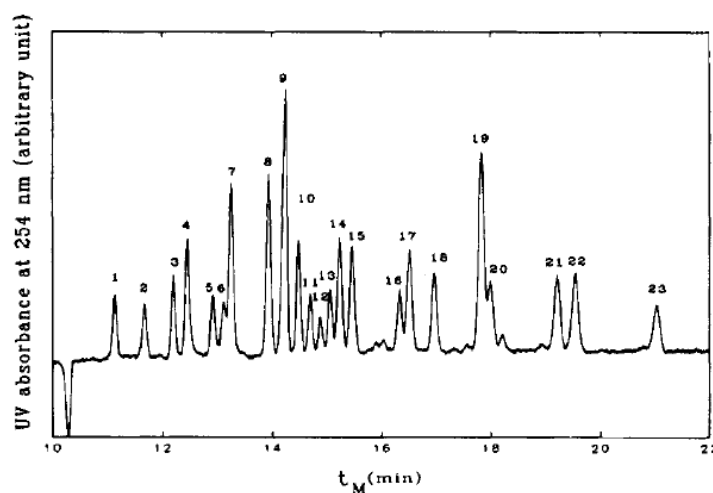


Fig. 14: Diethyl sulfosuccinate



**Fig. 15: Separation of nonionic aromatic compounds by hydrophobic interaction with DOSS.** Electrolyte: 50 mM sodium dioctyl sulfosuccinate, 8 mM sodium borate, 40% (v/v) acetonitrile, pH 9.0; applied voltage: 20 kV; Peak identification: **1:** acetophenone; **2:** nitrobenzene; **3:** unidentified; **4:** benzo[*f*]quinoline; **5:** benzophenone; **6:** azulene; **7:** naphthalene; **8:** acenaphthylene; **9:** acenaphthene; **10:** fluorene; **11:** 3-aminofluoranthene; **12:** 9,10-dimethylbenz[*a*]anthracene; **13:** benz[*a*]anthracene; **14:** phenanthrene; **15:** anthracene; **16:** fluoranthene; **17:** pyrene; **18:** benzo[*b*]fluorene; **19:** chrysene; **20:** benz[*a*]anthracene; **21:** perylene; **22:** benzo[*a*]pyrene; **23:** benzo[*ghi*]perylene. ([88] Reprinted with permission of the American Chemical Society)

An anionic surfactant was synthesized through treatment of the nonionic detergent Brij-30 with chlorosulfonic acid to yield  $C_{12}H_{25}(OCH_2CH_2)_4OSO_3^-Na^+$ , referred to as Brij-S (figure 16) [89]. This was used for the CE separation of a wide variety of neutral molecules in the counter migration mode. The migration times of different analytes could be adjusted by varying the surfactant concentration and the proportion of acetonitrile in the electrolyte buffer. A higher concentration of Brij-S led to longer migration times due to a stronger association, a higher percentage of acetonitrile shortened the migration times and at the same time increased the solubility of nonpolar compounds. Adjustments of these

parameters led to success in several difficult separations, for example the baseline separation of 20 PAHs (figure 17) and the separation of four isomers of methylbenz[*a*]anthracene. In later studies an acidic buffer was tested to eliminate the EOF; this influenced the migration order of the analytes [90].

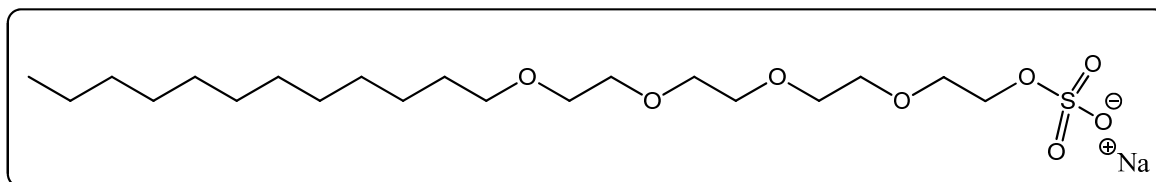
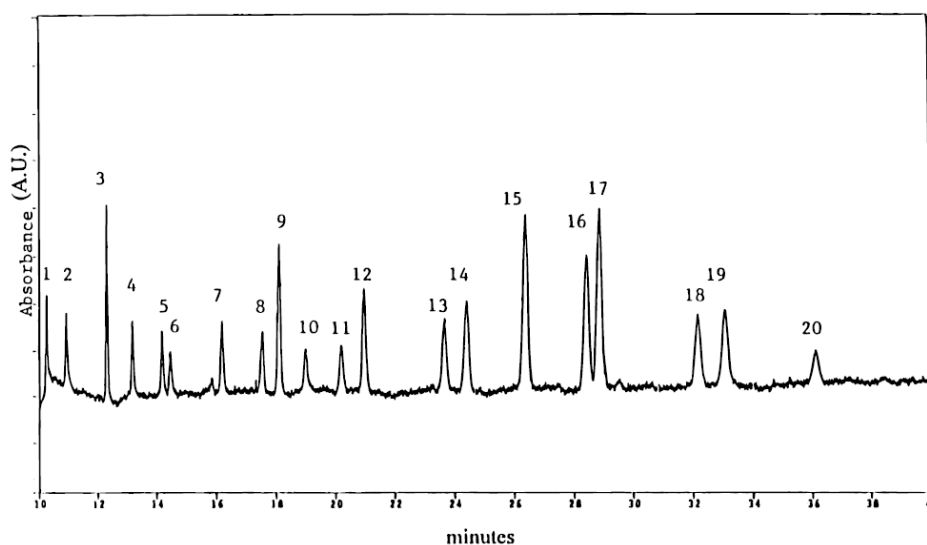


Fig. 16: Sulfonated Brij-30 (Brij-S)



**Fig. 17: Separation of PAHs by hydrophobic interaction with Brij-S.** Electrolyte: 40 mM Brij-S, 8 mM sodium borate, 40% (v/v) acetonitrile, pH 9.0; applied voltage 20 kV; current 68  $\mu$ A; injection time 30 s; detection 254 nm; capillary, 50  $\mu$ m i.d., 75 cm length. Peak identification: 1: acetophenone; 2: nitrobenzene; 3: benzo[*f*]quinoline; 4: benzophenone; 5: azulene; 6: naphthalene; 7: acenaphthylene; 8: acenaphthene; 9: fluorene; 10: 3-aminofluoranthene; 11: benz[*a*]anthracene; 12: anthracene; 13: fluoranthene; 14: pyrene; 15: 11*H*-benzo[*b*]fluorene; 16: chrysene; 17: benzo[*a*]anthracene; 18: perylene; 19: benzo[*a*]pyrene; 20: benzo[*ghi*]perylene.

([90] reprinted with permission of the American Chemical Society)

A high percentage of organic solvent - ideally 100 % - is desirable in the CE electrolyte for the separation of nonionic and nonpolar compounds since it leads to a better solubility of the analytes. Several ionic surfactants have been tested for nonaqueous CE (NACE) separation of PAHs [91], among them sodium dodecyl sulfate (SDS), the somewhat longer sodium tetradecyl sulfate (STS) and sodium hexadecyl sulfate (SHS) (figure 18). All three

ions allowed the separation of a standard mixture of five PAHs in pure methanol. The mobility of the analytes increased with higher concentration and longer chain lengths of the surfactant. Because the migration window for the tested analytes was rather small in pure methanol, the addition of low percentages of other solvents to the electrolyte buffer was investigated [91]. Surprisingly, the best results were obtained when the buffer contained 10 % to 25 % of water. It was postulated that water greatly influences the solvophobic interaction between the analytes and the surfactant as well as the dielectric constant and the viscosity of the binary methanol/water mixture. The concentration of water in the buffer had to be adjusted depending on the neutral analyte.

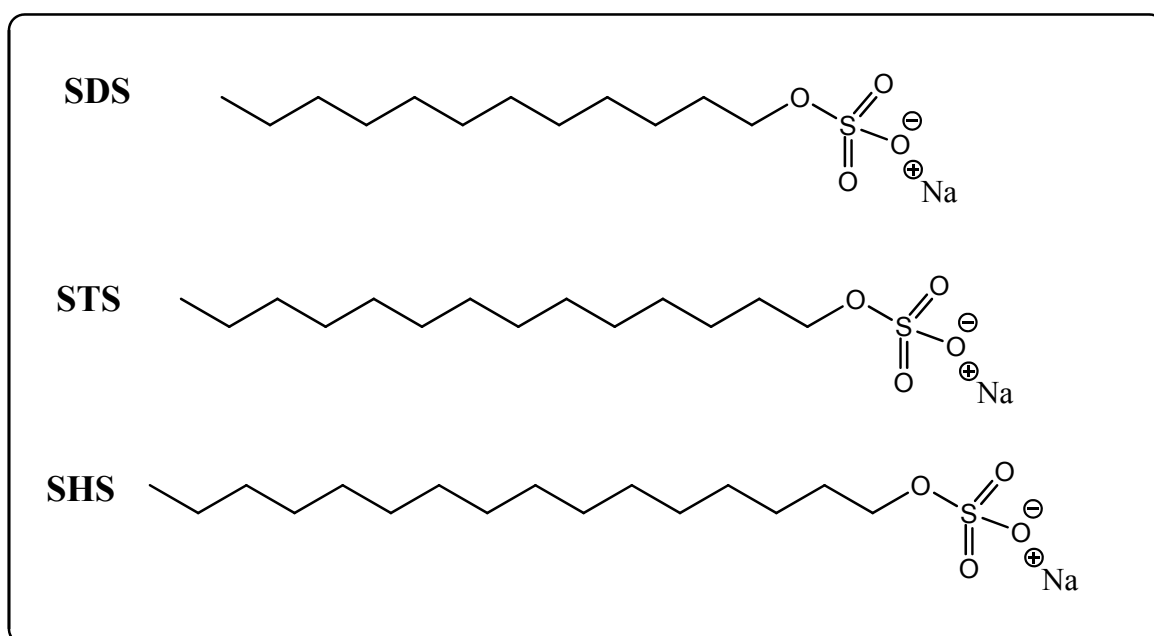


**Fig. 18: Sodium dodecyl sulfate (SDS), sodium tetradecyl sulfate (STS), sodium hexadecyl sulfate (SHS)**

With DOSS as additive and the separation window enlarged through the use of high concentrations of urea in the electrolyte buffer as practiced in MEKC, the 16 EPA PAHs could be separated using a variation of the above conditions [92]. Except for benzo[*a*]pyrene, benzo[*b*]fluoranthene and benzo[*k*]fluoranthene, complete separation was achieved. It was conjectured that the use of a more sensitive detector than UV may lead to a better separation since the peak width decreases with lower sample loading. With the high-sensitivity laser induced fluorescence detector the goal of baseline resolution of all the 16 PAHs was achieved.

Other buffer additives than urea can be used together with DOSS to increase the separation efficiency of the EPA PAHs, for instance cyclodextrins [93]. They are known to form inclusion complexes with the analytes and thereby influence the migration time. Separations aided by ionic cyclodextrins are discussed below.

The interaction between the surfactant and the PAHs can be made more selective if an aromatic group is included in the surfactant. Not only are solvophobic interactions observed but also  $\pi$ - $\pi$  interactions between the aromatic systems in the surfactant and the analytes. Sodium dodecylbenzenesulfonate (SDBS, figure 19) demonstrates this in the separation of 11 PAHs with ring numbers from 1 to 5 [94]. The formation of micelles was suppressed through a high concentration of organic modifier. The PAH mixture could be nicely separated with separation efficiencies between 130 000 and 230 000 theoretical plates/m.

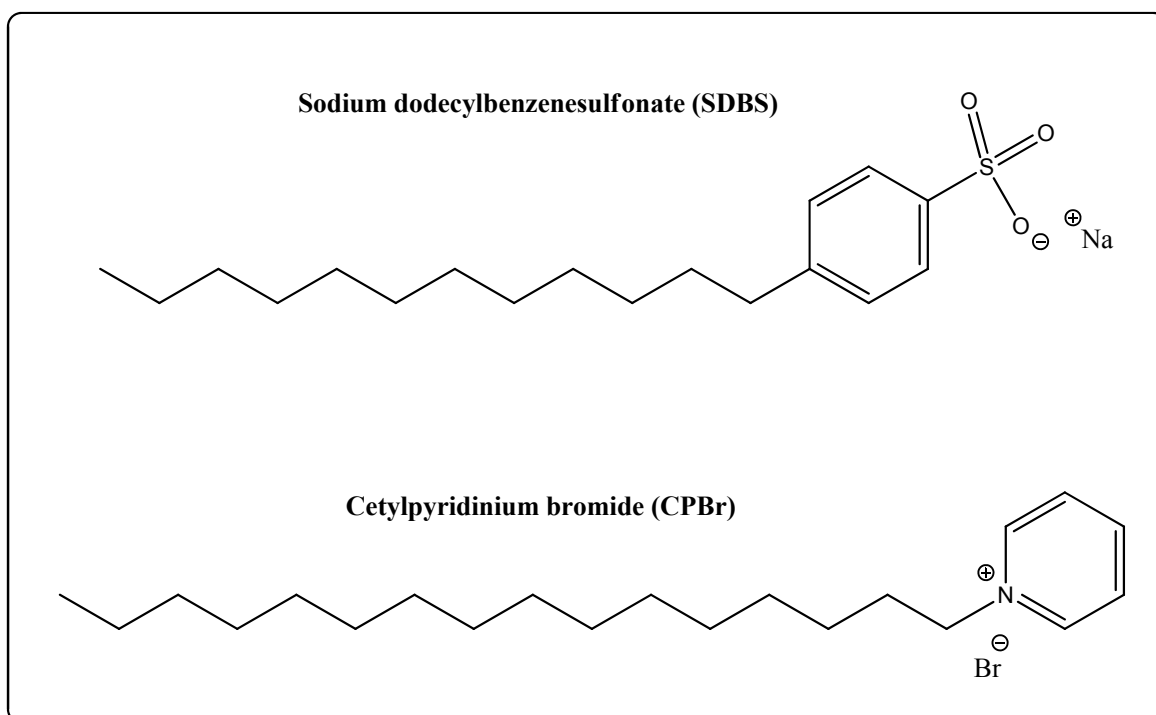


**Fig. 19: Structures of SDBS and CPBr**

The aromatic ring in the surfactant can play yet one more role if it contains nitrogen. A dynamic coating of the capillary wall is the result and hence a reversed electroosmotic flow is induced. Again, a high percentage of organic modifier prevents the formation of micelles. Such a cationic surfactant is cetylpyridinium bromide (CPBr) [95] (figure 19) that

interacts with the PAHs through solvophobic association and  $\pi$ - $\pi$  interactions so that that the largest PAHs have the greatest mobility and hence migrate last (figure 20).

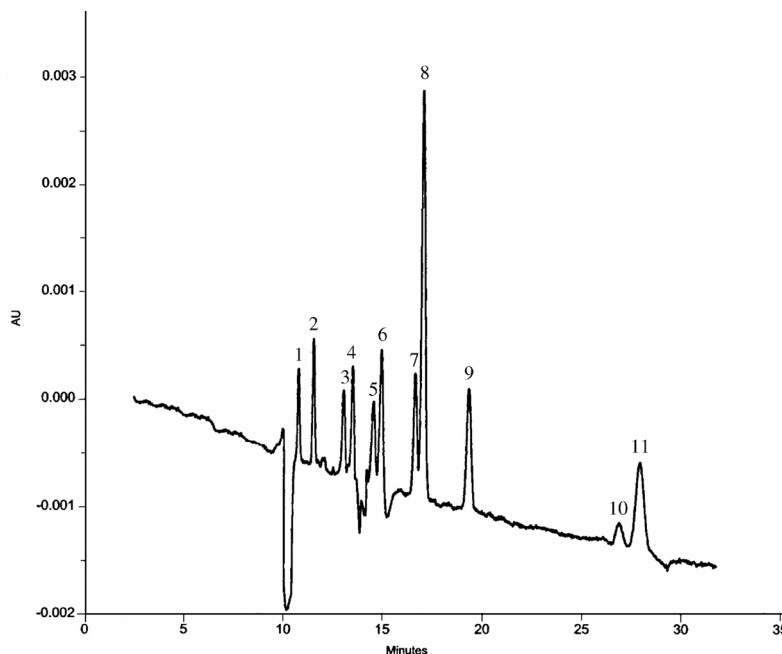


**Fig. 20: Electropherogram of PAHs separated by hydrophobic interaction and  $\pi$ - $\pi$  interactions with CPBr.** Electrolyte: 20 mM acetate, 50% MeCN, 40 mM CPBr, pH = 4.0. Voltage = -25 kV. Injection: 0.5 psi, 5 s, hydrodynamically. Wavelength = 254 nm. Peak identification: 1: nitrobenzene, 2: acetophenone, 3: benzophenone, 4: naphthalene, 5: acenaphthalene, 6: acenaphthene, 7: anthracene, 8: phenanthrene, 9: pyrene, 10: perylene, 11: benzo[*a*]pyrene. ([95], reprinted with permission of Taylor and Francis)

### 3.4 Separation through charge-transfer complexation with planar organic cations

A completely new approach to interactions of PACs with ionic compounds was described in 1997 [96]. As separations in nonaqueous media are desirable for solubility reasons of nonpolar and highly hydrophobic compounds, an ionic compound was needed capable of forming complexes with the analytes in 100 % organic solvents. The tropylium ion and the 2,4,6-triphenylpyrylium ion (figure 21) [96], both known to exhibit charge-transfer properties with electron rich compounds, work well as such carrier cations. The organic solvent was acetonitrile, being chemically inert to the organic cations and possessing a sufficient solvent strength for the carrier compounds. Separations of a mixture of 20 PAHs were performed using 30-40 mM of the planar organic cations. The PAHs were separated

according to their size, the largest analytes showed the shortest migration time due to their stronger interaction with the carriers. Some comigrations were observed for several compounds with both cations but mixtures of the two carrier ions improved the resolution, the best being an 80:20 mixture of triphenylpyrylium/tropylium ions with comigration of only two PAH isomer pairs (benz[*a*]anthracene/chrysene and anthracene/phenanthrene). Interactions of the organic cations with the negatively charged capillary wall led to variations in the EOF and therefore poor reproducibility. This problem was solved by rinsing the capillary between runs with an acidic solution to protonate the silanol groups.

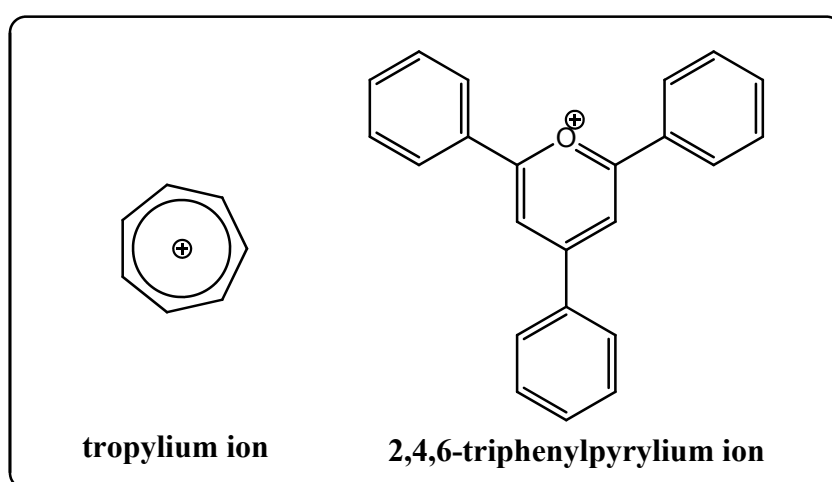


**Fig. 21: Tropylium ion and triphenylpyrylium ion**

The analytes gain higher electrophoretic mobility at higher carrier cation concentration as was revealed in a detailed investigation of the influence of the concentration of substituted pyrylium ions, the counter ion and the number of phenyl substituents [97]. Higher concentrations than 40 mM 2,4,6-triphenylpyrylium provided better resolution but led to an unstable baseline so that the analysis of the electropherogram became difficult. The identity of the counter ion had no effect on the separation as long as the carrier ion/counter ion completely dissociate in acetonitrile. The number of phenyl substituents on the carrier ion displayed a large effect on the electrophoretic mobility of the PAHs. Pyrylium ions with one to four phenyl substituents were tested and the maximum mobility for the analytes was obtained with three groups. Surprisingly, the mobility decreased when four phenyl groups were attached to the pyrylium ring and this was explained by steric

hindrance: four phenyl groups prohibit planarity of the pyrylium ion, leading to a weaker interaction with the analytes.

### 3.5 Separation through distribution into charged and uncharged cyclodextrins

Cyclodextrins (CD) are neutral cyclo-oligosaccharidic sugars of a cylindrical shape (figure 22). They possess a hydrophobic cavity whose size depends on the number of glucopyranose units in the ring. Their exterior is hydrophilic so that they show quite good solubility in aqueous media. Due to their hydrophobic cavity, they can form inclusion complexes with a variety of compounds. This effect is widely used in chromatography where cyclodextrin-containing phases are utilized for, i.a., the separation of enantiomeric compounds. This is the main use also in CE but occasionally they find use as additives in MEKC to influence the separation in the tertiary system buffer/micelles/cyclodextrins.

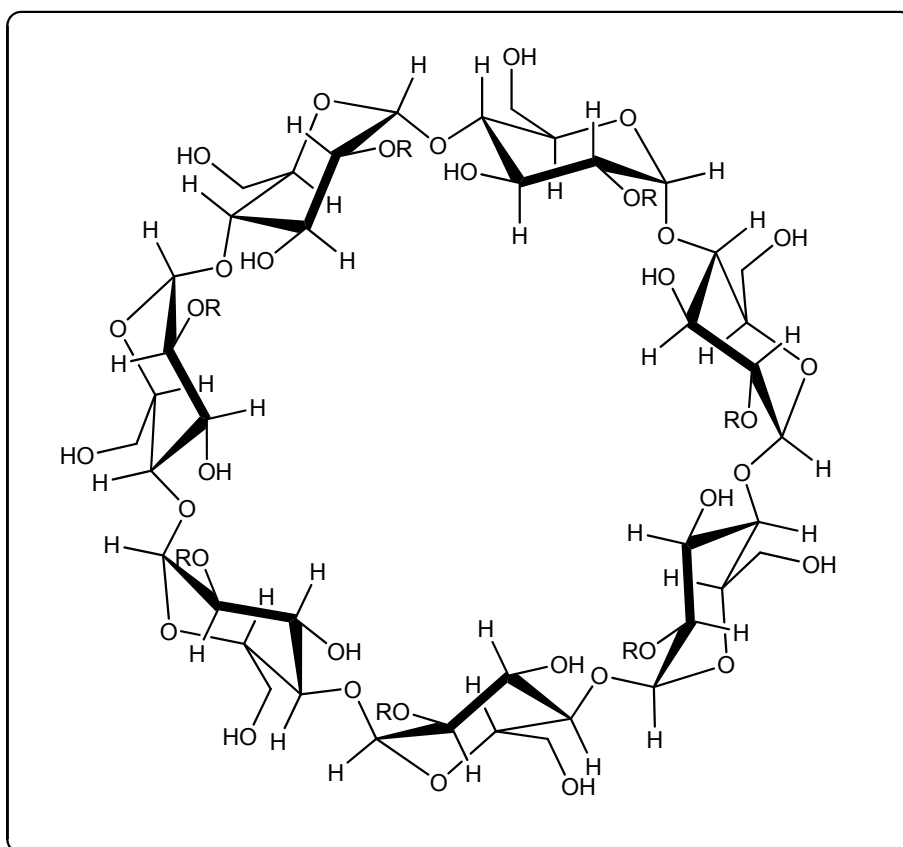


**Fig. 22:  $\beta$ -Cyclodextrin (with  $R = H$ ) with 7 glucopyranose units (carboxymethyl- $\beta$ -cyclodextrin:  $R = CH_2COO^-$ )**

The first separations of neutral PAHs aided by CDs in CE involved a dual CD system containing a native uncharged CD and a derivatized charged CD [98]. The latter (carboxymethyl- $\beta$ -cyclodextrin) operated as carrier for the neutral PAHs, imparting the necessary electrophoretic mobility to the PAHs. The native uncharged cyclodextrin in the buffer (hydroxypropyl- $\beta$ -cyclodextrin) provided a secondary pseudostationary phase. The analytes were thus distributed between retaining neutral CDs and the electrophoretically mobile charged CDs, thus increasing the selectivity of the separation. Anthracene and pyrene could easily be separated within five minutes. The separation efficiency with the dual CD phase was much higher than the one obtained with SDS-MEKC. Furthermore, tertiary CD phases can lead to even better separations [98]. A tertiary phase consisting of  $\beta$ -CD (7 glucose units),  $\gamma$ -CD (8 glucose units) and the charged carrier carboxymethyl- $\beta$ -CD enabled four PAHs (anthracene, pyrene, chrysene and benzo[*a*]pyrene) to be separated in 10 minutes, impossible by standard SDS-MEKC.

The size of the cavity and thus the interaction with analytes depends on the CD. The dual cyclodextrin phase provided an excellent selectivity and was especially useful for the separation of neutral isomeric compounds that do not differ in polarity and hence cannot be separated by standard MEKC [99]. Variations of the mixture of CDs allowed unique selectivities to be obtained with good resolution for the separation of alkyl substituted anthracenes. The retention of the PAHs could be controlled by the concentration and type of the CDs and it was possible to separate six anthracenes (anthracene, 1-methyl-, 2-methyl-, 9-methyl-, 9,10-dimethyl- and 2-ethylanthracene). A separation of the same compounds with MEKC is not possible due to their very similar polarity.

Attempts to use mixtures of neutral and charged CDs for differential partitioning of the analytes led to the realization that the migration time of the analytes is very difficult to predict as the separations vary dramatically when the CD phase composition is changed [100]. Hence each CD mixture has to be tested empirically for its applicability in a certain separation. An aqueous borate buffer containing methyl- $\beta$ -cyclodextrin and sulfobutyl- $\beta$ -cyclodextrin showed baseline separation for a mixture of ten of the EPA PAHs. The applicability to real world samples was demonstrated by separating the PAHs of an artificially contaminated soil sample (figure 23) [101].



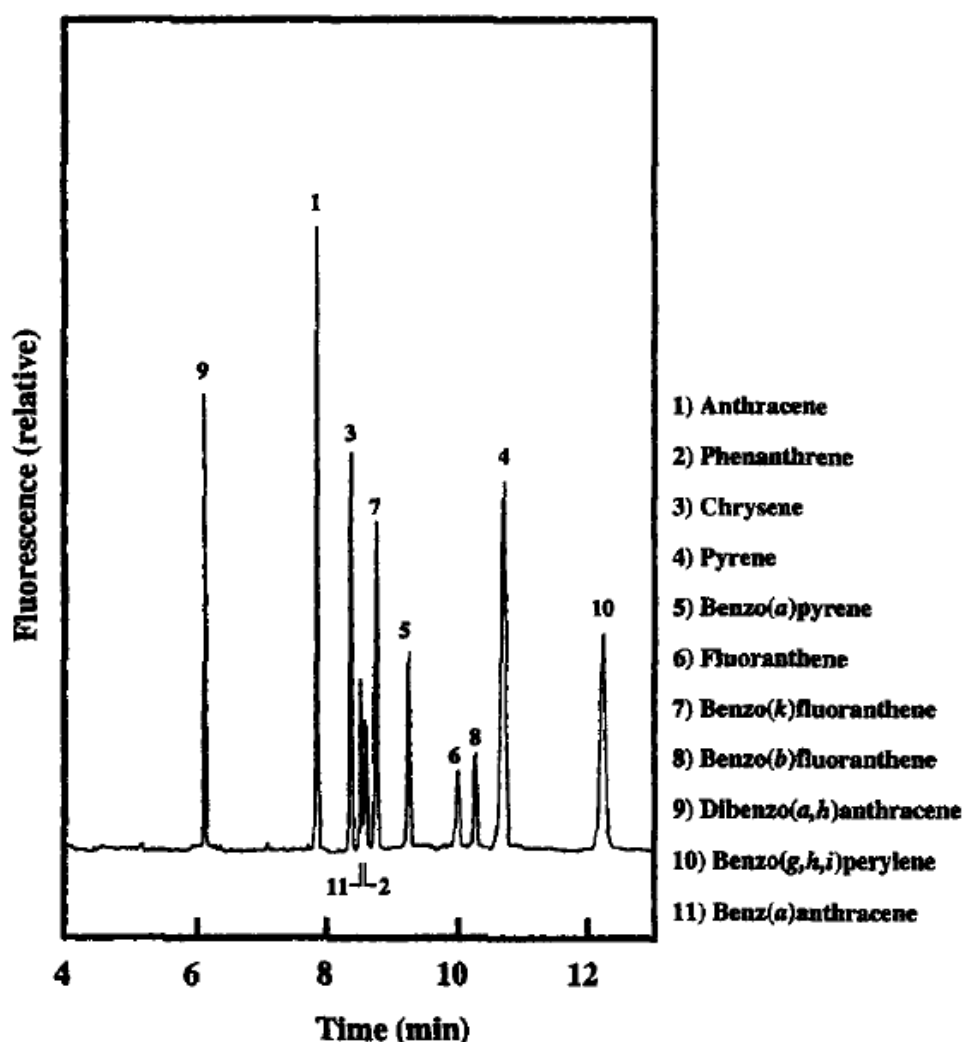


**Fig. 23:** CE separation of soil PAH mixture after Soxhlet extraction using a M- $\beta$ -CD/SB- $\beta$ -CD modified buffer. Soxhlet extract of soil in dichloromethane diluted in 60% methanol-water was injected into the capillary containing 20 mM methyl- $\beta$ -CD and 25 mM sulfobutyl- $\beta$ -CD in 50mM borate pH 9.1 at 30°C. Applied potential= 30 kV. ([101] reproduced with permission of Wiley VCH)

This mixed CD phase can resolve all 16 EPA priority pollutants in under 20 minutes with detection by either UV absorption or laser induced fluorescence (figure 24) [102]. The efficiency was better than 100 000 theoretical plates. This made it possible to separate the PAHs in a real contaminated soil sample that was favored over the artificially contaminated one used previously as more PAHs and matrix interferences occur. After being isolated through extraction with supercritical CO<sub>2</sub>, the extract was collected in a mixture of methanol and dichloromethane and then diluted in methanol/water. It was

directly injected und analyzed by CE. The separation provided very high resolution even for isomers with similar structure like benzo[*b*]fluoranthene and benzo[*k*]fluoranthene.

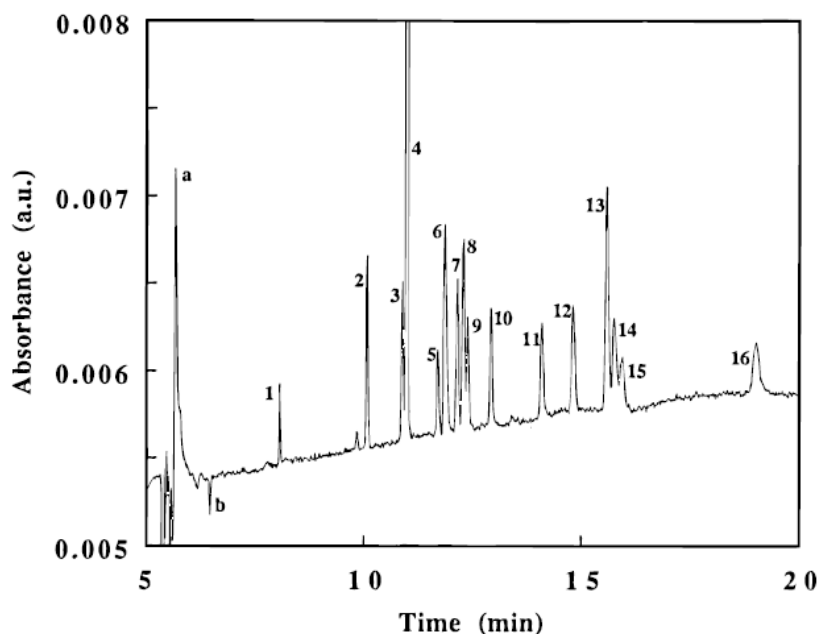


**Fig. 24: Electropherogram of a mixture of 16 EPA priority PAHs, using 35 mM sulfobutyl- $\beta$ -CD, 15 mM methyl- $\beta$ -CD. 50 mM borate buffer, pH 9.2, 30 °C, 30 kV, absorbance detection at 254 nm. Peaks a and b indicate methanol and dichloromethane. 1: dibenz[*a,h*]anthracene, 2: naphthalene 3: fluorene, 4: anthracene, 5: acenaphthene, 6: acenaphthylene, 7: chrysene, 8: phenanthrene, 9: benz[*a*]anthracene, 10: benzo[*k*]fluoranthene, 11: benzo[*a*]pyrene, 12: fluoranthene, 13: benzo[*b*]fluoranthene, 14: indeno[1,2,3-*cd*]pyrene, 15: pyrene, 16: benzo[*ghi*]perylene ([102] reproduced with permission of the American Chemical Society)**

Even this good separation can be improved as was shown with a ternary CD mixture [103]. Sulfobutyl- $\beta$ -cyclodextrin and methyl- $\beta$ -cyclodextrin provided the basis and other CDs were added to this buffer. Surprisingly the best results were obtained when the small  $\alpha$ -CD - which is not expected to form inclusion complexes with the large PAHs - was included while the large  $\gamma$ -CD did not show any effect. This optimized ternary buffer was used for samples obtained by solid phase microextraction. The first attempt to combine this preconcentration technique with CE showed very good results with UV detection. Despite the low concentration of the analytes in the sample (lower ppb range), they were extracted by SPME and redissolved in only 5-10 nL of methanol so that the effective concentration was high.

The CD based buffers can be combined with the charged surfactant DOSS (see above) for separating PAHs by solvophobic interactions [93]. A charged (sulfobutylether- $\beta$ -CD) and a neutral (hydroxypropyl- $\beta$ -CD) CD were added to the electrolyte buffer, influencing the separation of the PAHs by making possible the formation of completely different solvophobic association complexes with the DOSS on the one hand and with the cyclodextrins on the other hand. Because the selectivity of the analytes towards DOSS and the cyclodextrins is very different, the efficiency of the mixed mode separation was much better than that of the individual phases alone. An optimized running buffer led to a baseline separation of all 16 EPA PAHs in 35 minutes (figure 25).

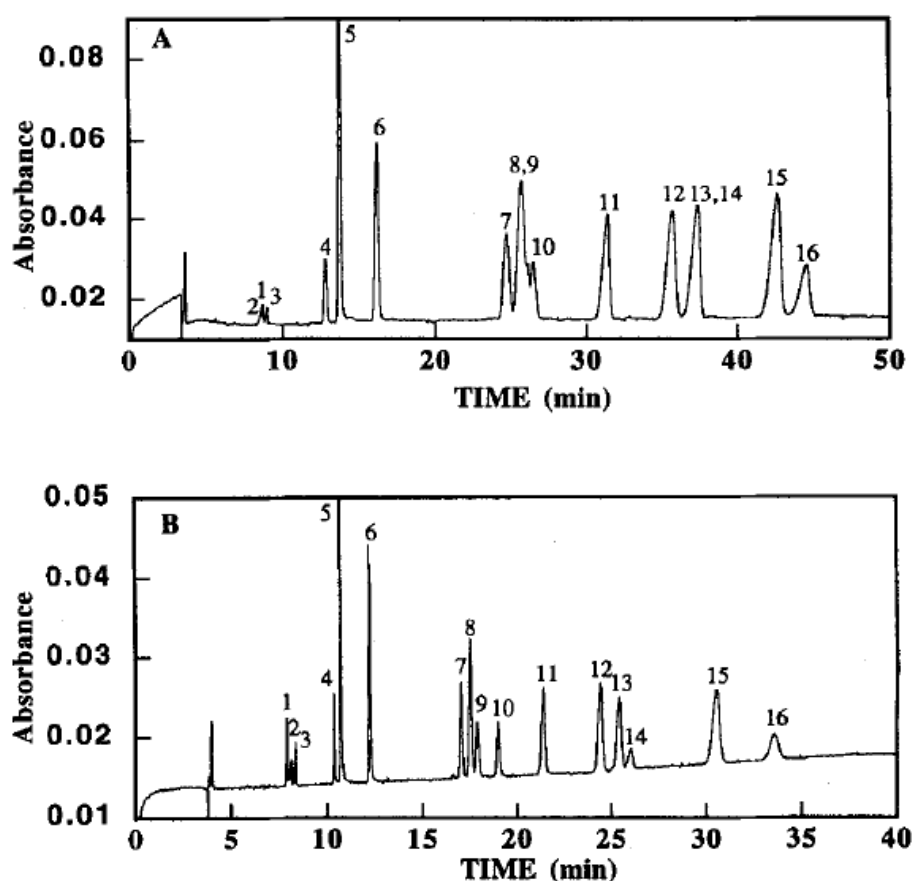


**Fig. 25: Separation of the 16 PAHs using two pseudo-stationary phases, DOSS and sulfobutyl- $\beta$ -CD, in mixed-mode EKC ((A) without hydroxypropyl- $\beta$ -CD and (B) with 5 mM hydroxypropyl- $\beta$ -CD). Electrolyte: 22.5 mM DOSS, 15 mM sulfobutyl- $\beta$ -CD, 15% ACN, and 6 mM borate, pH 9. Pressure injection for 3s at 0.5 psi and voltage of 20 kV. Peak identification: 1: naphthalene, 2: acenaphthene, 3: acenaphthylene, 4: fluorene, 5: anthracene, 6: phenanthrene, 7: chrysene, 8: benz[*a*]anthracene, 9: fluoranthene, 10: pyrene, 11: benzo[*k*]fluoranthene, 12: benzo[*a*]fluoranthene, 13: benzo[*a*]pyrene, 14: dibenz[*a,h*]anthracene, 15: indeno[1,2,3-*cd*]pyrene, 16: benzo[*ghi*]perylene ([93], reproduced with permission of Wiley VCH)**

The principle of using ionized CDs was demonstrated also with native  $\beta$ -CD which is uncharged at neutral and acidic pH. Since it contains weakly acidic secondary hydroxyl groups with a  $pK_a$  value of 12.1, it can be deprotonated at a pH above ca. 11.2. No electrophoretic mobility of the analyte PAHs occurred below pH 11.2 because of the nonionized secondary hydroxyl groups, and the transport is thus effected only by the EOF leading to complete comigration [104]. Electrophoretic mobility was observed at higher pH. The partition of the analytes into the CDs and the strength of the inclusion complexes led to a separation of the PAHs. Best results were obtained at a pH of 12.9, higher pH values caused a broadening of the peaks.

The separation of PAHs based on the distribution into CDs was put to good use in an unusual setting [105]. When PAHs need to be analyzed under extraterrestrial circumstances, simple and miniaturized systems must be used and here electrophoretic instruments possess an advantage. Operating without complex parts like pumps or a gas supply, as needed for HPLC and GC, they can easily be miniaturized. One field where these miniaturized “labs-on-a-chip” are used is aeronautic and extraterrestrial space research. The environmental conditions in this field are particularly adverse, so research has concentrated on analysis techniques that are robust and easy to run. The separation of PAHs using cyclodextrin modified CE on the Mars Organic Analyzer (MOA), a portable microchip CE instrument for amino acid analysis and extraterrestrial organic carbon detection, has been demonstrated [105]. The detection system of the MOA was laser induced fluorescence at 404 nm. With the optimized running buffer containing a charged (sulfobutyl- $\beta$ -CD) and a neutral CD (methyl- $\beta$ -CD) in a carbonate buffer, a mixture of seven PAHs found in extraterrestrial matter and two terrestrial PAHs was successfully separated. The method works for samples relevant to planetary exploration. Thus the PAHs of a Mars analogous sample from the Atacama Desert, containing 9,10-diphenylanthracene, anthracene, anthanthrene, fluoranthene, perylene and benzo[ghi]fluoranthene, could be nicely separated (figure 26).

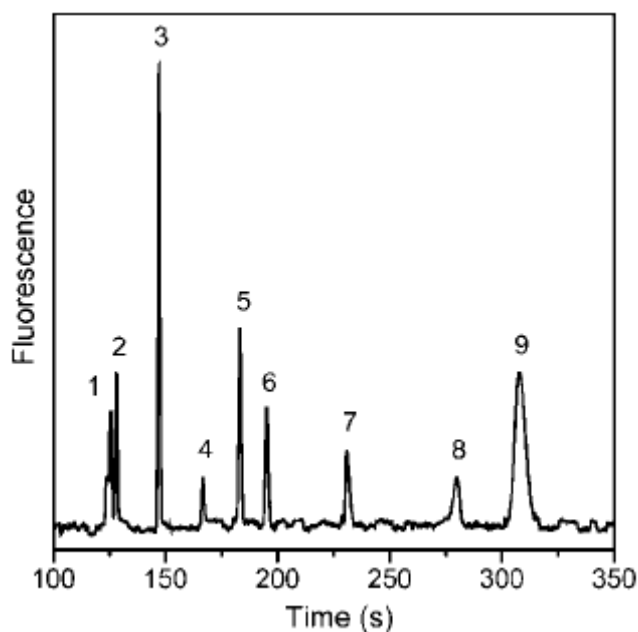


**Fig. 26: Separation of the Mars nine PAH standard by distribution into cyclodextrins.** Peak identification: **1:** 9,10 diphenylanthracene, **2:** dibenzo[*b,def*]chrysene, **3:** anthracene, **4:** anthanthrene, **5:** benzo[*a*]pyrene, **6:** benzo[*j*]fluoranthene, **7:** fluoranthene, **8:** perylene **9:** benzo[*ghi*]fluoranthene. Running buffer contains 10 mM sulfobutyl- $\beta$ -CD, 40 mM methyl- $\beta$ -CD, 5 mM carbonate buffer, pH 10, 20 °C. ([105], reproduced with permission of the American Chemical Society)

### 3.6 Separation through distribution into resorcarenes and calixarenes

Resorcarenes are macrocyclic compounds containing four alkylidene bridged resorcinol units (figure 27) and can easily be synthesized by condensing resorcinol with aldehydes. These compounds are known to form host-guest complexes with a variety of molecules and can be used as carrier molecules in CE separations [106]. The electrophoretic mobility of the host-guest complex is provided by the four negative charges in the macrocycle that arise through deprotonation of four hydroxyl groups. The stable structure of the tetraanion allows high concentrations of organic media in the buffer. A variety of substituted resorcarenes and the closely related macrocyclic compound calix[4]arene show interaction with PAHs [106]. Unsubstituted calix[4]arene and methyl substituted resorcarene show very poor selectivity and low capacity factors for PAHs. The analytes migrate unresolved shortly after the EOF, thus showing no host-guest interactions. Resorcarenes with longer alkyl chain or aromatic substituents lead to much improved results and twelve PAHs can be resolved (figure 28). The migration order of the analytes is similar to that obtained in

reversed phase chromatography. Therefore the alkyl substituents R seem to be the main contributors to the separation whereas the macrocycle itself mainly serves as a platform that carries and stabilizes the charges needed for the electrophoretic separation.

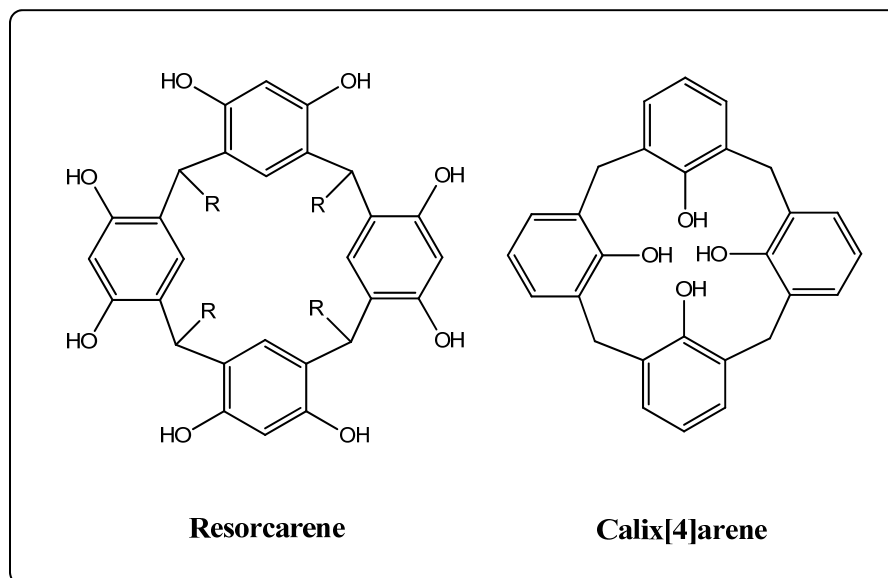


**Fig. 27: Carrier molecules resocarene (R=CH<sub>3</sub>, C<sub>5</sub>H<sub>11</sub>, C<sub>11</sub>H<sub>23</sub>, p-chlorophenyl) and calix [4]arene**

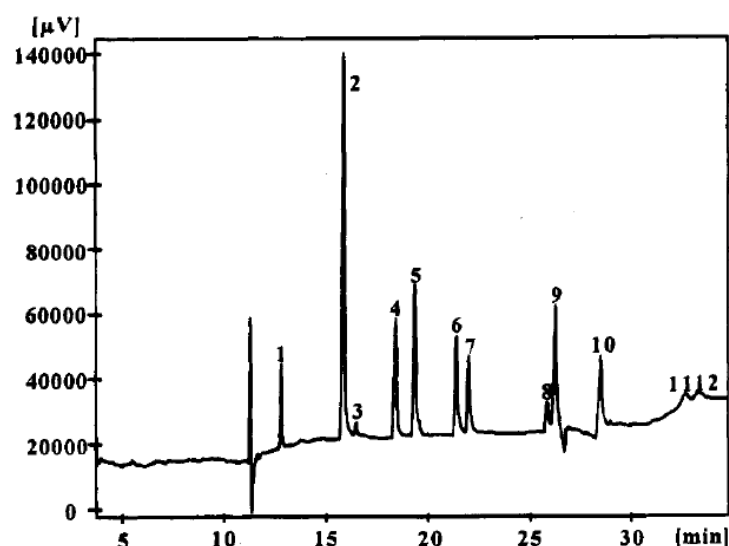


**Fig. 28: Separation of twelve PAHs with undecyl modified resorcarene (R=C<sub>11</sub>H<sub>23</sub>).** Electrolyte: 5.8 mM modified resorcarene, 5.0 % (v/v) acetonitrile, 6 M urea, pH = 13.25; capillary length 76 cm (62 cm to detector), i.d. 50 μm; injection hydrostatic 10 cm, 30 s; detection UV at 260 nm; voltage 20 kV; current 6 μA. Peak identification: **1:** naphthalene, **2:** phenanthrene, **3:** anthracene, **4:** fluoranthene, **5:** pyrene, **6:** triphenylene, **7:** chrysene, **8:** benzo[*k*]fluoranthene, **9:** benzo[*a*]pyrene, **10:** indeno[1,2,3-*cd*]pyrene, **11:** anthanthrene and **12:** benzo[*ghi*]perylene. ([106], reproduced with permission of the American Chemical Society)

Pure calix[4]arene was of no use but the host-guest interaction with PAHs were stronger with calixarenes derivatized with a carboxyethyl group (figure 29) [107]. This also increased the electrophoretic mobility of the carrier/analyte complex because the carboxylic groups are deprotonated under basic conditions and increase the negative charge of the compound. Derivatized calix[n]arenes with different ring sizes ( $n = 4-8$ ) were used for the separation of PAHs and polar substituted PAHs. The best resolution was obtained with the intermediate sized carboxyethyl-calixarenes with five to seven rings in the macrocycle. The smaller carboxymethyl-calix[4]arene probably possess a too small cavity for complexing with the PAHs. The poor resolution of the larger calixarenes was probably due to an unsuitable fit of the analytes. Low capacity factors were observed for all of the calixarenes but this drawback could be compensated by the high charge to mass ratio and the resulting high electrophoretic mobility of the host-guest complexes.

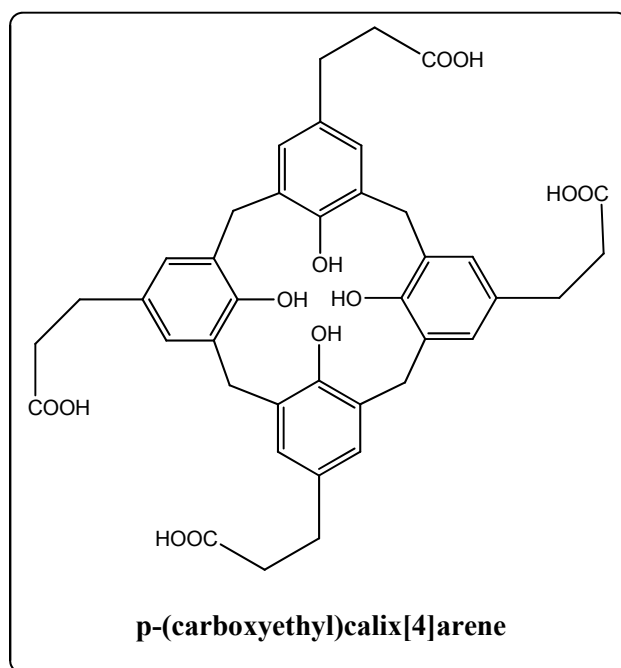


**Fig. 29: Structure of the carrier p-(carboxyethyl)calix[4]arene**

### 3.7 Conclusion

Different approaches were performed to separate PACs by capillary electrophoresis with charged buffer additives. However, the focus was mainly directed to the separation of the EPA-PAHs and only little efforts were done to separate other fuel related compounds or

real world samples. Indeed the presented methods are helpful to separate PACs of different ring size and different parental structure, but most of these methods can only provide baseline separation of these standard compounds, while the separation of compounds with different degrees of alkylation are awaited to be problematic and are hence not presented in the studies. Especially in case of complex PASH real world samples, where a large variety of alkylated dibenzothiophenes occur, the presented methods will fail. Comigration for most of the alkylated compounds is expected. Due to this reason, a further electrophoretic method for the separation of such compounds, basing on a different separation principle besides the interaction with buffer additives had to be found.

First reports of a completely different capillary electrophoretic method for the analysis of PASHs, basing on the derivatization of the sulfur atom, date back to 1998 where VALENZUELA demonstrated the separation of sulfonium and thiophenium ions, including the methylated forms of benzothiophene and dibenzothiophene [108,109]. No further research was done in this field until KÜNNEMEYER [110] introduced the CE separation of fuel related PASH standard compounds after derivatization in his diploma thesis in 2005. This research was picked up in the diploma thesis of NOLTE [23] afterwards and led to the successful separation of the PASH fraction from a desulfurized diesel fuel [111].



## **4 Scope of work**

One of the main advantages of the capillary electrophoretic separation of PASHs is that volatility of the compounds is not an issue. This leads to the assumption, that CE might be especially advantageous for the analytics of high boiling fuel fractions. In addition, the high resolution power of CE might provide better results than RP-HPLC, which lacks resolution power to separate complex samples, like PASHs, from fossil fuels.

In this work, the research on the capillary electrophoretic method for the separation of PASHs based on the derivatization of the sulfur atom of the analytes to produce charged species, is continued. Earlier studies revealed that this technique is especially useful for the separation of compounds with a different degree of alkylation and hence expected to be very useful for the separation of PASH real world samples [23]. The investigation of applicability of this method for the analysis of high molecular PASHs and PASH real world samples is the major aim of this work. For this reason, the work is split into two parts.

In the first part of the work the separation is demonstrated for different petroleum based standard compounds mainly by CE-UV. Different buffer additives, like cyclodextrins, are tested and comparisons to other separation methods like HPLC, GC and MEKC are done. Furthermore, capillary electrophoresis coupled to time-of-flight mass spectrometry (CE-TOF MS) is introduced for the analysis of standard PASHs.

The second part of the work concentrates on the separation of PASH-fractions from different desulfurized and non-desulfurized fuels and will demonstrate to what extent CE methods can be used for the analysis of such samples. The main focus within this part lies on the separation of PASH fractions by help of aqueous and nonaqueous capillary electrophoresis coupled to TOF MS to demonstrate the advantages of this coupling instead of UV. The results are compared with GC-MS and Orbitrap MS measurements.

## **5 Experimental introduction**

Within this work a variety of different analytical methods are used for the analysis of fossil fuel related PASHs. Three different techniques are employed: CE-UV, MEKC and CE-TOF MS. As the focus of this work lies in the capillary electrophoretic separation of PASHs, the experimental parameters for these methods are provided in the following. The experimental data for further techniques like GC, HPLC and Orbitrap MS will not be given in detail here but provided directly in the chapter dealing with these methods and in the appendix.

### **5.1 CE instrumentation**

#### **5.1.1 CE-UV and MEKC**

The used CE system for the CE-UV and MEKC measurements is a *PrinCE-Crystal 560* modul (*Prince Technologies B.V.*, Emmen, The Netherlands), which consists of the high voltage supply and the autosampler. The detector is a separate *Lambda 1010* UV-Vis detector from *Bischoff Chromatography*, Germany. Both of the modules are triggered by the software *WinPrince 6.0*, while data handling is performed with the *WinDAX 6.0* software from *Van Mierlo Software Consultancies*. For all experiments bare fused-silica capillaries (*Polymicro Technologies*, Phoenix, USA) with an internal diameter (i.d.) of 75  $\mu\text{m}$  were used. The effective length of the capillary was 56 cm, with a total length of 81 cm. The separations were performed at room temperature with a normal polarity between 20 and 30 kV, depending on the running buffer. Hydrodynamic injection was used by applying a pressure of 55 mbar for 3 s. The absorption wavelength was adjusted to 215 nm for the derivatized PASHs and 254 nm for the MEKC experiments.

Conditioning of new capillaries was done by rinsing with 1 M sodium hydroxide solution for 5 min, followed by electrolyte buffer for 30 min. In between the measurements, the capillary was reactivated by rinsing with 1 M sodium hydroxide for 1 min, 0.1 M sodium hydroxide for 1 min, and electrolyte buffer for 3 min.

### 5.1.2 CE-TOF MS

The measurements were performed on an *Agilent 7100* Capillary Electrophoresis System controlled by the software *ChemStation B.04.02*. The CE was coupled to an *Agilent 6520 Accurate-Mass Q-ToF MS* controlled by the *Mass Hunter B.03.01 software*. The flow of sheath liquid was operated by an *Agilent Isocratic Pump 1260*. For the CE-TOF MS fused-silica capillaries with an outer diameter of 364  $\mu\text{m}$  and an inner diameter of 50  $\mu\text{m}$  (*Polymicro Technologies*, Phoenix, AZ) were used. The length of the capillary for aqueous CE was 59.5 cm, while the length of the capillary used for NACE was 74.5 cm.

## 5.2 Procedures and conditions

### 5.2.1 CE-UV

For the background electrolyte, an exactly weighed amount of phosphoric acid 85 % was diluted with water and titrated with 1 M sodium hydroxide to exactly pH 2.15 afterwards. The buffer was diluted with distilled water to a total concentration of 50 mM. For further modifications, 10 mL of the stock solution was taken and isopropanol or cyclodextrins were added depending on the separation. The electrolytes were stored at 7 °C.

### 5.2.2 MEKC-UV

The MEKC-UV-measurements were performed with a buffer containing 100 mM SDS and 20 mM borate at a pH of 8.0. Cyclodextrins and organic modifiers were added as required.

### 5.2.3 CE-TOF MS

The aqueous CE-MS buffer was prepared by dissolving 300 mM acetic acid in water and titration to pH 4.0 with ammonia. Afterwards the buffer was mixed with isopropanol (1:1).

As nonaqueous CE-background electrolyte a solution of 4 % acetic acid in methanol with addition of 60 mM ammonium formate was used.

The sheath liquid for both aqueous and nonaqueous CE-TOF MS was 1 % acetic acid in a mixture of isopropanol and water (50:50). The solution was pumped into the CE/MS interface with the isocratic pump at a flow rate of 4.5  $\mu\text{L}/\text{min}$ . The pressure of the

nebulizer gas was 2 psi for the first 20 seconds and then increased to 6 psi to avoid air being sucked into the inlet when sample and buffer vials were changed. Dry gas was applied at 5 L/min at a temperature of 325 °C. The Agilent Q-ToF MS was operated in positive ion mode, with a mass scan range from 100 to 1700 m/z (Low Mass Range Mode).

### 5.3 Chemicals and reagents

All of the chemicals used for this work were of analytical grade. Standards and reference compounds were synthesized in the working group as far as they were not commercially available. A variety of 4,6-dialkylated dibenzothiophenes were synthesized during these studies. The corresponding synthesis instructions can be found in the appendix.

### 5.4 Ligand exchange chromatography

Modern transportation fuels contain less than 10 ppm sulfur. As this sulfur content is distributed over possibly hundreds of PASH compounds, single compounds are only present in very low concentrations. Especially when using CE coupled to a UV detector, the PASHs have to be concentrated to be able to analyze them. This can be achieved by using ligand exchange chromatography (LEC) which is usually applied in HPLC. To enable a sufficiently high concentration of PASHs for CE-UV, the HPLC-LEC method was adapted to open tubular column chromatography. The stationary phase used for the LEC contained palladium(II) ions immobilized on silica gel through mercaptopropano groups [18]. When a fossil fuel sample is brought onto the stationary phase, sulfur containing compounds coordinate to the palladium, while non-sulfur compounds can be washed off the column (figure 30). The PASH fraction can be released from the column by adding a competitive ligand (isopropanol) to the solvent. The exact procedure for the concentration of the PASHs with LEC is described in the following:

Ten grams of Pd-MPSG are washed into a column of 3 cm i.d. with cyclohexane. One milliliter of each diesel fuel fraction is applied and non-sulfur compounds are eluted with 150 mL of a cyclohexane-dichloromethane mixture (9:1 v/v). The PASH fractions are eluted by 250 mL cyclohexane-dichloromethane mixture (7:3 v/v), containing 1 vol.% of isopropanol. After removing the solvent on the aspirator, the residues are dissolved in 1.5 mL of 1,2-dichloroethane and stored in the refrigerator.

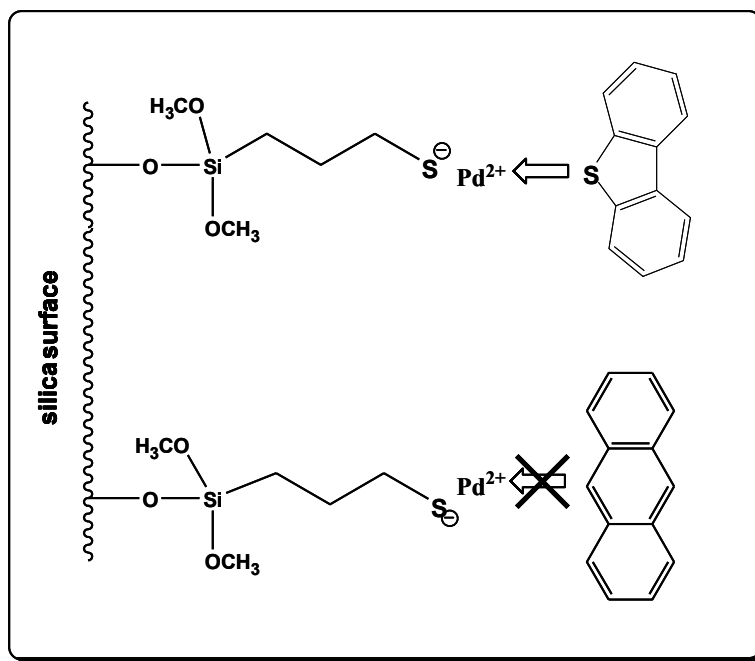


Fig. 30: Schematic pricipel of Pd-mercaptopropano silica gel

### 5.5 Derivatization of the PASHs

One problem that occurs when PASHs are separated by CE is that they do not contain a charge. However, charged analytes are needed for the CE separation to gain electrophoretic mobility. Unlike e.g. some nitrogen compounds, PASHs cannot easily be protonated or deprotonated. A direct CE separation is hence impossible. Nevertheless, these compounds can be electrophoretically separated, for example, by interactions with charged buffer additives as described for PACs in chapter 3.

PASHs contain one heteroatom in the structure which can be taken advantage of for the introduction of a charge into the molecule. The sulfur atom is incorporated into the aromatic system, but this position is not completely unreactive. The sulfur can be attacked by strong electrophiles like carbenium ions, which makes the position attractive for derivatization to impart electrophoretic mobility to the compounds. Two different derivatization methods were used during this work and will be presented in the following.

### 5.5.1 Methylation

The methylation reaction is based on the method of ACHESON and HARRISON where the sulfur atom is methylated to the corresponding thiophenium ion [112]. For the methylation of standard compounds, 2.0 mg of each PASH were dissolved in 2 mL of 1,2-dichloroethane and 100  $\mu$ L of methyl iodide was added. The vial was wrapped with aluminum foil to avoid decomposition through UV light. Sixty milligrams of silver tetrafluoroborate was added and the mixture stirred overnight. The precipitated silver iodide was removed by filtration and washed with 1,2-dichloroethane. The thiophenium salts were obtained by evaporation of the filtrate. Finally, the salts were dissolved in 1.5 mL acetonitrile and kept in the refrigerator at  $-18\text{ }^{\circ}\text{C}$ . The products were checked by mass spectrometry. For CE-UV measurements, the samples were dissolved 1:10, for CE-MS measurements, the samples were dissolved 1:1000. The reaction is schematically described in figure 31.

The PASHs of the different diesel fuel fractions were isolated by means of LEC as described before. For derivatization, 100  $\mu$ L of methyl iodide and 60 mg silver tetrafluoroborate were added to each sample. The mixtures were stirred over night and then filtered. Finally, the solvent was removed on the aspirator and the residues dissolved in 1.5 mL of acetonitrile and kept in the refrigerator at  $-18\text{ }^{\circ}\text{C}$ . For CE-UV measurements the samples could be used directly, for CE-MS measurements the samples were diluted 1:10.

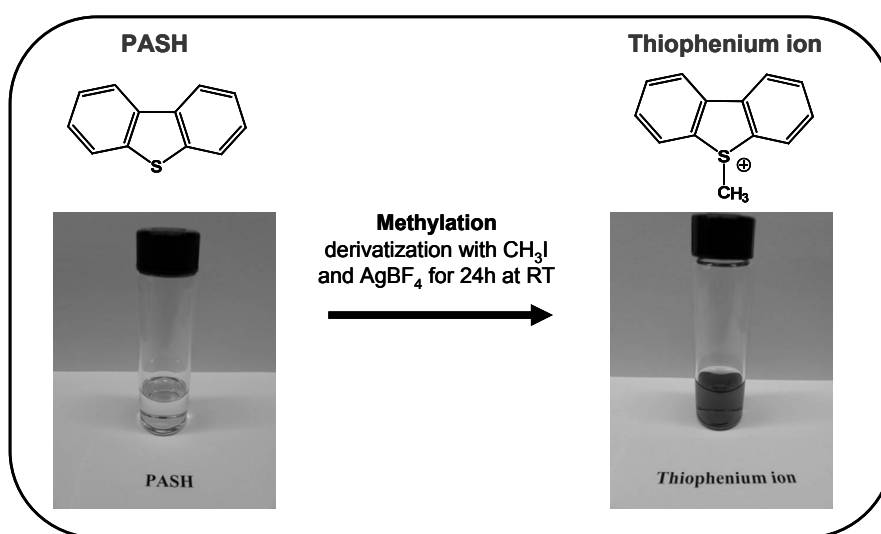


**Fig. 31: Methylation reaction for the formation of methyl thiophenium ions.**

### 5.5.2 Phenylation

The phenylation reaction is based on studies of KITAMURA who prepared S-phenyl-benzothiophenium triflates by treating benzothiophene with diphenyliodonium triflate in the presence of a catalyst [113, 114] (figure 32). For the derivatization of standard compounds by this method, 2 mg of each thiophene was dissolved in 2 mL of acetonitrile and 45 mg of the phenylation reagent diphenyliodonium triflate was added. After stirring for 30 min, a catalytic amount of copper acetate was added. The solvent was removed and the mixture was heated to 160 °C for 30 min under stirring. Finally, the reaction products were dissolved in 1.5 mL acetonitrile and stored in the refrigerator at -18 °C. The phenylated products were checked by MS.

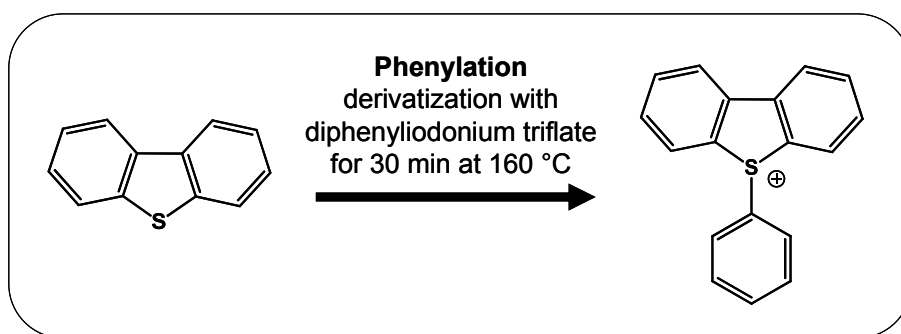


**Fig. 32: Phenylation reaction for the formation of phenyl-thiophenium ions.**

## 6 Capillary electrophoretic separation of standard compounds

Because the scope of this work was the separation of the PASHs found in fuels, the basic principles had to be investigated by separating standard compounds prior to dealing with real world samples. Some of this work has already been done in previous studies in our research group. The separation of PASHs with different ring sizes, different degrees of alkylation and different alkylation patterns was demonstrated [23,110]. Within this work, some of these results were used for further studies. In the following chapter the CE separation of PASHs in comparison to HPLC will be discussed as well as CE separations with the help of cyclodextrins as buffer additives and studies on the correlation between the molecular volume and the migration time. MEKC as well as aqueous and nonaqueous CE-TOF MS will be introduced as a further electrophoretic method for the separation of PASHs.

### 6.1 CE separation of fuel related PASHs in comparison to HPLC

Although CE is known for its superior resolution, a direct comparison of the CE separation of PASHs to the commonly used RP-HPLC has not been done so far. To close this gap, six PASHs (BT; 5-methyl-BT; DBT; 4-methyl-DBT; 4,6-dimethyl-DBT and 2,4,6,8-tetramethyl-DBT), that commonly occur in fuel related samples, were separated by both methods. For the CE analysis, all compounds were methylated to the corresponding S-methyl-benzothiophenium (SMBT) and S-methyl-dibenzothiophenium (SMDBT) ions as described in chapter 5.5.1. A mixture of all six compounds was analyzed using a CE electrolyte buffer of 50 mM phosphate at a pH of 2.15. The applied voltage for the separation was set to 20 kV. A baseline separation for all the compounds could easily be achieved in less than 10 minutes. However, for the compounds with longer migration time, a significant tailing of the signals could be observed. The tailing could be suppressed by adding isopropanol as additive to the electrolyte buffer. In addition to the suppression of the tailing, a further increase in resolution was observed. This effect can be explained by the higher viscosity of the running buffer that decreases the longitudinal diffusion of the analytes and hence a broadening of the signals. However, the addition of isopropanol leads to an increase in migration time, which is connected to the higher viscosity as well. Best results were obtained for buffers containing 20 to 40 %vol. isopropanol. The electropherogram for a separation performed with an addition of 20 % isopropanol can be



seen in figure 33a. The separation is finished in less than 25 min with superior baseline separation and a number of theoretical plates above 100.000 for all the compounds.

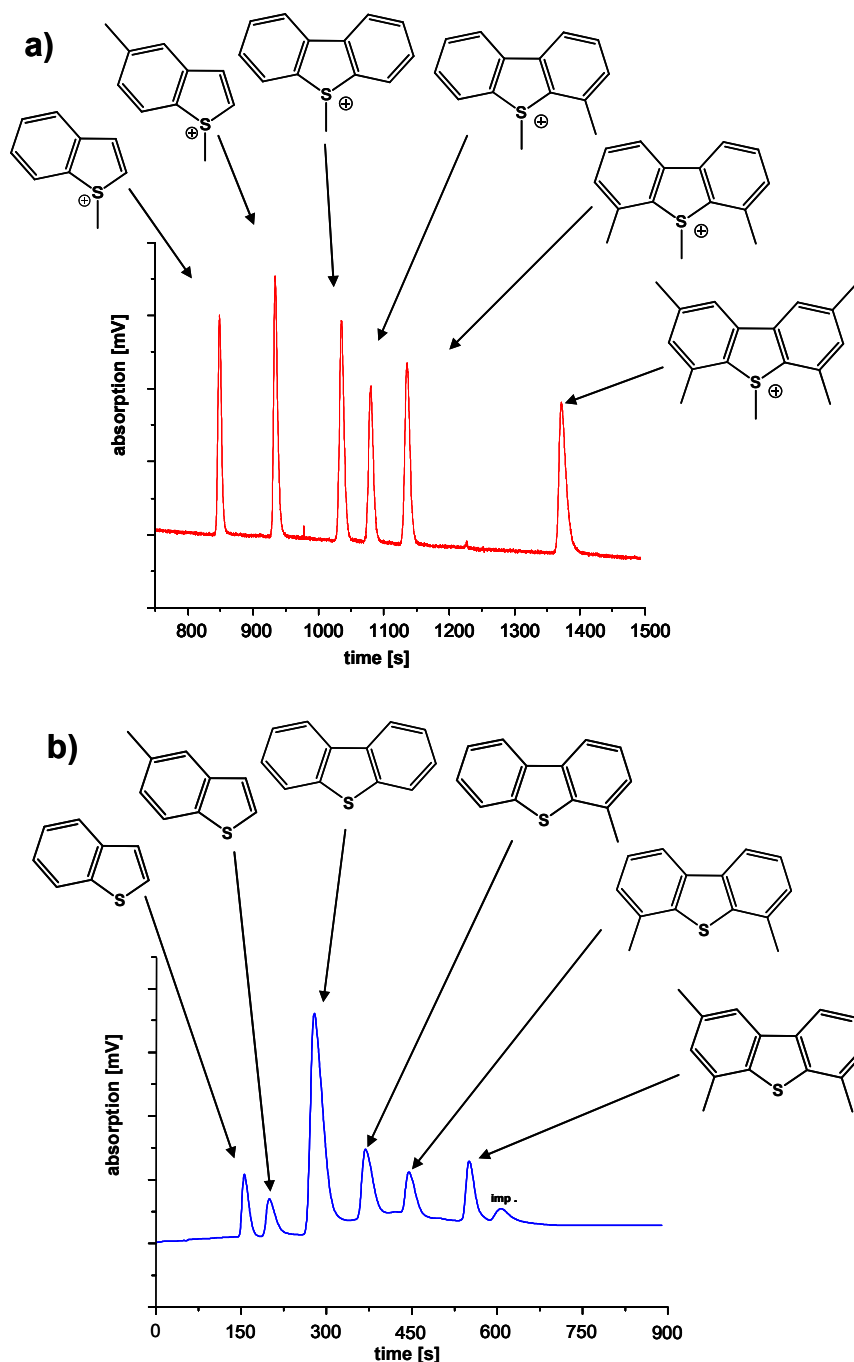


**Fig. 33: Separation of six fuel-related PASHs** with a) CE (SMBT; 5-methyl-SMBT; SMDBT; 4-methyl-SMDBT; 4,6-dimethyl-SMDBT; 2,4,6,8-tetramethyl-SMDBT) with phosphate buffer 50mM, pH 2.15, 20 % isopropanol at a voltage of 20 kV and b) RP-HPLC (BT; 5-methyl-BT; DBT; 4-methyl-DBT; 4,6-dimethyl-DBT; 2,4,6,8-tetramethyl-DBT; imp.: impurity) on a 150 mm RP18 column, 75-100 % acetonitrile in water, linear gradient 3 to 8 min, 2 mL/min.

Obviously the compounds are separated by size of the molecules. The S-methylated BT has the shortest migration time, while 2,4,6,8-tetramethyl-SMDBT has the highest migration time. The migration order is similar to what is expected from GC and HPLC. In GC, the longer retention time is related to the higher vaporization point, in RP-HPLC it is related to the stronger interaction with the stationary phase.

For the RP-HPLC separation of the PASHs, the nonderivatized standard compounds (BT; 5-methyl-BT; DBT; 4-methyl-DBT; 4,6-dimethyl-DBT and 2,4,6,8-tetramethyl-DBT) were used. The separation was performed on a 150 mm RP18 column (7  $\mu$ m particles) with 75-100 % acetonitrile in water with a linear gradient from 3 to 8 min at a flow rate of 2 mL/min. The separation was finished after 10 minutes with baseline separation for the six compounds. Nevertheless the resolution for this method is considerably lower than the one obtained with the CE method. The retention order is, as expected, the same as seen in the CE analysis. The use of a longer RP column as well as the use of smaller particle size (e.g. 3.5  $\mu$ m particles) would increase the resolution for the HPLC method. However, a longer column would be accompanied by longer retention times as well.

## **6.2 Comparison between the derivatization methods**

There are different possibilities to convert PASHs into ions. The most often used technique in this work is the methylation of the sulfur atom, so that the corresponding methyl-thiophenium ions are obtained. This can be done by using methyl iodide and silver tetrafluoroborate as described in chapter 5.5.1. A further method to convert PASHs to ions is the derivatization to phenyl-thiophenium ions. Using this technique, a phenyl ring is attached to the sulfur atom in the aromatic system instead of a methyl group. This can be performed by treating the PASHs with diphenyliodonium triflate as described in chapter 5.5.2. Both of the derivatization routes come with advantages and disadvantages. The methylation reaction is easy to perform and the chemicals used are very inexpensive. However, the reagents are toxic and the products are sensitive to light and heat. This makes storage in a cold and dark environment necessary. Contrary to that, the phenylated products do not show any sensitivity to light or heat. The additional aromatic group introduced into the compound increases UV absorption, which results in lower limits of detection for the analytes. The problem with this derivatization reaction is that the phenylation reagent itself is ionogenic so that a huge signal occurs when an excess of the

reagent is used. The migration time of the diphenyliodonium ion is very close to the most abundant PASHs in diesel fuels, so that signals tend to comigrate. A phenyl ring as derivatization group is larger and should hence increase the migration time of the compounds in comparison to the methylated products. Furthermore, the reagent for the phenylation reaction is very expensive.

These different advantages and disadvantages make a comparison of the derivatization methods necessary. For this reason, four standard PASHs (BT, DBT, 4-methyl-DBT and 4,6-dimethyl-DBT) were methylated in one reaction and phenylated in another reaction as shown in figure 34. A CE separation of each of the compound classes (S-methylthiophenium ions and S-phenylthiophenium ions) led to four baseline separated signals. The migration order corresponds to the size of the compounds as expected. The methylated and phenylated products of BT migrate fastest in their groups, while the derivatized products of 4,6-dimethyl-DBT migrate last within their class of compounds. In summary it could be observed, that the migration time for the phenylated compounds was to some extent longer than that of the methylated homologous. To get a better insight into the separation behavior, a combined analysis of all eight compounds was performed. The resulting electropherogram is presented in figure 35.

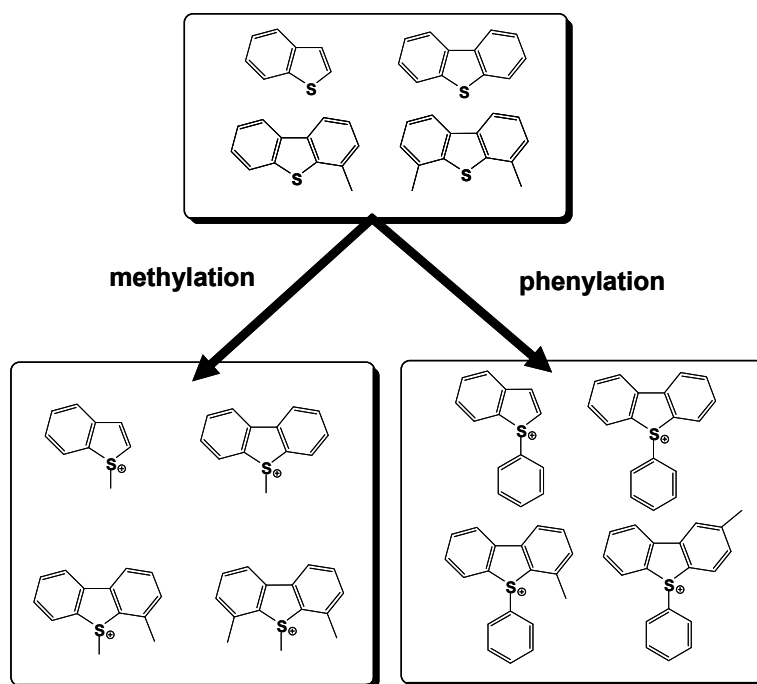


**Fig. 34: Derivatization of four PASHs to the corresponding methyl- and phenyl-thiophenium ions.**

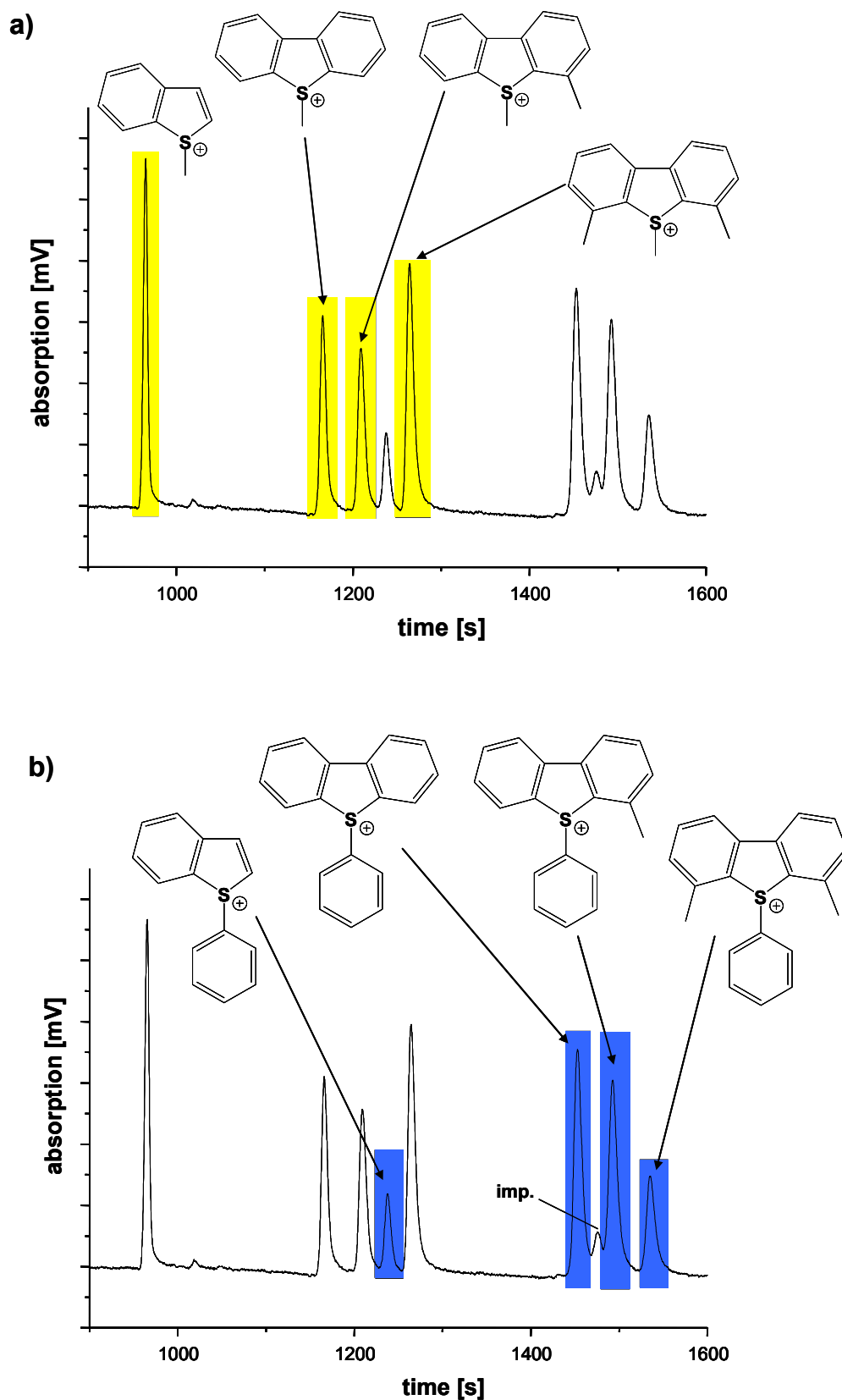


**Fig. 35:** CE-separation of a mixture of a) four methyl-thiophenium ions (marked in yellow) and b) four phenyl-thiophenium ions (marked in blue). Electrolyte: phosphate buffer 50 mM, pH 2.15, 25 % isopropanol at a voltage of 20 kV.

Each of the eight signals in the electropherogram can be associated with one of the compounds. In figure 35a, all the methylated products are marked in yellow, while in figure 35b, all the phenylated compounds are marked in blue. Interestingly the pattern for both of the compound classes is very similar, but can be observed with increased migration times for the phenylated compounds due to the more bulky derivatization group. The migration time difference for each of the pairs (for example S-methyl-DBT and S-phenyl-DBT) is close to 266 seconds as can be seen in figures 36a and 36b. The migration time difference seems to be independent from the structure of the parent compounds as it can be found for SMBT as well as SMDBTs. Even the alkylation pattern has no influence on this migration time difference.

It can thus be concluded that a different derivatization group mainly influences the migration time but has no positive effect on the resolution. The effect of a larger derivatization group can even be described as negative because the increased migration time of the phenylated compounds leads to broader signals that are related to the higher longitudinal diffusion. Obviously, the migration time is directly influenced by the derivatization group. All the phenylated compounds migrate 266 seconds later than the methylated homologous.

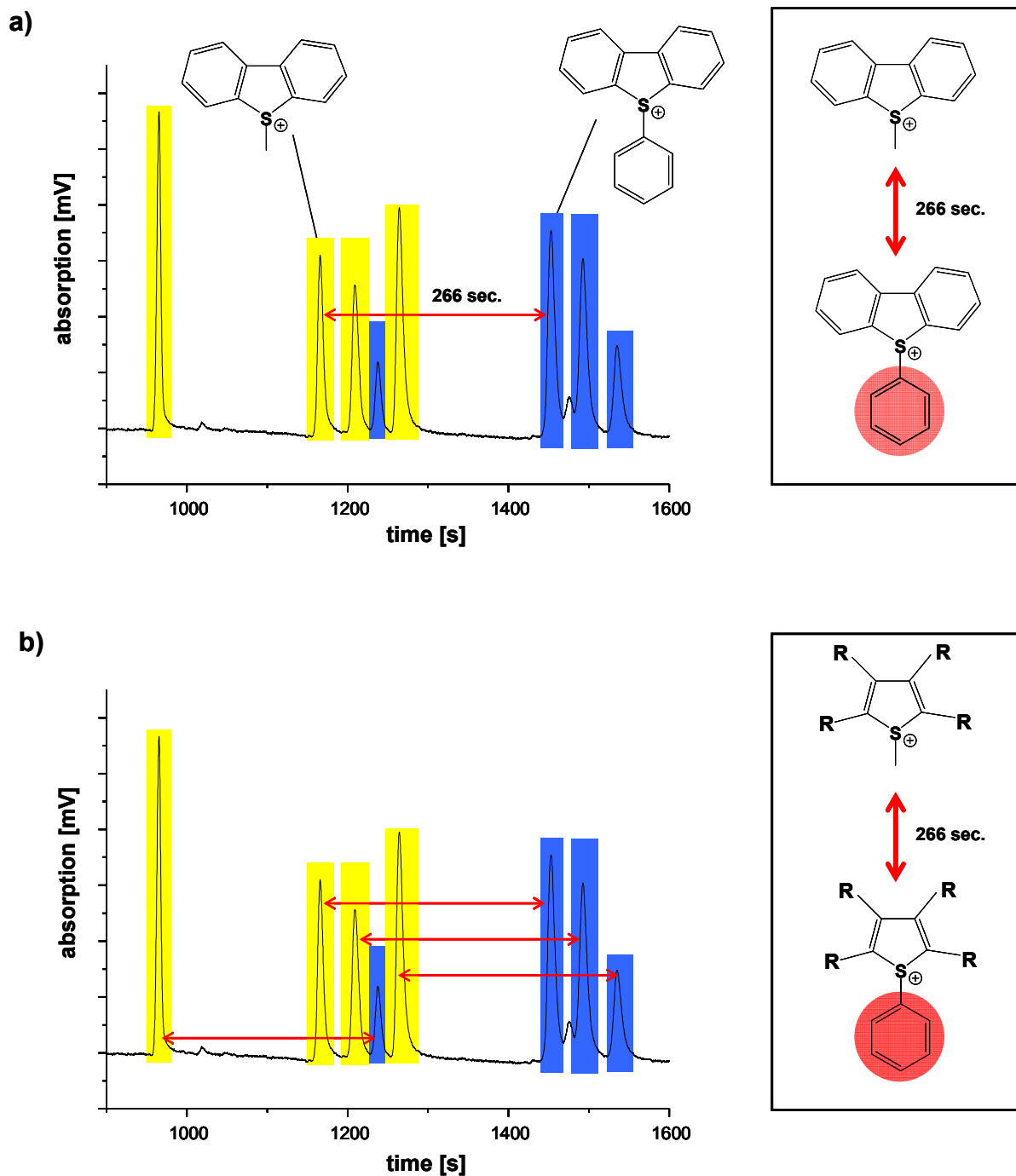


**Fig. 36: a) Migration time difference between S-methyl-DBT and S-phenyl-DBT and b) Migration time difference between all the methylated and phenylated products.**  
 Electrolyte: phosphate buffer 50 mM, pH 2.15, 25 % isopropanol at a voltage of 20 kV

### 6.3 Cyclodextrin supported separation of derivatized standard compounds

Different approaches toward the use of cyclodextrins in CE for the separation of PAHs, as described in chapter 3.5, can be found. This class of compounds can be used as carrier molecule. The neutral analytes form inclusion complexes with charged cyclodextrins and can hence be transported through the capillary when included in the cavity of the host.

For a wide variety of charged analytes, neutral cyclodextrins are used in CE to influence the migration time. Whenever a charged analyte forms an inclusion complex with a neutral cyclodextrin, the electrophoretic mobility is lower, because the mass-to-charge ratio of the complex is much higher. This technique is especially useful for the separation of isomers. Isomeric compounds with the same molecular weight tend to migrate with very similar migration time, so that comigration commonly occurs. Adding cyclodextrins to the CE running buffer can greatly increase the resolution, because isomers often have very different complex formation constants with the cyclodextrins and their mobility is therefore influenced very differently on dependence of the structure.

Furthermore, cyclodextrins are used for enantiomeric separation. Because enantiomers show exactly the same migration time during CE separations, enantiomeric separations can only be performed by adding enantiomeric complexing agents, like cyclodextrins, to the running buffer.

In this chapter the cyclodextrin supported separation of derivatized standard PASHs is described.

#### 6.3.1 Cyclodextrin supported enantiomeric separation of phenylated PASHs

PASHs lose their aromaticity in the derivatization step [114,115]. The S-substituted compounds are not planar but show a pyramidal structure at the sulfur atom (figure 37). This leads to the formation of two enantiomeric forms for all PASHs which do not have a mirror plane in the molecule before the derivatization.

To demonstrate this effect, 2-methyl-DBT was derivatized by the phenylation reaction to produce the corresponding phenylated ion 2-methyl-S-phenyl-DBT (2-methyl-SPDBT). Figure 38a shows the enantiomeric separation of this compound at different concentrations of  $\beta$ -cyclodextrin. The electropherogram was normalized to S-methyl-DBT as internal

standard (IS). A concentration of 15 mM  $\beta$ -cyclodextrin was sufficient to resolve the enantiomers. Symmetric compounds, such as 4,6-dimethyl-S-phenyl-dibenzothiophene, cannot form enantiomers and thus always give one signal. This is demonstrated in figure 38b where an enantiomeric separation cannot occur for 4,6-dimethyl-S-phenyl-dibenzothiophene (4,6-diMe-SPDBT).

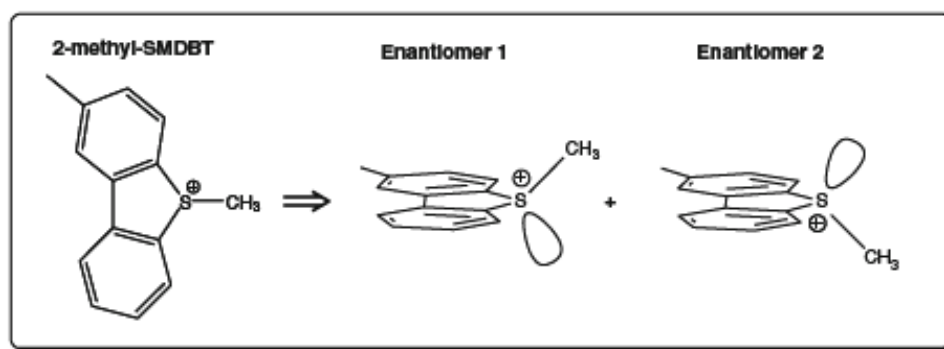


**Fig. 37: Formation of two enantiomeric structures during the derivatization reaction.**

### 6.3.2 Cyclodextrin supported separation of all monomethyl-BT isomers

Cyclodextrins are generally known to have a positive effect on the separation of isomers as already described in chapter 3.5 and 6.3. Due to these known positive effects, cyclodextrins were tested for the CE analysis of all the monomethyl-BT isomers. The six isomers (2-Me-BT, 3-Me-BT, 4-Me-BT, 5-Me-BT, 6-Me-BT and 7-Me-BT) and BT were derivatized to the according S-methyl thiophenium ions and separated by the common CE method without addition of cyclodextrins. The resulting electropherogram can be seen in figure 39a with the corresponding structures given in figure 40a. The migration time differences for the monomethyl-BT isomers are very small, comigration for nearly all of the compounds occurs. Only 2-methyl-BT and 3-methyl-BT migrate slightly faster and show individual signals. BT migrates first as it features no methyl group in 2- to 7-position. This result is according to the expectations. The small differences in molecule size make a separation of all the analytes difficult.

In the next measurement, a different CE buffer was used. Instead of adding isopropanol to the running buffer, 10 mM  $\beta$ -cyclodextrin was added. The resulting electropherogram is presented in figure 39b. The migration order of the isomers changes drastically. 7-methyl-BT now has the shortest migration time of the monomethyl-BTs, while it was



comigrating with 4-, 5- and 6-methyl-BT without CD. Enantiomeric separation of the compounds does not occur yet.

Because the solubility of  $\beta$ -cyclodextrin is limited in aqueous media, a hydroxypropyl-modified cyclodextrin should be used in the further measurements. In addition to the modification of the hydroxyl groups, a smaller cyclodextrin with only six glucose units was chosen. Because the monomethyl-BT isomers are relatively small, the interaction with smaller cyclodextrins was expected to be stronger, so hydroxypropyl- $\alpha$ -cyclodextrin was used in the following. The solubility in aqueous media of this compound is drastically increased by the hydroxypropyl-modification.

Due to the increased solubility, high concentrations of up to 300 mM could be used. Best results were obtained when the buffer contained 110 mM hydroxypropyl- $\alpha$ -cyclodextrin. The associated electropherogram is presented in figure 40b. The signals are marked according to the isomers given in figure 40a. A baseline separation of all the compounds is achieved except for 2-methyl-SMBT and 3-methyl-SMBT which are only near-baseline resolved. Four of the seven compounds show the enantiomeric peaks as well. Despite the fact that there are now eleven peaks visible from the seven compounds, it is a much better separation and all monomethyl-BTs can be separated from each other. A separation of all the isomers by GC has so far not been demonstrated, including stationary phases of higher polarity than those with 5 % phenyl groups [116].

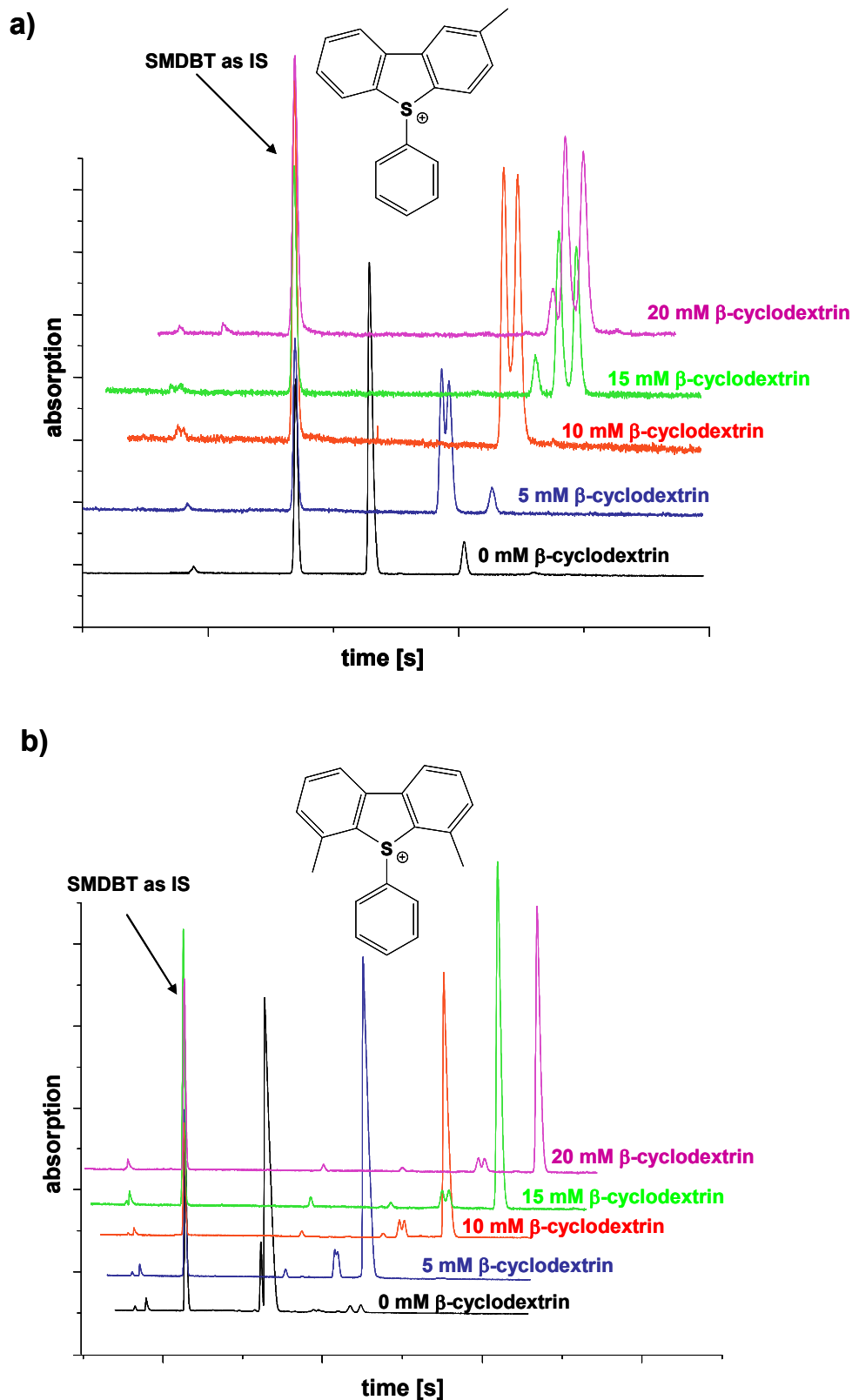


**Fig. 38: a) Enantiomeric separation of 2-methyl-SPDBT b) no enantiomeric separation for 4,6-dimethyl-SPDBT.** Electrolyte: phosphate buffer 50 mM, pH 2.15, at a voltage of 20 kV containing different concentrations of  $\beta$ -cyclodextrin.

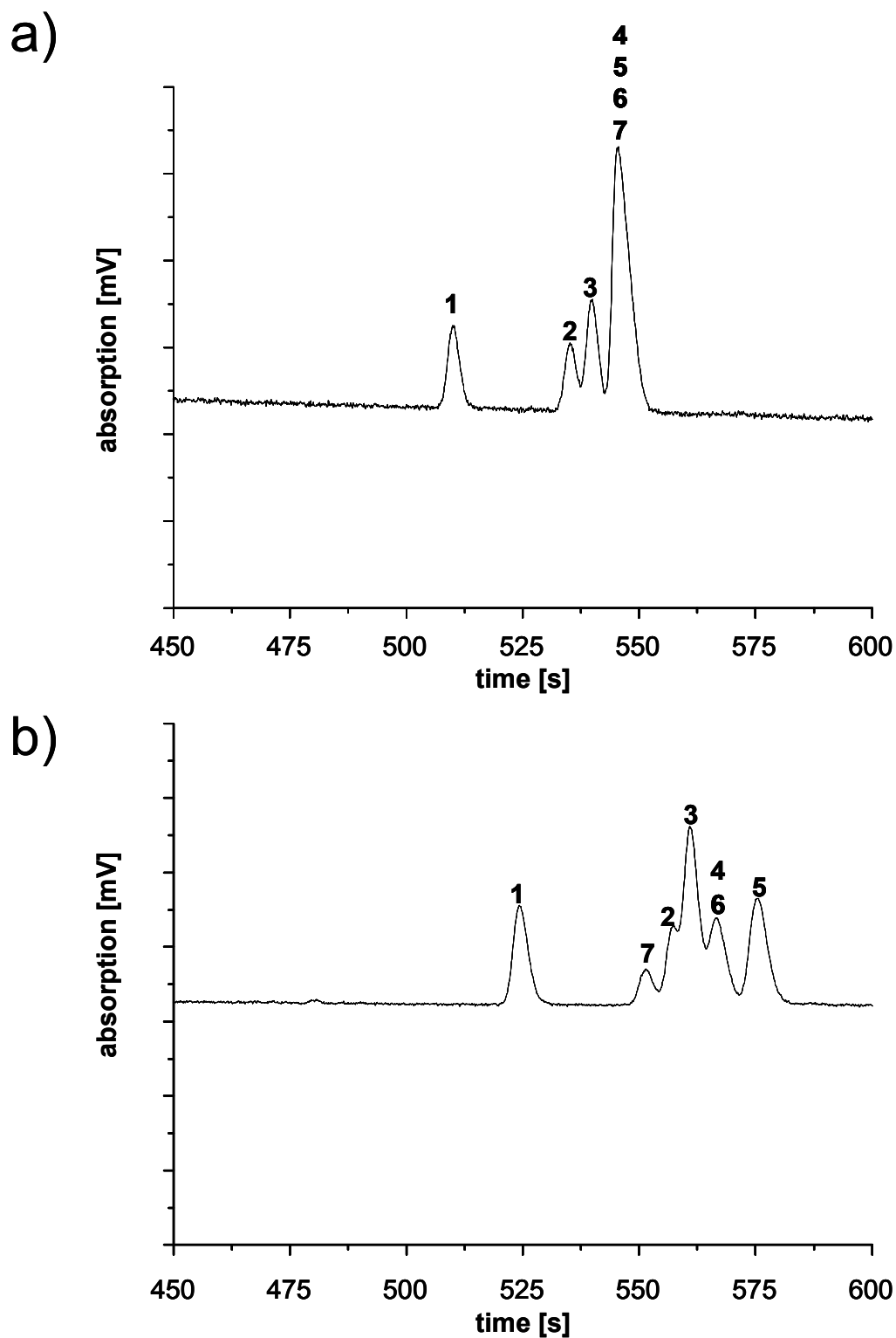


**Fig. 39: Capillary electrophoretic separations of a mixture containing seven S-methyl-benzothiophenium salts.** Peak identification: 1: SMBT, 2: 2-methyl- SMBT, 3: 3-methyl-SMBT, 4: 4-methyl-SMBT, 5: 5-methyl-SMBT, 6: 6-methyl-SMBT, 7: 7-methyl-SMBT. Electrolyte: a) Phosphate buffer 50 mM, pH 2.15, 10 % isopropanol, 20 kV b) Phosphate buffer 50 mM, pH 2.15, 10 mM  $\beta$ -cyclodextrin, 20 kV.

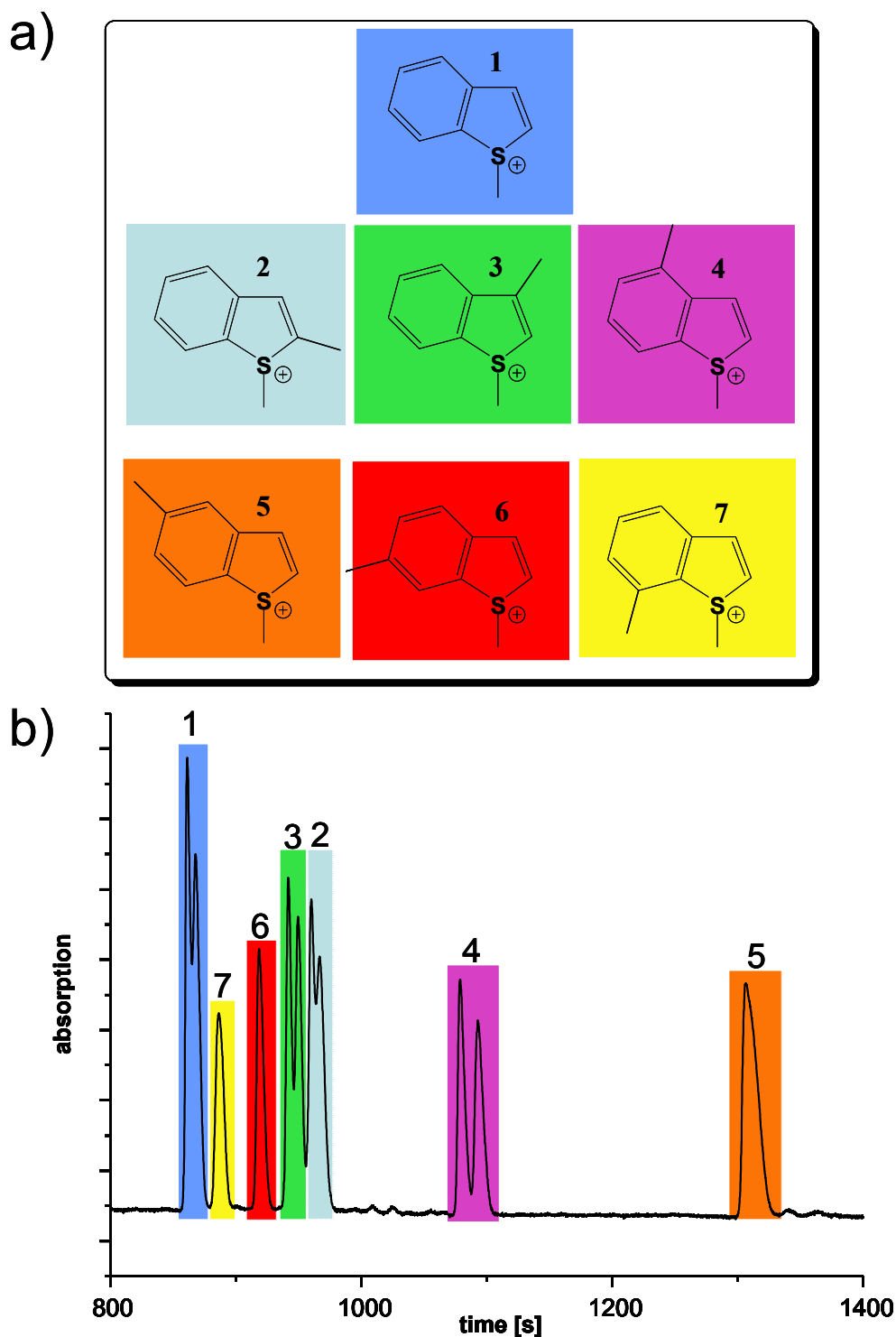


**Fig. 40: Structures of the analytes a) and electropherogram for the separation of a mixture containing seven S-methyl-benzothiophenium salts.** Structures given in a) 1: SMBT, 2: 2-methyl- SMBT, 3: 3-methyl-SMBT, 4: 4-methyl-SMBT, 5: 5-methyl-SMBT, 6: 6-methyl-SMBT, 7: 7-methyl-SMBT. b) Electropherogram for the separation; Electrolyte: phosphate buffer 50 mM, pH 2.15, 110 mM  $\alpha$ -hydroxypropyl-cyclodextrin, 20 kV.

#### 6.4 Correlation of molecular volume and migration time in CE-UV

Our preliminary studies revealed a linear correlation between the molecular volume and the migration time of the derivatized compounds. This linear correlation occurs due to the fact that all of the derivatized compounds have a net charge of +1. Because the migration of a compound in the electric field is influenced by the size/charge ratio, the correlation can be simplified to the molecular volume in case of derivatized PASHs [111].

A linear correlation of the calculated volume and the migration time is quite useful as it enables the prediction of migration times.

##### 6.4.1 Calculation of the molecular volume

The molecular volume of the derivatized PASHs can be calculated with PCModel, a molecular modeling software used for studies of organic and inorganic compounds.

The molecule to be calculated can be drawn on the desktop of the software. By using the option “minimize”, the geometry of the structure is adjusted by means of force field methods. The software analyzes the structure depending on atom type, bond type, angle and dihedral angle. The constants necessary for the calculation are provided by the database of the software.

The first step of the calculation is a derivative minimization of the drawn structure. The software tries to decrease the energy of the structure by moving atoms in the force field. Whenever the energy value of atoms begins to rise, or the difference in energy is below the error of measurement, the calculation is aborted. The resulting minimized energy value and the optimized structure are displayed on the desktop. By using the option “calculate volume”, the molecular volume of the optimized structure can be determined in the unit cubic Ångström. The calculated results for S-methyl-DBT and S-phenyl-DBT, including the molecular volume, are displayed in figure 41. The molecular volume of the molecules is displayed as a dotted area.

Because a molecule might have several minimal-energy-structures, it is always possible that only a local energetic minimum of the structure is found and further lower-energy structures exist. To avoid this problem, each structure was drawn three times and

optimized in individual calculations. The average values were determined and used for the correlation plots.

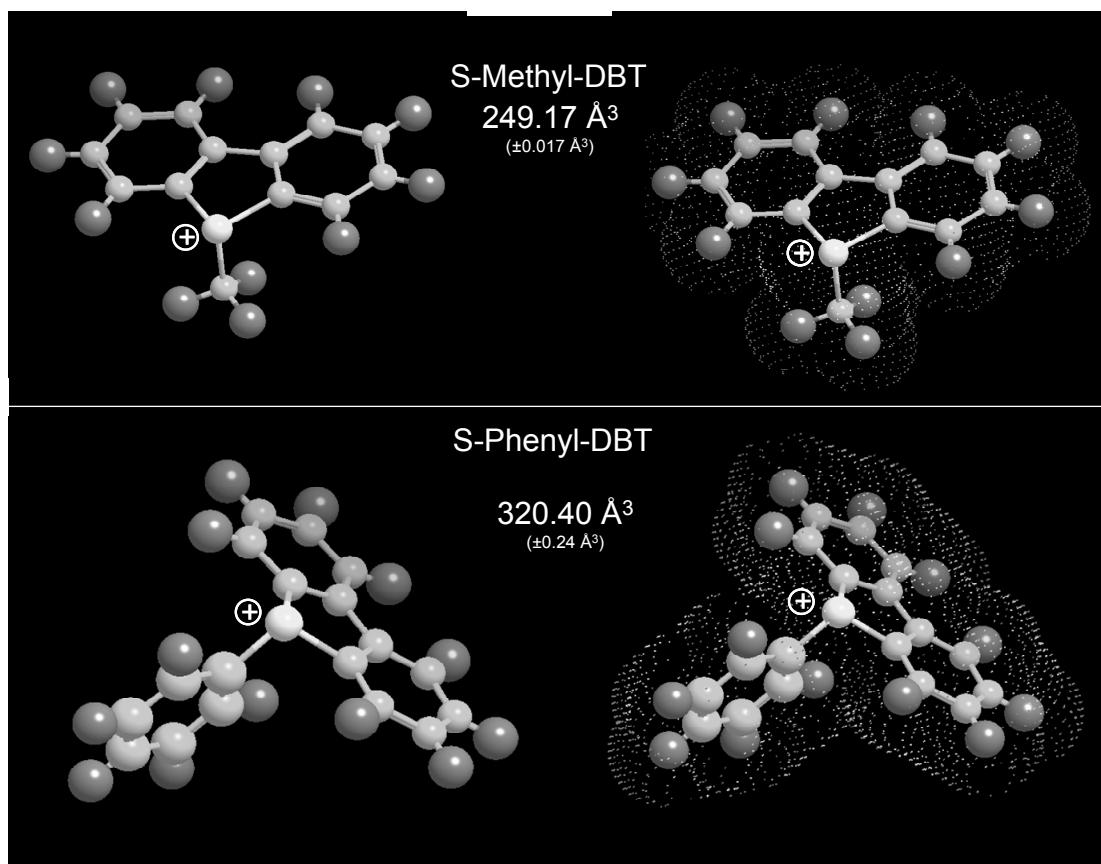


**Fig. 41: Optimized structures for S-methyl-DBT and S-phenyl-DBT with the calculated molecular volume by the software PCModel.**

#### 6.4.2 Correlation for PASHs with long alkyl chains

In earlier studies, the correlation of molecular volume and migration time was demonstrated for a complex mixture of fuel related PASHs [111]. Fourteen S-methyl thiophenium salts were mixed and the separation was performed in the commonly used CE buffer, but without the addition of isopropanol. It was possible to separate the analytes within 12 min. Near-baseline separation of the mixture was achieved and the number of theoretical plates (for all compounds) averaged 170.000. The electropherogram of this separation is displayed in figure 42a with a list of the analytes in 42b. The molecular volumes of the analytes were calculated as described in 6.4.1 and plotted against the

migration time. A linear correlation between calculated volume and migration time could be observed, the  $R^2$  value was determined to be 0.993.

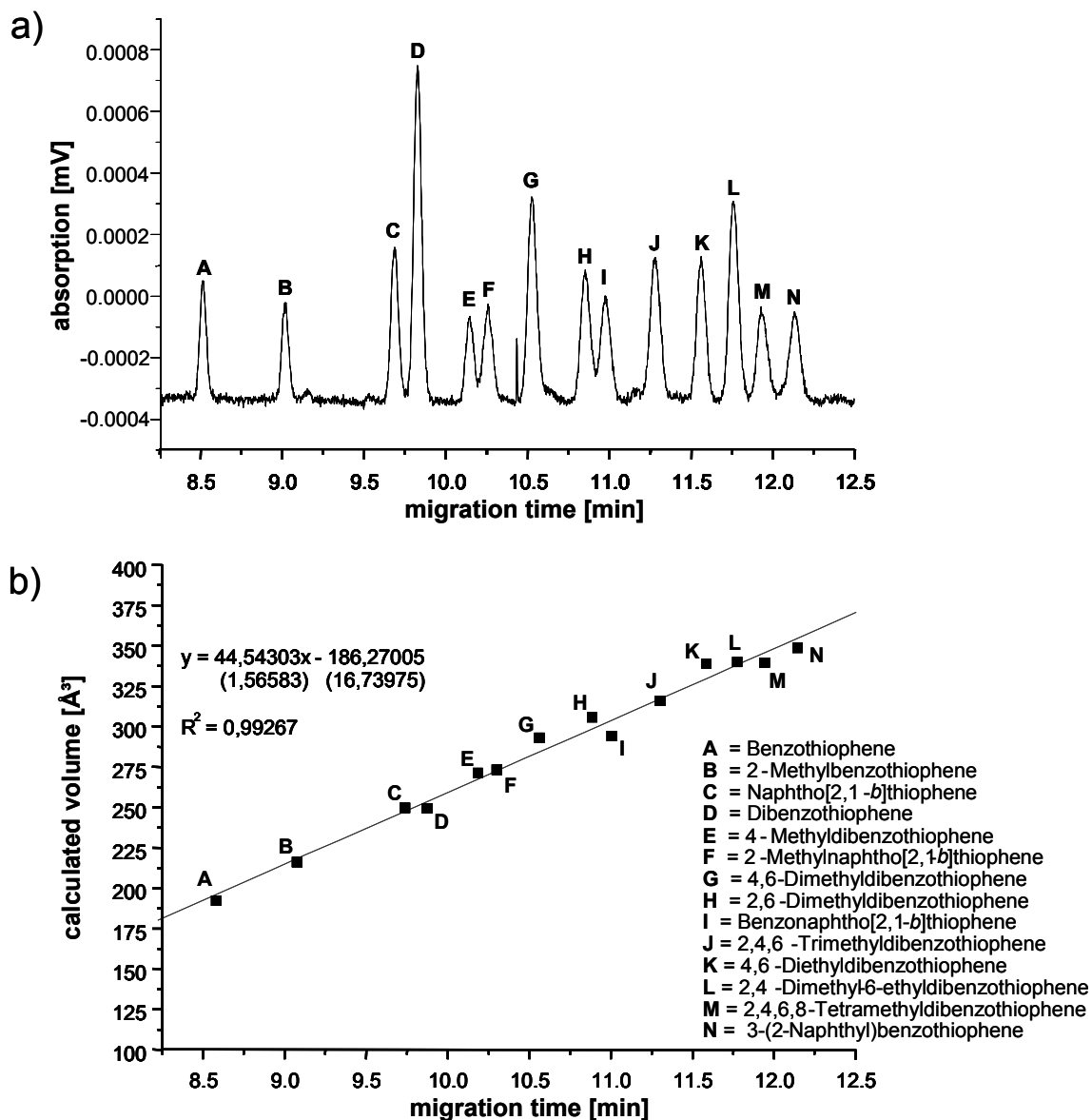


**Fig. 42:** a) Capillary electrophoretic separation of a mixture containing 14 PASH-methyl thiophenium salts. Electrolyte: phosphate buffer 50 mM, pH 2.15 at a voltage of 20 kV. b) Plot of calculated molecular volume vs. the migration time.

Because one major aim of this work was to evaluate to what extent the capillary electrophoretic method for the separation of PASHs can be applied to larger compounds, such as those occurring in high boiling fuel fractions, the linear correlation for PASHs with long alkyl chains was investigated. The synthesis of several highly alkylated PASHs was

necessary because these compounds are not commercially available. In the first step, 4,6-dipropyl-DBT, 4,6-dipentyl-DBT and 4,6-didecyl-DBT were synthesized. A synthesis instruction for these compounds can be found in the appendix 10.1.

A mixture of all the synthesized compounds including four further PASHs (structures for all compounds are given in figure 43) was derivatized by using the methylation reaction and subsequently separated by CE. In the following, the molecular volumes for all these analytes were calculated with PCModel and plotted against the migration time. The plot is displayed in figure 43. Obviously, the linear correlation ( $y = 24,101x - 156,070$ ) for PASHs with long alkyl chains in 4- and 6- position can be confirmed. The  $R^2$  value was determined to be 0.999, which supports the result.

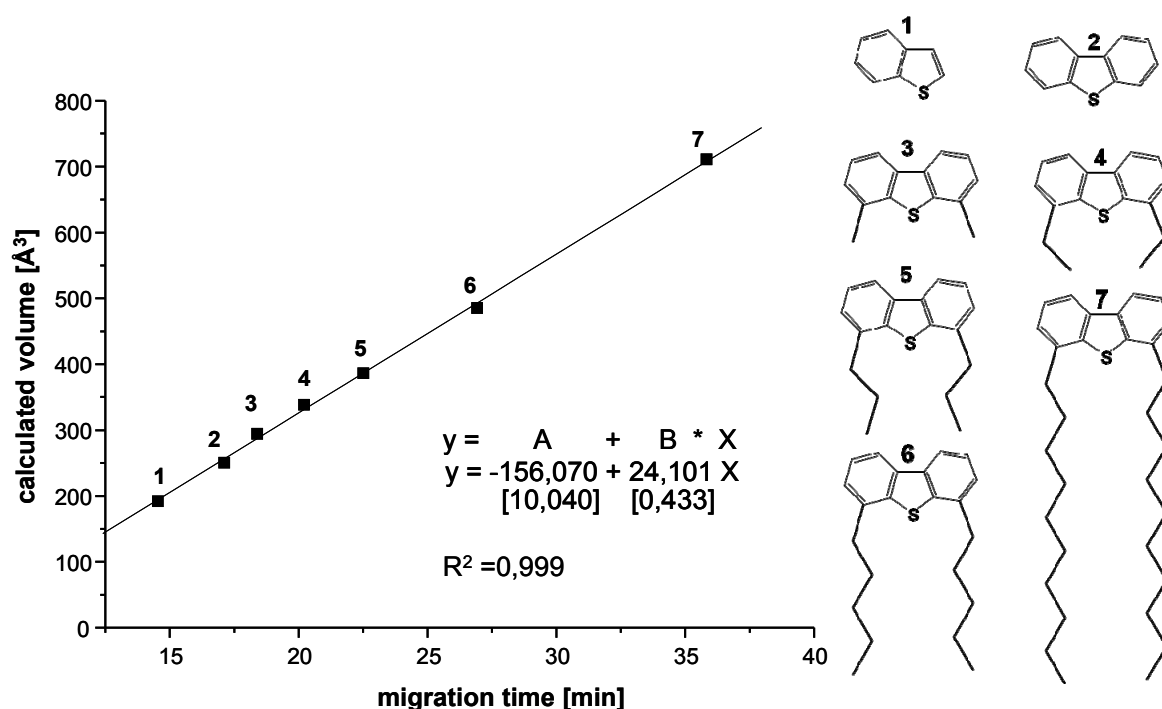


**Fig. 43: Plot of calculated molecular volume vs. the migration time for the separation of seven PASHs with five analytes containing alkylations in 4- and 6-positions.** Peak identification: 1: SMBT, 2: SMDBT, 3: 4,6-dimethyl-SMDBT, 4: 4,6-diethyl-SMDBT, 5: 4,6-dipropyl-SMDBT, 6: 4,6-dipentyl-SMDBT, 7: 4,6-didecyl-SMDBT; Electrolyte: phosphate buffer 50 mM containing 20 % isopropanol, pH 2.15 at a voltage of 25 kV

However, the linear correlation does not fit for all PASHs. Interestingly PASHs with only one long alkyl chain attached to the parent structure do not comply with the assumption



and differ significantly from the correlation. This effect was observed when a mixture of several mono-alkylated PASHs was separated by CE. The composition of the sample can be seen in figure 44. While the plot is linear for BT to 4-pentyl-DBT (signals 1 to 5), the signal for 4-decyl-DBT (signal 6) does not fit the correlation. The migration time of this compound is several minutes longer than expected. The correlation for the mono-alkylated DBTs seems to be better described as a quadratic function ( $y = 0,451x^2 + 39,067x - 281,195$ ) like it is presented in figure 44. This assumption is only based on the signal of 4-decyl-DBT so further measurements need to be performed.

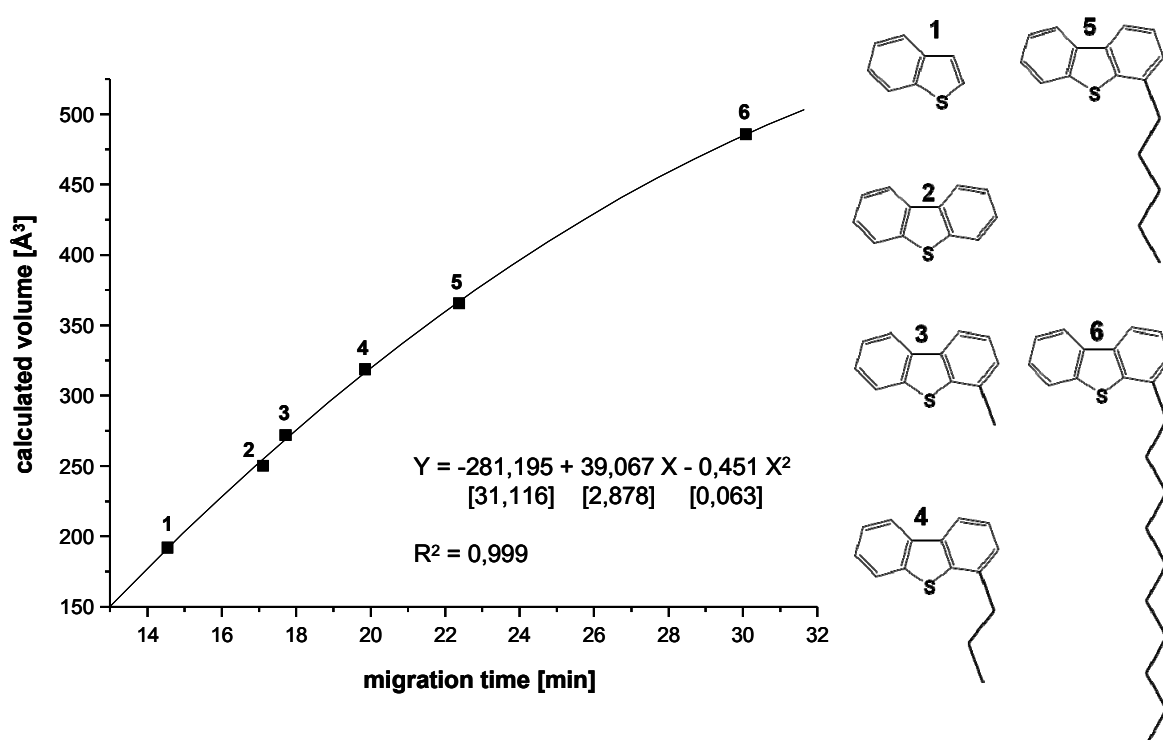


**Fig. 44: Plot of calculated molecular volume vs. the migration time for the separation of six PASHs with four analytes containing alkylations in 4-position.** Peak identification: 1: SMBT, 2: SMDBT, 3: 4-methyl-SMDBT, 4: 4-propyl-SMDBT, 5: 4-pentyl-SMDBT, 6: 4-decyl-SMDBT; Electrolyte: phosphate buffer 50 mM containing 20 % isopropanol, pH 2.15 at a voltage of 25 kV. Electrolyte: phosphate buffer 50 mM containing 20 % isopropanol, pH 2.15 at a voltage of 25 kV.

In the following, 4-octyl-DBT and 4,6-dioctyl-DBT were synthesized. The migration times of these compounds were predicted prior to the separation by using the linear correlation for 4,6-dioctyl-DBT and the quadratic function for 4-octyl-DBT.

The linear equation ( $y = 24,101x - 156,070$ ) was solved for  $x$  (migration time in minutes) with  $y = 619.26 \text{ \AA}^3$  as the molecular volume of for 4,6-dioctyl-DBT. The resulting migration time was calculated to be 32.17 min. The quadratic equation ( $y = 0,451x^2 + 39,067x - 281,195$ ) was solved for  $x$  with  $y = 439.19 \text{ \AA}^3$  as the molecular volume for 4-octyl-DBT. The result for the expected migration time of this compound was 26.62 min (60.00 min as second result neglected).

In the following, a mixture of different 4-alkylated and 4,6-dialkylated PASHs (**1** BT, **2** DBT, **3** 4-methyl-DBT, **4** 4,6-dimethyl-DBT, **5** 4-propyl-DBT, **6** 4,6-diethyl-DBT, **7** 4-pentyl-DBT, **8** 4,6-dipropyl-DBT, **9** 4,6-dipentyl-DBT, **10** 4-octyl-DBT, **11** 4-decyl-DBT, **12** 4,6-dioctyl-DBT, **13** 4,6-didecyl-DBT, structures given in figure 45a) including the two compounds with predicted migration times was derivatized and subsequently separated by CE. As expected, the 4,6-dialkylated analytes including 4,6-octyl-DBT (**4**, **6**, **8**, **9**, **12**, **13**) show a very good linear correlation between migration time and calculated volume. The measured migration time for 4,6-dioctyl-DBT was 33.35 min which deviates from the 32.17 min as the calculated migration time by 3.67 %. Both the calculated and the measured value are presented in figure 45b.

Analytes with only one alkyl group in 4-position (**3**, **5**, **7**, **10**, **11**) migrate slower than expected. The longer the alkyl chain is, the more significant is the deviation. In the performed measurement 4-octyl-DBT showed a migration time of 27.20 min which fits well to the calculated migration time of 26.62 min (2.19 % deviation). Both the measured and the calculated migration times are displayed in figure 45b. The correlation of molecular volume and migration time is more complex than assumed in the earlier studies. Especially compounds with long alkyl chains behave very differently and do not follow a linear correlation. This effect is probably based on the folding of the long alkyl chains in aqueous media. Obviously, the folding influences the shape of the molecules and hence the molecular volume. For this reason, the shape cannot be seen as ideal as calculated by the software. However, the software is only able to calculate the idealized structure of molecules in vacuum, while the actual structure in aqueous media might be very different. For this reason, further studies on the correlation for high molecular compounds were discontinued, as no software exists to calculate the structures of derivatized PASHs dissolved in water.

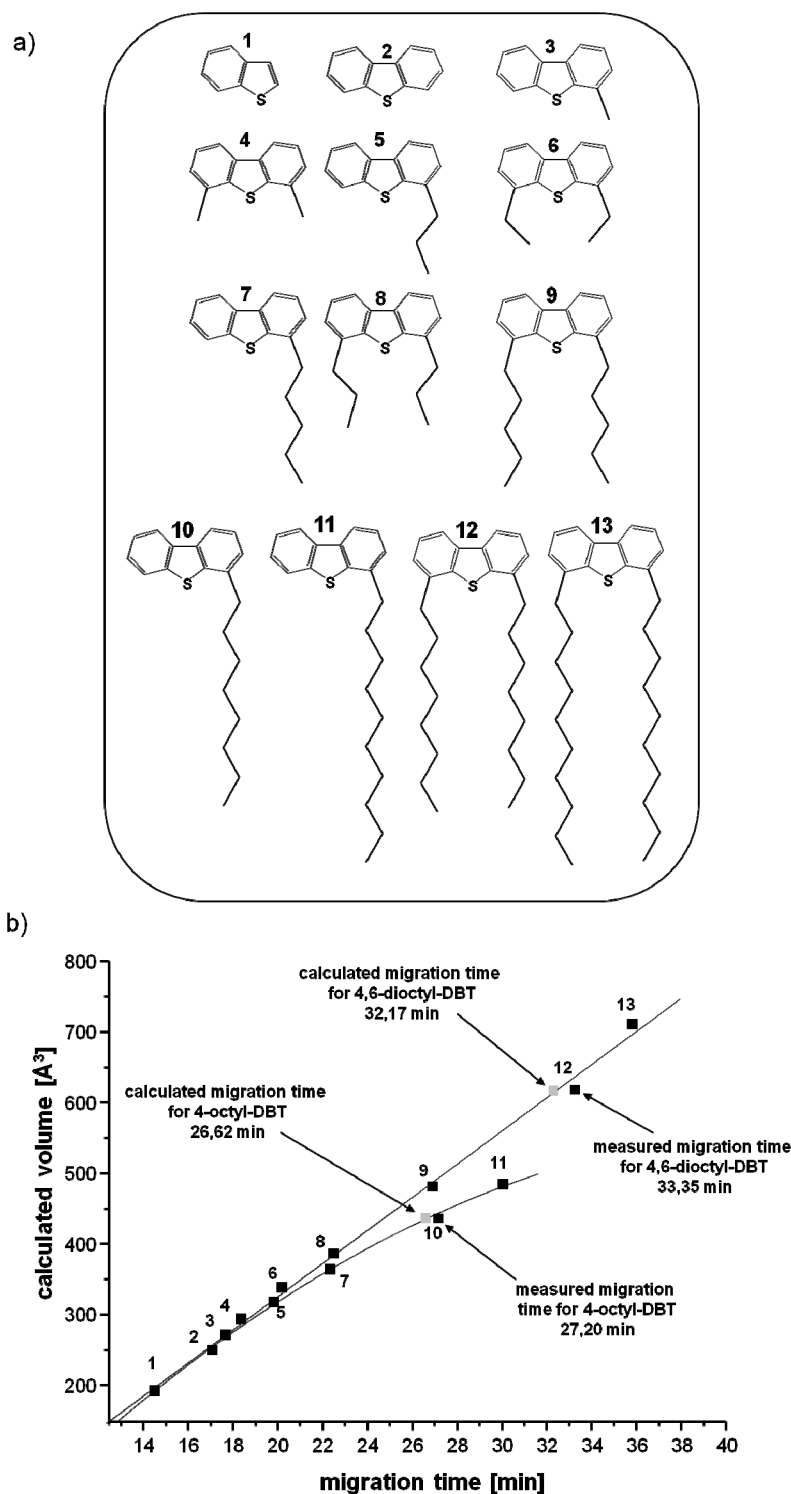


**Fig. 45:** a) Structures of the analytes and b) plot of calculated molecular volume vs. the migration time for the separation of 13 PASHs with different alkylations in 4- and 6-positions. Peak identification: 1: SMBT, 2: SMDBT, 3: 4-methyl-SMDBT, 4: 4,6-dimethyl-SMDBT, 5: 4-propyl-SMDBT, 6: 4,6-diethyl-SMDBT, 7: 4-pentyl-SMDBT, 8: 4,6-dipropyl-SMDBT, 9: 4,6-dipentyl-SMDBT, 10: 4-octyl-SMDBT, 11: 4-decyl-SMDBT, 12: 4,6-dioctyl-SMDBT, 13: 4,6-didecyl-SMDBT. Electrolyte: phosphate buffer 50 mM containing 20 % isopropanol, pH 2.15 at a voltage of 25 kV.

## 6.5 MEKC separation of standard compounds

Much research has been done on the separation of PAHs, especially the EPA-PAHs, by MEKC but the separation of PASHs with this method had not been tested when this work was carried out. To evaluate to what extent MEKC can be useful for the analysis of this compound class, the separation of a standard mixture of four PASHs (BT, DBT, 4,6-dimethyl-DBT and 2,4,6,8-tetramethyl-DBT) was optimized. Best results were obtained with a buffer containing 100 mM SDS, 20 mM borate at pH = 9.0. However this buffer was only able to separate BT from the other compounds while DBT, 4,6-dimethyl-DBT and 2,4,6,8-tetramethyl-DBT comigrated in one signal (figure 46). This can be explained by the strong interaction of these hydrophobic compounds with the interior of the micelles. All three compounds partition into the interior of the micelle and are therefore not separated. Only BT can be separated from the other compounds because the partition equilibrium does not lie completely on the side of the micelles. The signal for the EOF shows the beginning of the micellar window while the comigrating compounds define the end of the micellar window.

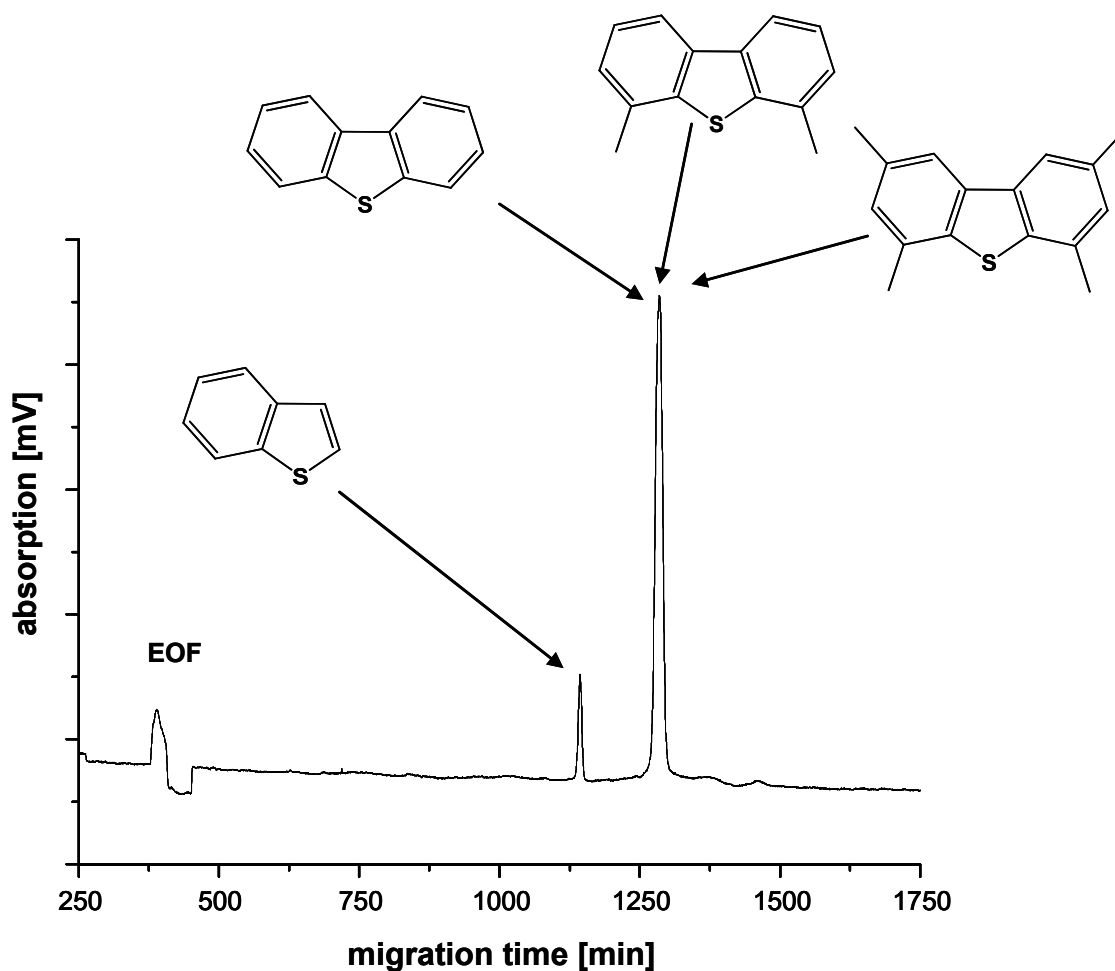


**Fig. 46: MEKC-separation of four PASH standard compounds.** (BT, DBT, 4,6-dimethyl-DBT and 2,4,6,8-tetramethyl-DBT) Electrolyte: 100 mM SDS, 20 mM borate at pH= 9.0.

### 6.5.1 Addition of organic modifier

In MEKC an addition of organic modifiers is widely used to enhance separation. If methanol is added to the running buffer, the analyte-micelle interactions of hydrophobic analytes can be decreased and hydrophobic compounds migrate earlier in the micellar window. SDS micelles are stable up to 25 % methanol as organic modifier.

A separation of the same test mixture as used before was performed with an addition of 10 % MeOH and 20 % MeOH to the running buffer. The results are shown in figure 47a and figure 47b.

The addition of 10 % MeOH increases the resolution but also leads to an increased migration time of all compounds, except for BT, which migrates earlier in the micellar window. Additionally a signal for DBT can be observed which is now separated from the other compounds. However, 4,6-dimethyl-DBT and 2,4,6,8-tetramethyl-DBT still comigrate in the last signal of the electropherogram.

An addition of 20 % MeOH strongly increases the migration time to nearly 5000 seconds but leads to baseline separation of all the compounds. Thus the number of theoretical plates only ranges from 66.000 for 2,4,6,8-tetramethyl-DBT to 113.000 for BT. Higher concentrations of organic modifiers were not tested because the migration time would increase further and the micelles might collapse due to instability in organic media. Because a good separation between 4,6-dimethyl-DBT and 2,4,6,8-tetramethyl-DBT could not be obtained, the sole usage of organic modifiers is not auspicious.

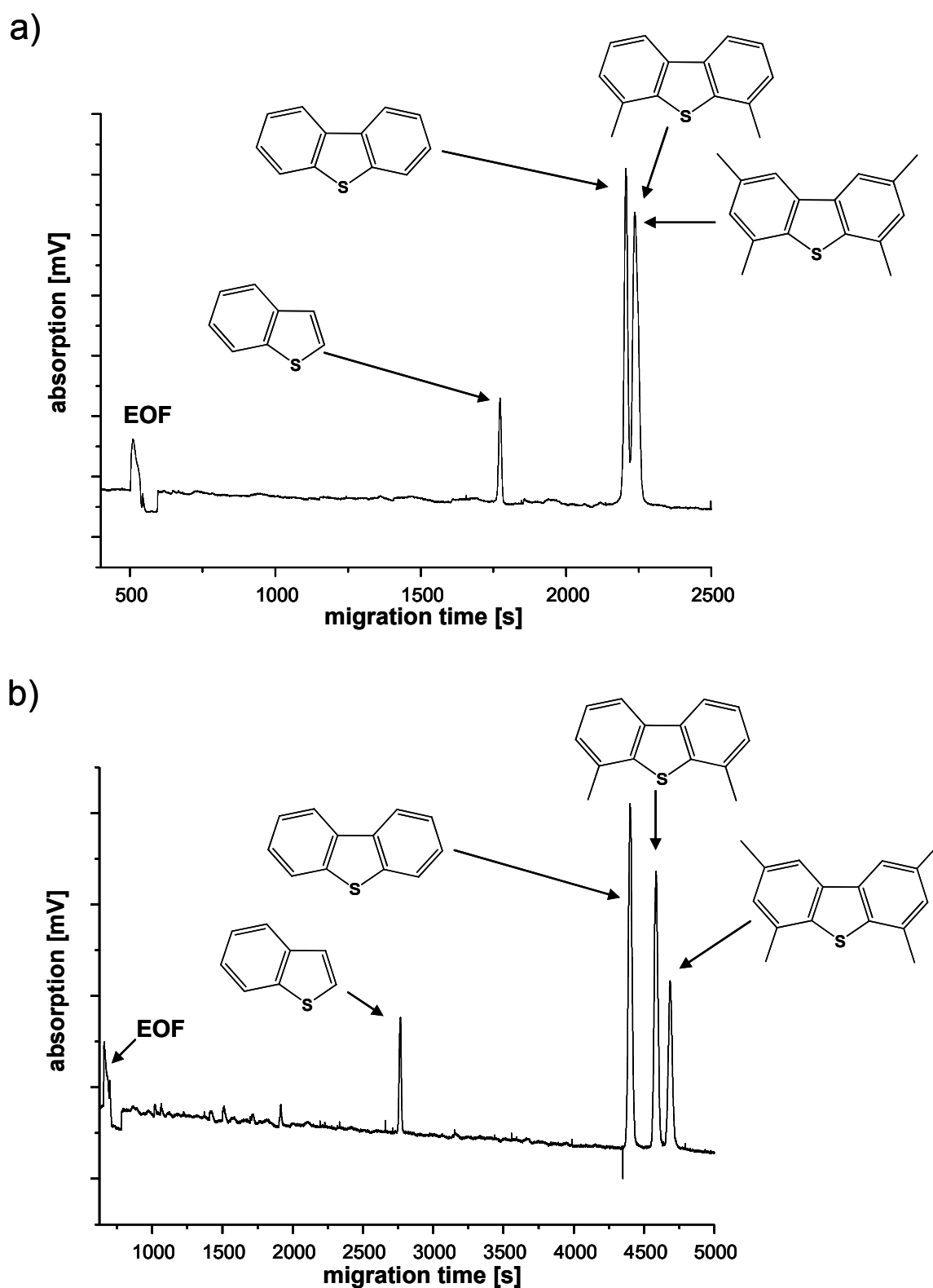


**Fig. 47: MEKC-separation of four PASH standard compounds with addition of organic modifier.** (BT, DBT, 4,6-dimethyl-DBT and 2,4,6,8-tetramethyl-DBT) Electrolyte: a) 100 mM SDS, 20 mM borate, pH = 9.0 containing 10 % methanol b) 100 mM SDS, 20 mM borate, pH = 9.0 containing 20 % methanol.

### 6.5.2 Addition of cyclodextrin

Cyclodextrins can be used in MEKC separations as well. Whenever a PASH compound partitions into a cyclodextrin, it is only affected by the EOF, as the mobility of the cyclodextrin-PASH-complex is zero. This leads to earlier migration of the compound in the micellar window without influencing the overall migration times.

For the separation, the cyclodextrin of choice was a hydroxypropyl modified  $\beta$ -cyclodextrin (HP- $\beta$ -cyclodextrin) because of its high solubility in aqueous media.

With an addition of 166 mmol/L of HP- $\beta$ -cyclodextrin to the running buffer, the resolution of the separation could be slightly improved (figure 48a). The larger compounds are partly separated and do not comigrate in one signal, as seen for the pure running buffer. The analysis time of the separation is not significantly influenced.

A further increase of the cyclodextrin concentration up to 332 mmol/L leads to a separation of all four compounds with a somewhat decreased migration time (figure 48b). The decreased migration time can only be explained by the expected effect: The PASHs partly partition into the cyclodextrins and are hence transported to the detector somewhat faster. Due to the fast separation and narrow peaks the numbers of theoretical plates are somewhat higher compared to the usage of organic modifier (BT: 145.000; DBT: 127.000; 4,6-dimethyl-DBT: 111.000; 2,4,6,8-tetramethyl-DBT: 94.000). Higher concentrations of cyclodextrin in the buffer could not be used because the solution was already saturated.



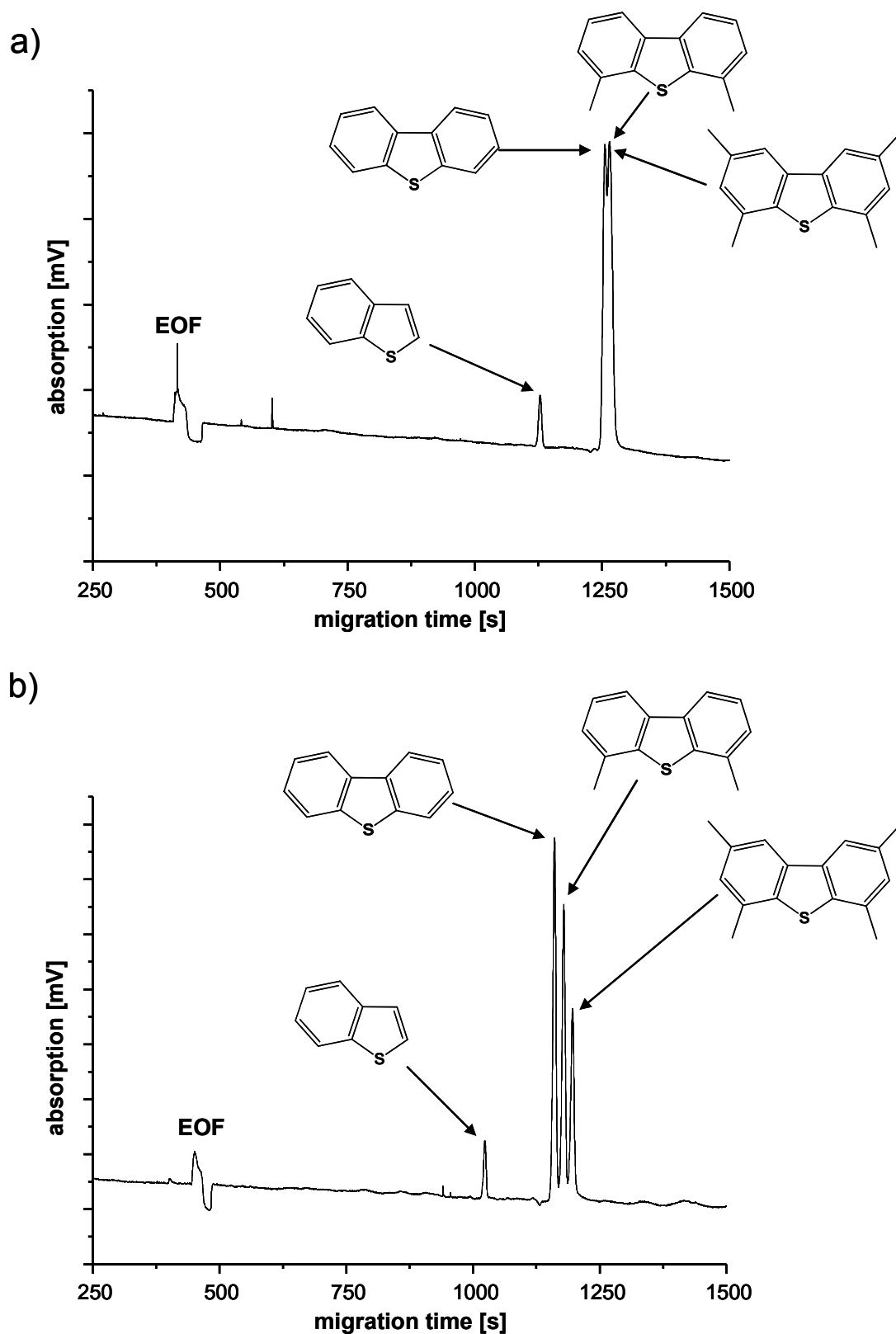


**Fig. 48: MEKC-separation of four PASH standard compounds with addition of cyclodextrins.** (BT, DBT, 4,6-dimethyl-DBT and 2,4,6,8-tetramethyl-DBT) Electrolyte: a) 100 mM SDS, 20 mM borate, pH= 9.0 containing 166 mmol/L of HP- $\beta$ -cyclodextrin b) 100 mM SDS, 20 mM borate, pH= 9.0 containing 332 mmol/L of HP- $\beta$ -cyclodextrin.

### 6.5.3 Combination of organic modifier and cyclodextrins

Because both the organic modifier and the cyclodextrins improved the separation of the PASH standard compounds, a combination of both methods was used. As the cyclodextrins had a positive effect without increasing the migration time, a MEKC buffer saturated with 332 mM HP- $\beta$ -cyclodextrin was used and the concentration of organic modifier was varied from 10 % vol. to 20 % vol.

A separation with 332 mM HP- $\beta$ -cyclodextrin and 10 %vol. of methanol in the MEKC buffer leads to a baseline separation of all four compounds, the electropherogram is displayed in figure 49a. The migration time for 2,4,6,8-tetramethyl-DBT is about 2250 seconds, exactly the same migration time when using a buffer, which is only modified with 10 % methanol without cyclodextrins. This demonstrates that the positive effect of both, organic modifier and cyclodextrins is additive and is not accompanied by disadvantages. This effect can also be observed in the number of theoretical plates for this measurement, which range from 115.000 for 2,4,6,8-tetramethyl-DBT to 170.000 for BT.

With 20 % of organic modifier and 332 mM cyclodextrins in the buffer, a very good separation of the four PASH standard compounds can be obtained (figure 49b). The migration time for the separation is 4250 seconds and hence even shorter compared to a buffer that only contains 20 % methanol as additive. However, the number of theoretical plates is lower in this measurement due to the intensely increased migration time (BT: 145.000; DBT: 129.000; 4,6-dimethyl-DBT: 125.000; 2,4,6,8-tetramethyl-DBT: 85.000).

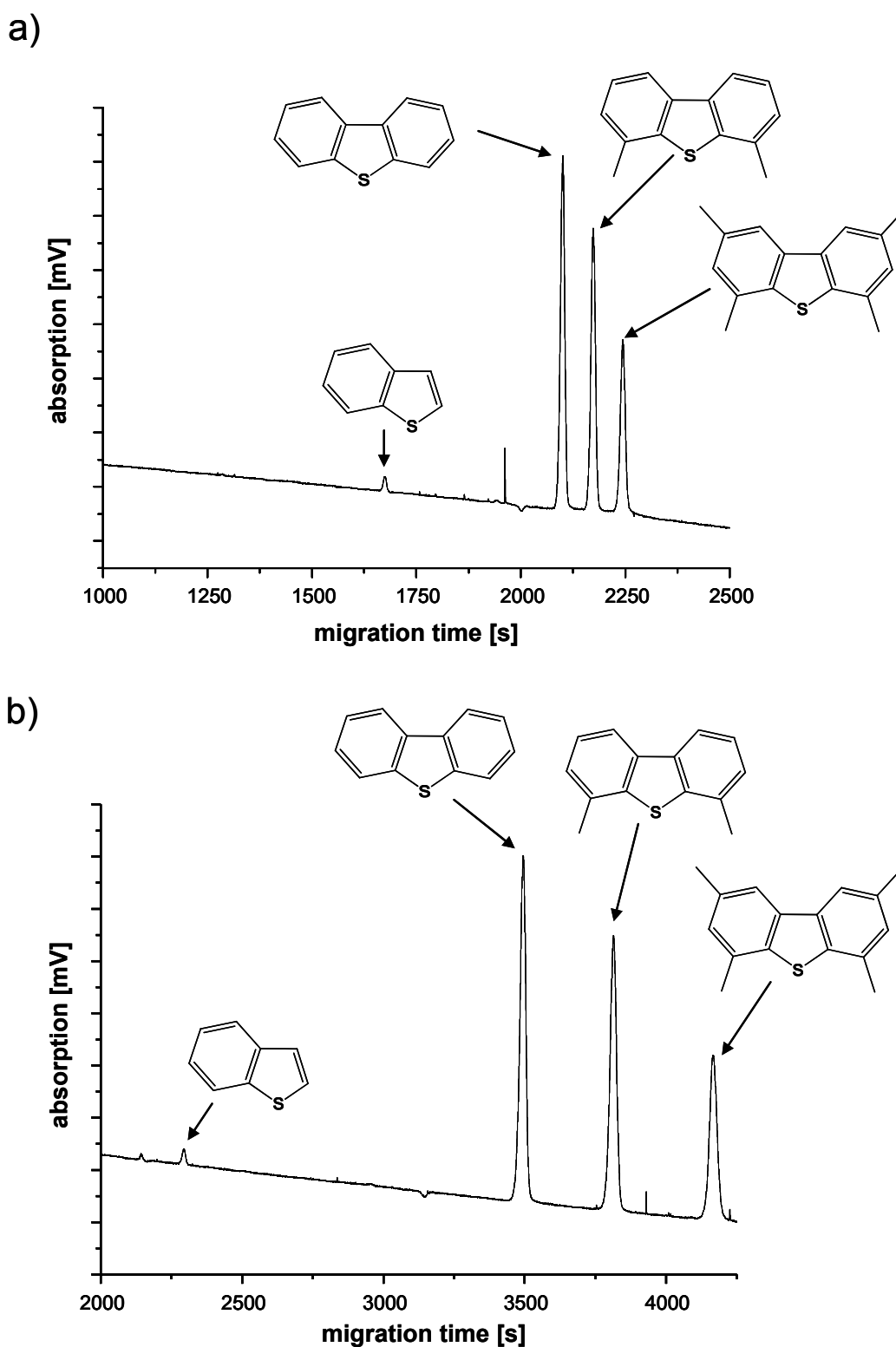


**Fig. 49: MEKC-separation of four PASH standard compounds with combined addition of organic modifier and cyclodextrins.** (BT, DBT, 4,6-dimethyl-DBT and 2,4,6,8-tetramethyl-DBT) Electrolyte: a) 100 mM SDS, 20 mM borate, pH= 9.0 containing 10 % methanol and 332 mmol/L of HP- $\beta$ -cyclodextrin b) 100 mM SDS, 20 mM borate, pH = 9.0 containing 20 % methanol and 332 mmol/L of HP- $\beta$ -cyclodextrin.

## 6.6 CE-TOF MS separation of standard compounds

The coupling of CE to TOF MS has the advantage that a second dimension is added to the separation. Compounds can hence not only be separated by migration time but according to their masses as well. A comigration of compounds is not a problem if the compounds have different masses. Especially for the separation of complex samples, as expected in real world samples, this coupling technique delivers a lot more detailed results in comparison to CE-UV. Before this technique was applied to the separation of PASH fractions from diesel fuels, the separation of standard compounds was necessary to optimize the method.

### 6.6.1 Aqueous CE-TOF MS

Because the TOF MS is incompatible with the typically used phosphate CE buffer (precipitation of the non-volatile phosphate), a completely new buffer had to be found. Best results for a buffer only containing volatile compounds were achieved with 300 mM acetic acid in water, titrated with ammonia solution to a pH of 4.0. This buffer was mixed with isopropanol 1:1. The resulting CE-buffer was used for the separation of standard compounds as described in the following.

A standard mixture of DBT, 4-methyl-DBT, 4,6-dimethyl-DBT and 4,6-diethyl-DBT, which are compounds known to occur in desulfurized diesel fuels, were methylated (figure 50) and the corresponding S-methyl-DBT ions were analyzed by CE-TOF MS.

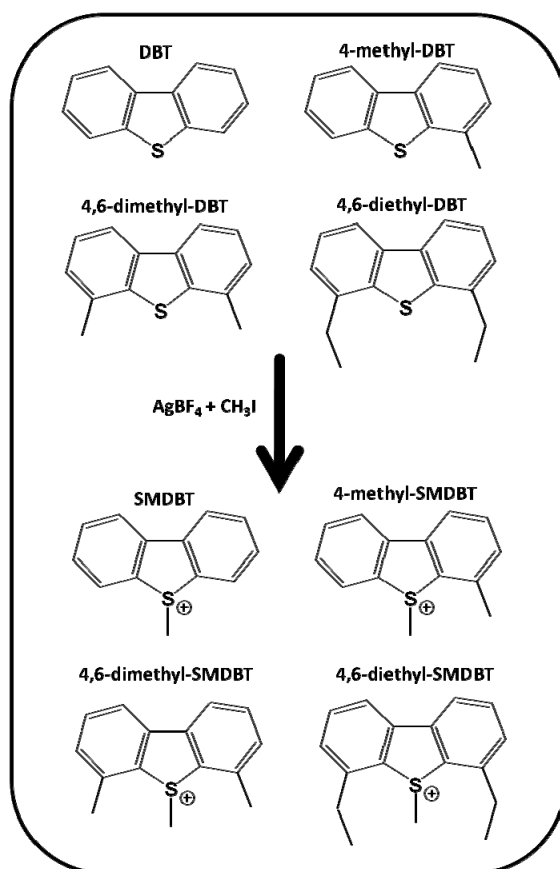


**Fig. 50: Derivatization of four standard PASHs for CE-TOF MS measurements.**

Baseline separation for all of the four compounds could easily be achieved within 16 minutes as seen in the electropherograms (figure 51). The peaks are very symmetric and no tailing was observed as sometimes found for the phosphate CE buffer. As known from previous CE-UV studies, the compounds were separated by size in aqueous buffers with the smaller compounds migrating faster than the larger ones. S-methylated DBT has the shortest migration time with 13.3 min followed by 4-methyl-S-MDBT (13.7 min), 4,6-dimethyl-S-MDBT (14.2 min) and finally 4,6-diethyl-S-MDBT (15.5 min). Each additional methyl group added to the S-methyl-DBT parent structure increases the migration time of the molecule. The extracted ion chromatograms exactly fit the calculated masses of the S-methylated PASHs.

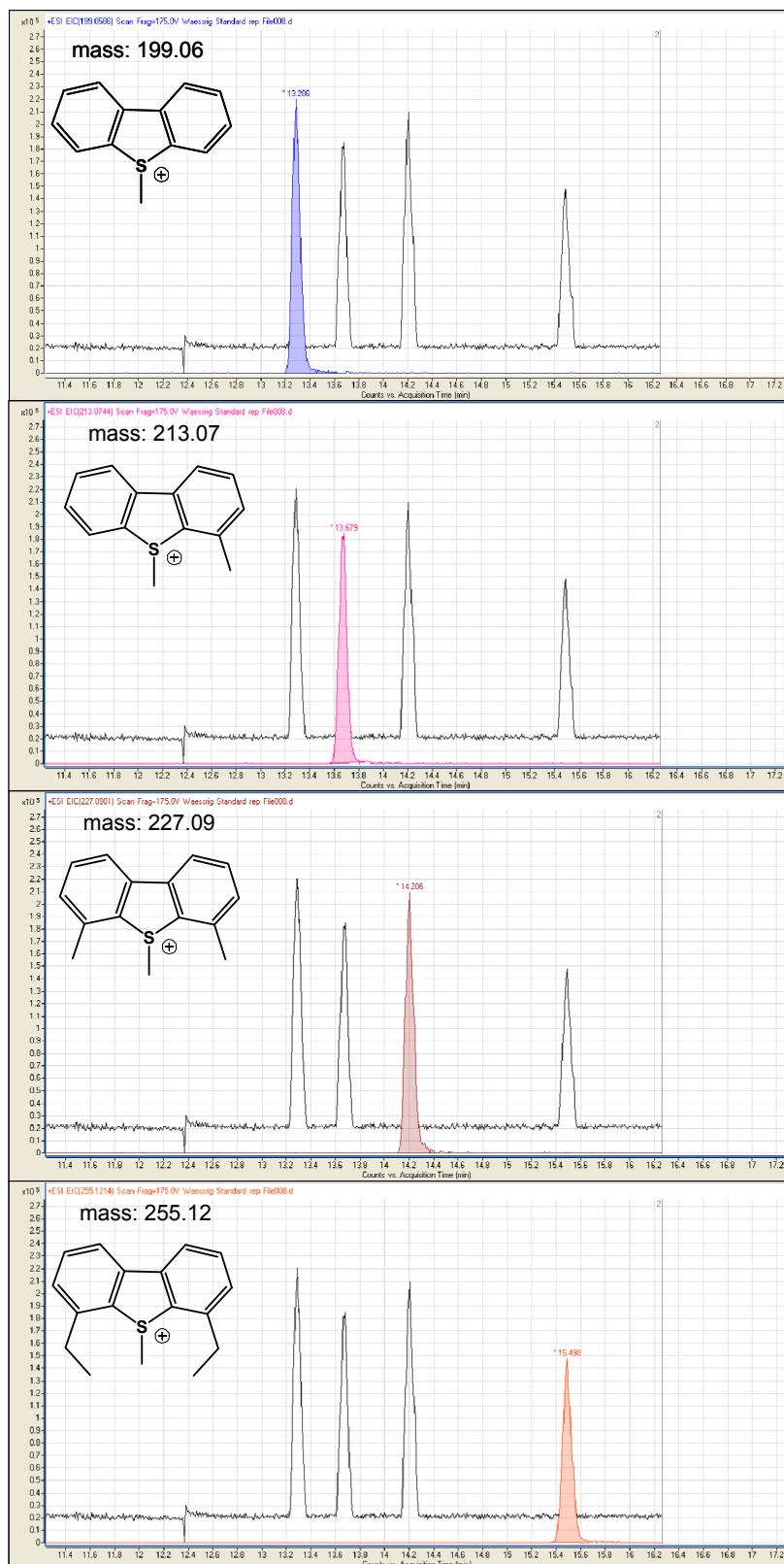


**Fig. 51: Electropherogram of the aqueous CE-TOF MS separation with extracted masses for the four analytes. (SMDBT, 4-methyl-SMDBT, 4,6-dimethyl-SMDBT and 4,6-diethyl-SMDBT) Electrolyte: 300 mM acetic acid in water, titrated to pH 4.0 with ammonia, mixed with isopropanol 1:1.**

### 6.6.2 Non-aqueous CE-TOF MS

During previous studies [23] it was demonstrated that the separation of thiophenium ions can be performed in completely nonaqueous media. Because this technique had a major influence on resolution, a CE-TOF MS separation of standard compounds using nonaqueous CE was of interest.

The previously used standard mixture of DBT, 4-methyl-DBT, 4,6-dimethyl-DBT and 4,6-diethyl-DBT was methylated and the corresponding SMDBTs analyzed by nonaqueous CE-TOF MS. The used electrolyte buffer was composed of 4 % acetic acid in methanol with an addition of 60 mM ammonium formate. A separation of all four compounds was finished within 9.5 minutes, as can be seen in the electropherogram (figure 52). Differing from the results of aqueous CE, the compounds were not separated by size. The migration order changes when purely organic media is used. The fastest migrating compound is 4-methyl-DBT which comigrates with 4,6-dimethyl-DBT. The compound with the longest migration time is 4,6-diethyl-DBT, while the compound with the smallest molecular volume, DBT, migrates in-between the other compounds. Nevertheless, the extracted ion electropherograms exactly fit the calculated masses of the S-methylated PASHs and the signals show a good resolution with symmetric peaks.

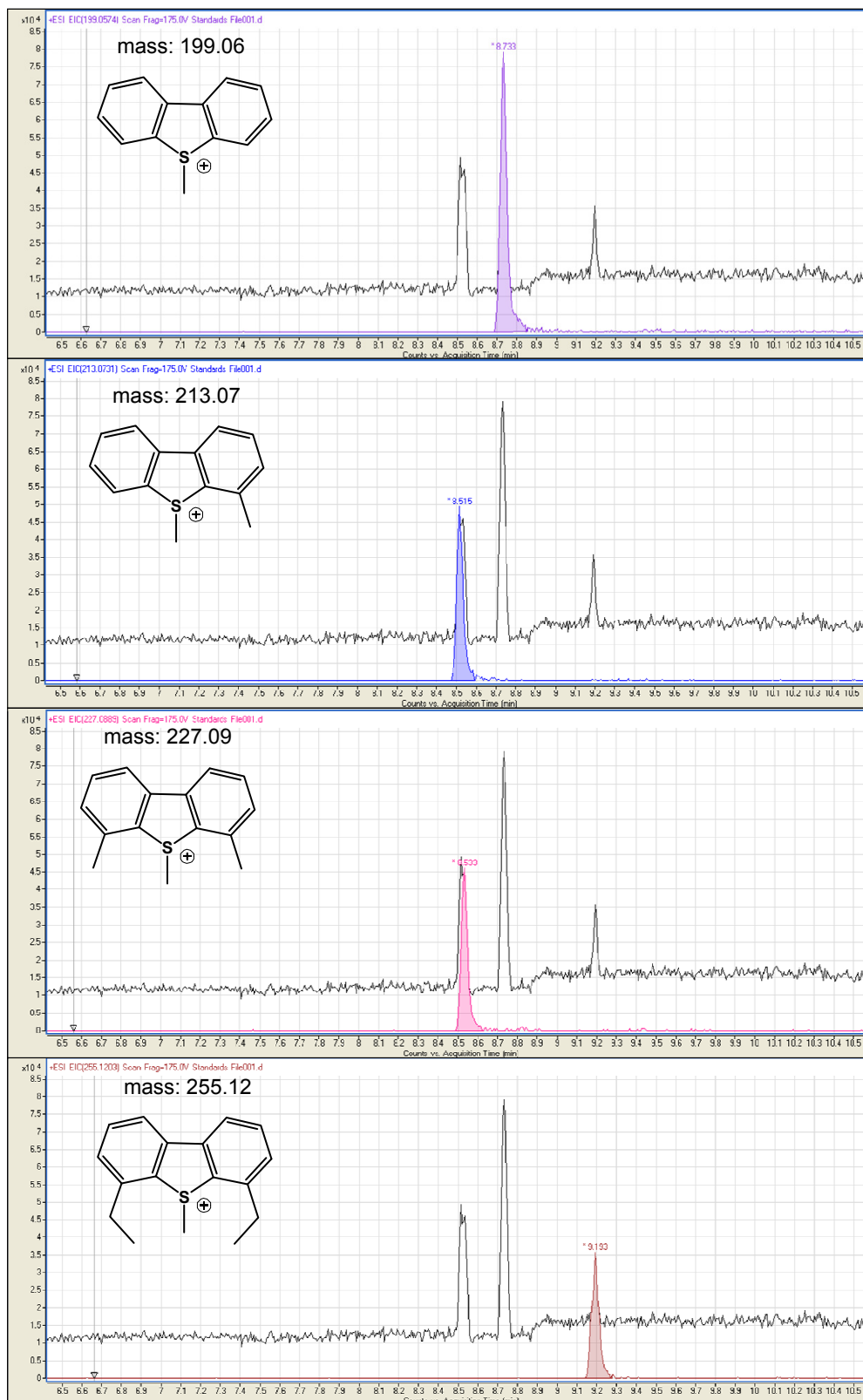


**Fig. 52: Electropherogram of the nonaqueous CE-TOF MS separation with extracted masses for the four analytes. (SMDBT, 4-methyl-SMDBT, 4,6-dimethyl-SMDBT and 4,6-diethyl-SMDBT) Electrolyte: 4 % acetic acid in methanol with addition of 60 mM ammonium formate.**



## 6.7 Discussion

In the last chapter different electrophoretic methods and techniques for the separation of standard PASHs were introduced. The studies focussed on the separation of derivatized compounds.

The derivatization of the compounds is necessary to gain electrophoretic mobility for the analytes. Two techniques for the derivatization of the PASHs were introduced, the methylation and the phenylation reaction. The results reveal that the phenylation reaction is accompanied by several drawbacks. Due to the bulky derivatization group, these compounds are larger and hence they migrate more slowly. The increased migration time leads to a higher longitudinal diffusion which results in broader signals and reduced resolution. Due to that reason, the phenylation reaction was not used for further derivatizations of PASHs.

The addition of cyclodextrins to the running buffer was introduced as a technique that can increase the resolution of the separation. This was clearly demonstrated by the separation of all the monomethyl-BT isomers which is impossible with standard GC methods, including stationary phases with higher polarity. Nevertheless, this technique comes with a major drawback: When higher concentrations of cyclodextrins are used in the separation, an additional enantiomeric separation of the derivatized PASHs occurs. This means that for nearly all of the compounds two signals appear. This may not be regarded as a problem if non-complex samples are used but might be disadvantageous for the separation of real world samples which contain hundreds of different compounds. The amount of signals would double due to the enantiomeric separation and thus destroy the positive effect on the resolution by the cyclodextrins. Nevertheless the enantiomeric separation of S-methyl- and S-phenylthiophenium salts is of interest since some of these compounds can be used for asymmetric alkylations [117] and cationic polymerization [118-120].

The correlation of the calculated volume and the migration time is an interesting aspect, because the prediction of migrations times is possible. Moreover, the migration time of a compound might give hints as to the structure of an unknown compound. However, this correlation cannot be used for all of the derivatized PASHs. It seems to work quite well up to a certain degree of alkylation of the compounds. Derivatized monoalkylated dibenzothiophenes with long alkyl chains showed a higher migration time than expected by

the calculations so that a prediction of migration times was only possible by using a quadratic function. The reason for this might be the folding of the long alkyl chains in aqueous media. Because the software used for the calculation is limited to the energy minimization for compounds in vacuum, the optimized structure in aqueous media might be very different. As no software exists that can calculate the behavior of derivatized PASHs with long alkyl chains dissolved in aqueous media, the correlation between molecular volume and migration time is limited. Further studies on the structures of a large variety of PASHs would be necessary to be able to apply this method to real world samples, including high-boiling PASHs.

SDS-MEKC was introduced as a method in which the analytes themselves do not need to be charged, because they are transported in charged micelles. Using this method for the separation of PASHs is very attractive, because the time consuming derivatization reaction can be avoided. Nevertheless, this method has some disadvantages. The analytes show a very strong interaction with the micelles so that most PASHs migrate with  $t_m$ . Especially compounds with more alkyl groups in the side chains interact strongly with the micelles, so that a separation can only be achieved by using different buffer additives. An addition of organic modifier and cyclodextrins led to a nice separation of several standard PASHs with up to four methyl groups. For the separation of real world samples this buffer might, however, still be insufficient. High-boiling samples are expected to contain compounds with 10 and more carbon atoms in the side chains. These compounds are highly hydrophobic and for that reason might not be separable by MEKC.

At the end of the last chapter the coupling of CE to TOF MS for the separation of derivatized PASHs was demonstrated. This method is quite promising because a lot of additional information can be gained. Especially for the separation of complex samples it might be advantageous because comigration is not a problem if the masses of the analytes differ. The peak shapes for both aqueous and non-aqueous CE-TOF MS were superb, so that maximal resolution can be expected. The use of completely organic media has the major advantage that the solubility of high-molecular derivatized PASHs might be better in such media than in aqueous solution. Additionally, nonaqueous CE leads to shorter migration times which might be an explanation for the narrow peaks: the longitudinal diffusion of the analytes in the capillary is minimized by the short analysis time.

## 7 CE separation of PASHs from real world samples

The studies dealing with the electrophoretic separation of PASH standard compounds were used as a basis for the analysis of PASHs from real world samples. In the course of this work, a large variety of real world samples was separated by CE. However, only a part of these samples will be presented in the following chapter to focus the work on the techniques used. These samples, mostly provided by *Synchrude Canada*, ranged from low-boiling gas oils to high boiling gas oils, both desulfurized and non-desulfurized. To evaluate the different CE methods, in most cases comparisons with commonly used techniques like GC-FID were performed. Each of the different real world samples will be briefly introduced in the individual chapters.

### 7.1 Danish diesel fuel

The Danish diesel fuel is the first real world sample that was used for the CE separation of PASHs. First attempts of the separation of this sample were done in the previous diploma thesis [23]. Because the sample dates back to 2001, it is only desulfurized to 50 ppm of sulfur content, which simplified the analysis with CE-UV. During the diploma thesis, the CE-UV separation of this sample was compared with a GC measurement, with atomic emission detection, and it was obvious that the electropherogram looked very similar to the chromatogram (figure 53). However, the separation efficiency of the CE method was still lower than the one obtained by GC-AED.

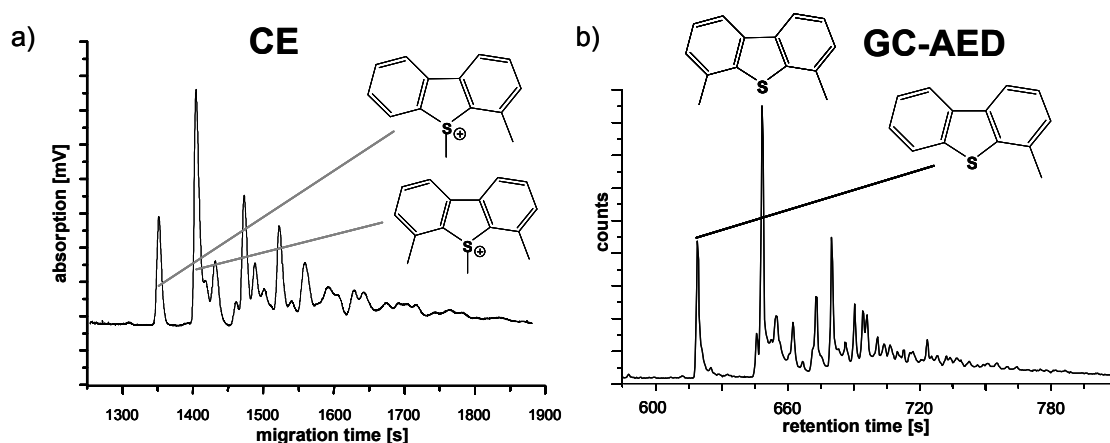


**Fig. 53:** a) Capillary electrophoretic separation of the methylated PASH fraction of a desulfurized diesel fuel. Electrolyte: phosphate buffer 50 mM, pH 2.15, 20 % isopropanol at a voltage of 20 kV b) GC-AED separation of a PASH fraction of a desulfurized diesel fuel.

In this work, the sample was used for the comparison with the commonly used RP-HPLC. Furthermore the addition of cyclodextrins to the electrophoresis buffer was tested for this real world sample.

The ligand exchange procedure described in chapter 5.4 was used for the isolation of the PASHs from the diesel fuel matrix.

### 7.1.1 Comparison to HPLC

The CE analysis of PASH standard compounds demonstrated that separations can be obtained with very good resolutions. To compare the resolution with the commonly used techniques, a measurement of the PASH fraction of this fuel with RP-HPLC was performed. The PASHs were isolated from the Danish diesel fuel sample by LEC and afterwards divided into two parts. One part was methylated for the CE-UV measurements while the other part was directly used for the HPLC separation, without prior derivatization.

The resulting electropherogram and the RP-HPLC chromatogram are shown in figure 54. The resolution of the CE method is significantly higher than of the RP-HPLC. While the most abundant analytes in the sample, 4-methyl-DBT and 4,6-dimethyl-DBT, are completely baseline separated by the CE method, they elute only scarcely baseline separated in RP-HPLC. The larger compounds seem to be better resolved for CE, because more individual signals can be observed in the electropherogram, while coelution can be observed in HPLC. A large difference in the analysis time is noticeable. While the CE separation is finished after roughly 2000 seconds, the HPLC method needs about 5000 seconds before the last compounds elute. However, both methods have a lower resolution than GC. An identification of single compounds is very difficult because severe comigration and accordingly coelution for both methods occur.

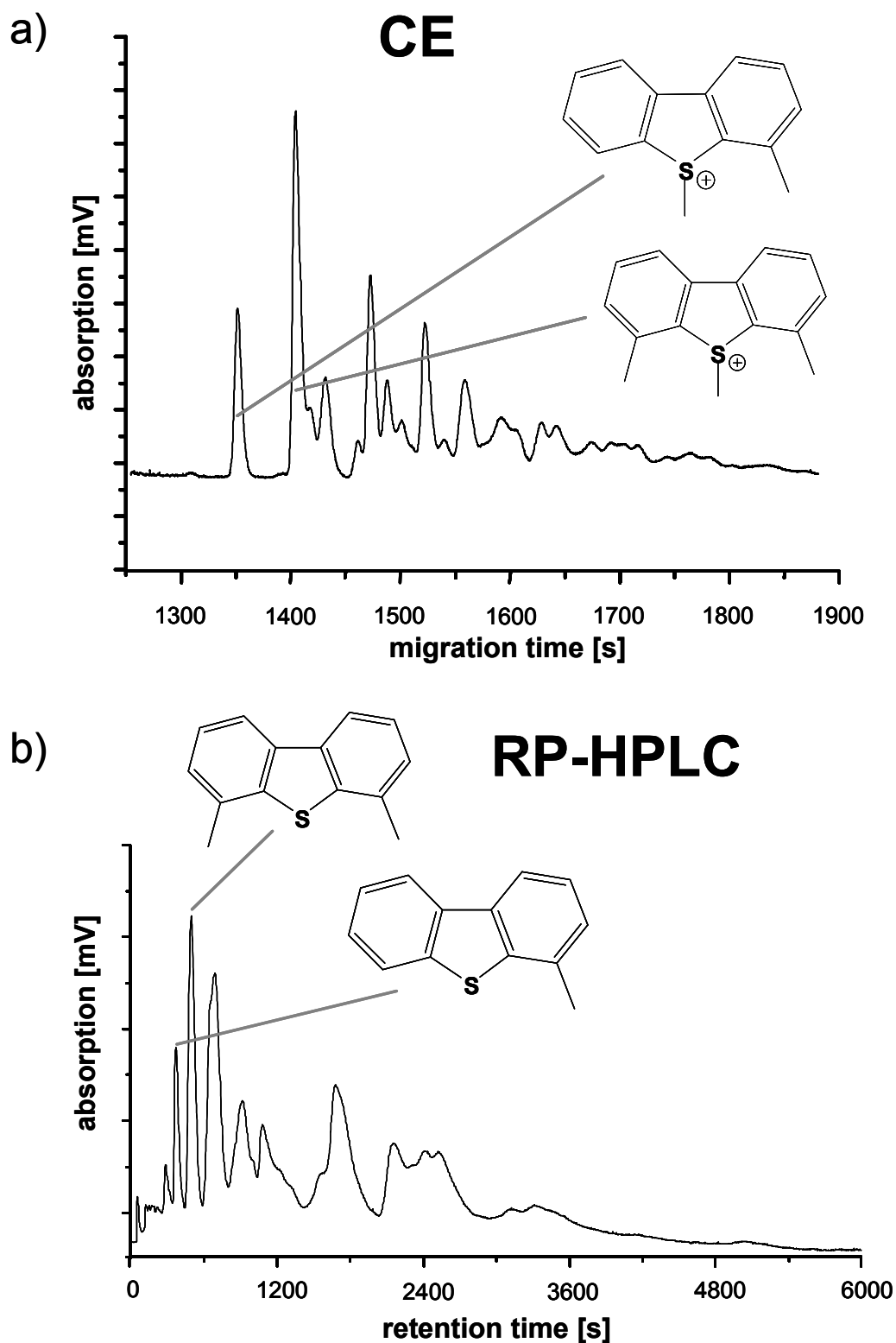


**Fig. 54: a) Capillary electrophoretic separation of the methylated PASH fraction of a desulfurized diesel fuel.** Electrolyte: phosphate buffer 50 mM, pH 2.15, 20 % isopropanol at a voltage of 20 kV **b) HPLC separation of a PASH fraction of a desulfurized diesel fuel.** (150 mm RP18 column, 60 % acetonitrile in water, without gradient, 1 mL/min)

### 7.1.2 Addition of cyclodextrins

Very good results were obtained for the CE separation of PASH standard compounds when cyclodextrin was added to the running buffer. The resolution could be increased and even the separation of all six monomethyl-benzothiophene isomers was possible. However, due to the additional enantiomeric separation of the compounds, the amount of signals in the electropherograms increased. The applicability of this method to the separation of real world samples was hence doubtful. A complex real world sample would probably come with a drastically increased complexity due to a doubling of the peaks. To evaluate the effect, the methylated PASH fraction of the Danish diesel fuel sample was separated by CE, once with the normal CE buffer and once with a buffer modified with cyclodextrins. The cyclodextrin of choice was  $\beta$ -cyclodextrin, because in contrast to hydroxypropyl- $\alpha$ -cyclodextrin no direct enantiomeric separation of methylated PASH was observable. The electropherograms for both separations are displayed in figure 55.

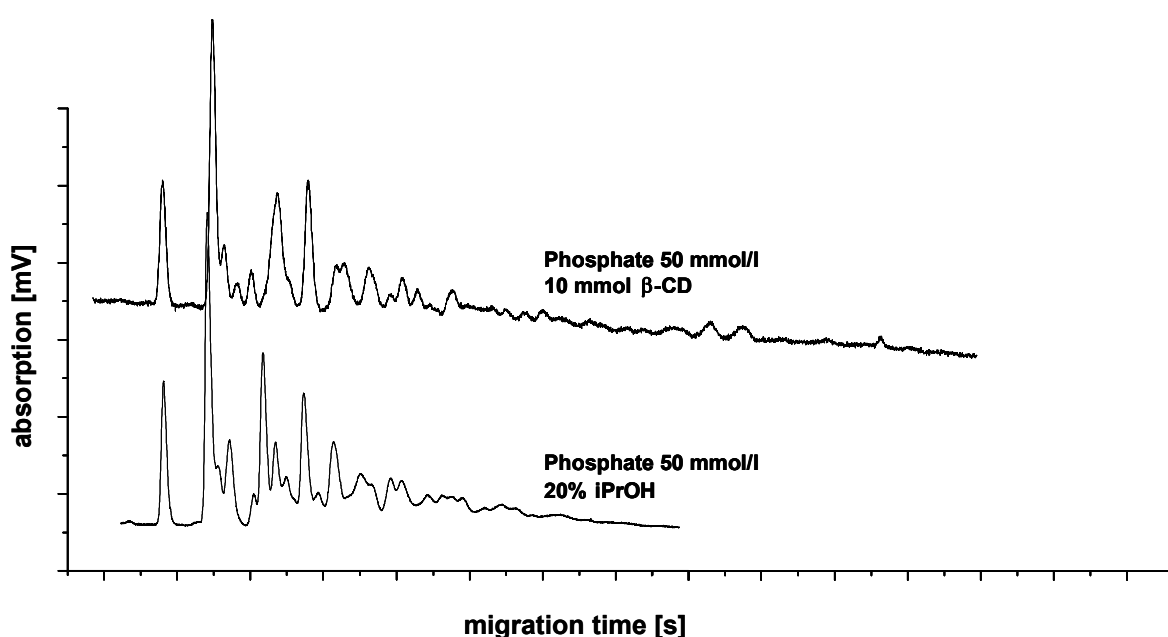


**Fig. 55:** Separation of a real world sample (diesel fuel Denmark, 2001) with and without  $\beta$ -CD. Electrolyte: phosphate buffer 50 mM, pH 2.15, 10 mM  $\beta$ -cyclodextrin and 20 % isopropanol at a voltage of 20 kV.

The resolution of the first signals, which belong to 4-methyl-DBT and 4,6-dimethyl-DBT is not strongly influenced by the addition of cyclodextrins to the running buffer. Especially for 4-methyl-DBT, no enantiomeric peak occurs, a result of the low concentration of

$\beta$ -cyclodextrin. An influence on the resolution can be found for the larger compounds and is related to the size of the cavity of the cyclodextrins. The larger compounds fit better into the cavity and are hence more strongly influenced. The migration times of these analyte-cyclodextrin complexes are longer, because the whole complex is larger, but still only contains a charge of +1, so that the electrophoretic mobility is decreased. This explains why the signals in the upper electropherogram migrate later. Nevertheless it is difficult to say if some of the compounds show enantiomeric separations as well. Especially for some of the later migrating signals it seems like double peaks occur. To avoid this increase of complexity, for all following separations of real world samples, no cyclodextrins were used in the running buffer.

## **7.2 Desulfurized Syncrude light gas oils**

Three samples of light gas oil (LGO) gathered from different desulfurization steps during the refining process were provided by Syncrude. The first of the three samples originated from the feedstock of the fuel before desulfurization. The second sample was partly treated by HDS in a first desulfurization step. The third sample was the completely hydrodesulfurized product that can be used directly as transportation fuel. Due to the fact that this sample has a very low boiling range, most of the sulfur content can easily be removed during the HDS. While the feedstock sample was expected to contain a variety of small to middle sized PASHs, the partly and completely hydrodesulfurized samples were expected to contain very low quantities of sulfur. A capillary electrophoretic separation of the PASH fractions of all three LGOs was performed to demonstrate that the CE method is applicable to fuels from different HDS stages. In addition to the commonly used phosphate CE buffer, a nonaqueous CE buffer was tested for the separation of the derivatized PASHs. Furthermore, an MEKC analysis of the LGO-feedstock sample was performed to evaluate if MEKC can be applied to real world samples as well.

### **7.2.1 Separation of the three derivatized LGO samples**

The PASHs of all three samples (feedstock, first-HDS-step, final) were isolated by LEC and the isolated fractions were derivatized using the methylation reaction. The derivatized feedstock PASHs were separated by CE and some of the components identified by spiking the sample (figure 56). The shape of the electropherogram is very complex, the identification of any single compounds nearly impossible. Only the first part of the

electropherogram is shown, as no information was obtained from migration times beyond 2000 seconds, because here the resolution was so low that no individual signals were obtained. The signal reaches the baseline after 3500 seconds. Nevertheless, low concentrations of BT can be identified in the sample and signals for DBT, 4-methyl-DBT and 4,6-dimethyl-DBT are found, although comigration with other compounds occurs. The complexity of the sample can be explained by the fact that the feedstock is not desulfurized. This also explains the high concentrations of alkylated BTs in the sample that can be found at migration times around 1250 seconds. Because these low boiling sulfur compounds can easily be removed during the desulfurization process, they should only be present in this sample but not in the other two HDS treated samples.

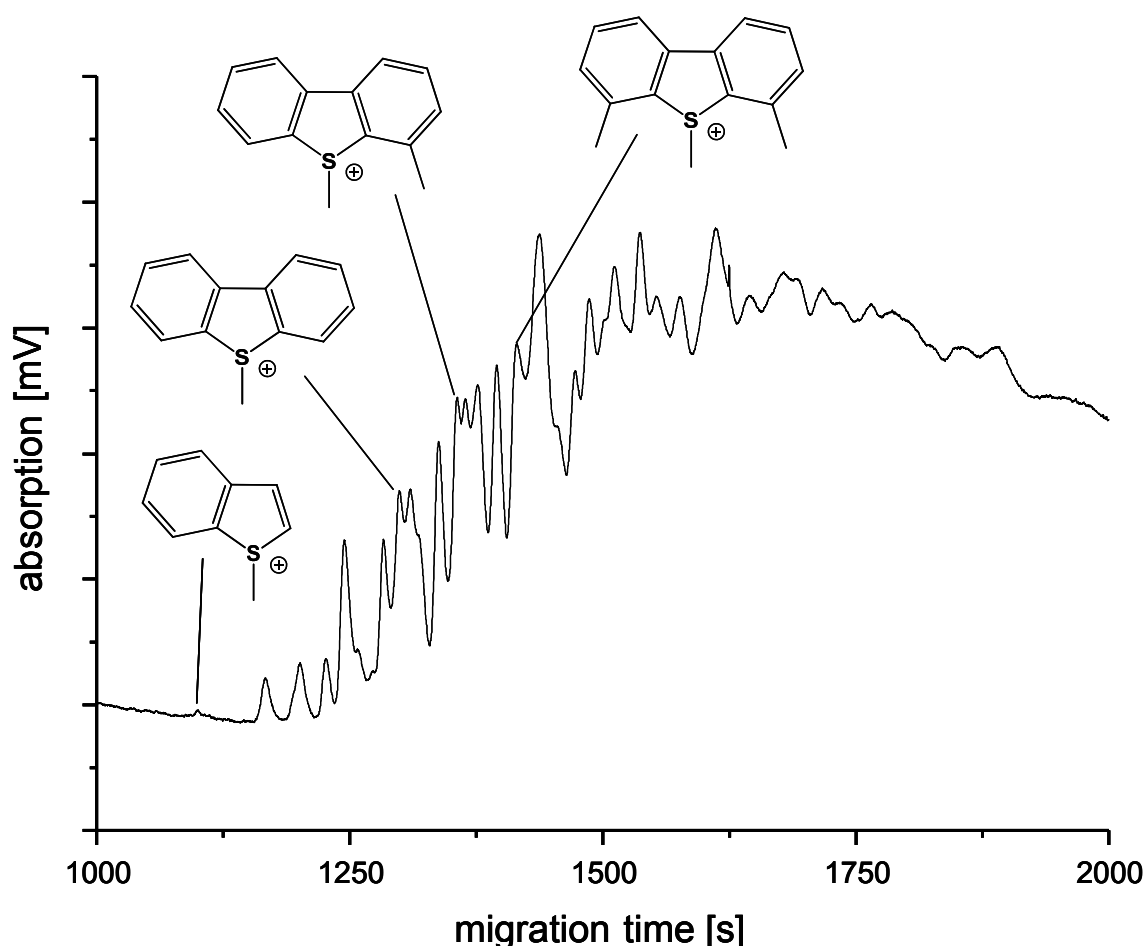


**Fig. 56: Electropherogram of the separation of the feedstock LGO PASHs.** Electrolyte: phosphate buffer 50 mM, pH 2.15 and 20 % isopropanol at a voltage of 20 kV.



This assumption was confirmed by the separation of the second LGO sample which was treated in a first desulfurization stage. The electropherogram is less complex and it is much easier to identify individual compounds (figure 57). The smallest compound identified by spiking is DBT, followed by 4-methyl-DBT. Signals for BT or alkylated BTs, as present in the feedstock sample, cannot be observed for the first stage HDS product.

The separation of the final stage product did not lead to evaluable results that could be interpreted. The signals were hardly detectable in the signal noise of the measurement. Apparently, most of the sulfur containing compounds were removed by HDS in this sample. As the CE was coupled to a common UV detector, the detection was limited. Better results might be obtained by using CE-fluorescence or CE-MS.

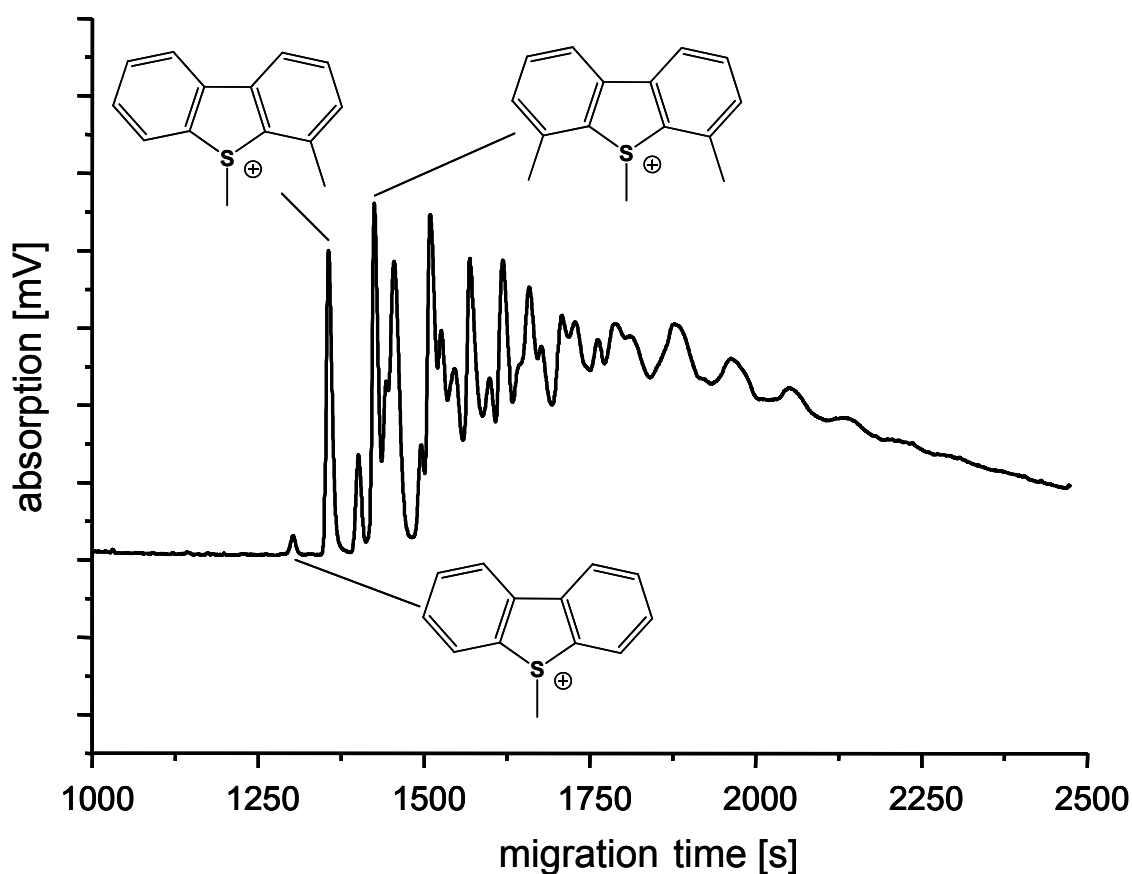


**Fig. 57: Electropherogram of the separation of the first-stage LGO PASHs.** Electrolyte: phosphate buffer 50 mM, pH 2.15 and 20 % isopropanol at a voltage of 20 kV.

### 7.2.2 Partly-aqueous and non-aqueous CE of the first stage sample

In previous studies, the separation of derivatized PASH in completely organic media was demonstrated. This kind of nonaqueous CE massively influences the resolution of the separation and the migration of the compounds. A separation of a real world sample in completely organic media had not been performed so far. Because the first stage desulfurized LGO sample was not too complex in its PASH composition and the main constituents were known, a nonaqueous CE separation of this sample was carried out to examine the effects of nonaqueous running buffers on the separation of complex samples. The CE buffer used for this separation was prepared by dissolving 4 % acetic acid in methanol with an addition of 60 mM ammonium formate. In addition to this separation, an increase of the isopropanol concentration for the normal phosphate buffer from 20 % to 40 % was tested to determine the influence on the separation of real world samples.

The electropherograms for all separations as an overlay (different migration times on x-axis) are presented in figure 58. The migration times of the different measurements were very different but are left out in this diagram. The electropherogram of the sample with a completely organic buffer is obviously more compact than the other ones. It is difficult to identify individual compounds in the sample because most of the signals comigrate. In comparison to the typically used buffer with 20 % isopropanol, the resolution is lower. An increase of the isopropanol concentration from 20 % to 40 % results in better resolution, especially for the later migrating compounds but was accompanied by longer migration times. Concentrations higher than 40 % of isopropanol were not tested, as the baseline became unstable and the measurements were aborted.

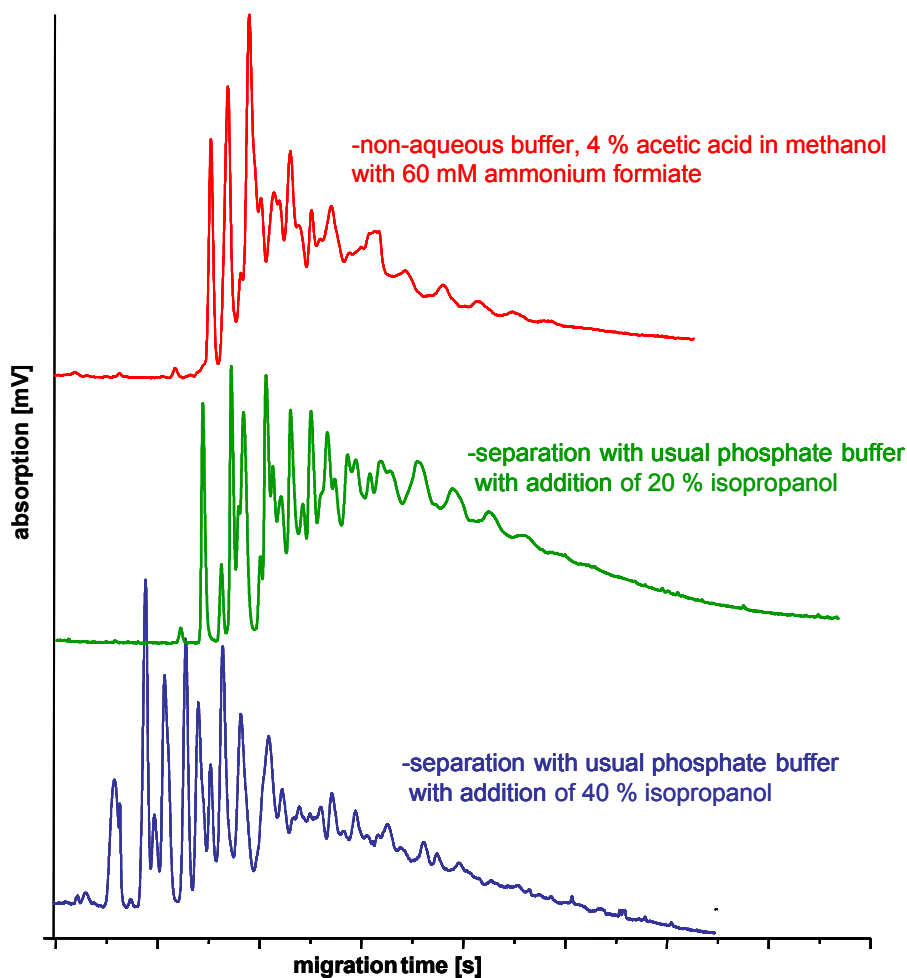


**Fig. 58: Electropherogram for the separation of the first-stage LGO PASHs with nonaqueous CE and aqueous CE with addition of different isopropanol concentrations.** (Different time scales on x-axis in the three electropherograms) Electrolyte: nonaqueous CE (red electropherogram) 4 % acetic acid in methanol with 60 mM ammonium formate; aqueous CE with 20 % isopropanol (green electropherogram) phosphate buffer 50 mM, pH 2.15 and 20 % isopropanol at a voltage of 20 kV; aqueous CE with 40 % isopropanol (blue electropherogram) phosphate buffer 50 mM, pH 2.15 and 20 % isopropanol at a voltage of 20 kV.

### 7.2.3 MEKC of the feedstock sample

In chapter 6.5 the separation of underivatized PASH standard compounds by MEKC was demonstrated. However, the applicability to real world samples was questionable because it was difficult to separate the higher molecular compounds. Due to their hydrophobicity the interaction with the micelles is very strong and a sufficient separation can only be performed when an organic modifier and cyclodextrins are added to the buffer. The buffer

that gave the best results for the separation of the standard compounds was hence tested for the separation of a complex real world sample.

The PASH fraction of the feedstock sample was isolated by ligand exchange chromatography and afterwards separated by MEKC using a buffer containing 20 % methanol and 332 mM of HP- $\beta$ -cyclodextrin additionally to the SDS. The resulting electropherogram is displayed in figure 59.

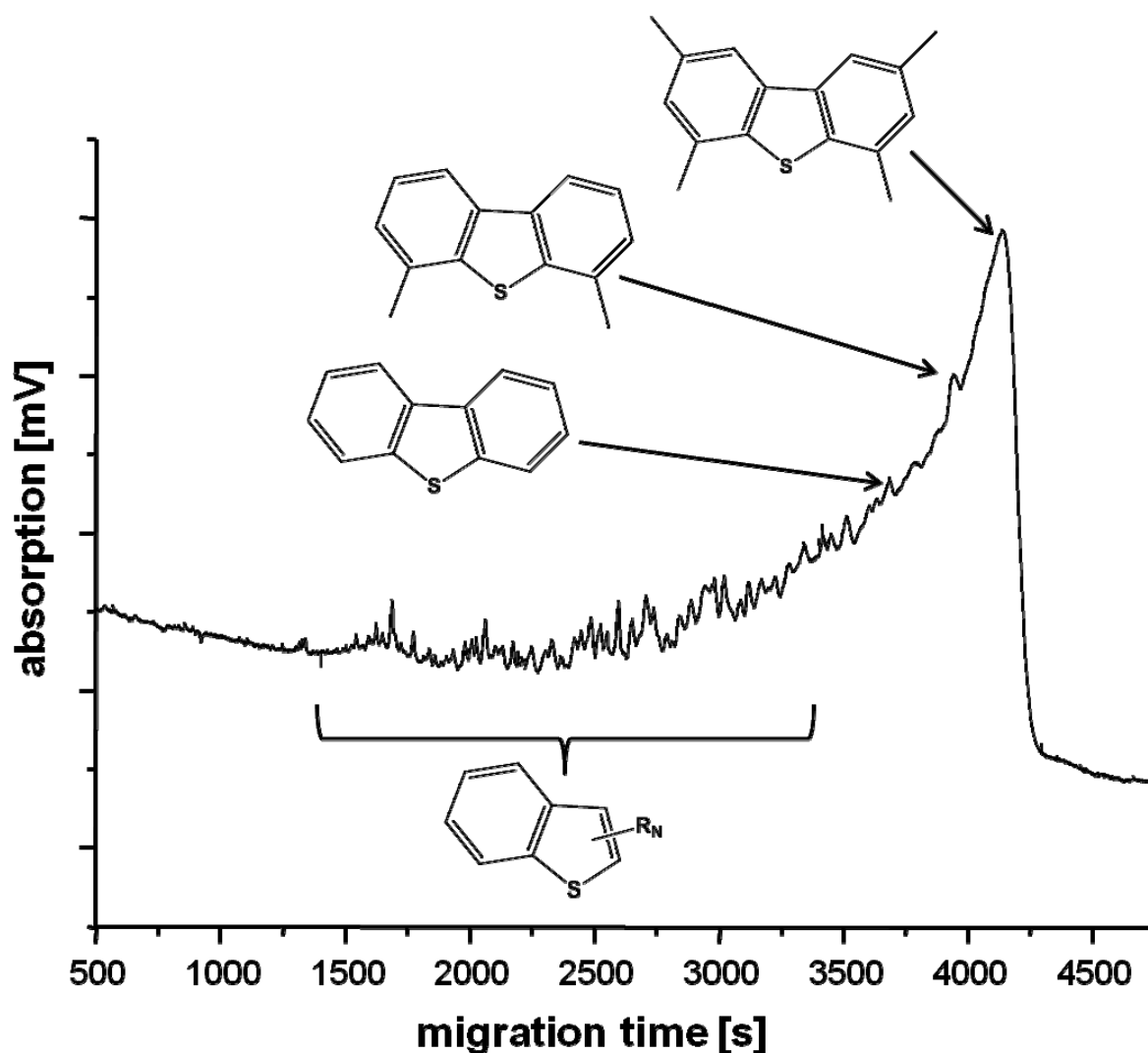


**Fig. 59: MEKC separation of the LGO feedstock PASHs.** Electrolyte: 100 mM SDS, 20 mM borate, pH = 9.0 containing 20 % methanol and 332 mmol/L of HP- $\beta$ -cyclodextrin.

As expected, a separation, especially of the higher molecular compounds, is impossible. All these compounds migrate at the end of the micellar window, so that at a migration time

of 4000 seconds, a large signal for all these compounds occurs. The signals for DBT, 4-methyl-DBT and 2,4,6,8-tetramethyl-DBT can only roughly be identified by spiking the sample with the references. Nevertheless, the separation shows a good resolution for the smaller compounds, like alkylated benzothiophenes. For the analysis of desulfurized fuels though, MEKC is not useful because the expected compounds are too hydrophobic to be separated.

### **7.3 Syncrude heavy gas oils at different desulfurization stages**

A series of three samples, derived from different hydrodesulfurization stages of a heavy gas oil, was provided by Syncrude. The first sample was the untreated feedstock of the heavy gas oil, while the other two samples were hydrodesulfurized at 370 °C and 385 °C. The PASH fractions of all three samples were isolated by LEC and analyzed by gas chromatography to get a first insight into the composition of the sample. The corresponding GC parameters are given in the appendix (chapter 10.6). The GC analysis of the PASH fraction of the HGO feedstock in comparison to the LGO feedstock that was used in the last chapter demonstrates the higher boiling range of this sample (figure 60). An additional measurement with three standard PASHs (DBT, 4-methyl-DBT and 4,6-dimethyl-DBT) reveals that these compounds are among the smallest ones to expect in the HGO sample additionally to low concentrations of alkylated BTs.

In the next step, the isolated PASHs from the feedstock were methylated and subsequently separated by CE. The resulting electropherogram (figure 61) is extremely complex, only the smallest compounds can be separated, while massive comigration for all the larger compounds occurs. The separation was terminated after 3000 seconds although the signal had not reached the baseline at that time. As already seen for the LGO feedstock, non-desulfurized samples are far too complex for the analysis by CE GC analysis of these samples has a significantly higher resolution.

The three reference compounds that were used in GC can be identified in the electropherogram as well. Low concentrations of DBT are observed as the smallest PASH compound in the feedstock. 4-methyl-DBT is present in slightly higher concentrations. However, comigration with other compounds is likely. Between these two signals (DBT and 4-methyl-DBT), small signals of other compounds can be found. These should be higher alkylated BTs, because 4-methyl-DBT is the smallest (and hence fastest migrating)

of the monoalkylated DBTs. This result corresponds quite well to the GC-measurements, which showed small concentrations of alkylated BTs as well.

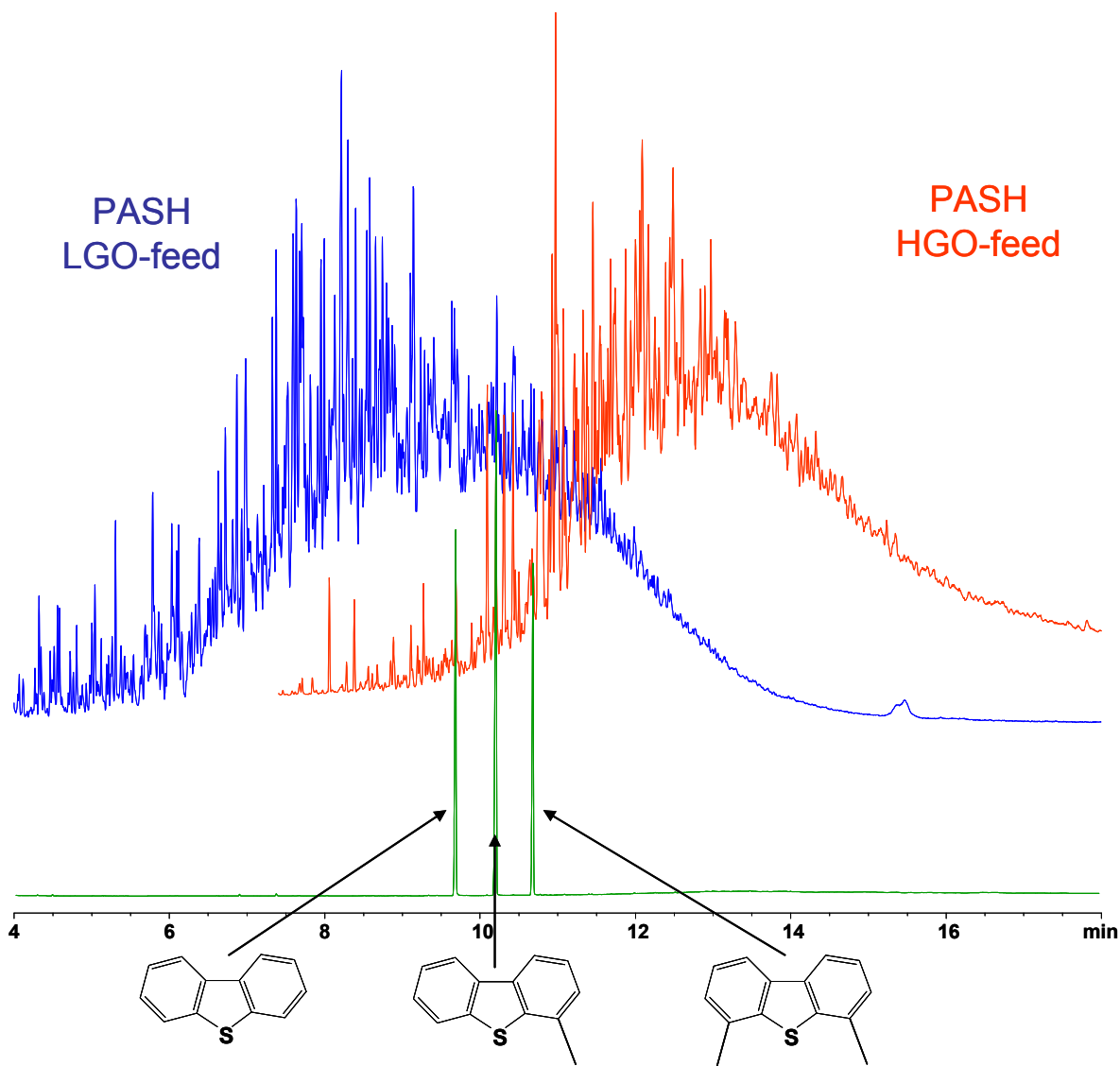


**Fig. 60: GC-separation of LGO-feedstock (blue) and HGO-feedstock (red) PASHs with the identification through reference compounds (green).**

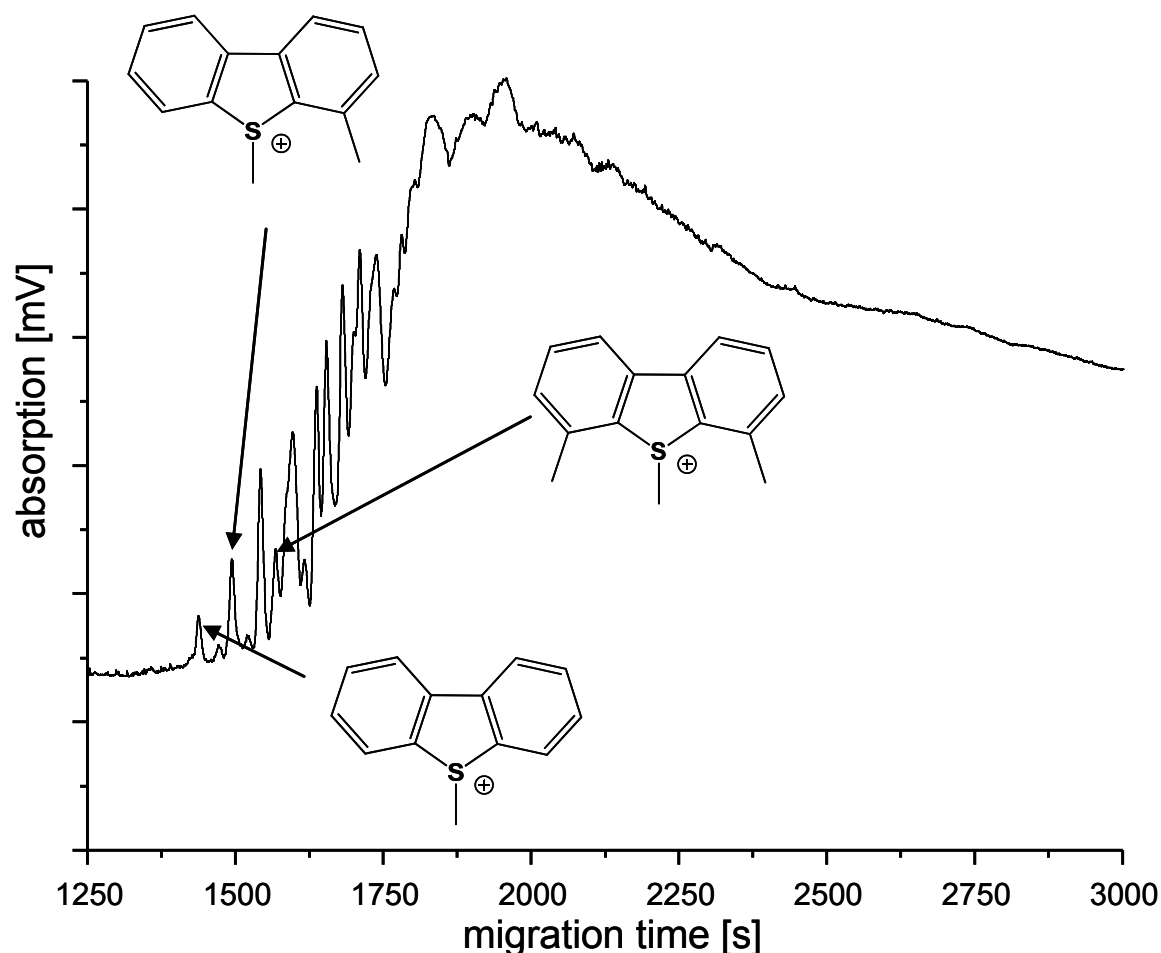


**Fig. 61: CE-separation of the HGO-feedstock PASHs.** Electrolyte: phosphate buffer 50 mM, pH 2.15 and 20 % isopropanol at a voltage of 20 kV.

The next samples to be analyzed were the two HGOs, which were treated at different temperatures during the HDS process. Due to the fact that a temperature increase of 15 °C during HDS should only have a small effect on the pattern of the recalcitrant PASHs, both samples were expected to be very similar. This assumption was supported by a GC measurement presented in figure 62. The complexity of the samples is obviously lower than that of the feedstock. High concentrations of 4-methyl-DBT and 4,6-dimethyl-DBT can be identified in the sample. The high concentration of these two compounds can easily be explained by their low reactivity during the HDS process: the methyl groups in 4- and 6- position inhibit an approach of the sulfur atom to the HDS catalyst, so that these compounds are desulfurized less efficiently than other ones as explained in chapter 1.4. The concentration of the less recalcitrant compounds in the hydrotreated product was therefore lower, while the concentration of the recalcitrant compounds did not decrease in

the same extent. This led to an enrichment of these PASHs in the samples. DBT is now the smallest compound, probably followed by 4-methyl-DBT as this is the fastest migrating C1-DBT.

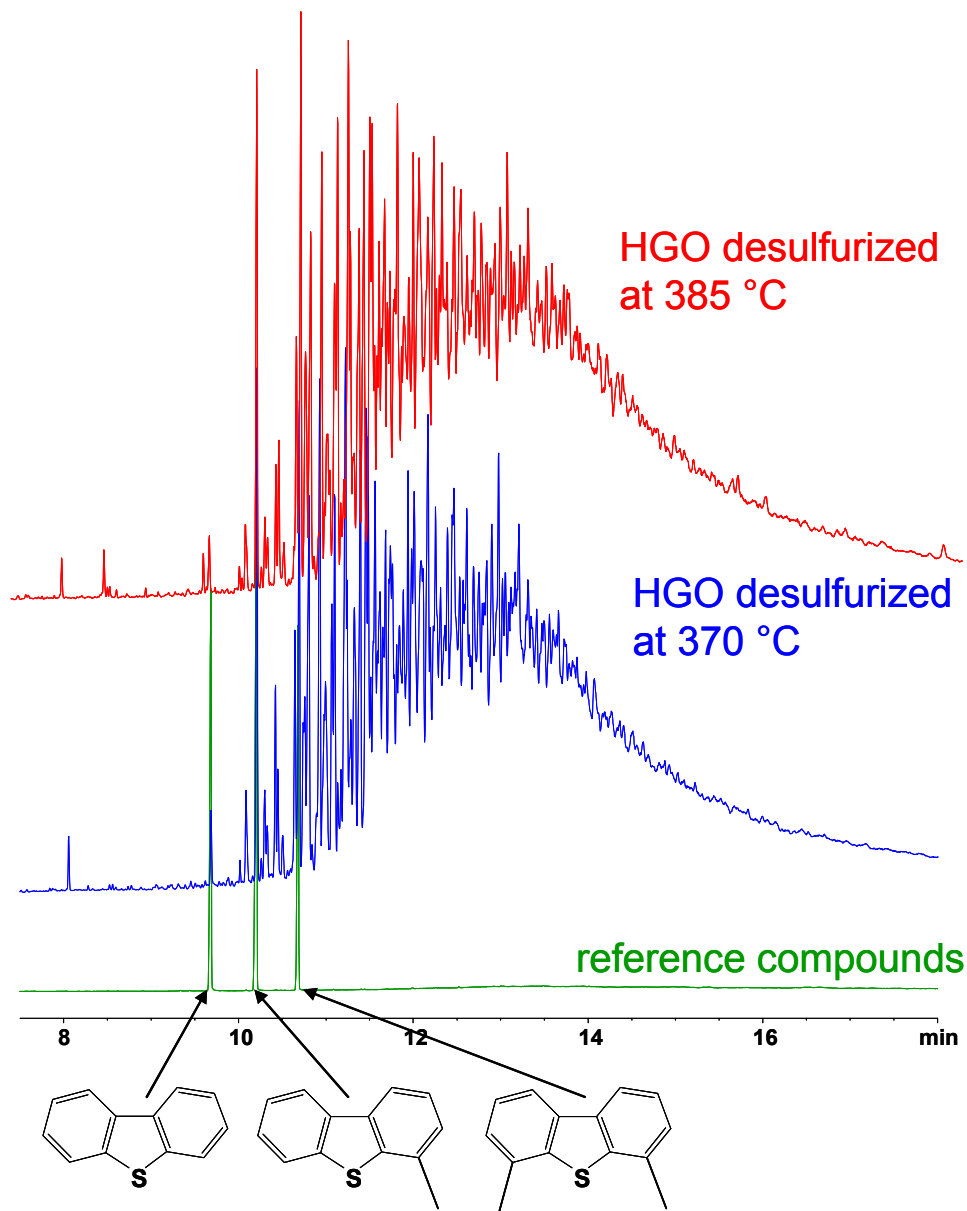


**Fig. 62: GC-separation of desulfurized HGO PASHs after desulfurization at 385 °C (red) and desulfurization at 370 °C (blue) and reference compounds (green).**

The information on the sample, gained by the GC analysis, is supported by the results from the CE measurements presented in figure 63. In both samples the smallest PASH found is DBT, followed by 4-methyl-DBT as smallest of the C1-DBTs. Alkylated BTs or thiophenes are not present in this sample, because these compounds were removed during



the hydrotreatment. Only low concentrations of DBT are left after the desulfurization at both temperatures. The concentrations for 4-Me-DBT and 4,6-DiMe-DBT are quite similar which supports the results from the GC analysis. The electropherograms for both samples are very similar, only small differences in the pattern can be observed. For migration times exceeding 2400 seconds, the electropherogram gets too complex, thus this part is not displayed in figure 63. To compare the electropherograms with respect to the desulfurization pattern, a graphic fitting was performed (figure 64). The size of the signals was normalized so that the signal intensity for 4,6-dimethyl-DBT - the most recalcitrant substance - was the same in both electropherograms. Then the signal intensity for all other compounds could be compared.

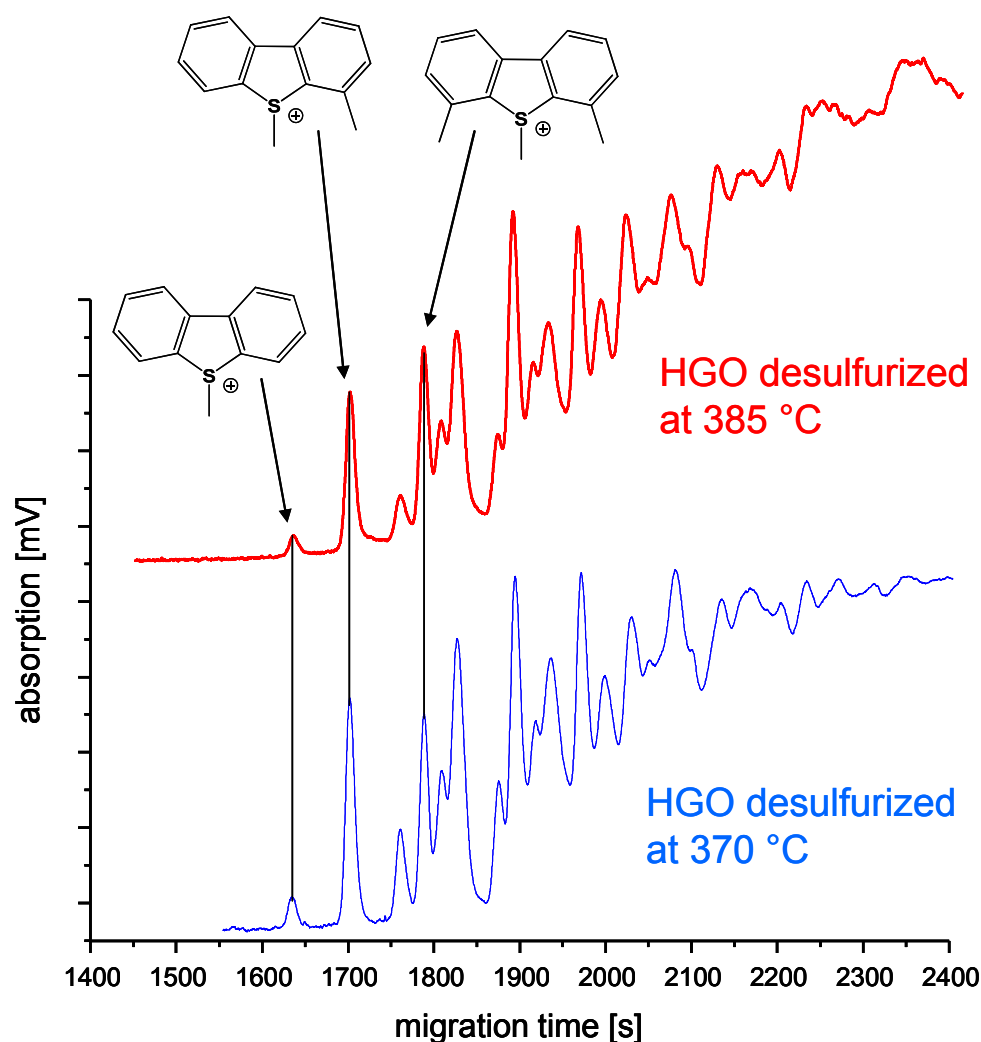


**Fig. 63:** CE-separation of desulfurized HGO samples with desulfurization at 385 °C (red) and desulfurization at 370 °C (blue). Electrolyte: phosphate buffer 50 mM, pH 2.15 and 20 % isopropanol at a voltage of 20 kV.

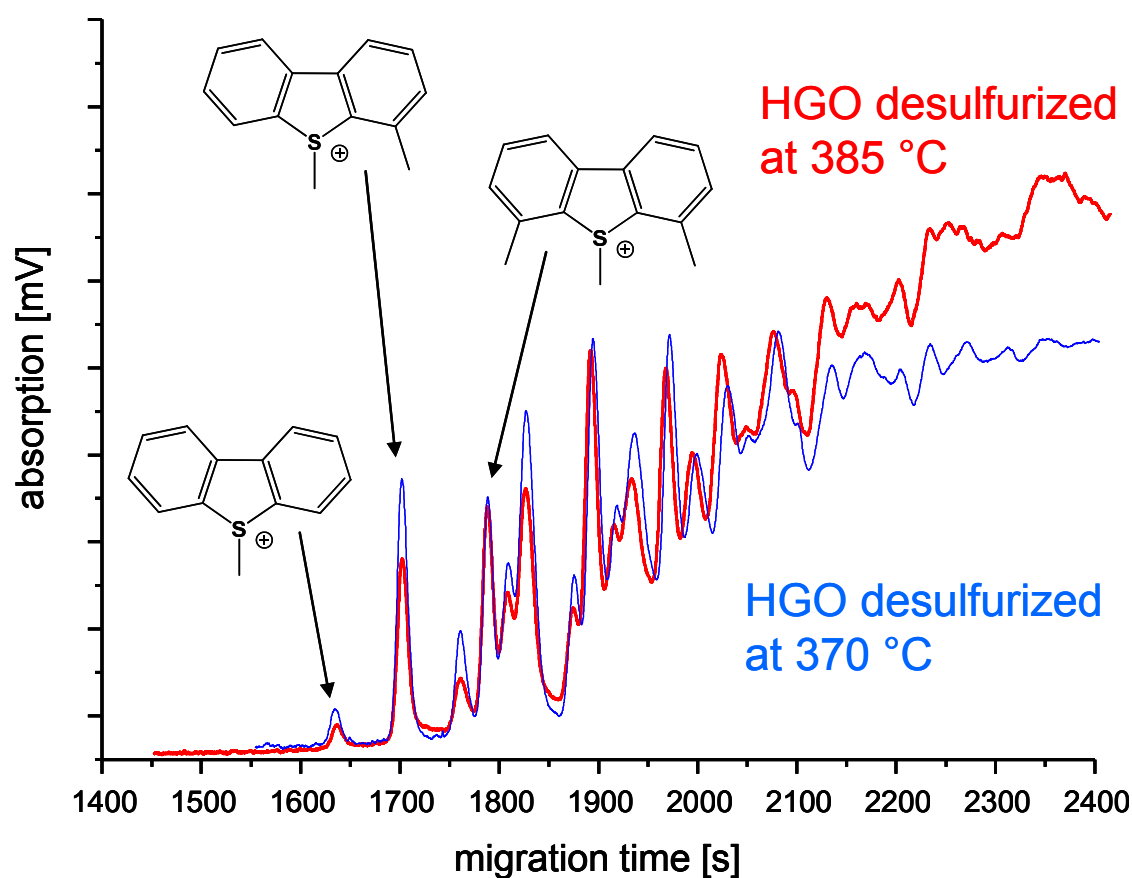


**Fig. 64:** Overlay of the electropherograms of desulfurized HGO samples with desulfurization at 385 °C (red) and desulfurization at 370 °C (blue). Electrolyte: phosphate buffer 50 mM, pH 2.15 and 20 % isopropanol at a voltage of 20 kV.

For the sample desulfurized at higher temperatures, the concentration of DBT, 4-Me-DBT and other compounds is lower. This demonstrates the decrease of the total concentration of these compounds in comparison to the most recalcitrant substance.

#### 7.4 Separation of different boiling fractions of Syncrude HGOs by CE-TOF MS

Three samples of an HGO were analyzed with different methods to evaluate the CE-TOF MS separation of real world sample PASHs. The HGO samples were fractions of a desulfurized Syncrude high boiling gas oil. The first sample consisted of the parent HGO, the second one corresponded to the boiling range from the initial boiling point (IBP) to 343 °C, and the third boiling fraction from 343-524 °C. The difference between the

samples became directly obvious because the high boiling fraction showed a high viscosity while the sample with a boiling range from IBP to 343 °C had a low viscosity. The parent HGO from which these fractions were obtained showed an intermediate viscosity. A GC analysis of the three samples illustrates the differences in the boiling ranges (figure 65).

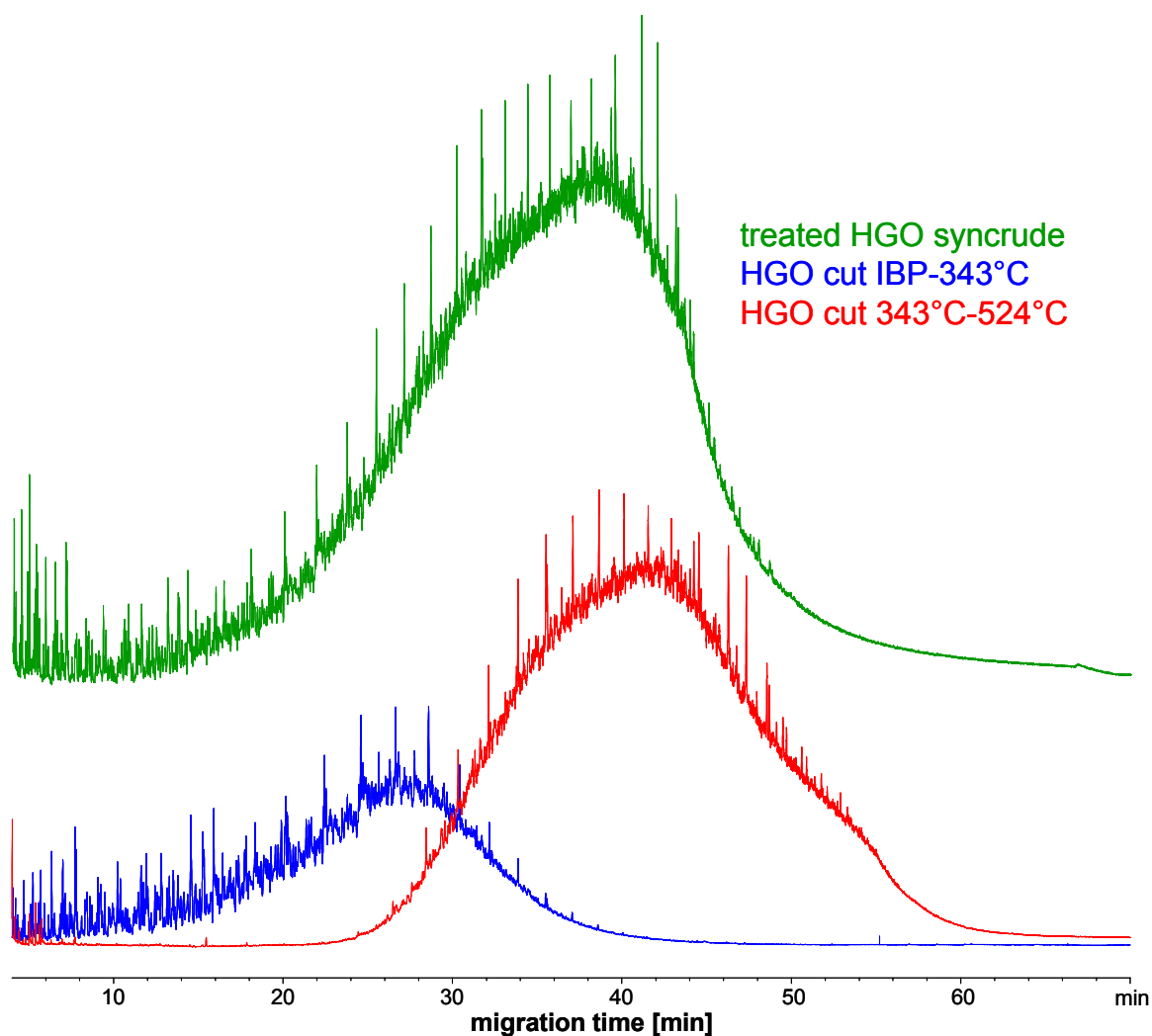


**Fig. 65: GC-separation of the desulfurized HGO (green) with the corresponding low boiling fraction (blue, IBP-343 °C) and high boiling fraction (red, 343 °C – 524 °C).**

In the fraction from IBP-343 °C most of the compounds elute within the first 40 minutes of the GC analysis, while the fraction from 343-524 °C begins at about 25 minutes ranging to retention times of over 60 minutes (figure 66). The parental desulfurized HGO covers the whole retention area of the chromatogram.

In the following, the PASHs of each of the samples were isolated by LEC and again analyzed by GC. The identification of DBT, 4-methyl-DBT and 4,6-dimethyl-DBT was done by measuring the corresponding reference substances. Relatively high concentrations of DBT were found in the low boiling fraction, while only minimal concentrations were found in the high boiling fraction. The parental sample possessed an intermediate concentration of DBT, as the two fractions were derived by distillation from this sample. Significant concentrations of 4-methyl-DBT and 4,6-dimethyl-DBT were found in all of the samples, with highest concentrations in the low boiling fraction of the HGO.

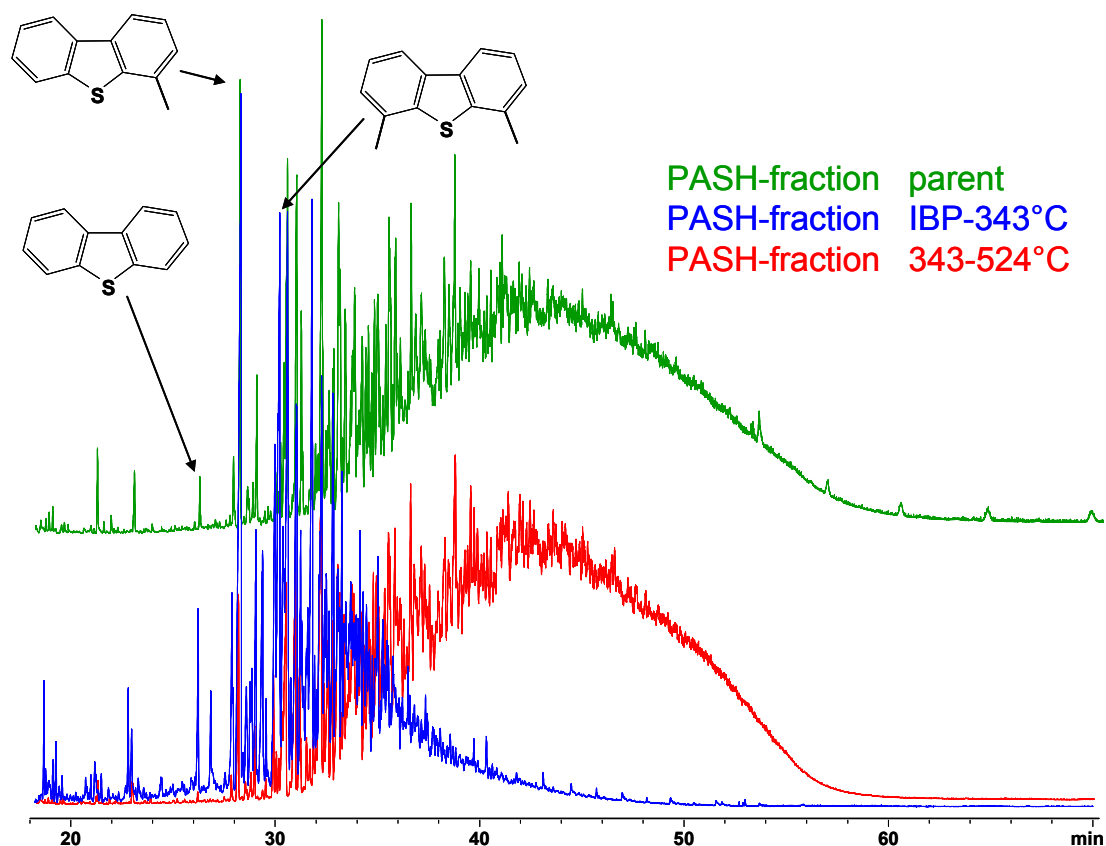


**Fig. 66:** GC-separation of the desulfurized HGO PASHs (green) with the corresponding low boiling fraction PASHs (blue, IBP-343 °C) and high boiling fraction PASHs (red, 343 °C – 524 °C).

#### 7.4.1 Aqueous CE-TOF MS

Following the GC-FID analysis, the different PASH fractions were methylated and subsequently separated with aqueous CE-TOF MS. The first real world sample that was separated was the low boiling PASH fraction because the complexity of this sample was expected to be moderate. Alkylated DBTs were estimated to be the most abundant PASHs

in this sample, based on the information from the previous GC analysis. This assumption was supported by the CE-TOF MS measurement. While the electropherogram for this low boiling sample looks quite complex (figure 67) due to the larger number of different PASHs, it is considerably simplified, when single masses are extracted from the electropherogram (figure 68).

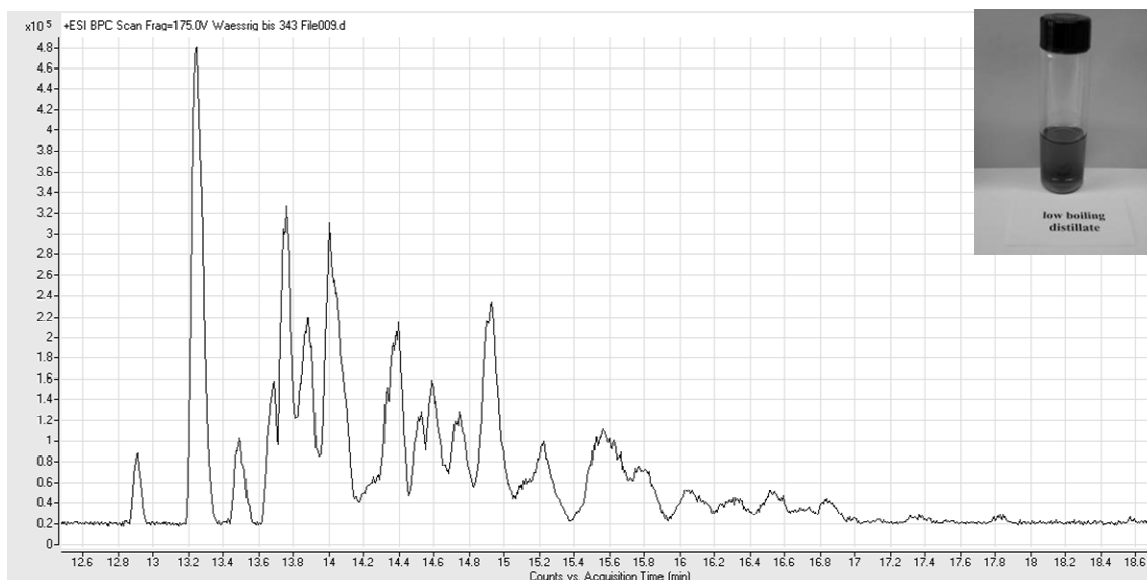


**Fig. 67: Aqueous CE-TOF MS electropherogram of the low boiling fraction PASHs.** Electrolyte: 300 mM acetic acid in water titrated to pH 4.0 with ammonia and mixed with isopropanol 1:1.

SMDBT was the compound with the shortest migration time, which indicates that no smaller PASHs can be found in this diesel fuel fraction and agrees with the information from GC. For mass 213.07 three signals are present. This exactly fits the distribution of C1-DBT-isomers in diesel fuels. Because a methyl group in 4-position restrains an approach of the molecule to the HDS catalyst this compound can be found in significant concentrations in desulfurized diesel fuels and can be identified as the largest signal at a migration time of 13.3 min in the electropherogram. The isomer with the methyl group in 3-position is less recalcitrant to HDS and hence its concentration is lower. This signal can be found at a migration time of 13.7 min. A very small signal for 2-methyl-DBT can be observed at 14.1 min while 1-methyl-DBT cannot be found in the sample. This compound is expected to migrate in between the 4-methyl- and 3-methyl-isomers which was determined by separations of standard compounds earlier.

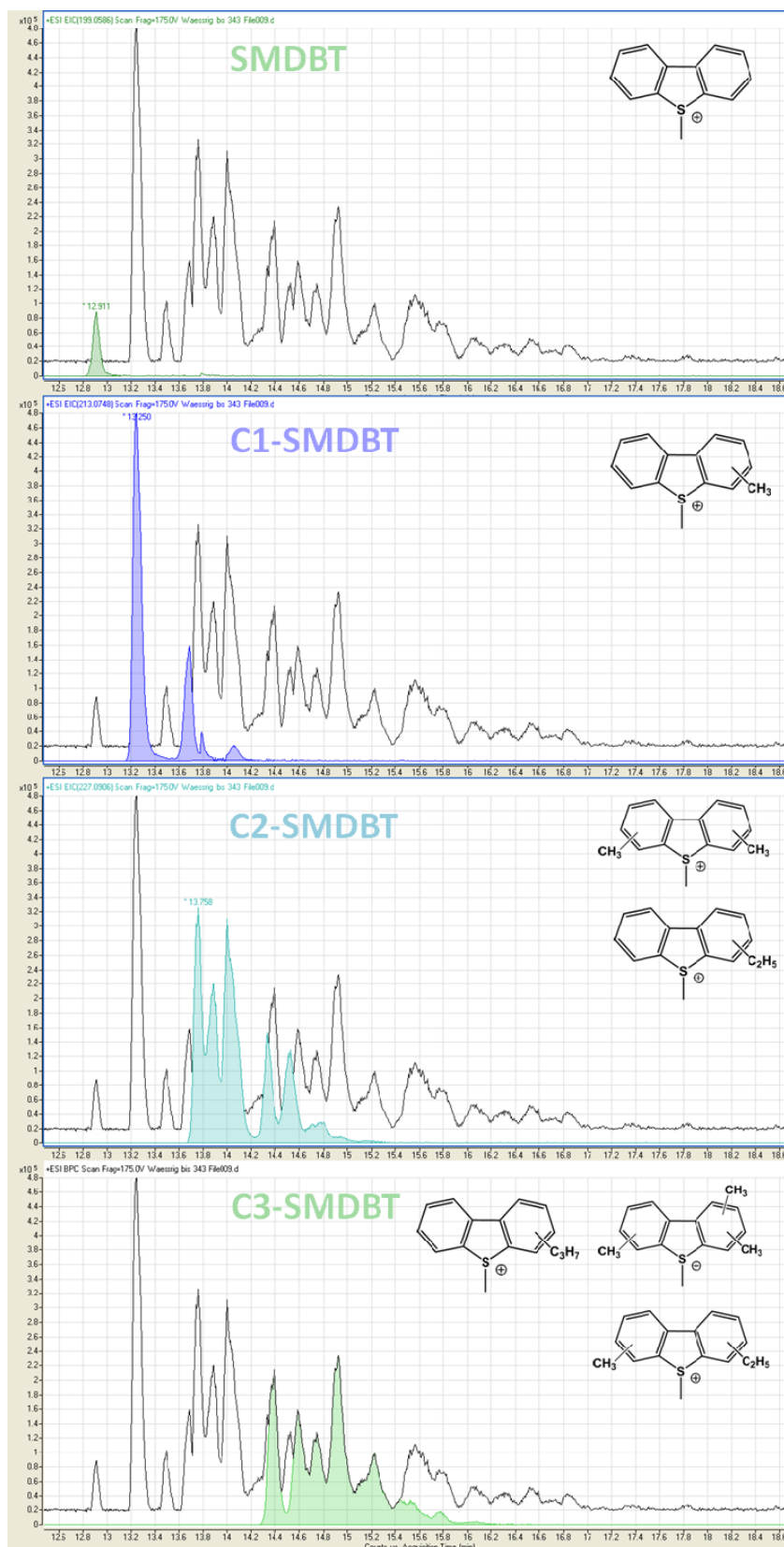


**Fig. 68: Extracted ion electropherograms of the low boiling fraction PASHs from SMDBT to C3-SMDBT.**

For mass 227.09 the signals get more complex because a large variety of isomers for C2-DBTs are possible. Different recalcitrant dimethyl-DBTs and ethyl-DBTs are commonly found in desulfurized diesel, which explains the pattern for the mass of 227.09. The most recalcitrant compound is known to be 4,6-dimethyl-DBT, as both methyl groups are flanking the sulfur and inhibit an approach to the HDS catalyst. The signal of this compound is the one with the lowest migration time in the measurement, because it has the most compact molecular shape and hence migrates fastest.

Alkylated DBTs are the major constituents of the analyzed diesel fuel fraction. This can easily be demonstrated by overlaying the extracted ion electropherograms for alkylated DBTs, ranging from DBT to C7-DBTs (figure 69). As expected, the pattern for the larger compounds is increasingly complex because the number of isomers increases strongly with each additional carbon atom. An overlay of the electropherograms of the alkylated DBTs from DBT to C7-DBT reveals that some signals do not belong to this class of compounds and have not been identified so far.

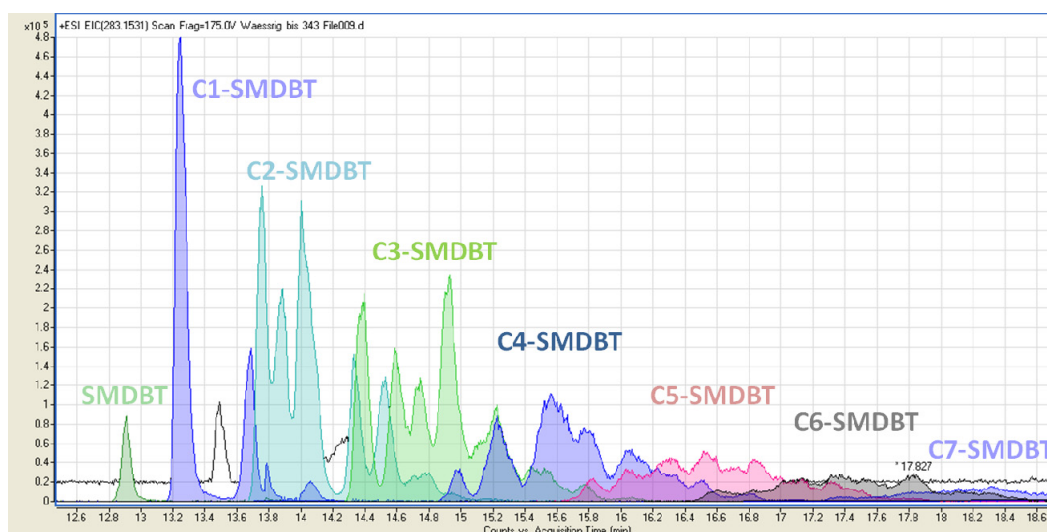


**Fig. 69: Overlay of SMDBT to C7-SMDBT extracted ion electropherograms of the low boiling fraction.**

The signal at a migration time of 13.5 min has a mass of 217.10 and could be identified as the S-methylated form of 4-methyltetrahydrodibenzothiophene. Tetrahydrodibenzothiophenes (THDBT) belong to a class of compounds that are generated through a competitive reaction to the HDS that leads to a hydrogenation of

dibenzothiophenes during the process (figure 70). An overlay of the extracted ion electropherograms of C1- to C4-THDBTs shows that significant amounts of this compound class can be found in the fraction. Interestingly, the mass for S-methyl-THDBT itself cannot be found in the sample. This can be explained by the fact that hydrodesulfurization for this compound occurs faster than a hydrogenation of the aromatic ring. Because 4-methyl-DBT eludes the hydrodesulfurization, there is enough time for hydration of the aromatic ring, leading to 4-methyl-THDBT. This also clarifies the fact that only extremely small amounts of isomers (with a methyl group in 3- or 2-position) can be found for C1-THDBT. Further isomers are possible where the alkyl group is not positioned at the aromatic ring, but at the hydrogenated ring. However, GC-MS measurements revealed that these isomers do not occur in the sample. The fragmentation pattern of this compound shows a loss of 28 masses which corresponds to a  $C_2H_4$  fragment from the hydrogenated ring. If the methyl group was positioned at the hydrogenated ring, the fragment was expected to have a mass of 43 due to the methyl group attached to the  $C_2H_4$  fragment, but these fragments could not be observed in the sample. Homologous of THDBTs with more than one alkyl group can be found in the electropherogram of the sample as presented in figure 71.

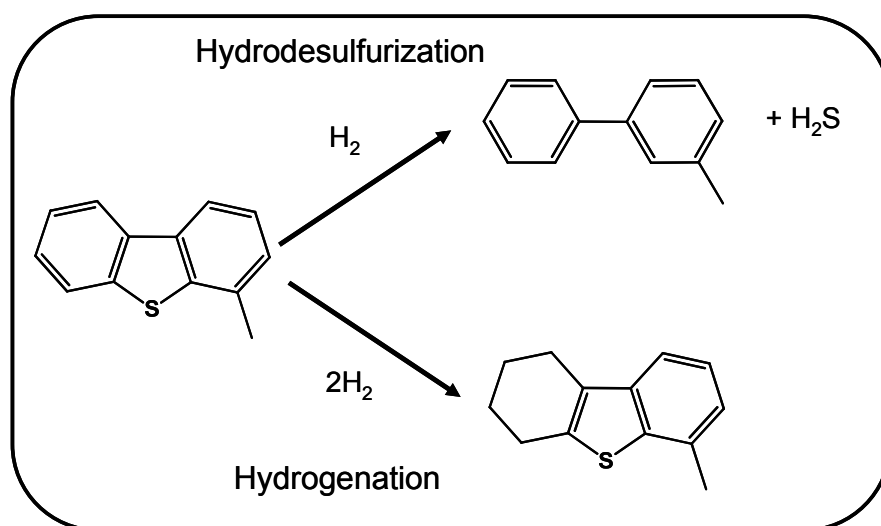


**Fig. 70: Formation of tetrahydrodibenzothiophenes by hydrogenation as competitive reaction to the hydrodesulfurization.**



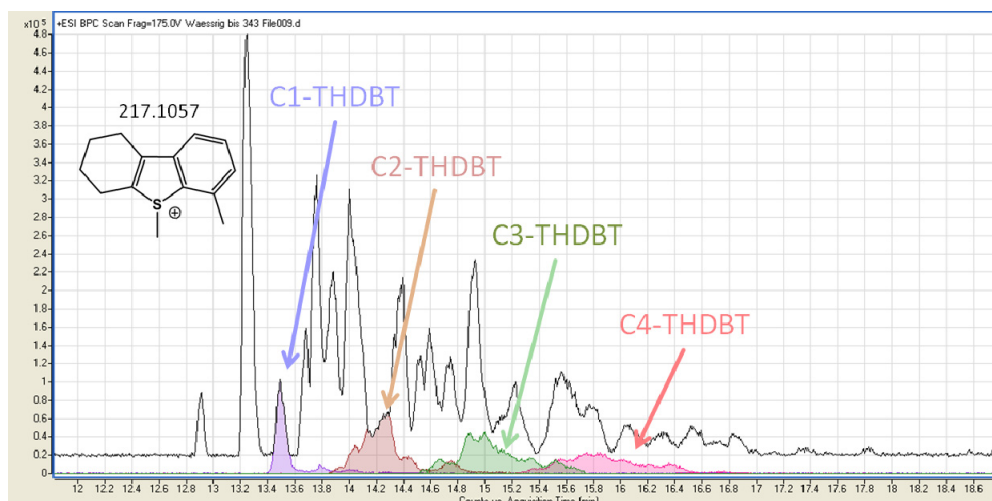


**Fig. 71: Overlay of methylated C1-THDBT to C4-THDBT extracted ion electropherograms.**

The analysis of the higher boiling fraction of the HGO was performed in the same way as the low boiling PASH fraction. As already shown in the GC analyses, the boiling range of this material is higher (343 °C to 524 °C), so that the longer migration times of the compounds in this sample were to be expected. Additionally the sample should be more complex. These assumptions were easily verified as shown by the resulting electropherogram (figure 72). The migration time for the separation of the sample increased to ca. 22 minutes vs. ca. 18 minutes for the low boiling sample.

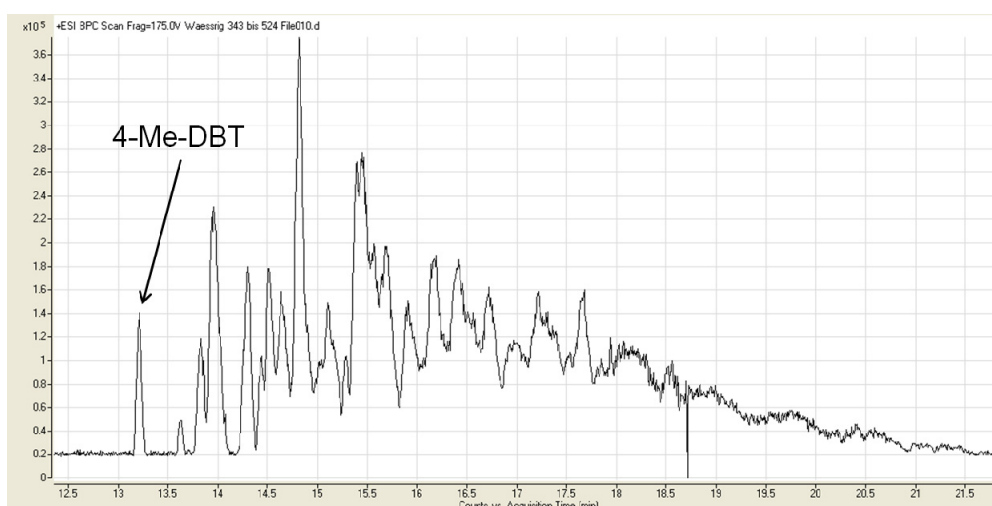


**Fig. 72: Aqueous CE-TOF MS electropherogram of the higher boiling fraction PASHs.** Electrolyte: 300 mM acetic acid in water titrated to pH 4.0 with ammonia and mixed with isopropanol 1:1.

Only minimal concentrations of S-methyl-DBT can be found in this sample, which fits the observations from the GC measurements. The signal for 4-methyl-SMDBT is the first that can be seen in the electropherogram. Again, the signal for 4-methyl-DBT is accompanied by two further signals of the same mass that can be related to 3-methyl-DBT and 2-methyl-DBT (figure 73). Again, for C2- and C3-DBTs, an increase in complexity for the signals due to isomeric diversity can be observed.

In the low boiling fractions the C1-DBTs were one of the main constituents but for the high boiling sample the C1-DBTs are marginal. Higher mass compounds like C3- and C4-DBTs constitute the main components of this PASH fraction, going up to C12-DBTs that are found in the later part of the electropherogram. An overlay of the extracted ion chromatograms for all alkylated DBTs shows that this compound class is the major one as was observed for the low boiling fraction (figure 74). THDBTs that were found in the low boiling fractions can be found in low concentrations in this sample as well, but are not a major constituent (figure 75). The signal at 15.28 min, which is not part of the DBT homologous, showed a mass of 267.1219 and belongs to a further class of homologous in this sample. The exact structure of this class of compounds could not be determined because a chromatographic separation is not possible and fragmentation patterns did not lead to an elucidation of the structure. Most probably these homologous belong to tetrahydrobenzonaphthothiophenes (THBNT) and dihydrophenanthro[4,5bcd]thiophenes (DHPT) that are known to occur in the distillable aromatic fraction of Athabasca bitumen [121] which is the origin of the used real world samples. Tetrahydrobenzonaphthothiophenes were furthermore found in desulfurized petroleum fuels [122, 123], while phenanthro[4,5-*bcd*]thiophenes were reported to be present in tar [124] and can be hydrogenated to the corresponding dihydrophenanthro[4,5-*bcd*]thiophenes during desulfurization. An additional class of compounds that would fit the mass of this signal are phenylbenzothiophenes but as these compounds were only found in lignite and coal so far [125, 126] it is unlikely that they are present in the sample. The mass 267.1219 hence belongs to C1-tetrahydrobenzonaphthothiophenes or C2-dihydrophenanthro[4,5-*bcd*]thiophenes. The mass 239.0913 is the lowest mass of this homologous series found in the sample and the electropherogram shows three small signals (figure 76). Because the mass of methylated tetrahydrobenzonaphthothiophene itself is

253, this signal most likely belongs to C1-dihydrophenanthro[4,5-*bcd*]thiophenes which would also be an explanation for the small amount of isomer signals for this mass.

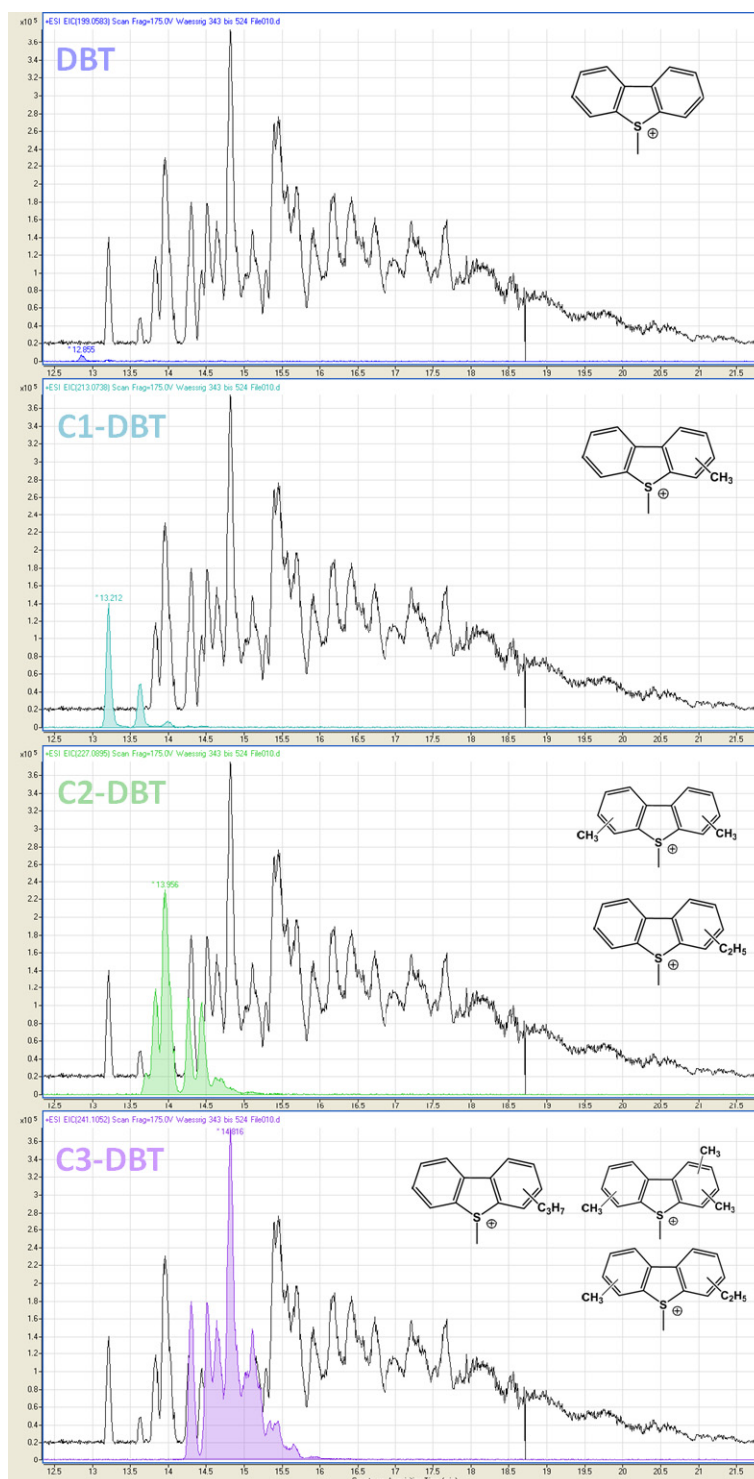


**Fig. 73: Extracted ion electropherograms of the higher boiling fraction PASHs from SMDBT to C3-SMDBT.** Electrolyte: 300 mM acetic acid in water titrated to pH 4.0 with ammonia and mixed with isopropanol 1:1.

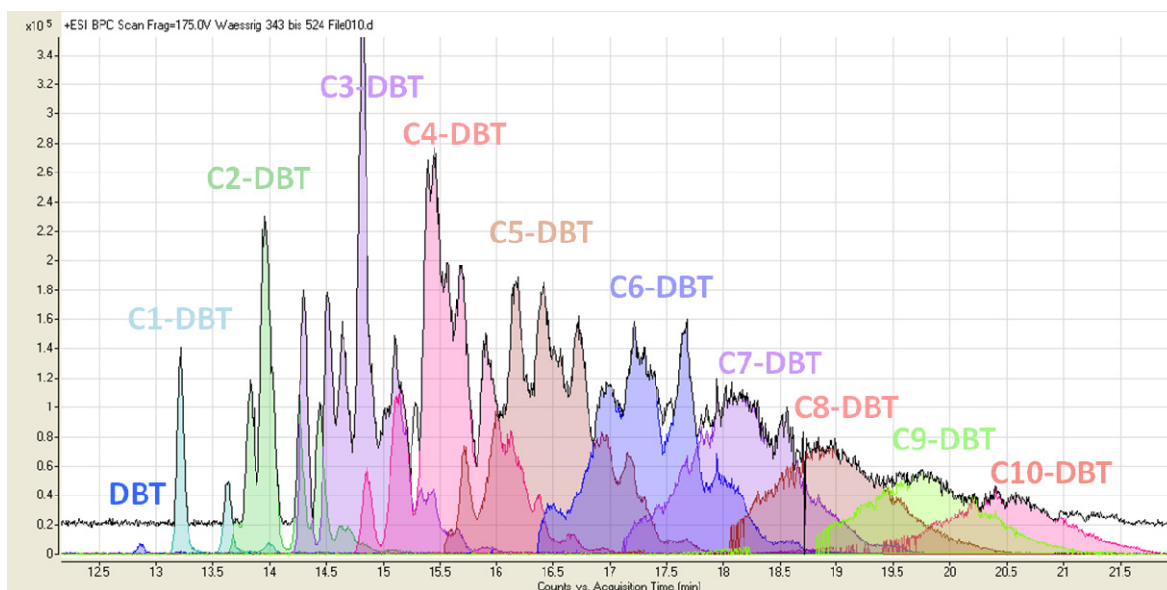


**Fig. 74: Overlay of methylated DBT to C10-DBT extracted ion electropherograms of the higher boiling fraction.** Electrolyte: 300 mM acetic acid in water titrated to pH 4.0 with ammonia and mixed with isopropanol 1:1.

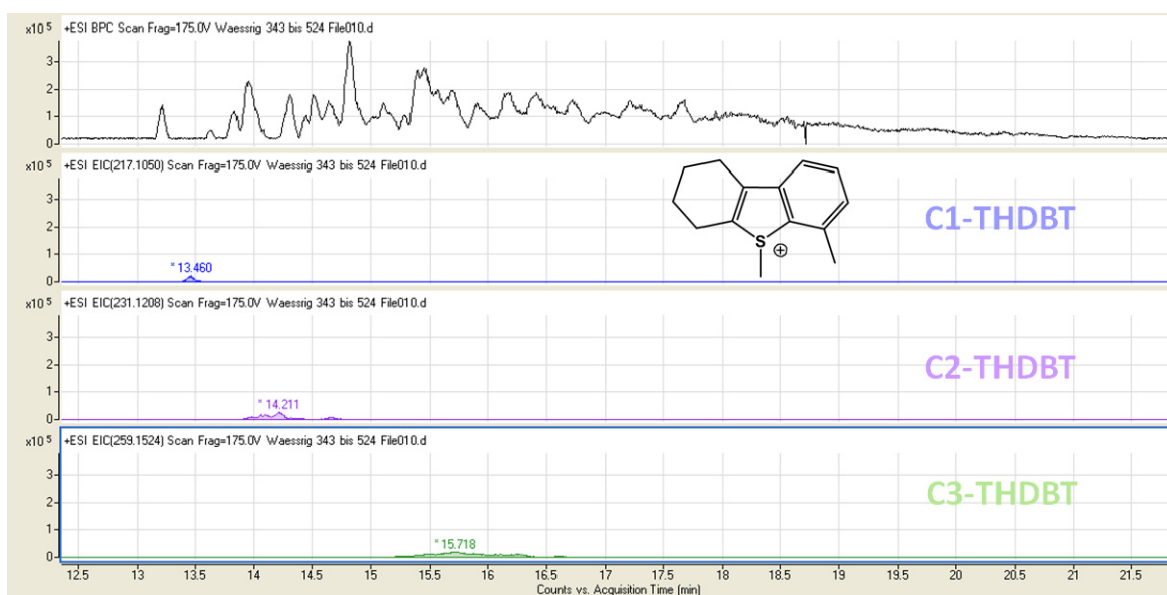


**Fig. 75: Extracted ion electropherograms for methylated C1 to C3-THDBTs of the higher boiling fraction.** Electrolyte: 300 mM acetic acid in water titrated to pH 4.0 with ammonia and mixed with isopropanol 1:1.

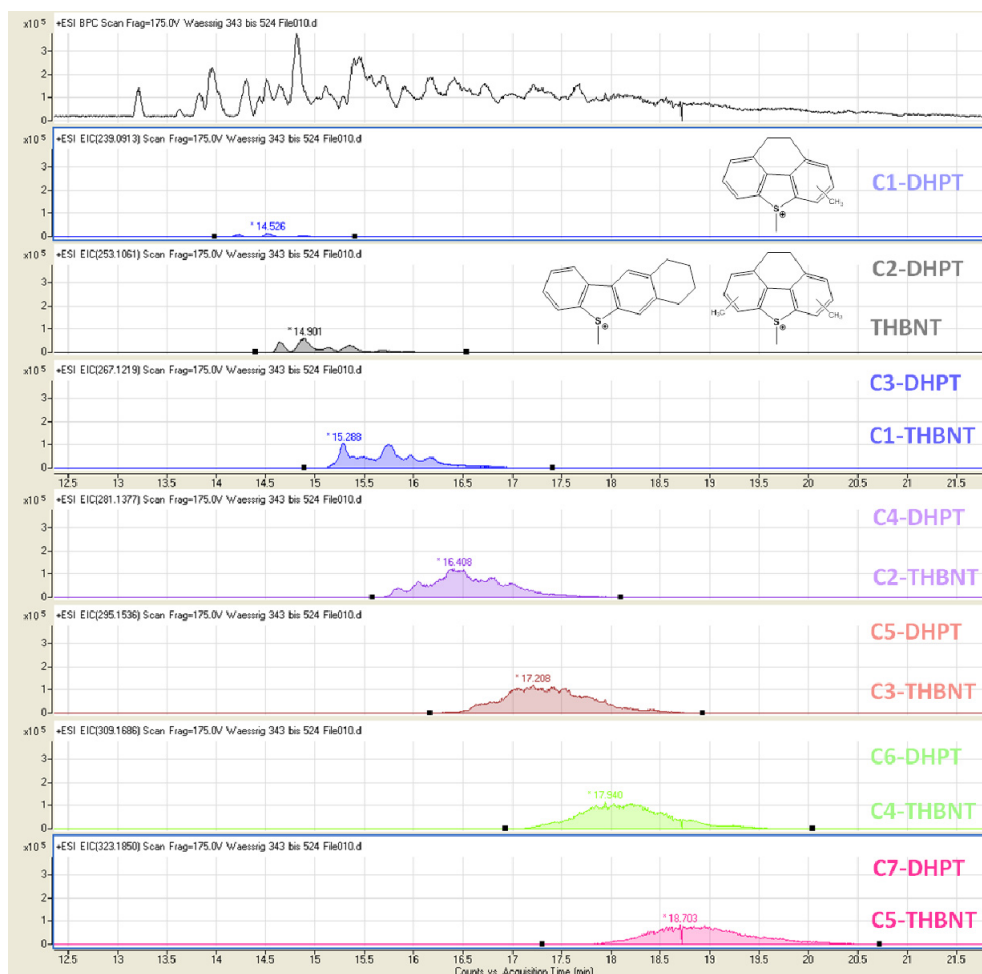


**Fig. 76: Extracted ion electropherograms for THBNTs and DHPTs from the parent HGO sample after separation with aqueous CE-TOF MS. Electrolyte: 300 mM acetic acid in water titrated to pH 4.0 with ammonia and mixed with isopropanol 1:1.**

The third real world sample represents the parent desulfurized HGO that was not fractionated. Based on this information, the parent sample should contain all the constituents that were found for the other real world samples measured before.

The sample was separated by aqueous CE and the results compared with the measurements from the low boiling fraction and the higher boiling fraction measured before. In the parent sample, again, alkylated DBTs are the main constituents and show more than 10 carbon atoms in the side chains. An overlay of the extracted ion chromatograms for DBT to C9-DBT is presented in figure 77.

The THDBTs that are produced during the HDS process are found in the parent sample as well. At a migration time of 13.34 min the signal for 4-methyl-THDBT occurs. An overlay of the extracted ion electropherograms for C1-THDBTs to C7-THDBT is presented in figure 78. The THBNTs and DHPTs that were found in the higher boiling fraction of the HGO can also be found in the parent fraction with masses up to 351 and higher (figure 79). Again, only a signal for C1-DHPT can be found, while a signal for DHPT without alkylations cannot be observed.

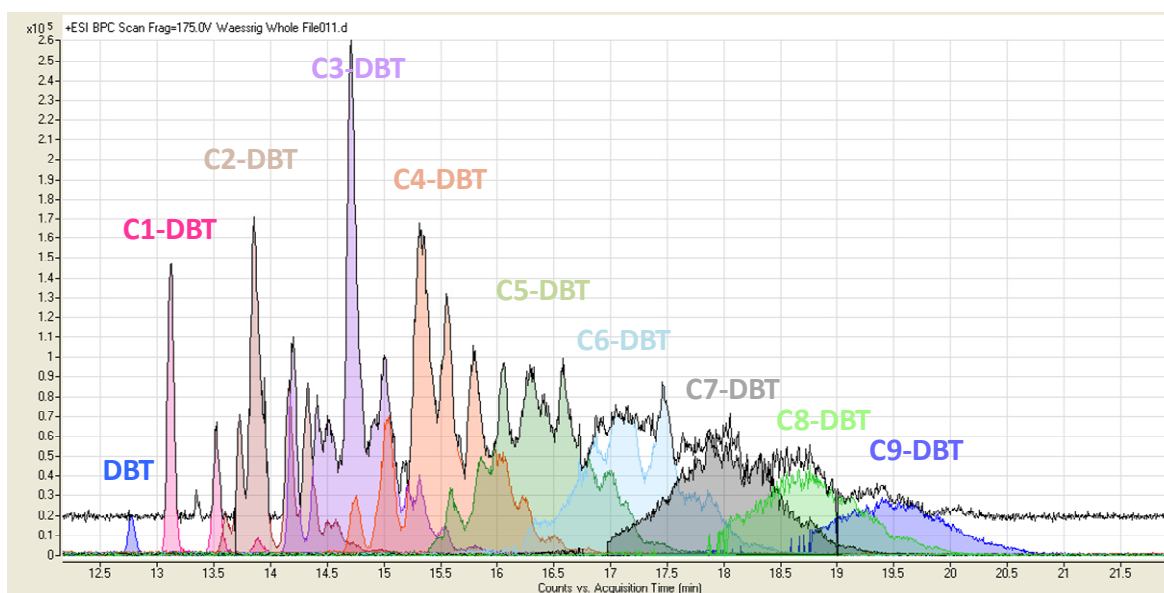


**Fig. 77: Overlay of methylated DBT to C9-DBT extracted ion electropherograms of the parent HGO PASH fraction obtained with aqueous CE-TOF MS. Electrolyte: 300 mM acetic acid in water titrated to pH 4.0 with ammonia and mixed with isopropanol 1:1.**



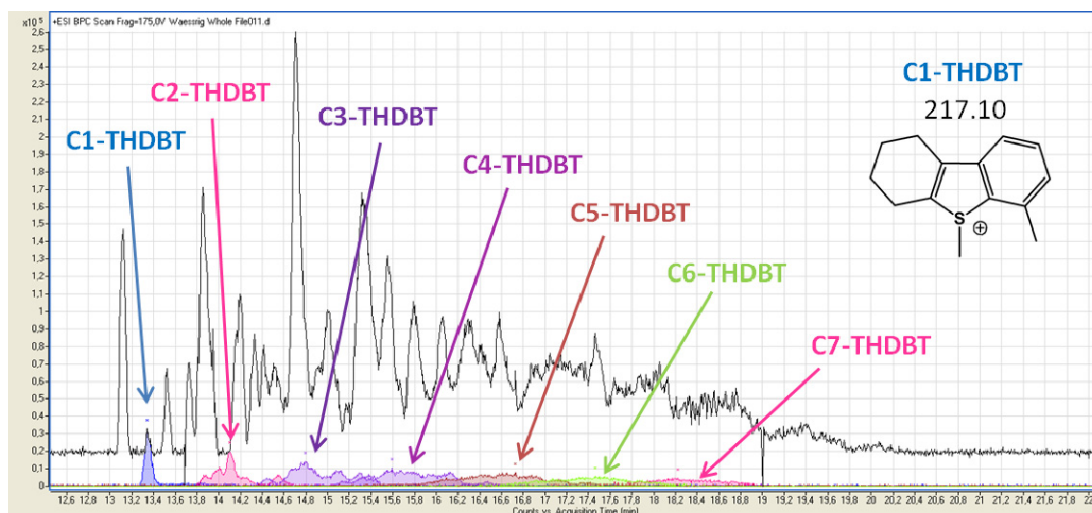


**Fig. 78:** Overlay of methylated THDBT to C7-THDBT extracted ion electropherograms of the parent HGO PASH fraction obtained with aqueous CE-TOF MS. Electrolyte: 300 mM acetic acid in water titrated to pH 4.0 with ammonia and mixed with isopropanol 1:1.

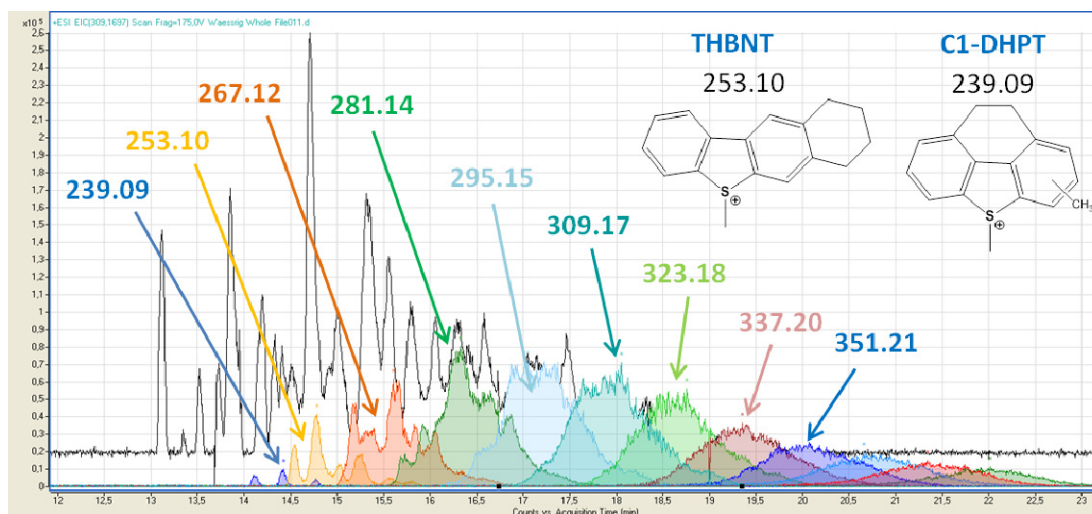


**Fig. 79:** Overlay of THBNTs and DHPTs extracted ion electropherograms of the parent HGO PASH fraction obtained with aqueous CE-TOF MS. Electrolyte: 300 mM acetic acid in water titrated to pH 4.0 with ammonia and mixed with isopropanol 1:1.

#### 7.4.2 Nonaqueous CE-TOF MS

As already presented for the standard compounds in chapter 6.6.2, it is possible to separate the derivatized PASHs in completely nonaqueous media. Advantages of this method are

shorter migration times and a better solubility of the analytes. A major disadvantage is the change of migration order for several compounds. The compounds are not separated by size anymore, as could be seen for the separation of four standard PASHs (figure 52).

The same real world samples as used for the aqueous CE were used for the nonaqueous CE-TOF MS separation as well. The purely organic buffer for the separation was a mixture of 4 % acetic acid in methanol with an addition of 70 mM ammonium formate, as was already used for the nonaqueous CE-TOF MS of the standard compounds.

The first real world sample separated with this method was the low boiling fraction of the HGO (figure 80). As known from the GC measurements and from aqueous CE-TOF MS, S-methylated DBT was expected to be the smallest PASH in the sample. The extracted ion signal for this analyte can be found in the middle part of the electropherogram at a migration time of 8.4 minutes. This demonstrates the change in migration order between the aqueous and the nonaqueous separation again. The signals for the methylated C1-DBT isomers can be found at 8.2 min (4-methyl-DBT), 8.6 min (3-methyl-DBT) and 8.8 minutes (2-methyl-DBT) migration time. A signal for 1-methyl-DBT cannot be found in the electropherogram, verifying the results from aqueous CE. The extracted signals for the C2-DBTs show a much more complex pattern. The variety of ethyl- and dimethyl substituted isomers leads to at least 10 resolved signals but comigration of the compounds can be observed as well. The C3-DBT signals exhibit a further increase in complexity as now the isomers may consist of propyl-, ethyl-methyl- and trimethyl-substituted DBTs. Single compounds cannot be resolved any more so that comigration occurs for most of the compounds. It is noteworthy that all the compounds from DBT to C3-DBT migrate between 8.2 and 9.8 minutes. The electropherogram is hence more compact than the one obtained with aqueous CE where migration times of these compounds vary a lot more. However, the resolution for the separation with nonaqueous CE seems to be better because the signals are very narrow. This can especially be seen for the C2-DBTs: in aqueous CE, only six comigrating signals were obtained while in the nonaqueous CE ten, mostly baseline separated, signals were obtained.

An overlay of all the extracted ion electropherograms for alkylated DBTs can be seen in figure 81. DBTs with up to seven C-atoms in the side chains can be found, which is similar to the results from aqueous CE. The THDBTs that were found in aqueous CE can be found



in nonaqueous CE as well (figure 82). The most abundant THDBT is the C1-THDBT, which migrates at 7.9 minutes and is hence the fastest migrating compound in nonaqueous CE.

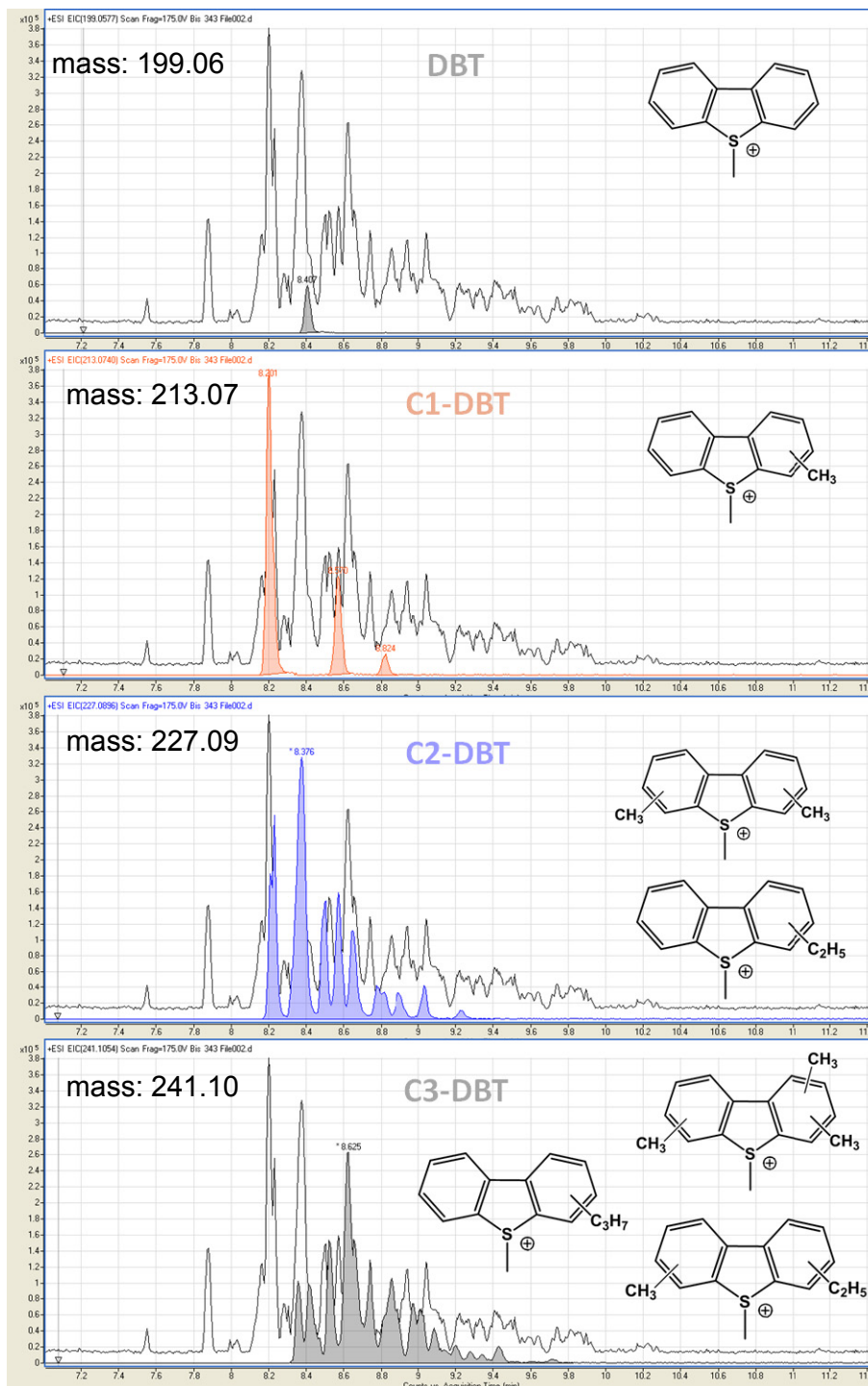


**Fig. 80:** Extracted ion electropherograms for methylated DBT to C3-DBTs for the low boiling HGO PASHs with nonaqueous CE. Electrolyte: 4 % acetic acid in methanol with addition of 70 mM ammonium formate.

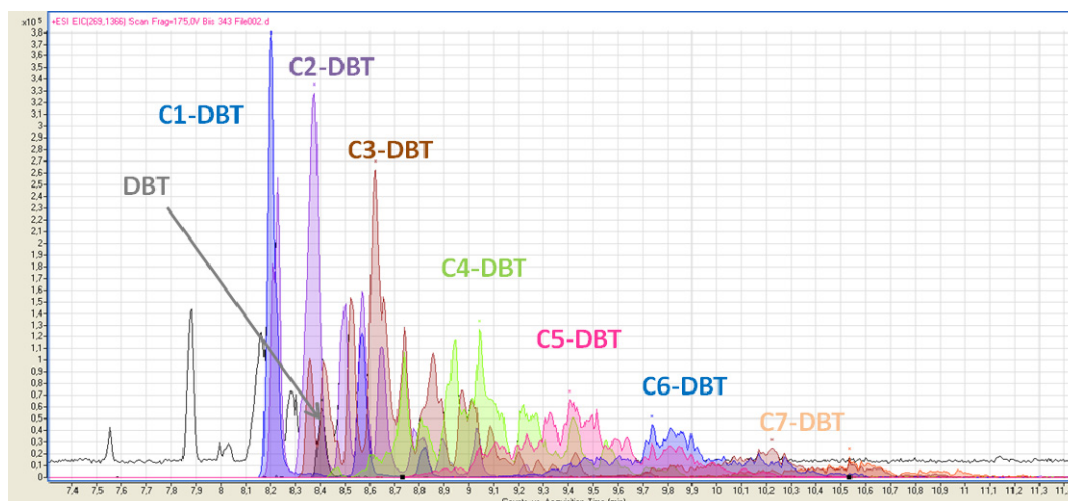


**Fig. 81: Overlay of methylated DBT to C7-DBT extracted ion electropherograms of the low boiling fraction PASHs.** Electrolyte: 4 % acetic acid in methanol with addition of 70 mM ammonium formate.

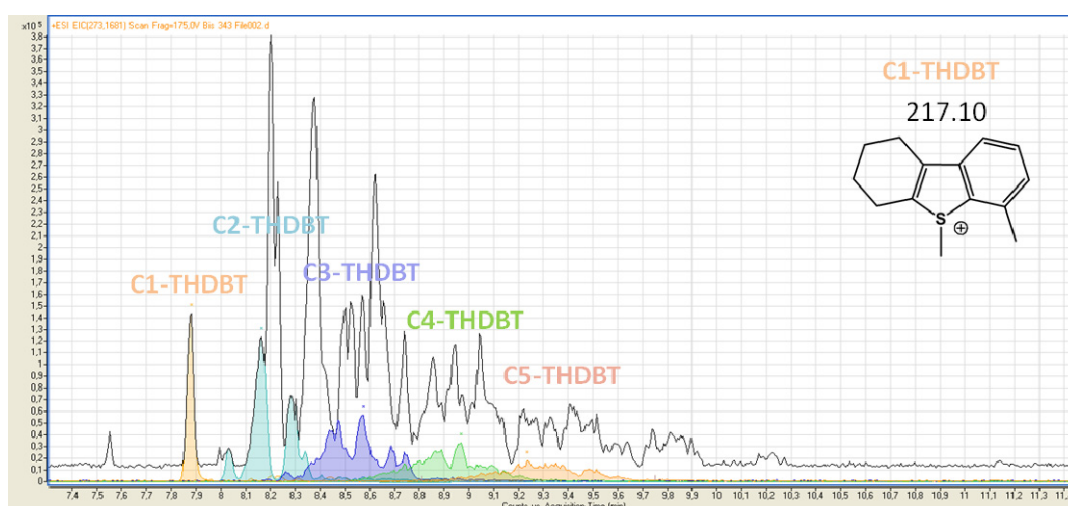


**Fig. 82: Overlay of methylated C1-THDBT to C5-THDBT extracted ion electropherograms of the low boiling HGO sample by nonaqueous CE-TOF MS.** Electrolyte: 4 % acetic acid in methanol with addition of 70 mM ammonium formate.

The separation of the higher boiling fraction of the HGO fuel led to results in agreement with the aqueous CE-TOF MS. Only low concentrations of DBT occur in this sample and the pattern for the C1-DBTs is similar. The main constituents are C3-DBTs and higher as seen in figure 83 where all the extracted ion electropherograms for DBT to C8-DBT are

presented. However, DBTs with longer alkyl chains of up to twelve carbon atoms in the side chains can be recorded.

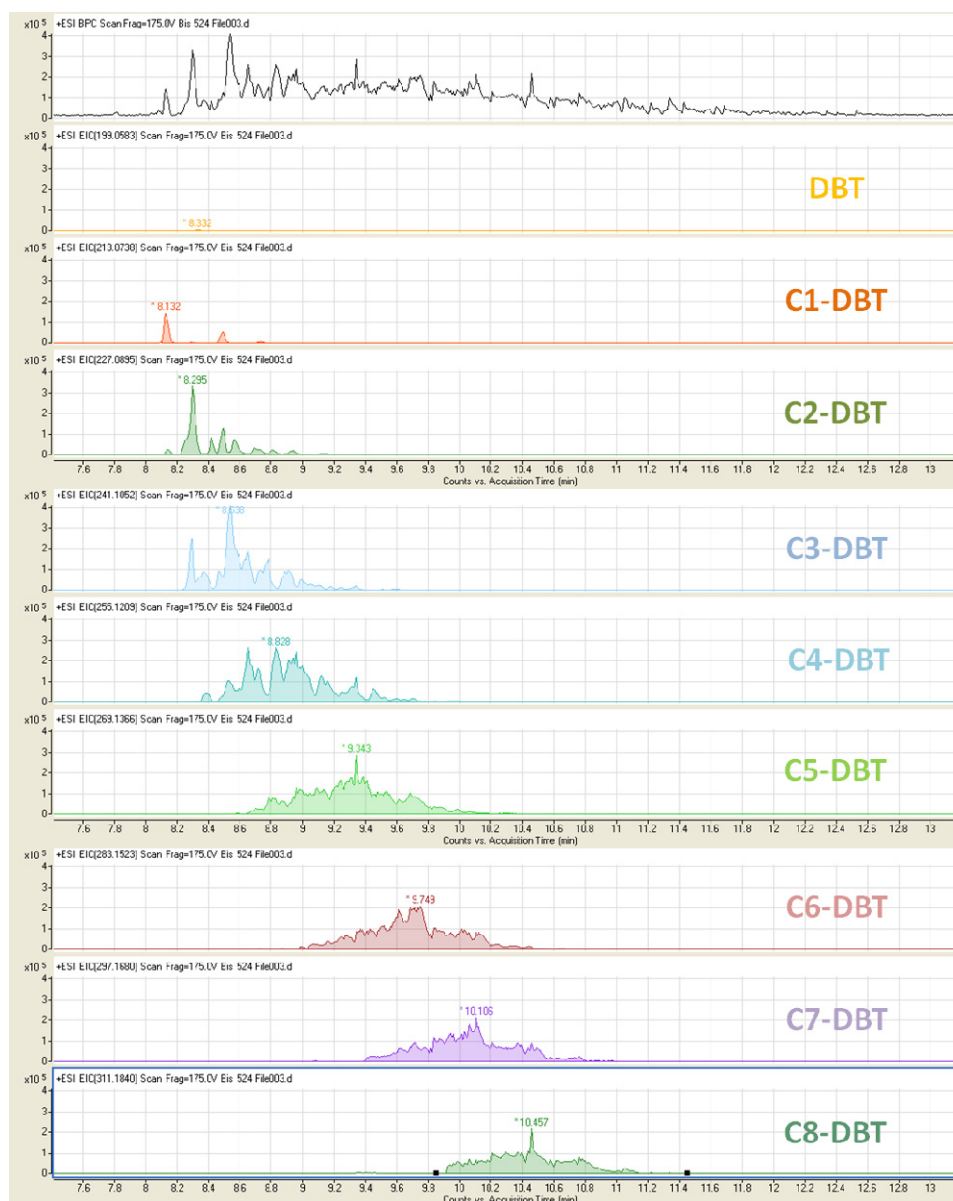


**Fig. 83: Extracted ion electropherograms of DBT to C8-DBT for the higher boiling HGO sample by nonaqueous CE-TOF MS. Electrolyte: 4 % acetic acid in methanol with addition of 70 mM ammonium formate.**

THDBTs are present, but only in low concentrations (figure 84). As seen in the aqueous CE-TOF MS, THBNTs and DHPTs play an important role in this fraction. Figure 85 presents an overlay of the extracted ion electropherograms of these compounds with masses up to 379 and higher, corresponding to the results from aqueous CE.

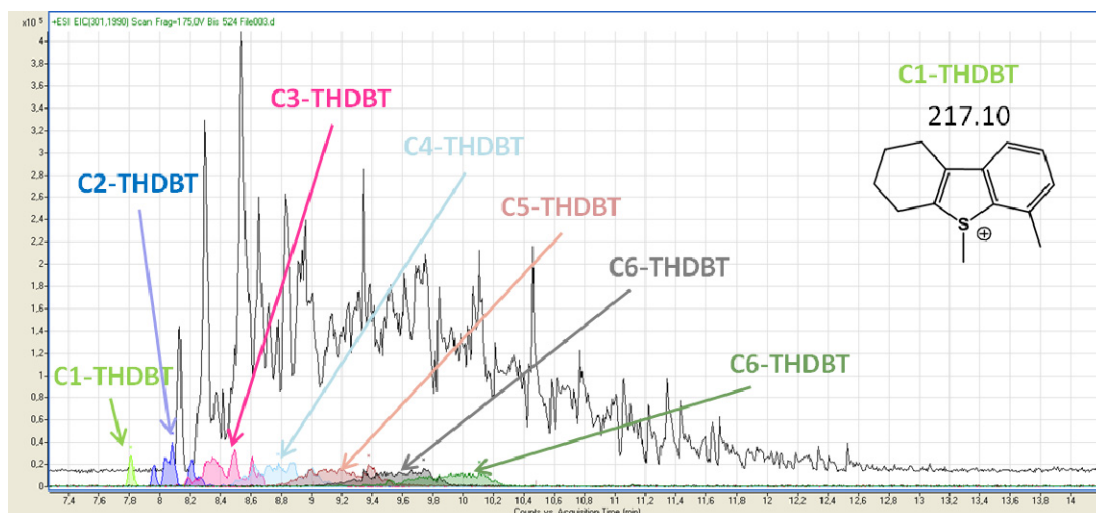


**Fig. 84:** Overlay of methylated C1-THDBT to C6-THDBT extracted ion electropherograms of the higher boiling HGO sample by nonaqueous CE-TOF MS. Electrolyte: 4 % acetic acid in methanol with addition of 70 mM ammonium formate.

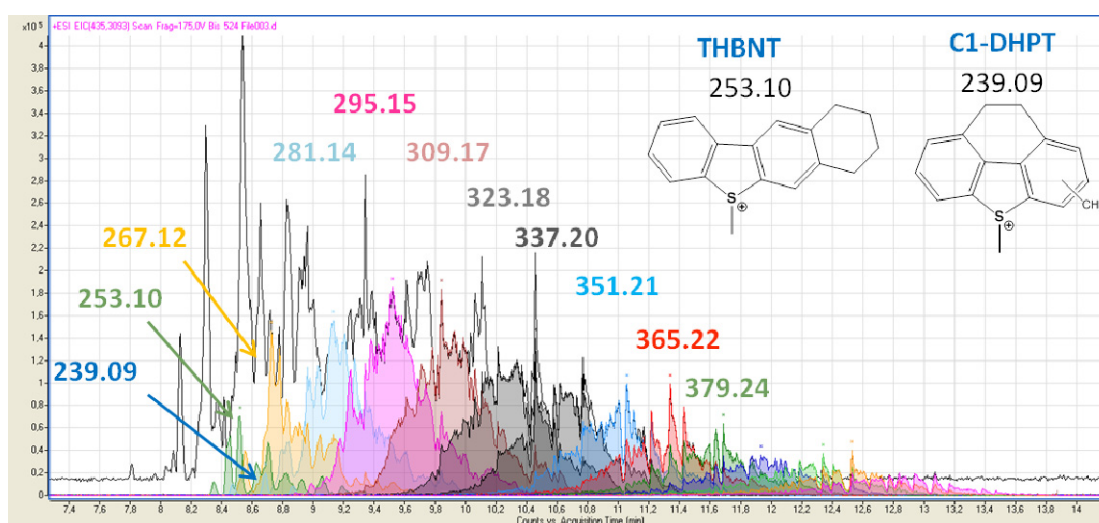


**Fig. 85:** Overlay of the extracted ion electropherograms of methylated THBNTs and DHPTs of the higher boiling HGO sample by nonaqueous CE-TOF MS. Electrolyte: 4 % acetic acid in methanol with addition of 70 mM ammonium formate.

The third real world sample measured by nonaqueous CE-TOF MS was again the parent desulfurized HGO, which is expected to contain all the compound classes found in the previous fractions. DBT can be found in low concentrations in the sample (figure 86). The pattern for C1-DBT to C3-DBT is very similar to the results from the higher boiling

fraction which agrees with the assumption that the parental crude mostly contains high boiling compounds that end up in the gas oil fraction.

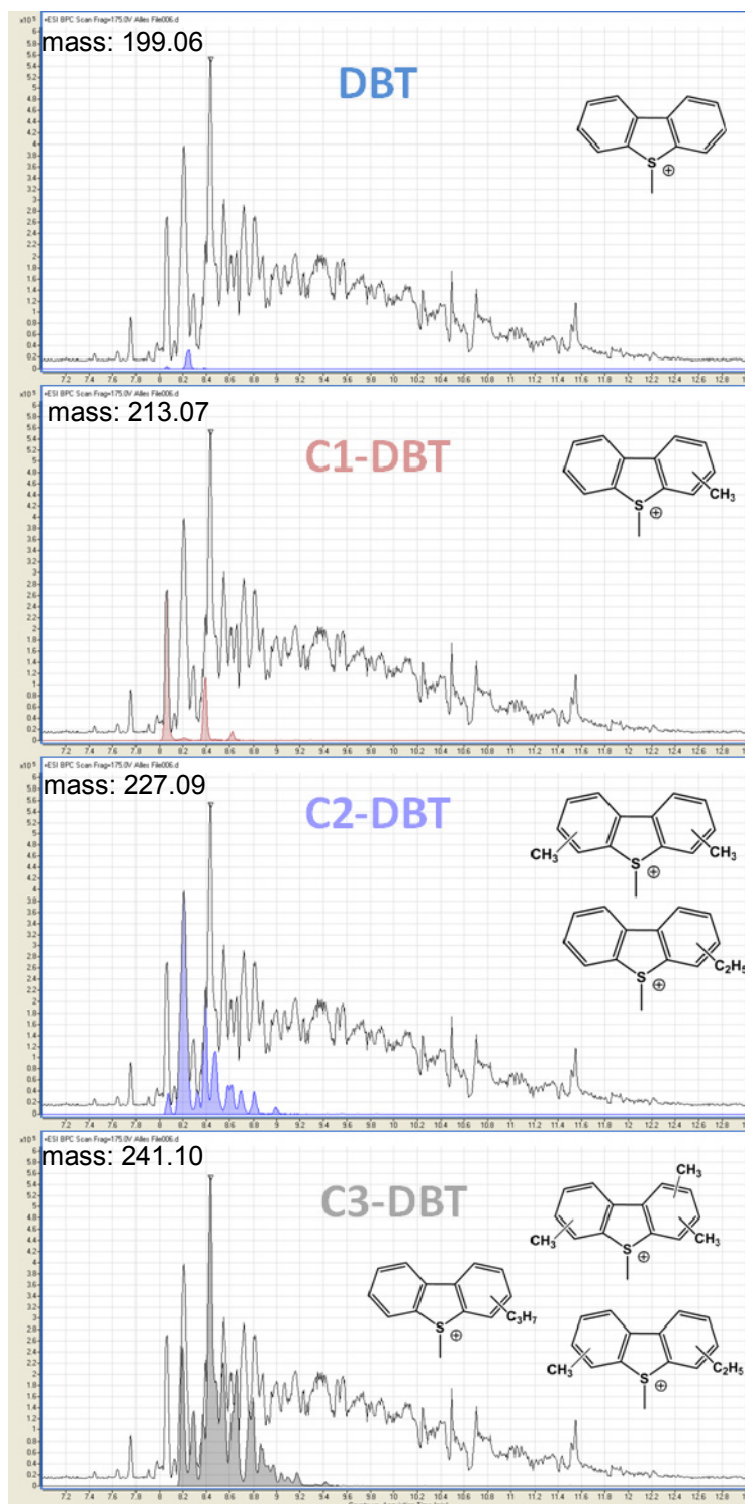


**Fig. 86: Extracted ion electropherograms for methylated DBT to C3-DBTs for the parent HGO PASHs with nonaqueous CE-TOF MS. Electrolyte: 4 % acetic acid in methanol with addition of 70 mM ammonium formate.**



An overlay of all the extracted electropherograms of alkylated DBTs demonstrates that DBTs with up to ten or more carbon atoms in the side chains can be found (figure 87). THDBTs are present in the first part of the electropherogram. An overlay of the extracted ion electropherograms for the C1- to C6-homologous can be seen in figure 88. THBNTs and DHPTs are found in high concentrations, like it was previously seen in aqueous CE-TOF MS. An overlay of the extracted ion electropherograms up to a mass of 393 for these compounds is shown in figure 89.

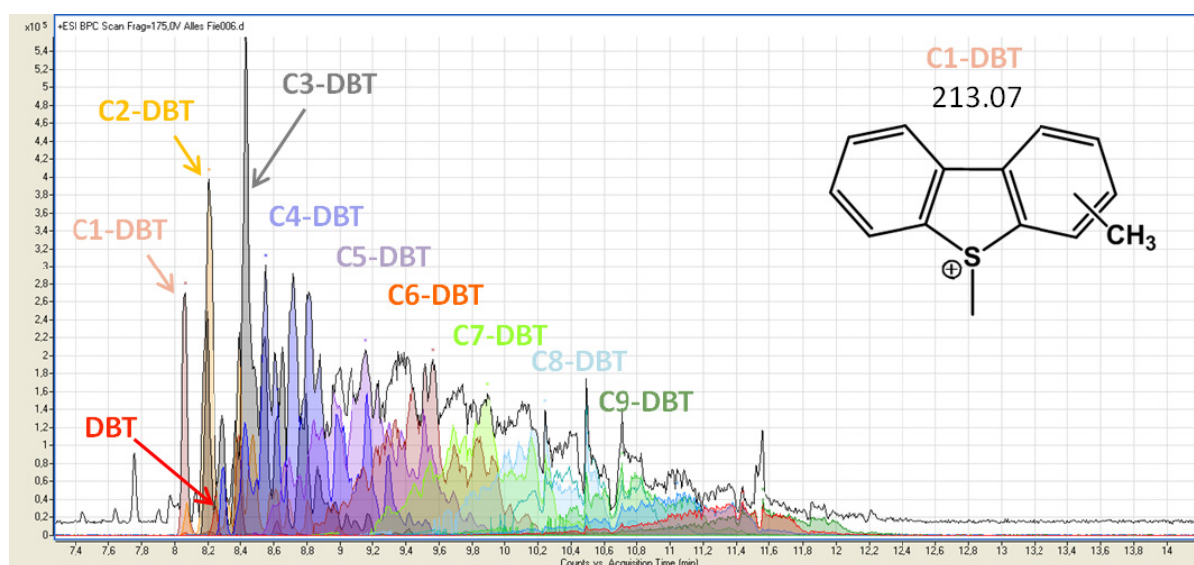


**Fig. 87: Overlay of methylated DBT to C12-DBT extracted ion electropherograms of the parental HGO sample by nonaqueous CE-TOF MS. Electrolyte: 4 % acetic acid in methanol with addition of 70 mM ammonium formate.**

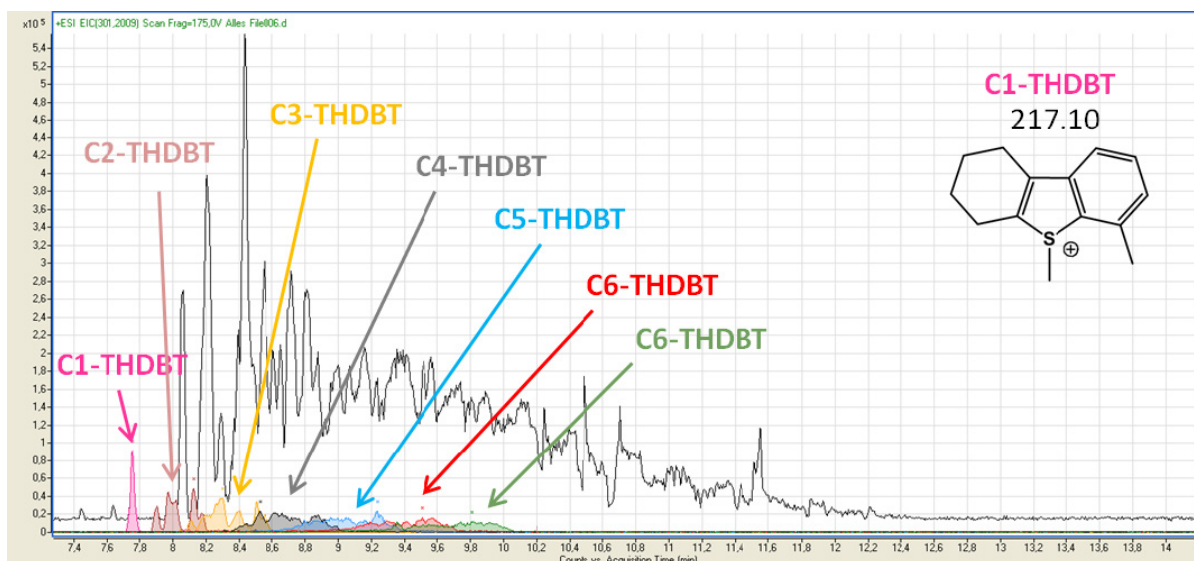


**Fig. 88:** Overlay of methylated C1-THDBT to C6-THDBT extracted ion electropherograms of the parental HGO sample by nonaqueous CE-TOF MS. Electrolyte: 4 % acetic acid in methanol with addition of 70 mM ammonium formate.

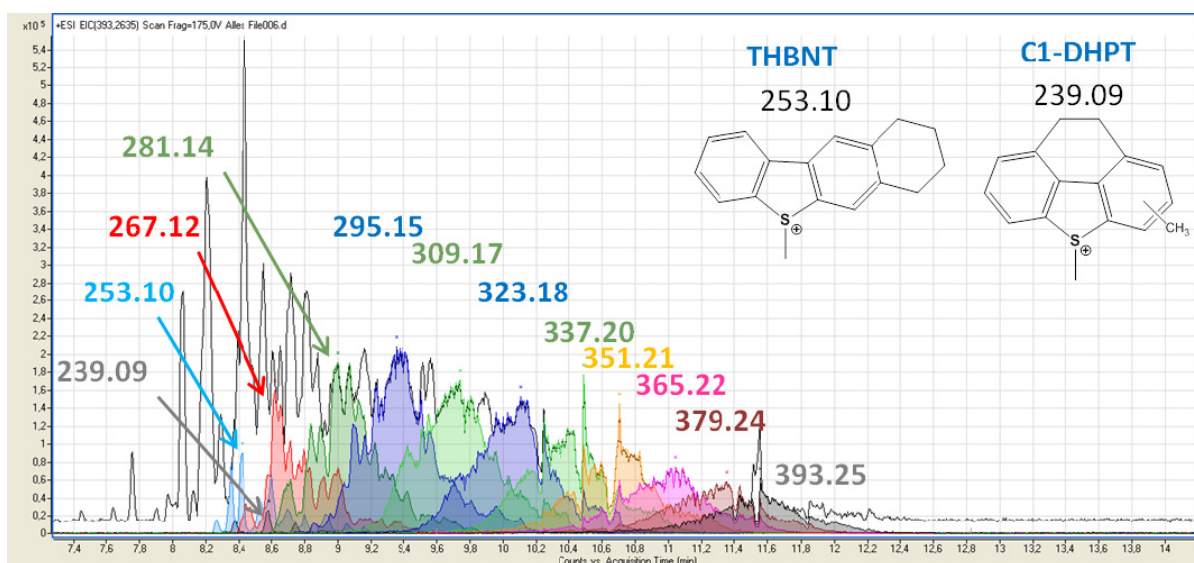


**Fig. 89:** Overlay of extracted ion electropherograms of methylated THBNTs and DHPTs of the parental HGO sample by nonaqueous CE-TOF MS. Electrolyte: 4 % acetic acid in methanol with addition of 70 mM ammonium formate.

### 7.4.3 Comparison with GC-MS

Although the results from the capillary electrophoretic separations of real world sample PASHs are quite promising, a direct comparison with other methods for the analysis of such samples has not been done so far, except for RP-HPLC. A comparison of the electrophoretic results with results obtained by GC-MS would be helpful to evaluate the CE separation of PASHs. For this reason the PASH fractions of the three HGOs that were used for the CE-MS measurements were collected by ligand exchange chromatography and measured by GC-MS. The GC-MS parameters are provided in the appendix (10.7).

The chromatogram for the low boiling PASH fraction shows DBT at the retention time of 25.86 min (figure 90). Significant concentrations of C1-DBTs can be found, with 4-methyl-DBT as the most abundant one. The molecular ion signal for this compound occurs at a migration time of 27.86 min in the mass spectrum (figure 90). Further signals can be assigned to the other isomers of C1-DBTs (28.36 min and 28.78 min). The rest of the signals are derived from fragmentation of larger compounds. C2-DBTs are found in high concentrations as well with 4,6-dimethyl-DBT as the most abundant compound. It was identified at a retention time of 29.88 min through its molecular ion signal (figure 91). 4-Ethyl-DBT was found at a migration time of 30.79 min and could be identified by its molecular ion signal (mass: 212) and the loss of 15 masses, which leads to the 4-methyl-DBT radical cation fragment with a mass of 197 (figure 91). THDBTs, which were present in the samples with the CE-TOF MS method, can be observed by GC-MS as well. The signal at the retention time of 27.45 min can be assigned to 4-methyl-THDBT. The mass spectrum shows the molecular ion signal for the substance ( $m = 202$ ) and a loss of 28 masses from the loss of a  $C_2H_2$  fragment of the hydrogenated ring in the molecule (figure 91). Higher molecular THDBTs are found in significant concentrations as presented in figure 92.



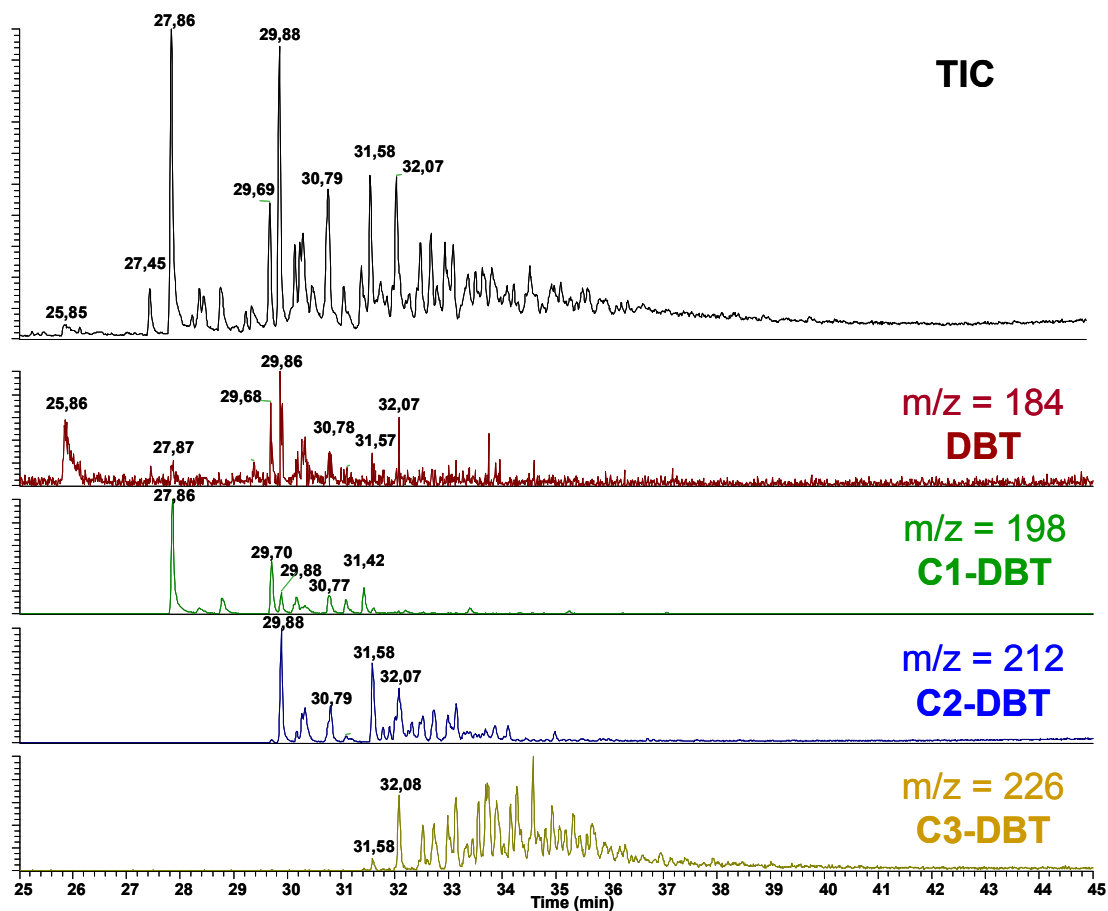
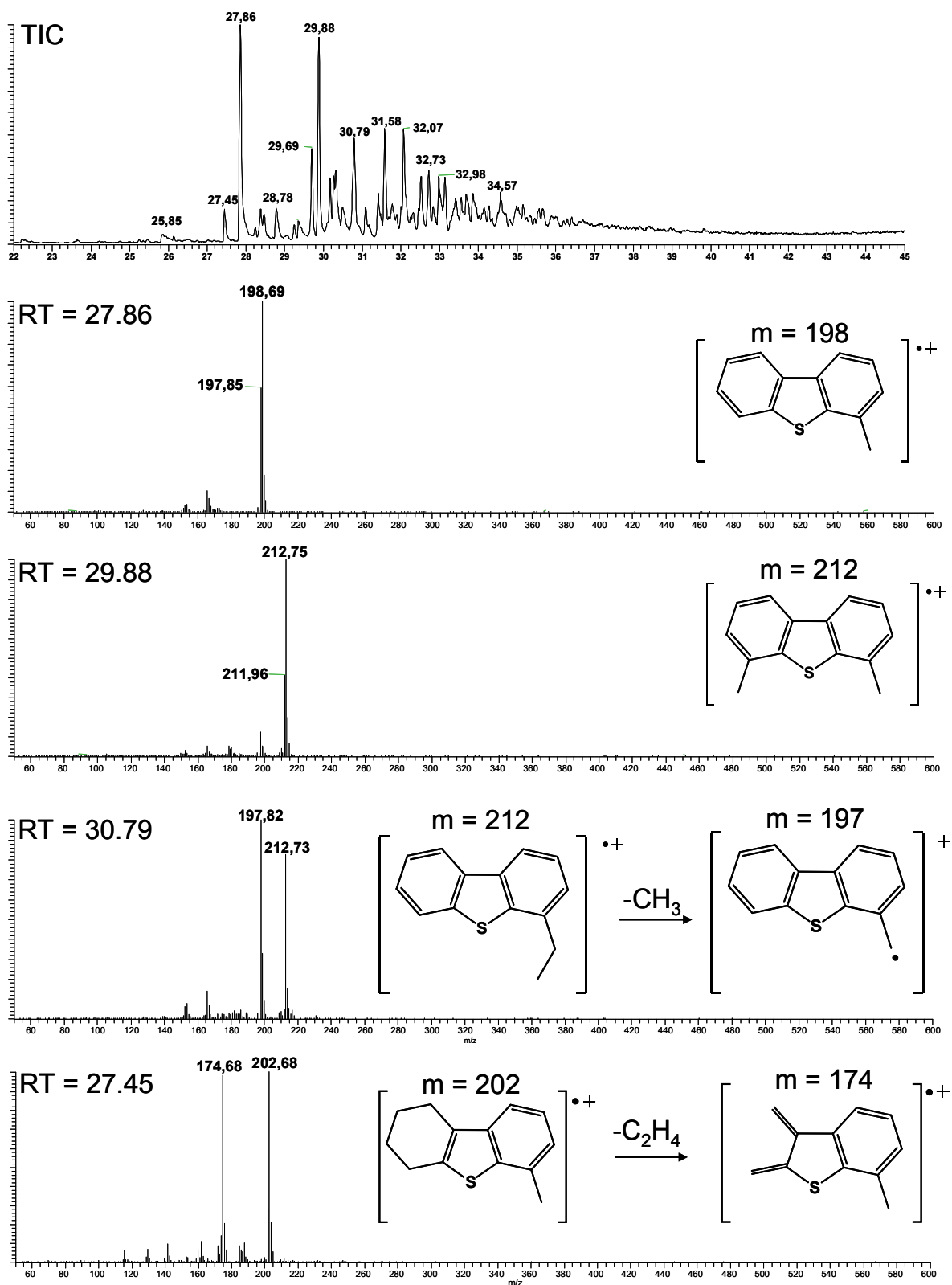
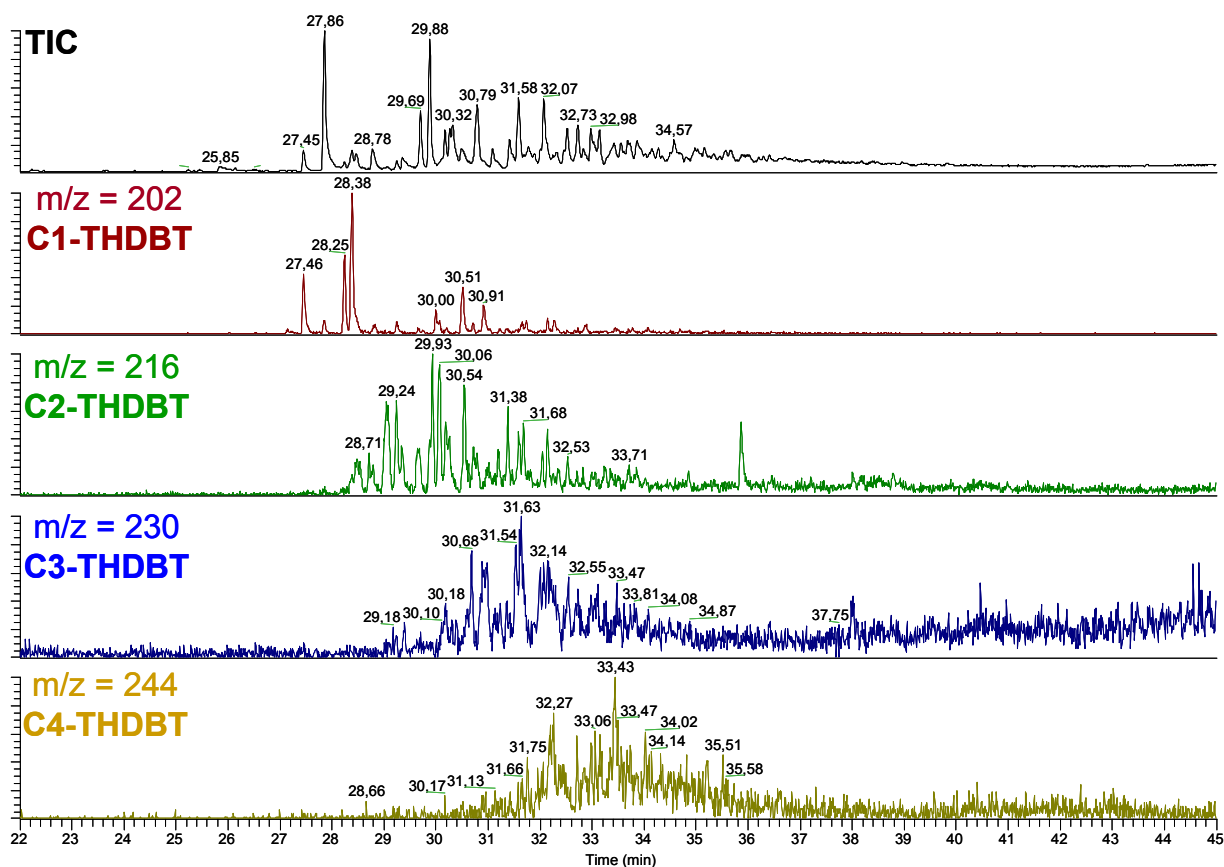


Fig. 90: GC-MS chromatogram of the low boiling sample PASHs with the extracted ion chromatograms for DBT to C3-DBTs.



**Fig. 91: GC-MS chromatogram of the low boiling sample PASHs with identification of different compounds by fragmentation pattern.**



**Fig. 92: GC-MS chromatogram of the low boiling sample PASHs with the extracted ion chromatograms for C1-THDBTs to C4-THDBTs.**

For the higher boiling fraction of the HGO it is obvious that the usual GC-MS-methods are not sufficient for the analysis of such samples. The compounds cannot completely be eluted from the column. Even methods with slower temperature gradients were used without the separation being finished. Compounds up to the masses of C12-DBT and even higher occur in the sample, according to the results from CE-MS. The extracted ion chromatograms for DBT to C6-DBTs are presented in figure 93.

## TIC

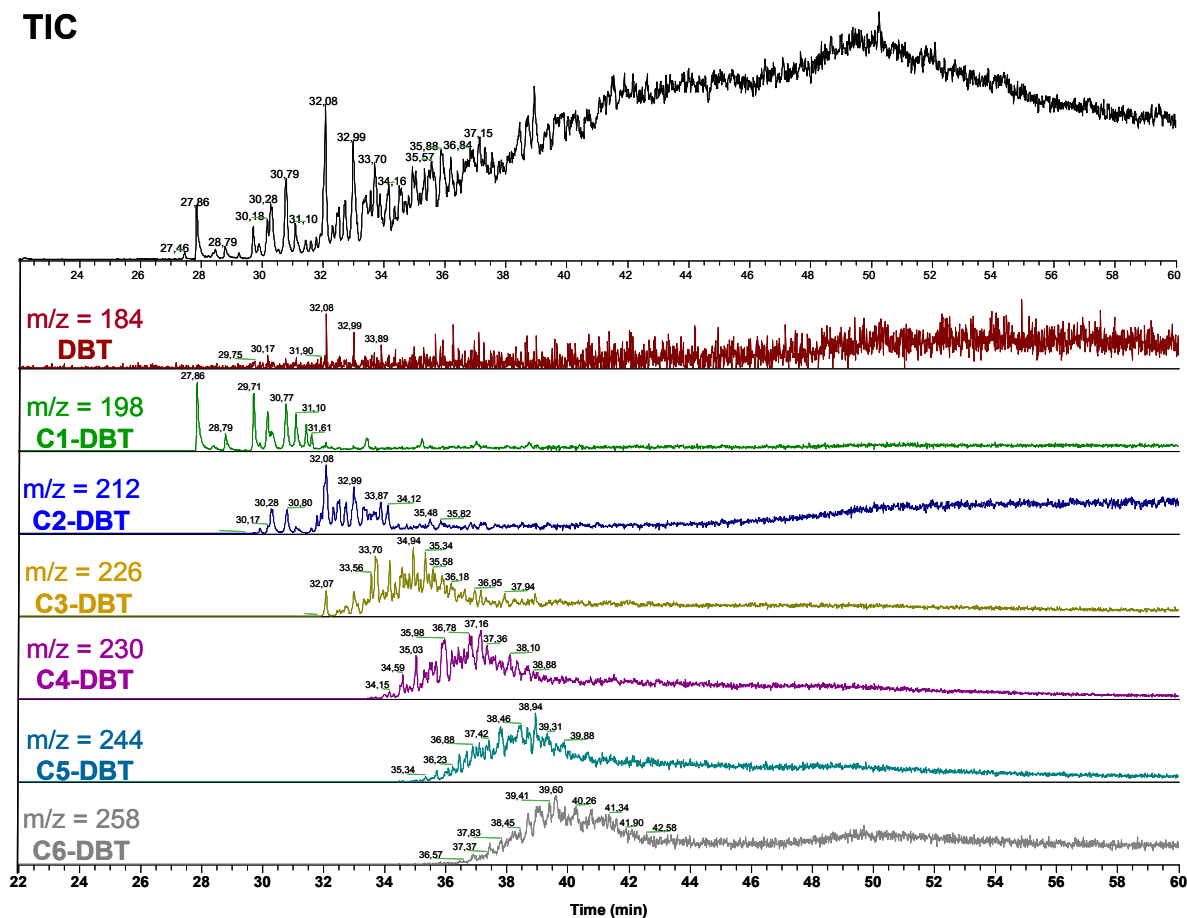


**Fig. 93: GC-MS chromatogram of the higher boiling sample PASHs with the extracted ion chromatograms for DBT to C6-DBTs.**

THDBTs are only found in extremely small concentrations in the early part of the chromatogram. This result agrees with the CE-MS analysis of the sample where minimal THDBT concentrations were observed.

The masses for the homologous series of THBNTs and DHPTs can be found in the GC analysis of the sample, in agreement with the results from CE-MS. The chromatograms for the extracted masses 224 to 280 are presented in figure 94. In the CE-MS measurements THBNTs and DHPTs with 10 to 13 carbon atoms in the side chains were observed, which fits quite well to the results from GC-MS.

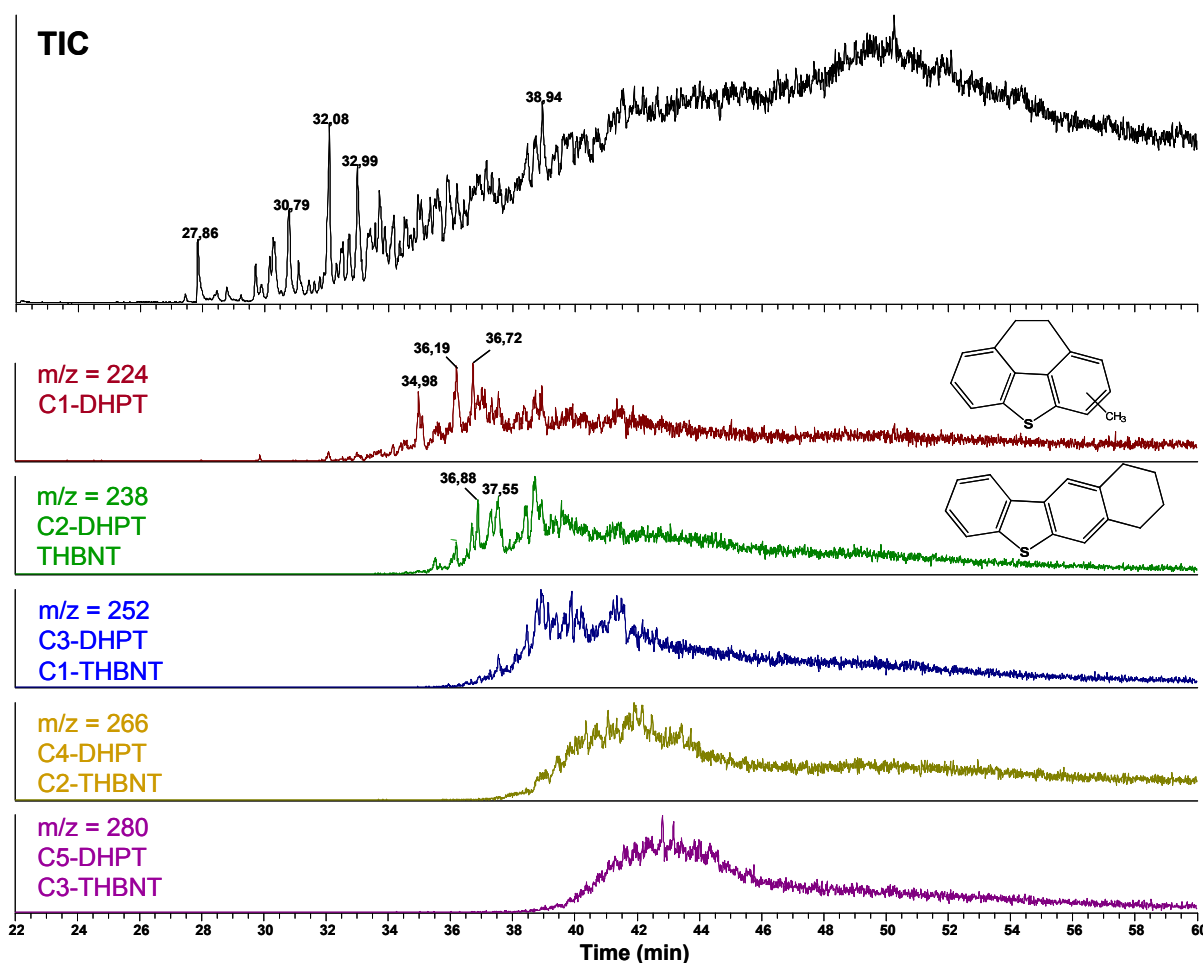


**Fig. 94: GC-MS chromatogram of the higher boiling sample PASHs with the extracted ion chromatograms for the homologous series of THBNTs and DHPTs.**

The parental HGO sample was again expected to contain all the constituents detected in the low- and higher boiling fraction. DBT can be observed in low concentrations, in agreement with previous results. The extracted ion chromatograms for DBT to C6-DBTs are presented in figure 95. DBT homologous with up to 12 carbon atoms in the side chains can easily be recorded in the sample. The concentration of THDBTs in the parental sample is low (figure 96). This result again agrees with the results obtained by CE-MS. The masses for the homologous series of THBNTs and DHPTs were found in the parent sample according to the results from the GC-MS analysis of the higher boiling sample. The extracted ion chromatograms for the masses 224 to 280 are presented in figure 97.

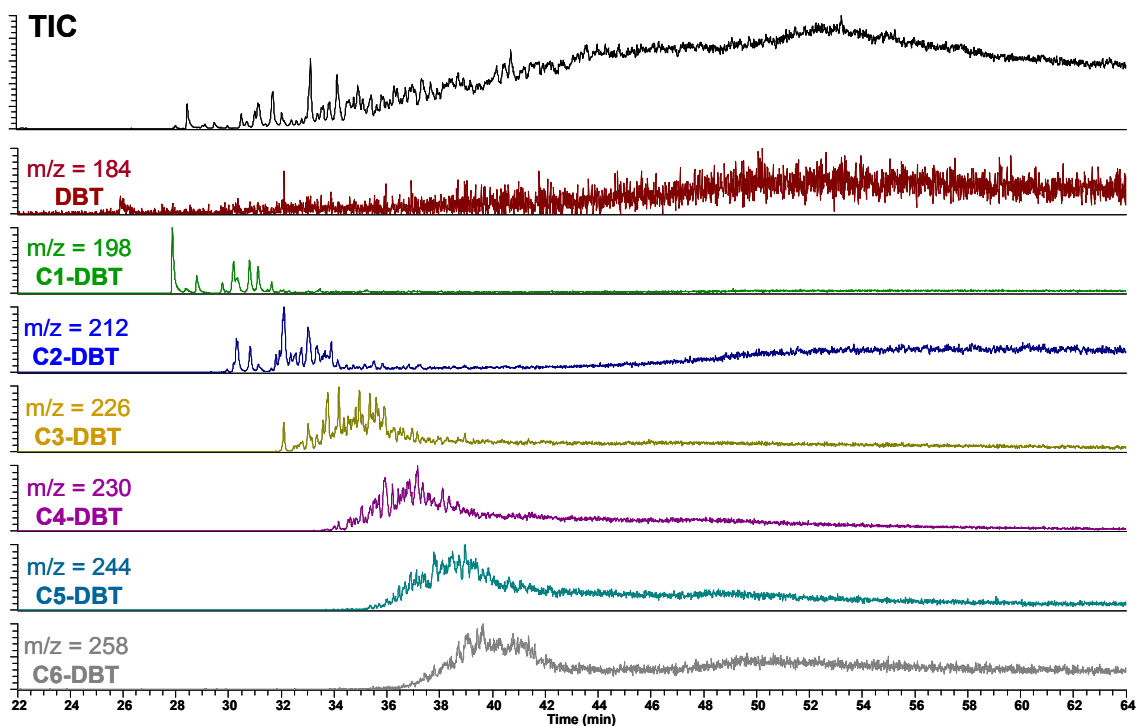


**Fig. 95:** GC-MS chromatogram of the parental sample PASHs with the extracted ion chromatograms for DBT to C6-DBTs.

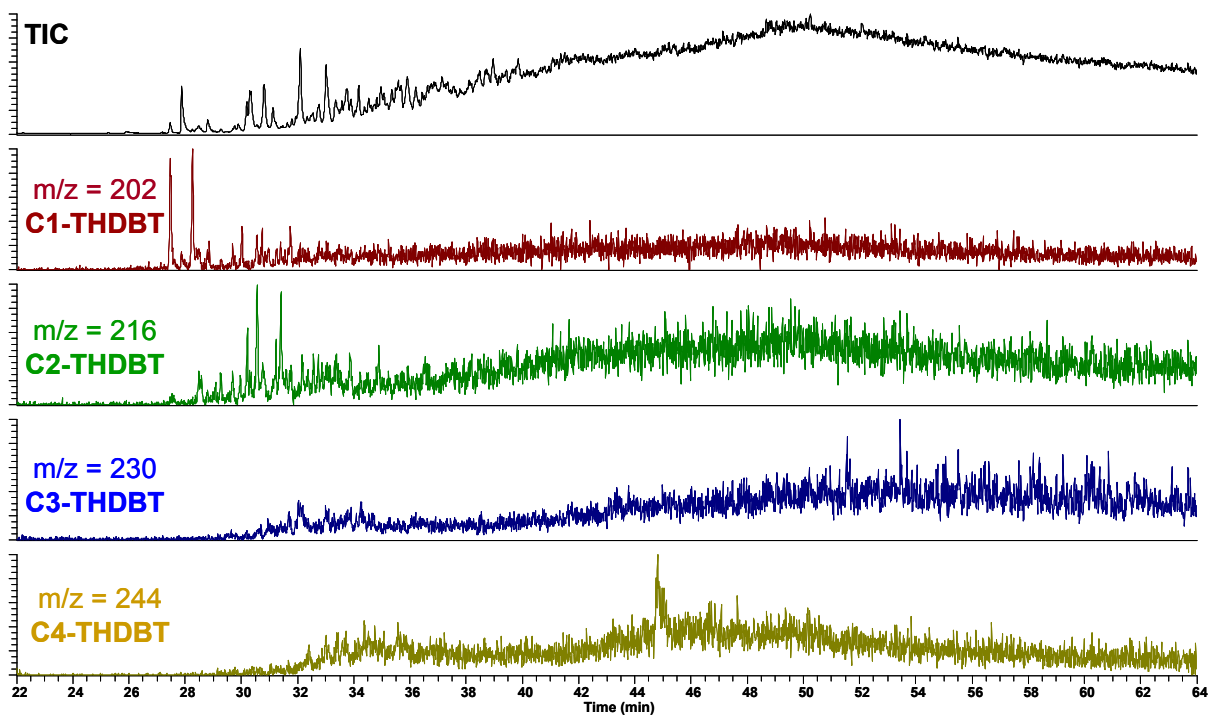


**Fig. 96:** GC-MS chromatogram of the parental sample PASHs with the extracted ion chromatograms for C1-THDBTs to C4-THDBTs.

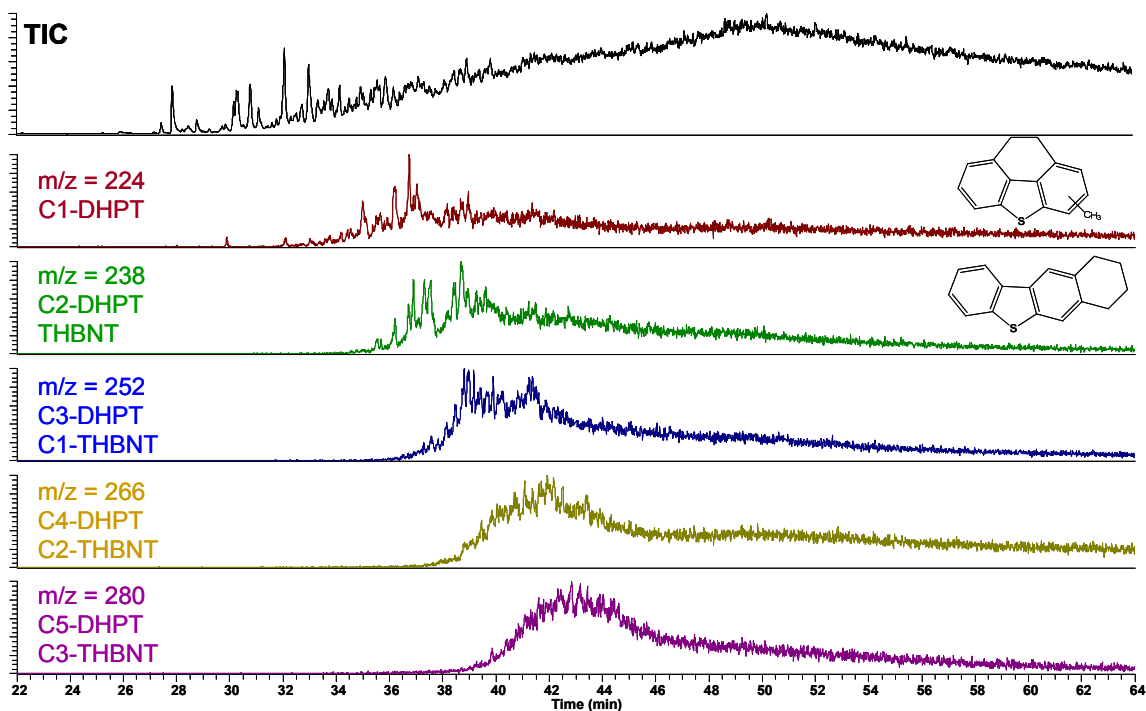


**Fig. 97:** GC-MS chromatogram of the parental sample PASHs with the extracted ion chromatograms for the homologous series of THBNTs and DHPTs.

Obviously, the results obtained by GC-MS verify the results of the CE-MS measurements. The same compound classes with similar degrees of alkylation can be found in the sample with both CE-MS and GC-MS methods. This demonstrates the applicability of the CE-method. The GC analysis of the higher boiling fraction and the parent sample was problematic due to the fact that a sufficient volatility was not displayed by many compounds. These problems did not occur in CE-MS as all the compounds migrated through the capillary and the signal reached the baseline at the end of the separation. However, the resolution of CE is still lower than the one obtained by GC.

#### 7.4.4 Comparison to Orbitrap MS

FT-ICR MS and Orbitrap MS gain more and more prominence in the analysis of fossil fuel samples. Due to the extremely high resolution, it is possible to obtain a lot more information about highly complex samples than with other methods. PASHs are typically analyzed by this method after isolating them by means of LEC followed by the same derivatization reaction that is used for the CE measurements of these analytes.

Because the Orbitrap analysis of fossil fuel PASHs also includes the derivatization step, it was interesting to see if the results agree with the CE measurements. The PASH-fractions from the parental HGO and its two distilled fractions were therefore derivatized and analyzed by Orbitrap MS.

The first sample was the low boiling fraction of the LGO. From CE-TOF MS and GC-MS it is known that the main constituents of this sample are alkylated DBTs. This result is obviously achieved by Orbitrap MS as well (figure 98). Low concentrations of DBT can be found in agreement with the results of the other methods. C2- to C4- alkylated DBTs are the main constituents in this sample while DBTs with up to ten carbon atoms in the side chains are found. This result is slightly different from the ones obtained by CE-MS analysis. The problem is that higher alkylated DBTs give a very broad signal in CE due to the different migration times of all the isomers. This means that, for example, all of the C8-DBTs are spread out over a migration time window of more than four minutes. Hence, the signal for each of the many different isomers is very small. The signal in Orbitrap MS is generated by all the isomers since they all have the same mass. A comparison of the intensities can hence only be done by integrating the signals for all the isomers in CE-MS.

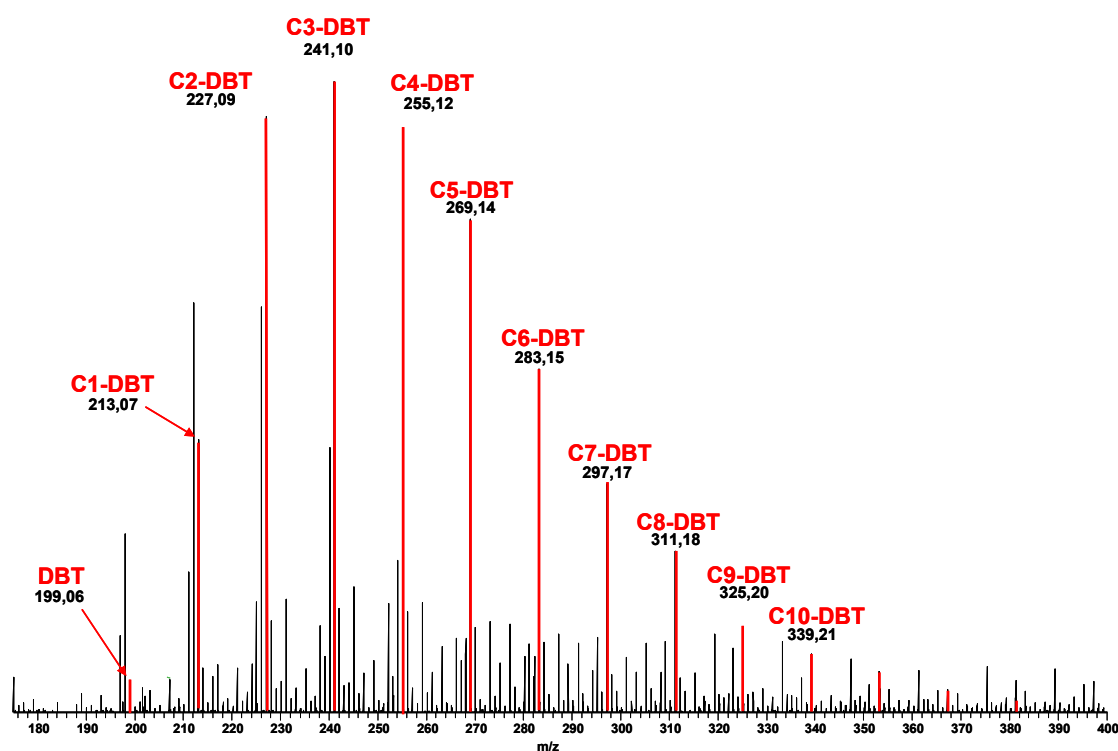


**Fig. 98:** Orbitrap MS spectrum of the low boiling HGO PASHs with alkylated DBTs marked in red.



A further homologous series of signals can be observed in the spectra, beginning with a mass of 184.03 (figure 99). Interestingly, the exact masses of the signals completely match the masses of underivatized DBT homologous. The Orbitrap MS, for example, shows a mass of 198.0492 in the spectra while the calculated mass for a C1-DBT radical cation is 198.0498. This good agreement of the measured and the calculated mass leads to the assumption, that the homologous series is derived from demethylated species of DBTs. Demethylation reactions are known to occur for the methylated products [127] and a loss of the methyl group during MS measurements has already been observed in earlier studies [112]. The exact species of the demethylated products is not known but expected to be a radical cation. The age of the sample as well as the instrumental parameters of the MS measurements have a significant influence on the occurrence of the demethylated products, so that it is difficult to say if they are produced during the derivatization itself or are generated during the MS. An Orbitrap measurement of methylated benzophenanthro[9,10-*d*]thiophene is shown in figure 100 (measured by M. NOCUN). The mass 299.09 belongs to the methylated species while the mass 284.07 corresponds to the demethylated product. The homologous series beginning with the mass 184.03 in the Orbitrap MS of the low boiling HGO sample can hence be related to alkylated dibenzothiophenes. These compounds cannot be seen in the electrophoretic measurements as they are probably only stable in the ESI-spray, but not in aqueous media during CE separations. Reactions of the radical cations with the buffer constituents will probably yield neutral, uncharged species that are not separated by CE.

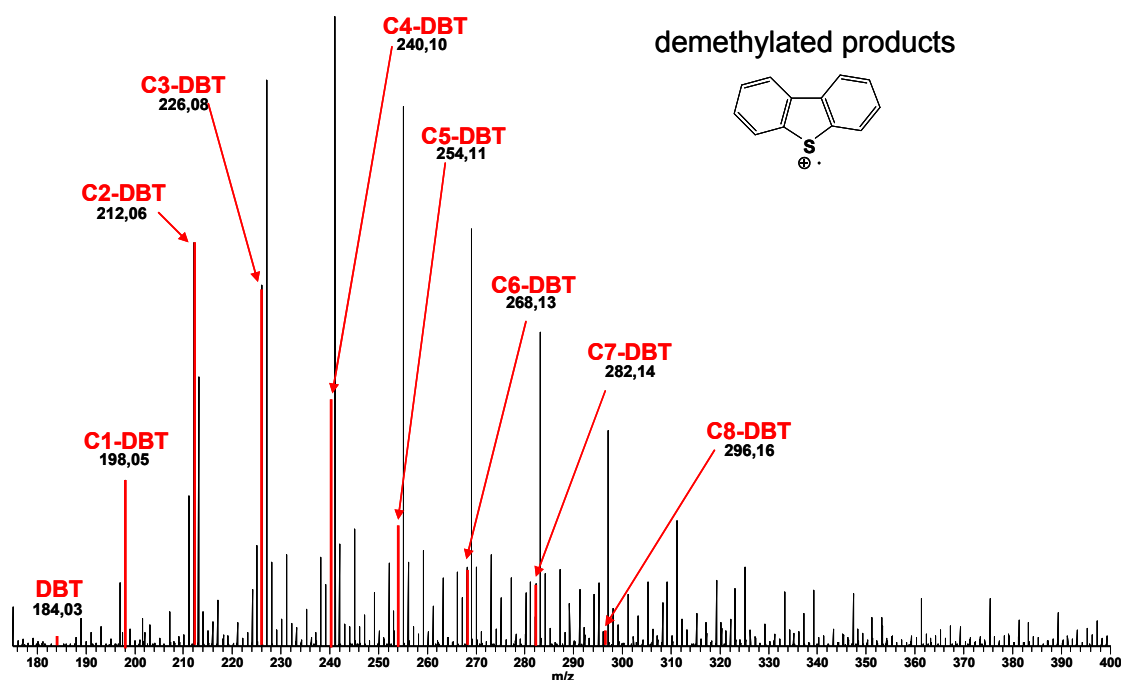


**Fig. 99:** Orbitrap MS spectrum of the low boiling HGO PASHs with demethylated DBT radical cations marked in red.

THDBTs were found by Orbitrap MS as well (figure 101) with more than seven carbon atoms in the side chains. This result is again in accordance with CE-MS and GC-MS.

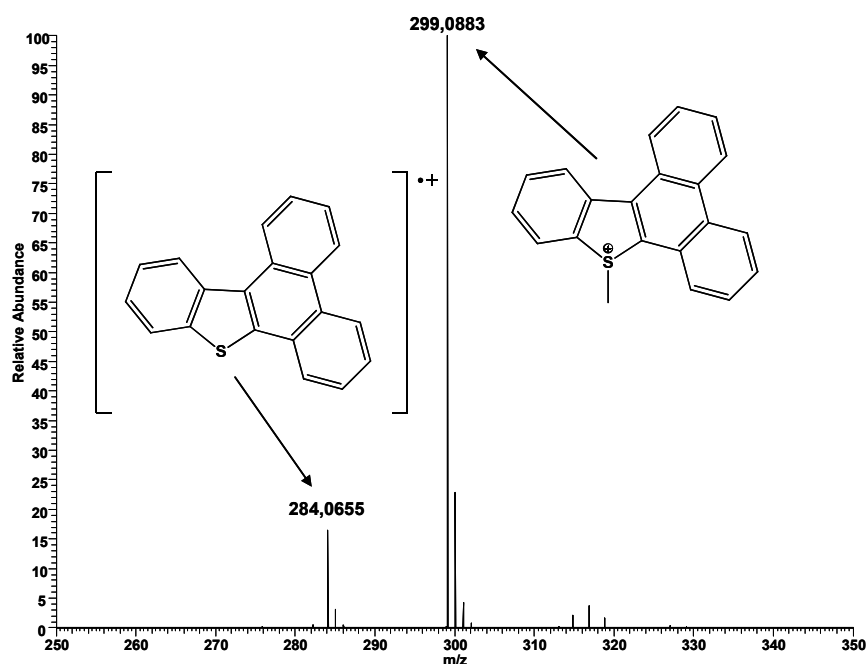


**Fig. 100:** Orbitrap MS spectrum of methylated benzophenanthro[9,10-*d*]thiophene.

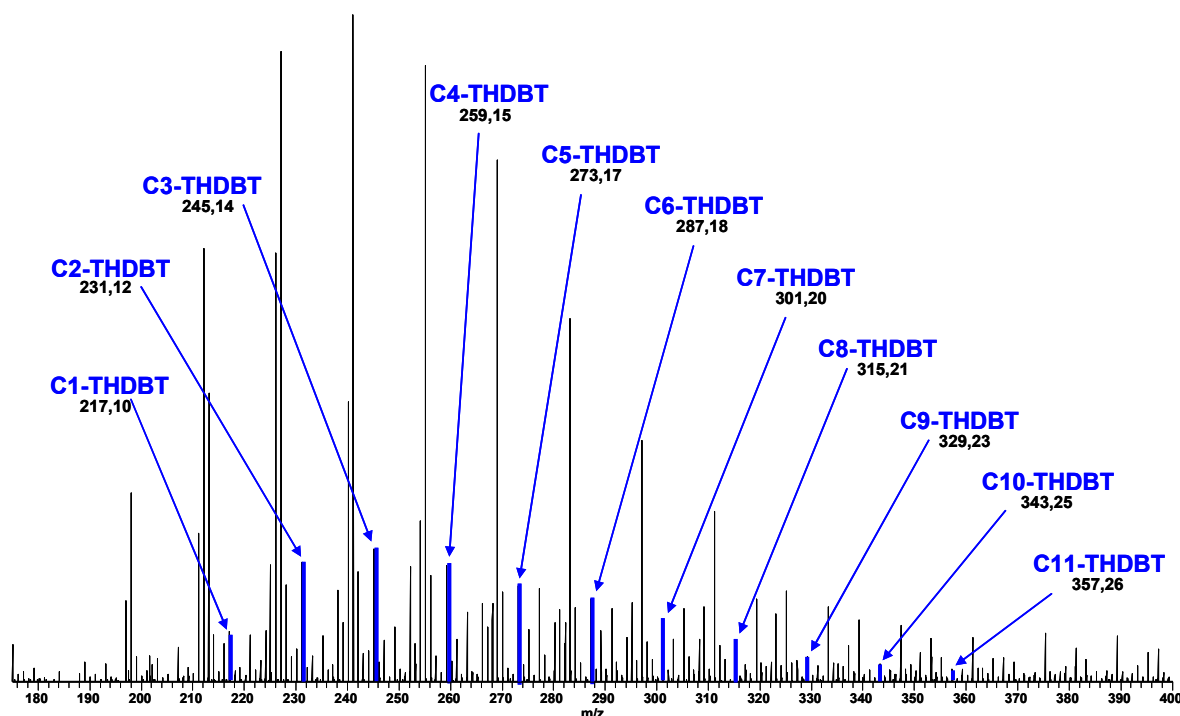


**Fig. 101: Orbitrap MS spectrum of the low boiling HGO PASHs with alkylated THDBTs marked in blue.**

In the higher boiling fraction of the HGO, no signal for DBT could be detected, in agreement with the CE-MS results where only very low concentrations were found. Alkylated DBTs ranging from C1-DBT to C20-DBT can be observed with C5- to C9-DBTs as the most abundant compounds (figure 102). Signals for demethylated DBT radical cations can be found as well, but in lower concentrations than in the previous sample. In CE-MS the C5-DBTs were identified as the most abundant DBTs. This difference can again be explained by the spread out signals in the electropherograms of the isomers. The signal intensities of the higher alkylated DBTs are hence smaller but the sum of their integrals would indicate the true concentrations. However integration of the CE measurements was not performed so that a direct comparison was not possible. In addition to the alkylated DBTs, the homologous series of THBNTs and DHPTs belongs to the main constituents of the higher boiling fraction. These compound classes can as well be detected with masses of up to 550 (figure 103).

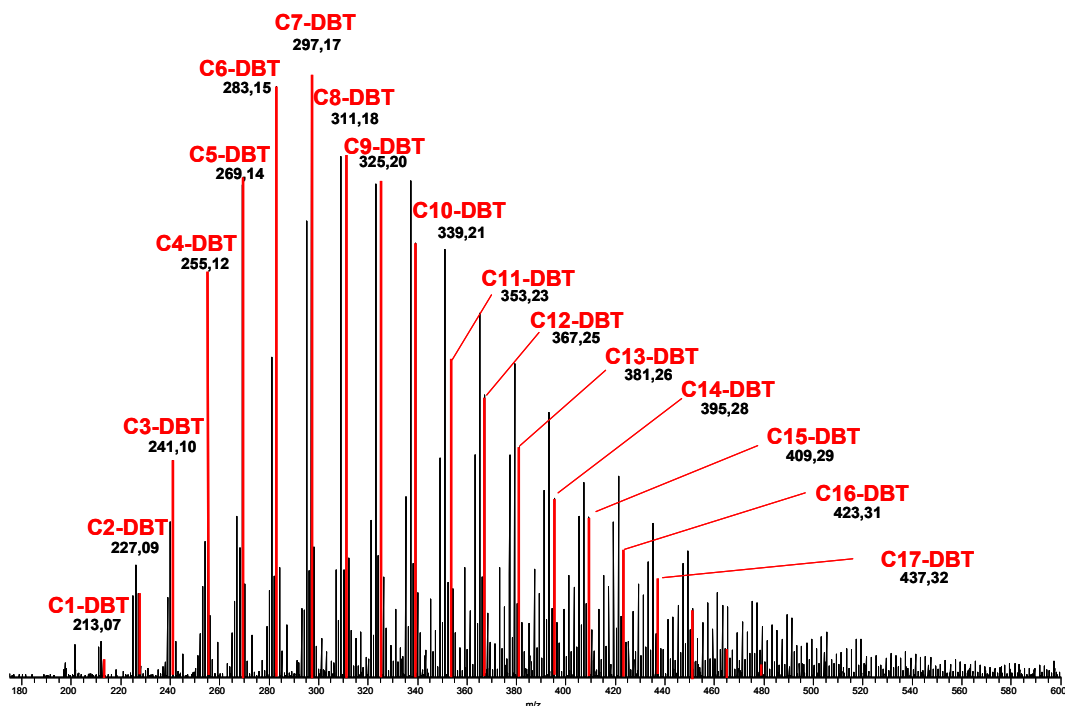


Fig. 102: Orbitrap MS spectrum of the higher boiling HGO PASHs with alkylated DBTs marked in red.

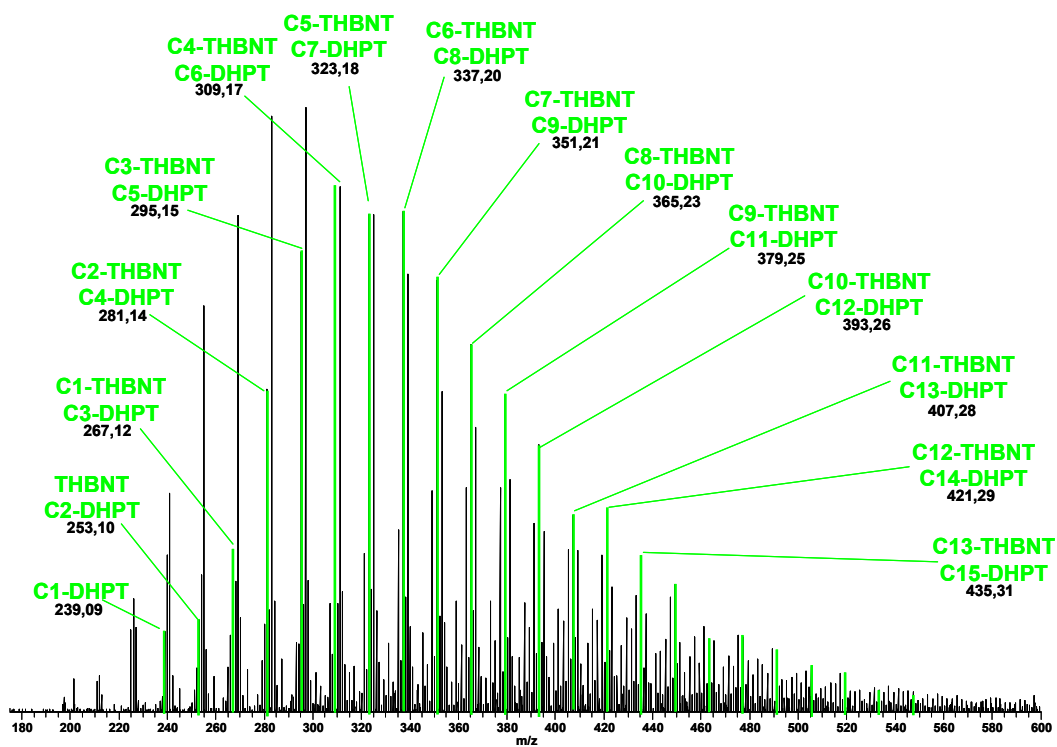
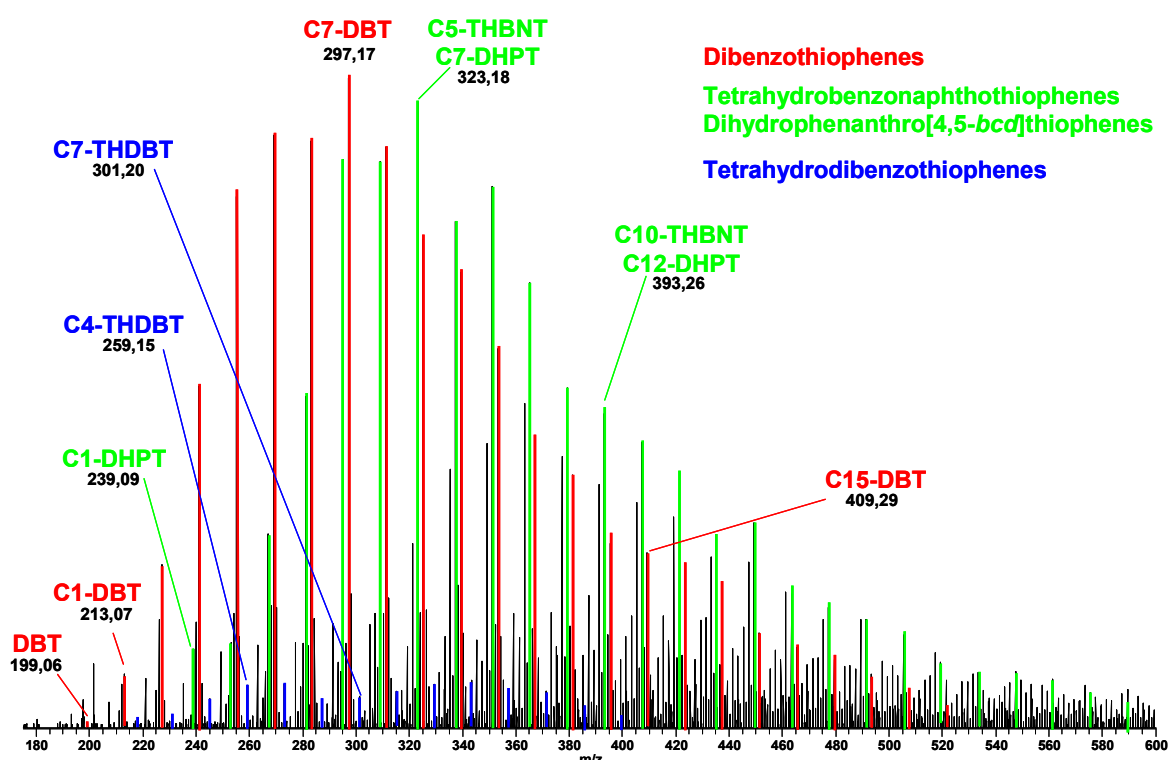


Fig. 103: Orbitrap MS spectrum of the higher boiling HGO PASHs with alkylated THBNTs and DHPTs marked in green.

The parent HGO sample contains all the compound classes found in the distilled samples. DBTs with more than 20 carbon atoms in the side chains can be detected, a very small signal can be observed for DBT itself (figure 104). Very low concentrations for demethylated compounds can be observed as well. THDBTs can be observed as well, but in low concentrations. THBNTs and DHPTs are the other main constituents in the sample with the mass 323.18 as the most abundant one.



**Fig. 104:** Orbitrap MS spectrum of the parental HGO PASHs with alkylated DBTs marked in red, THBNTs and DHPTs marked in green and alkylated THDBTs marked in blue.

In summary, the results from the Orbitrap MS measurements agree well with the results from the CE-MS analysis. However, the analysis of higher mass compounds by CE-MS is difficult because the analytes of a given mass are widely distributed over the electropherogram due to their different mobility. The signal for each isomer is hence quite small, so that especially the signals of larger compounds can be lost in the background noise.

## 7.5 Discussion

Within the last chapter a broad variety of real world sample PASHs was separated by different capillary electrophoretic methods. The commonly used technique was the separation after derivatization with either CE-UV or CE-TOF MS. The CE-UV measurements demonstrated that the resolution of the separation can compete with RP-HPLC analysis of the samples. However, the resolution is still lower than the one obtained with GC methods.

Cyclodextrins were successfully used to increase the resolution of the separation of standard compounds but this technique is not applicable to real world samples. Due to the additionally occurring enantiomeric separation, the number of signals in the electropherogram increases, making it even more complex. Further experiments dealing with the application of cyclodextrins for the separation of derivatized PASHs were discontinued for this reason.

Especially when the samples have not been desulfurized, the electropherogram is crowded with unresolved signals. This could clearly be seen in the separation of the LGO feedstock sample, where even the identification of DBT, 4-methyl-DBT and 4,6-dimethyl-DBT was difficult due to the comigration with other compounds. Especially in the later part of the electropherogram, all compounds comigrated, so that no individual signals were obtained and the overall signal only slowly decreased back to the baseline.

Nonaqueous and partly aqueous CE-UV was introduced for the separation of the first step desulfurized LGO PASHs. A separation in a buffer consisting of 4 % acetic acid in methanol with the addition of 70 mM ammonium formate showed that the electropherogram is a lot more compact and the overall resolution is hence smaller. Identification of single compounds was difficult due to comigration. However, this technique demonstrated its advantages for the CE-TOF MS measurements discussed later. The partly nonaqueous separation with addition of 40 % isopropanol led to increased migration times but also showed improved separation.

MEKC was tested for the separation of the PASHs in the LGO feedstock real world sample. As expected from the separation of standard compounds, the analysis of real world samples with MEKC is not successful. While the smaller and more polar constituents of

the sample, like BT, are nicely separated, all the larger compounds comigrate at the end of the micellar window, although a buffer with an organic modifier and addition of cyclodextrins was used. An identification of individual compounds is impossible. The MEKC method might be of interest for the analysis of PASH mixtures with smaller analytes but cannot be used for the analysis of compounds that are much larger than DBTs. The interaction of these compounds with the micelle interior is so strong that a successful separation is impossible.

CE-UV was used to compare the progress in desulfurization for two HGOs that were desulfurized at different temperatures. A direct comparison of the electropherograms made it possible to see differences in the pattern. The concentration of the less recalcitrant compounds decreased in comparison with the most recalcitrant compound 4,6-dimethyl-DBT when a higher temperature was used during the HDS process. However, the differences in the pattern could only be observed for the smaller PASHs, as all the larger ones comigrate so that individual compounds in this area are not resolved.

Both aqueous and nonaqueous CE coupled to TOF MS are introduced as new analysis methods for PASHs from fossil fuels. Both methods were successful in analyzing the PASH fractions of desulfurized fuels. The main difference between the two methods is found in the migration order of the analytes. While the analytes in aqueous CE migrate according to their size, a change in migration behavior can be observed in nonaqueous CE which makes the electropherograms more complex. However, the resolution for nonaqueous CE exceeds the one obtained by aqueous CE and additionally migration times are shorter for the nonaqueous method. Nevertheless both methods succeeded in the identification of the main constituents of the samples and delivered similar results. To verify the capillary electrophoretic method, analyses of the same sample were performed with other analytical methods.

GC-MS provided results that were in agreement with the CE-MS results on the one hand, and demonstrated the volatility problems with high boiling samples on the other hand.

The Orbitrap MS measurements verified the results from previous measurements and demonstrated its practicability especially for high boiling samples. While highly alkylated DBTs can easily be found in the Orbitrap spectra, these signals disappear in the background of the CE-MS measurements.

## 8 Summary and outlook

Capillary electrophoresis is not generally thought of as a typical technique for the separation of PASHs from fossil fuels because a variety of methods already exist to analyze these compounds. However, this technique can now be added to the list of possible methods. Within this work, an overview of different capillary electrophoretic techniques to separate PASHs was established. Most of the analyses were based on the separation of the analytes after derivatization. This step was necessary to impart electrophoretic mobility into the compounds. The separation of standard PASHs by CE was successful and a comparison to RP-HPLC demonstrated the high efficiency of the electrophoretic separations. However, this technique has drawbacks when real world samples are separated. Non-desulfurized samples were far too complex for an electrophoretic separation. Massive comigration of the compounds occurred. The identification of individual compounds in the electropherograms was possible, but quantification was impossible due to the comigration of the signals. High boiling samples showed the problem that, especially for the higher molecular analytes, no resolution could be obtained, due to peak broadening of the later migrating compounds and the increased complexity of the sample in this part. Hence, the most suitable samples for the capillary electrophoretic analysis of PASHs from fuels were partly desulfurized LGOs. The complexity of these samples is limited, due to the partial desulfurization, and the rather small size of the analytes. However, this severely limits the applicability of the method.

The addition of cyclodextrins to the running buffer for the CE-separation of PASHs led to very different results for standard compounds and real world samples. While these additions increased the resolution of the separation of standard compounds and led to even better results than obtainable with GC, the addition of cyclodextrins failed for the separation of real world samples. Due to the formation of enantiomers during the derivatization step, an additional signal for all non-symmetric analytes occurred, which further complicated the electropherogram.

The correlation of migration time and calculated volume that was found for the capillary electrophoretic separation of derivatized PASHs earlier becomes problematic for compounds with longer alkyl chains. Hence, the application to real world samples is not possible, because analytes with long alkyl chains are expected in fossil fuels. From the



Orbitrap MS measurements it is known that DBTs with up to 20 carbon atoms in the side chains exist in HGOs. Significant deviations from the linear correlation were, however, already observed for DBTs with more than five carbon atoms in the side chains. The migration times of even isomeric compounds can differ greatly for this reason. This can, for example, be observed during the CE-TOF MS measurements. The signals for C10-DBT are widely spread out over big parts of the electropherogram. This can be explained by a different folding of the alkyl chains in aqueous media and hence a different molecular shape, because the calculated molecular volumes are not expected to vary to a large extent. The only way to solve this problem is to use a different software for the calculation that is capable of calculating behavior of alkyl chain folding in aqueous media.

MEKC was introduced as an electrophoretic technique that does not require a derivatization of the analytes. This technique is not applicable to the separation of PASHs when normal MEKC buffers are used. When cyclodextrins and organic modifier were added, the PASHs could be separated. However, this problem could be solved by using a buffer that contains high concentrations of HP- $\beta$ -cyclodextrin and methanol which led to a good baseline separation of four standard PASHs. Nevertheless, the additives were not sufficient for the separation of real world samples. Comigration of all the higher molecular PASHs of the sample could be observed at the end of the micellar window. MEKC for the analysis of higher boiling real world samples is hence not applicable.

The most promising capillary electrophoretic method for the analysis of PASHs is the coupling of CE to MS. The results obtained from CE-TOF MS measurements greatly improve on the results from the other methods. Due to the fact that a further dimension of separation is added, the electropherograms are less complex. Individual compounds and compound classes can easily be identified as demonstrated. The results agree with measurements of other chromatographic and mass spectrometric methods. However, further studies in this field have to be performed. Especially the analysis of high boiling samples is of interest because these are difficult to deal with when GC methods are used. Further buffer systems and additives could be tested to increase the resolution of the signals. The exact composition of the real world samples is of special interest because it could not be determined whether tetrahydrobenzonaphthothiophenes or dihydrophenanthrothiophenes occur in the high boiling samples. This problem could be solved by developing a chromatographic pre separation of the samples according to the

structure of the compounds. Concerning the Orbitrap measurements, further studies on the demethylation of the derivatized PASH have to be done. Single compounds can be derivatized and artificially be aged to look for the demethylation products.

In summary it can be stated that capillary electrophoresis was introduced as a new technique for the separation of PASHs that can compete with RP-HPLC and GC depending on the sample. The main drawback is that electrophoretic mobility has to be imparted to the analytes via derivatization which makes the analysis more laborious than other techniques. However, this disadvantage can be balanced by very high resolution and independence of volatility of the compounds. Especially for less complex samples the capillary electrophoretic method showed superior resolution that even exceeded the resolution obtained by GC. This feature could be used for the analysis of chromatographically pre-separated samples. Argentation chromatography could, for example, be used to separate real world samples according to their ring size [19] followed by a capillary electrophoretic separation of the different fractions. As presented in chapter 7.3, CE can be used to compare the sulfur pattern of gas oils at different stages during the desulfurization process. This technique might be of interest in industry as far as the analysis times are kept very short. This aim can be achieved by minimizing the time used for the derivatization. Recent studies in the working group indicate that the derivatization reaction is quantitatively finished after several minutes. Combining this shortened derivatization with a fast separation on short capillaries or even microchips would lead to very short analysis times. MEKC can not be used for the analysis of compounds with high masses but shows nice resolution for smaller analytes. This method could hence be adapted for the separation of small PASHs, like they occur in petroleum condensates. Other micelle surfactants or polymeric surfactants could be used to improve the separation.

## 9 Literature

- [1] Online reference source: „Entwurf eines dreizehnten Gesetzes zur Änderung des Atomgesetzes, 22.06.2011“, draft law of the Federal Government of Germany (<http://dipbt.bundestag.de/dip21/btd/17/062/1706246.pdf>), last access 03.10.2011
- [2] Online reference source: <http://www.oilscenarios.info/>, last access 03.10.2011
- [3] Online reference source: <http://www.theglobeandmail.com/report-on-business/international-news/european/norway-oil-gas-find-may-be-its-third-biggest/article2186042/>, last access 03.10.2011
- [4] Online reference source: Association for the Study of Peak Oil and Gas [http://energiekrise.de/erdoel/images\\_sections/Grafik5.gif](http://energiekrise.de/erdoel/images_sections/Grafik5.gif), last access 03.10.2011
- [5] Czogalla C.D. and F. Boberg. 1983. Sulfur compounds in fossil fuels. I. Annulated thiophenes in crude oils, oil shales, tar sands, syncrudes, and extracts from coals. *Sulfur Reports*, 3:121-167.
- [6] Purdy, K., Munson, M., Nedwell, D. and T. Martin Embley. 2002. Comparison of the Molecular Diversity of the Methanogenic Community at the Brackish and Marine Ends of a UK Estuary. *FEMS Microbiology Ecology*, 39:17-21.
- [7] Holmer, M. and P. Storkholm. 2001. Sulphate Reduction and Sulphur Cycling in Lake Sediments: a Review. *Freshwater Biology*, 46:431-451.
- [8] Online reference source: U.S. Energy Information Administration, [http://www.eia.gov/dnav/pet/pet\\_pri\\_wco\\_k\\_w.htm](http://www.eia.gov/dnav/pet/pet_pri_wco_k_w.htm), last access 03.10.2011
- [9] Younes, M. A., Hegazi, A. H., El-Gayar, M. S. and J. T. Andersson. 2007. Petroleum Biomarkers as Environment and Maturity Indicators for Crude Oils from the Central Gulf of Suez, Egypt. *Oil Gas-European Magazine*, 33:15-21.
- [10] Online reference source: <http://www.dieselnet.com/standards/eu/ld.php>, last access 03.10.2011
- [11] Nag, N.K., Sapre, A.V., Broderick D.H. and B.C. Gates. 1979. Hydrodesulfurization of Polycyclic Aromatics Catalyzed by Sulfided CoO-MoO<sub>3</sub>-Gamma-Al<sub>2</sub>O<sub>3</sub> – Relative Reactivities. *Journal of Catalysis*, 57:509-512.
- [12] Houalla, M., Nag, N.K., Sapre, A.V., Broderick, D.H. and B.C. Gates. 1978. Hydrodesulfurization of Dibenzothioethene Catalyzed by Sulfided CoO-MoO<sub>3</sub>- Al<sub>2</sub>O<sub>3</sub>: The Reaction Network. *A. I. Ch. E.*, 24:1015-1021.
- [13] Ma, X.L., Sakanishi, K.Y. and I. Mochida. 1994. Hydrodesulfurization Reactivities of Various Sulfur-Compounds in Diesel Fuel. *Industrial & Engineering Chemistry Research*, 33:218-222.
- [14] Maghsoudi, S., Vossoughi, M., Kheirilomoom, A., Tanaka, E. and S. Katoh. 2001. Biodesulfurization of Hydrocarbons and Diesel Fuels by *Rhodococcus* sp Strain P32C1. *Biochemical Engineering Journal*, 8:151-156.

- [15] Ohshiro, T. and Y. Izumi. 1999. Microbial Desulfurization of Organic Sulfur Compounds in Petroleum. *Bioscience Biotechnology and Biochemistry*, 63:1-9.
- [16] Kim, B. H., Kim, H. Y., Kim, T. S. and D. H. Park. 1995. Selectivity of Desulfurization Activity of *Desulfovibrio-Desulfuricans* M6 on Different Petroleum-Products. *Fuel Processing Technology*, 43:87-94.
- [17] Manufacturers of Emission Controls Association. 2000. "Catalyst-Based Diesel Particulate Filters and NO<sub>x</sub> Adsorbers: A Summary of the Technologies and the Effects of Fuel Sulfur".
- [18] Schade, T., Roberz, B. and J.T. Andersson. 2002. Polycyclic aromatic sulfur heterocycles in desulfurized diesel fuels and their separation on a novel palladium(II)-complex stationary phase. *Polycyclic Aromatic Compounds*, 22:311-320.
- [19] Nocun, M. and J. T. Andersson. 2011. Argentation chromatography for the separation of polycyclic aromatic compounds according to ring size. *Journal of Chromatography A*, accepted for publication.
- [20] Panda, S.K., Andersson, J.T. and W. Schrader. 2008. Fourier transform ion cyclotron resonance mass spectrometry in the speciation of high molecular weight sulfur heterocycles in vacuum gas oils of different boiling ranges. *Analytical and Bioanalytical Chemistry*, 392:839-848.
- [21] Hegazi, A. H., Roberz, B. and J. T. Andersson. 2006. Polycyclic aromatic sulfur heterocycles as information carriers in environmental studies. *Analytical and Bioanalytical Chemistry*, 386:891-905.
- [22] Marshall, A.G., Hendrickson, C.L. and G.S. Jackson. 1998. Fourier transform ion cyclotron resonance mass spectrometry: a primer. *Mass Spectrometry Reviews*, 17:1-35.
- [23] T. Nolte: Kapillarelektrophoretische Trennung derivatisierter polyaromatischer Schwefelheterocyclen. Diploma thesis. Westfälische Wilhelms-Universität, Münster/Germany. 2008.
- [24] K. Cammann. 2001. Instrumentelle Analytische Chemie – Verfahren, Anwendungen und Qualitätssicherung. *Spektrum Akademischer Verlag GmbH, Heidelberg/Germany*.
- [25] Skoog, D. A., Holler, F. J. and S. R. Crouch. 2007. Principles of Instrumental Analysis. *Thomson Brooks/Cole Publishing, Belmont/CA*.
- [26] Simó, C., Barbas, C. and A. Cifuentes. 2005. Capillary electrophoresis-mass spectrometry in food analysis. *Electrophoresis*, 26:1306-1318.
- [27] Kelly, J. F., Ramaley, L. and P. Thibault. 1997. Capillary Zone Electrophoresis-Electrospray Mass Spectrometry at Submicroliter Flow Rates: Practical Considerations and Analytical Performance. *Analytical Chemistry*, 69:51-60.
- [28] Smith, R. D., Barinaga, C. J. and H. R. Udseth. 1988. Improved electrospray ionization interface for capillary zone electrophoresis-mass spectrometry. *Analytical Chemistry*, 60:1948-1952.

- [29] Schmitt-Kopplin, P. and M. Frommberger. 2003. Capillary electrophoresis – mass spectrometry: 15 years of developments and applications. *Electrophoresis*, 24:3837-3867.
- [30] Brocke, A.v., Nicholson, G. and E. Bayer. 2001. Recent advances in capillary electrophoresis/electrospray-mass spectrometry. *Electrophoresis*, 22:1251-1266.
- [31] Lee, E. D, Muck, W., Henion, J. D. and T. R. Covey. 1989. Liquid junction coupling for capillary zone electrophoresis/ion spray mass spectrometry. *Biomedical and Environmental Mass Spectrometry*, 18:844-850.
- [32] Reinhoud, N. J., Niessen, W. M. A., Tjaden, U. R., Gramberg, L. G., Verheij, E. R. and J. van der Greef. 1989. Performance of a liquid-junction interface for capillary electrophoresis mass spectrometry using continuous-flow fast-atom bombardment. *Rapid Communications in Mass Spectrometry*, 3:348-351.
- [33] Pleasance, S., Thibault, P. and J. F. Kelly. 1992. Comparison of liquid-junction and coaxial interfaces for capillary electrophoresis-mass spectrometry with application to compounds of concern to the aquaculture industry. *Journal of Chromatography*, 591:325-339.
- [34] Wahl, J. H., Gale, D. C. and R. D. Smith. 1994. Sheathless capillary electrophoresis-electrospray ionization mass spectrometry using 10  $\mu$ m I.D. capillaries: Analyses of tryptic digests of cytochrome c. *Journal of Chromatography*, 659:217-222.
- [35] Olivares, J.A., Nguyen, N.T., Yonker, C.R. and R.D. Smith. 1987. On-line mass spectrometric detection for capillary zone electrophoresis. *Analytical Chemistry*, 59:1230-1232.
- [36] Barceló-Barrachina, E., Moyano, E. and M. T.Galceran. 2004. State-of-the-art of the hyphenation of capillary electrochromatography with mass spectrometry. *Electrophoresis*, 25:1927-1948.
- [37] Waterval, J. C. M., Bestebreurtje, P., Versluis, C., Heck, A. J. R., Bult, A., Lingeman, H. and W. J. M. Underberg. 2001. Robust and cost-effective capillary electrophoresis-mass spectrometry interfaces suitable for combination with on-line analyte preconcentration. *Electrophoresis*, 22:2701-2708.
- [38] Online reference source: [http://www.ucl.ac.uk/ich/services/lab-services/mass\\_spectrometry/metabolomics/hplc](http://www.ucl.ac.uk/ich/services/lab-services/mass_spectrometry/metabolomics/hplc) , last access 03.10.2011
- [39] Watanabe, T., Mazumder, T. K., Yamamoto, A., Nagai, S., Arimoto-Kobayashi, S., Hayatsu, H. and S. Terabe. 1999. A simple and rapid method for analyzing the Monascus pigment-mediated degradation of mutagenic 3-hydroxyamino-1-methyl-5H-pyrido[4,3-b]indole by in-capillary micellar electrokinetic chromatography. *Mutation Research*, 444:75-83.
- [40] Terabe, S., Otsuka, K. and T. Ando. 1985. Electrokinetic chromatography with micellar solution and open-tubular capillary. *Analytical Chemistry*, 57:834-841.

- [41] Kim, J. and S. Terabe. 2003. On-line sample preconcentration techniques in micellar electrokinetic chromatography. *Journal of Pharmaceutical and Biomedical Analysis*, 30:1625-1643.
- [42] Cugat, M. J., F. Borrull and M. Calull. 1999. Influence of organic solvents in the capillary zone electrophoresis of polycyclic aromatic hydrocarbon metabolites. *Chromatographia*, 49:261-267.
- [43] Huang, C. W., Jen, H. P., Wang, R. D. and Y. Z. Hsieh. 2006. Sweeping technique combined with micellar electrokinetic chromatography for the simultaneous determination of flunitrazepam and its major metabolites. *Journal of Chromatography A*, 1110:240-244.
- [44] Culbertson, C. T. and K. W. Hoeman. 2009. A novel, environmentally friendly sodium lauryl ether sulfate-, cocamidopropyl betaine-, cocamide monoethanolamine-containing buffer for MEKC on microfluidic devices. *Electrophoresis*, 29:4900-4905.
- [45] Hadley, M. R., Harrison, M. W. and A. J. Hutt. 2003. Use of chiral zwitterionic surfactants for enantiomeric resolutions by capillary electrophoresis. *Electrophoresis*, 24:2508-2513.
- [46] Online reference source: [http://mackerell.umaryland.edu/fig\\_micelle\\_files/sds\\_waterbox\\_trim.png](http://mackerell.umaryland.edu/fig_micelle_files/sds_waterbox_trim.png), last access 03.10.2011
- [47] Terabe, S., Y. Miyashita, O. Shibata, E. R. Barnhart, L. R. Alexander, D. G. Patterson, B. L. Karger, K. Hosoya and N. Tanaka. 1990. Separation of highly hydrophobic compounds by cyclodextrin-modified micellar electrokinetic chromatography. *Journal of Chromatography*, 516: 23-31.
- [48] Fu, X., J. Lu and A. Zhu. 1990. Micellar electrokinetic capillary chromatography with mixed ethanol-water solvent. *Fenxi Huaxue*, 18:791-795.
- [49] Yik, Y. F., C. P. Ong, S. B. Khoo, H. K. Lee and S. F. Y. Li. 1992. Separation of polycyclic aromatic hydrocarbons by micellar electrokinetic chromatography with cyclodextrins as modifiers. *Journal of Chromatography*, 589: 333-338.
- [50] Copper, C. L., T. D. Staller and M. J. Sepaniak. 1993. Characterization of polyaromatic hydrocarbon mixtures by micellar electrokinetic capillary chromatography. *Polycyclic Aromatic Compounds*, 3:121-135.
- [51] Otsuka K, M. Higashimori, R. Koike, K. Karuhaka, Y. Okada and S. Terabe. 1994. Separation of lipophilic compounds by micellar electrokinetic chromatography with organic modifiers. *Electrophoresis*, 15:1280-1283.
- [52] Jinno, K. and Y. Sawada. 1994. Relationships between capacity factors and hydrophobicity of polycyclic aromatic hydrocarbons in cyclodextrin-modified micellar electrokinetic capillary chromatography. *Journal of Capillary Electrophoresis*, 1:106-111.
- [53] Kaneta, T., T. Yamashita and T. Imasaka. 1995. Separation of polycyclic aromatic hydrocarbons by micellar electrokinetic chromatography with laser fluorescence detection. *Analytica Chimica Acta*, 299:371-375.

- [54] Jinno, K. and Y. Sawada. 1995. Relationships between capacity factors and hydrophobicity of polycyclic aromatic hydrocarbons in cyclodextrin-modified micellar electrokinetic chromatography using surface treated capillaries. *Journal of Liquid Chromatography*, 18:3719-3727.
- [55] Brueggemann, O. and R. Freitag. 1995. Determination of polycyclic aromatic hydrocarbons in soil samples by micellar electrokinetic capillary chromatography with photodiode-array detection. *Journal of Chromatography A*, 717:309-324.
- [56] Jinno, K. and Y. Sawada. 1995. Comparison of cyclodextrin modified micellar electrokinetic capillary chromatography and reversed-phase liquid chromatography for separation of polycyclic aromatic hydrocarbons. *Journal of Capillary Electrophoresis*, 2:151-155.
- [57] Dabek-Zlotorzynska, E. and E. P. C. Lai. 1996. Separation of polynuclear aromatic hydrocarbons by micellar electrokinetic capillary chromatography using sodium taurodeoxycholate modified with organic solvents. *Journal of Capillary Electrophoresis*, 3:31-35.
- [58] Issaq, H. J., P. L. C. Horng, G. M. Janini and G. M. Muschik. 1997. Micellar electrokinetic chromatography using mixed sodium dodecyl sulfate and sodium cholate. *Journal of Liquid Chromatography and Related Technology*, 20:167-182.
- [59] Jimenez, B., D. G. Patterson, J. Grainger, Z. Liu, M. J. Gonzalez and M. L. Marina. 1997. Enhancement of the separation selectivity of a group of polycyclic aromatic hydrocarbons using mixed cyclodextrin-modified micellar electrokinetic chromatography. *Journal of Chromatography A*, 792:411-418.
- [60] Fu, X; J. Lu and Y. Chen. 1998. Separation of polycyclic aromatic hydrocarbons by micellar electrokinetic chromatography with aqueous short-chain alcohol solvent. *Talanta*, 46:751-756.
- [61] Nakagawa, M., J.-M. Lin, T. Nakagama, K. Uchiyama and T. Hobo. 1999. *Bunseki Kagaku*, 48:239-244.
- [62] Bermudez-Saldana, J. M., M. A. Garcia, M. J. Medina-Hernandez and M. L. Marina. 2004. Micellar electrokinetic chromatography with bile salts for predicting ecotoxicity of aromatic compounds. *Journal of Chromatography A*, 1052:171-180.
- [63] Song, G.-Q., Z.-L. Peng and J.-M. Lin. 2006. Comparison of two capillary electrophoresis online stacking modes by analysis of polycyclic aromatic hydrocarbons in airborne particulates. *Journal of Separation Science*, 29:2065-2071.
- [64] do Rosario, P. M. A. and J. M. F. Nogueira. 2006. Combining stir bar sorptive extraction and MEKC for the determination of polynuclear aromatic hydrocarbons in environmental and biological matrices. *Electrophoresis*, 27:4694-4702.

- [65] Alzola, R., B. Pons, D. Bravo and A. Arranz. 2008. Determination of polynuclear aromatic hydrocarbons (PAHs) in sewage sludge by micellar electrokinetic capillary chromatography and HPLC-fluorescence detection: a comparative study. *Environmental Technology*, 29:1219-1228.
- [66] Whitaker, K. W. and M. J. Sepaniak. 1994. Nonaqueous packed capillary electrokinetic chromatographic separations of large polycyclic aromatic hydrocarbons and fullerenes. *Electrophoresis*, 15:1341-1345.
- [67] Ding, J. and P. Vouros. 1997. Capillary electrochromatography and capillary electrochromatography-mass spectrometry for the analysis of DNA adduct mixtures. *Analytical Chemistry*, 69:379-384.
- [68] Asiaie, R., X. Huang, D. Farnan and C. Horvath. 1998. Sintered octadecylsilica as monolithic column packing in capillary electrochromatography and micro high-performance liquid chromatography. *Journal of Chromatography A*, 806:251-263.
- [69] Adam, T., K. K. Unger, M. M. Dittmann and G. P. Rozing. 2000. Towards the column bed stabilization of columns in capillary electroendosmotic chromatography. Immobilization of microparticulate silica columns to a continuous bed. *Journal of Chromatography A*, 887:327-337.
- [70] Garguilo, M. G., D. H. Thomas, D. S. Anex and D. J. Rakestraw. 2000. Laser-induced dispersed fluorescence detection of polycyclic aromatic compounds in soil extracts separated by capillary electrochromatography. *Journal of Chromatography A*, 883:231-248.
- [71] Chirica, G. S. and V. T. Remcho. 2000. Fritless capillary columns for HPLC and CEC prepared by immobilizing the stationary phase in an organic polymer matrix. *Analytical Chemistry*, 72:3605-3610.
- [72] Yao, Z., G. Jiang, M. Ye and H. Zou. 2001. Analysis of polycyclic aromatic hydrocarbons by reversed phase capillary electrochromatography. *International Journal of Environmental Analytical Chemistry*, 81:15-24.
- [73] Norton, D. and S. A. Shamsi. 2003. Capillary electrochromatography of methylated benzo[a]pyrene isomers. II. Effect of stationary phase tuning. *Journal of Chromatography A*, 1008:217-232.
- [74] Norton, D., J. Zheng and S. A. Shamsi. 2003. Capillary electrochromatography of methylated benzo[a]pyrene isomers. I. Effect of mobile phase tuning. *Journal of Chromatography A*, 1008:205-215.
- [75] Droste, S., M. Schellentrager, M. Constapel, S. Gab, M. Lorenz, K. J. Brockmann, T. Benter, D. Lubda and O. J. Schmitz. 2005. A silica-based monolithic column in capillary HPLC and CEC coupled with ESI-MS or electrospray-atmospheric-pressure laser ionization-MS. *Electrophoresis*, 26:4098-4103.



- [76] Zheng, J., S. A. A. Rizvi, S. A. Shamsi and J. Hou. 2007. Photopolymerized sol-gel monolithic column for capillary electrochromatography (CEC) and CEC coupled to atmospheric pressure photoionization mass spectrometry. *Journal of Liquid Chromatography and Related Technology*, 30:43-57.
- [77] Xie, R. and R.Oleschuk. 2007. Photoinduced polymerization for entrapping of octadecylsilane microsphere columns for capillary electrochromatography. *Analytical Chemistry*, 79:1529-1535.
- [78] Qu, Q.-S., S. Wang, Mangelings, D., C.-Y. Wang, G.-J. Yang, X.-Y. Hu and C. Yan. 2009. Monolithic silica xerogel capillary column for separations in capillary LC and pressurized CEC. *Electrophoresis*, 30:1071-1076.
- [79] Ou, J., G. T. T. Gibson and R. D. Oleschuk. 2010. Fast preparation of photopolymerized poly(benzyl methacrylate-co-bisphenol A dimethacrylate) monoliths for capillary electrochromatography. *Journal of Chromatography A*, 1217:3628-3634.
- [80] Wang, M.-M., H.-F. Wang, D.-Q. Jiang, S.-W. Wang and X.-P. Yan. 2010. A strong inorganic acid-initiated methacrylate polymerization strategy for room temperature preparation of monolithic columns for capillary electrochromatography. *Electrophoresis*, 31:1666-1673.
- [81] Nolte, T. and J. T. Andersson. 2011. Capillary Electrophoretic Methods for the Separation of Polycyclic Aromatic Compounds. *Polycyclic Aromatic Compounds*, 31:287-338.
- [82] Walbroehl, Y. and J. W. Jorgenson. 1986. Capillary Zone Electrophoresis of Neutral Organic Molecules by Solvophobic Association with Tetraalkylammonium Ion. *Analytical Chemistry*, 58:479-481.
- [83] Nie, S., R. Dadoo and R. N. Zare. 1993. Ultrasensitive Fluorescence Detection of Polycyclic Aromatic Hydrocarbons in Capillary Electrophoresis. *Analytical Chemistry*, 65:3571-3575.
- [84] Shi, Y. and J. S. Fritz. 1994. Capillary Zone Electrophoresis of Neutral Organic Molecules in Organic-Aqueous Solution. *Journal of High Resolution Chromatography*, 17:713-718.
- [85] Muijselaar, P. G., H. B. Verhelst, H. A. Claessens and C. A. Cramers. 1997. Separation of hydrophobic compounds by electrokinetic chromatography with tetraalkylammonium ions. *Journal of Chromatography A*, 764:323-329.
- [86] Koch, J. T., B. Beam, K. S. Phillips and J. F. Wheeler. 2001. Hydrophobic interaction electrokinetic chromatography for the separation of polycyclic aromatic hydrocarbons using non-aqueous matrices. *Journal of Chromatography A*, 914:223-231.
- [87] Kavran Belin, G., F. B. Erim and F. O. Gülacar. 2006. Effect of cetyltrimethylammonium bromide on the migration of polyaromatic hydrocarbons in capillary electrokinetic chromatography. *Talanta*, 69:596-600.

- [88] Shi, Y. and J. S. Fritz. 1995. HPCZE of Nonionic Compounds Using a Novel Anionic Surfactant Additive. *Analytical Chemistry*, 67:3023-3027.
- [89] Ding, W. and J. S. Fritz. 1997. Separation of Nonionic Compounds by CE Using a Lauryl Poly(oxethylene) Sulfate Additive. *Analytical Chemistry*, 69:1593-1597.
- [90] Ding, W. and J. S. Fritz. 1998. Separation of Neutral Compounds and Basic Drugs by Capillary Electrophoresis in Acidic Solution Using Laurylpoly(oxyethylene) Sulfate as an Additive. *Analytical Chemistry*, 70:1859-1865.
- [91] Li, J. and J. S. Fritz. 1999. Nonaqueous media for separation of nonionic organic compounds by capillary electrophoresis. *Electrophoresis*, 20:84-91.
- [92] Luong, J. H. T. 1998. The combined effect of acetonitrile and urea on the separation of polycyclic aromatic hydrocarbons using sodium dioctyl sulfosuccinate in electrokinetic chromatography. *Electrophoresis*, 19:1461-1467.
- [93] Luong, J. H. T. and Y. Guo. 1998. Mixed-mode separation of polycyclic aromatic hydrocarbons (PAHs) in electrokinetic chromatography. *Electrophoresis*, 19:723-730.
- [94] Kavran Belin, G. and F. B. Erim. 2002. Separation of polycyclic aromatic hydrocarbons with sodium dodecylbenzenesulfonate in electrokinetic chromatography. *Journal of Chromatography A*, 949:301-305.
- [95] Kavran Belin, G., F. B. Erim and F. Gülar. 2004. Capillary electrokinetic separation of polycyclic aromatic hydrocarbons using cetylpyridinium bromide. *Polycyclic Aromatic Compounds*, 24:343-352.
- [96] Miller, J. L., M. G. Khaledi and D. Shea. 1997. Separation of Polycyclic Aromatic Hydrocarbons by Nonaqueous Capillary Electrophoresis Using Charge Transfer Complexation with planar organic Cations. *Analytical Chemistry*, 69:1223-1229.
- [97] Miller, J. L., M. G. Khaledi and D. Shea. 1998. Separation of Hydrophobic Solutes by Nonaqueous Capillary Electrophoresis through Dipolar and Charge-Transfer Interactions with Pyrylium Salts. *Journal of Microcolumn Separations*, 10:681-685.
- [98] Sepaniak, M. J., C. L. Copper, K. W. Whitaker and V. C. Anigbogu. 1995. Evaluation of a Dual-Cyclodextrin Phase Variant of Capillary Electrokinetic Chromatography for Separations of Nonionizable Solutes. *Analytical Chemistry*, 67:2037-2041.
- [99] Whitaker, K. W., C. L. Copper and M. J. Sepaniak. 1996. Separation of Alkyl-Substituted Anthracenes Using Cyclodextrin Distribution Capillary Electrochromatography. *Journal of Microcolumn Separations*, 8:461-468.
- [100] Szolar, O. H. J., R. S. Brown and J. H. T. Luong. 1995. Separation of PAHs by Capillary Electrophoresis with Laser-Induced Fluorescence Detection Using Mixtures of Neutral and Anionic  $\beta$ -Cyclodextrins. *Analytical Chemistry*, 67:3004-3010.

- [101] Brown, R. S., O. H. J. Szolar, and J. H. T. Luong. 1996. Cyclodextrin-aided Capillary Electrophoretic Separation and Laser-induced Fluorescence Detection of Polynuclear Aromatic Hydrocarbons (PAHs). *Journal of Molecular Recognition*, 9:515-523.
- [102] Brown, R. S., J. H. T. Luong, O. H. J. Szolar, A. Halasz and J. Hawari. 1996. Cyclodextrin-Modified Capillary Electrophoresis: Determination of Polycyclic Aromatic Hydrocarbons in Contaminated Soils. *Analytical Chemistry*, 68:287-292.
- [103] Nguyen, A.-L. and J. H. T. Luong. 1997. Separation and Determination of Polycyclic Aromatic Hydrocarbons by Solid Phase Microextraction/Cyclodextrin-Modified Capillary Electrophoresis. *Analytical Chemistry*, 69:1726-1731.
- [104] Bächmann, K., A. Bazzanella, I. Haag and K.-Y. Han. 1997. Charged native  $\beta$ -cyclodextrin as a pseudostationary phase in electrokinetic chromatography. *Fresenius Journal of Analytical Chemistry*, 357:32-36.
- [105] Stockton A. M., T. N. Chiesl, J. R. Scherer and R. A. Mathies. 2009. Polycyclic Aromatic Hydrocarbon Analysis with the Mars Organic Analyzer Microchip Capillary Electrophoresis System. *Analytical Chemistry*, 81:790-796.
- [106] Bächmann, K., A. Bazzanella, I. Haag and K.-Y. Han. 1995. Resorcarenes as Pseudostationary Phases with Selectivity for Electrokinetic Chromatography. *Analytical Chemistry*, 67:1722-1726.
- [107] Sun, S., M. J. Sepaniak, J.-S. Wang and C. D. Gutsche. 1997. Capillary Electrokinetic Chromatography Employing p-(Carboxyethyl)calix[n]arenes as Running Buffer Additives. *Analytical Chemistry*, 69:344-348.
- [108] Valenzuela, F.A., Green, T.K. and D.B. Dahl. 1998. Capillary zone electrophoretic separation of sulfonium and thiophenium ions. *Journal of Chromatography A*, 802:395-398.
- [109] Valenzuela, F.A., Green, T.K. and D.B. Dahl. 1998. Enantiomeric separation of sulfonium lone by capillary electrophoresis using neutral and charged cyclodextrins. *Analytical Chemistry*, 70:3612-3618.
- [110] Künnemeyer, J.: Kapillarelektrophoretische Trennung derivatisierter polyaromatischer Schwefelheterocyclen. Diploma thesis. Westfälische Wilhelms-Universität, Münster/Germany. 2005.
- [111] Nolte, T. and J. T. Andersson. 2009. Capillary electrophoretic separation of polycyclic aromatic sulfur heterocycles. *Analytical and Bioanalytical Chemistry*, 395:1843-1852.
- [112] Acheson, R.M. and D.R. Harrison. 1970. Synthesis, Spectra, and Reactions of Some S-Alkylthiophenium Salts. *Journal of the Chemical Society C-Organic*, 13:1764-1771.

- [113] Kitamura, T., Yamane, M., Zhang, B. Z. And Y. Fujiwara. 1998. 1-Phenyl-1-benzothiophenium triflates by a direct S-phenylation with diphenyliodonium triflate. *Bulletin of the Chemical Society of Japan*, 71:1215-1219.
- [114] Kitamura, T., Yamane, M., Furuki, R., Taniguchi, H. and Motoo Shiro. 1993. Preparation and Crystal Structure of a Parent 1-Arylbenzo[*b*]thiophenium Triflate and its Derivatives. *Chemistry Letters*, 22:1703-1706.
- [115] Kitamura, T., Zhang, B. X. and Y. Fujiwara. 2003. Novel [4+2]-cycloaddition of 1-phenyl-1-benzothiophenium salts with dienes. Experimental evidence for a lack of aromaticity in the thiophene ring. *Journal of Organic Chemistry*, 68:731–735.
- [116] J. T. Andersson. 1986. Gas chromatographic retention indices for all C1- and C2-alkylated benzothiophenes and their dioxides on three different stationary phases. *Journal of Chromatography*, 354:83-98.
- [117] Umemura, K., Matsuyama, H., Watanabe, N., Kobayashi, M. and N. Kamigata. 1989. Asymmetric alkylation of  $\beta$ -keto esters with optically active sulfonium salts. *Journal of Organic Chemistry*, 54:2374–2383.
- [118] Sundell, P. E., Jönsson, S. and A. Hult. 1991. Thermally induced cationic polymerization of divinyl ethers using iodonium and sulfonium salts. *Journal of Polymer Science, Part B: Polymer Chemistry*, 29:1535-1543.
- [119] Hamazu, F., Akashi, S., Koizumi, T., Takata, T. and T. Endo. 1991. Synthesis and activity of aryl benzyl methyl sulfonium salts as cationic initiators: Effect of substituent on aryl group. *Journal of Polymer Science, Part B: Polymer Chemistry*, 29:1845-1851.
- [120] Hamazu, F., Akashi, S., Koizumi, T., Takata, T. and T. Endo. 1991. Novel benzyl sulfonium salt having an aromatic group on sulfur atom as a latent thermal initiator. *Journal of Polymer Science, Part B: Polymer Chemistry*, 29:1675-1680.
- [121] Strausz, O. P., Lown, E. M., Morales-Izquierdo, A., Kazmi, N., Montgomery, D. S., Payzant, J. D. and J. Murgich. 2011. Chemical Composition of Athabasca Bitumen: The Distillable Aromatic Fraction. *Energy & Fuels*, 25:4552-4579.
- [122] Sapre, A. V., Broderick, D. H., Fraenkel, D., Gates, B. C. and N. K. Nag. 1980. Hydrodesulfurization of Benzo[*b*]naphtho[2,3-*d*]thiophene Catalyzed by Sulfided CoO-MoO<sub>3</sub>  $\gamma$ -Al<sub>2</sub>O<sub>3</sub>: The Reaction Network. *AIChE Journal*, 26:690-694.
- [123] Guida, A., Levache, D. and P. Geneste. 1983. Hydrodesulfurization of polycyclic sulfided aromatic molecules over nickel-molybdenum/ $\gamma$ -aluminum oxide: benzo[*b*]naphtho[1,2-*d*]thiophene and 8,9,10,11-tetrahydrobenzo[*b*]naphtho[1,2-*d*]thiophene. *Bulletin de la Societe Chimique de France*, 2:170-174.
- [124] Thomas, D., Crain, S. M. and P. G. Sim. 1995. Application of Reversed Phase Liquid Chromatography with Atmospheric Pressure Chemical Ionization Tandem Mass Spectrometry to the Determination of Polycyclic Aromatic Sulfur Heterocycles in Environmental Samples. *Journal of Mass Spectrometry*, 30:1034-1040.

- [125] Del Rio, J. C., Gonzalez-Vila, F. J. and F. Martin. 1992. Variation in the content and distribution of biomarkers in two closely situated peat and lignite deposits. *Organic Geochemistry*, 18:67-78
- [126] W. H. Calkins. 1994. The chemical forms of sulfur in coal: a review. *Fuel*, 73:475-484
- [127] Shiraishi, Y., Taki, Y., Hirai, T. and I. Komasaawa. 2001. A Novel Desulfurization Process for Fuel Oils Based on the Formation and Subsequent Precipitation of S-Alkylsulfonium Salts. 1. Light Oil Feedstocks. *Industrial & Engineering Chemistry Research*, 40:1213-1224.

## 10 Appendix

### 10.1 Synthesis of 4,6-dipropyl-DBT

19 mL of a 1.6 M solution of n-butyl lithium (30 mmoles) were added at 0 °C to a solution of 4.5 mL TMEDA (30 mmoles) in 10 mL of dry hexane. After stirring for 30 min at 0 °C and 30 min at room temperature, 10 mL of hexane was added. Then a solution of 1.84 g dibenzothiophene in 10 mL of hexane was added dropwise to the reaction mixture. The temperature was increased to 60 °C and held for 2 h. After cooling the mixture to 0°C, 100 mmoles of propyl iodide was added all at once.

After stirring over night, the reaction mixture was poured into 100 mL of ice-water. The product was extracted three times with methylene chloride, and after acidification with 1 M HCl washed with water. The organic phase was dried over magnesium sulphate and the solvents were removed under vacuum. The obtained oil was vacuum distilled. The product was checked by GC-FID and NMR.

GC-FID measurements showed two main products, one belonging to the monoalkylated product, the other one to the dialkylated product. Small remains of the starting material can be observed as well. The yield of 4,6-dipropyl-DBT was calculated to be 76 % based upon the relative peak areas.

The NMR data represent the mixture of monoalkylated and dialkylated product.

$\delta_H$  (300 MHz,  $CDCl_3$ ;  $Me_4Si$ ): 0.91-1.09 (m,  $CH_3$ ), 1.73-1.89 (m,  $CH_2$ ), 2.78-2.90 (m,  $CH_2$ ), 7.14-7.24 (d,  $H_{arom}$ ), 7.29-7.42 ppm (m,  $H_{arom}$ ), 7.65-8.24 ppm (m,  $H_{arom}$ )

$\delta_C$  (75 MHz,  $CDCl_3$ ;  $Me_4Si$ ): 14.22 (s,  $CH_3$ ), 22.51 (s,  $CH_2$ ), 37.34 (s,  $CH_2$ ), 77.15 ( $CDCl_3$ ), 119.27 (s,  $C_{arom}$ ), 119.42 (s,  $C_{arom}$ ), 120.70 (s,  $C_{arom}$ ), 121.75 (s,  $C_{arom}$ ), 122.75 (s,  $C_{arom}$ ), 124.27 (s,  $C_{arom}$ ), 124.75 (s,  $C_{arom}$ ), 126.11 (s,  $C_{arom}$ ), 126.24 (s,  $C_{arom}$ ), 126.33 (s,  $C_{arom}$ ), 126.61 (s,  $C_{arom}$ ), 136.37 (s,  $C_{arom}$ ), 136.86 (s,  $C_{arom}$ ), 138.95 (s,  $C_{arom}$ ).

### 10.2 Synthesis of 4,6-dipentyl-DBT

The reaction for the synthesis of 4,6-dipentyl dibenzothiophene was performed in the same way as for 4,6-dipropyldibenzothiophene. To increase the yield, the amount of added alkyl iodide was increased to 300 mmoles. After addition of the alkyl iodide, the temperature was increased to 60 °C. The obtained oil was vacuum distilled and the product checked by GC-FID and NMR.

GC-FID measurements showed two main products, one belonging to the monoalkylated product, the other one to the dialkylated product. Small remains of the starting material can be observed as well. The yield of 4,6-dipentyl-DBT was calculated to be 71 % based upon the relative peak areas.

The NMR data represent the mixture of monoalkylated and dialkylated product.

$\delta_H$  (300 MHz,  $CDCl_3$ ;  $Me_4Si$ ): 0.71-0.89 (m,  $CH_3$ ), 1.18-1.40 (m,  $CH_2$ ), 1.61-1.77 (m,  $CH_2$ ), 2.68-2.85 (m,  $CH_2$ ), 7.05-7.16 (d,  $H_{arom}$ ), 7.18-7.35 ppm (m,  $H_{arom}$ ), 7.50-8.15 ppm (m,  $H_{arom}$ )

$\delta_C$  (75 MHz,  $CDCl_3$ ;  $Me_4Si$ ): 14.18 (s,  $CH_3$ ), 22.68 (s,  $CH_2$ ), 29.00 (s,  $CH_2$ ), 31.86 (s,  $CH_2$ ), 35.25 (s,  $CH_2$ ), 77.15 ( $CDCl_3$ ), 119.36 (s,  $C_{arom}$ ), 122.83 (s,  $C_{arom}$ ), 124.34 (s,  $C_{arom}$ ), 124.82 (s,  $C_{arom}$ ), 136.38 (s,  $C_{arom}$ ), 137.12 (s,  $C_{arom}$ ), 138.93 (s,  $C_{arom}$ ).

### 10.3 Synthesis of 4,6-dioctyl-DBT

The reaction for the synthesis of 4,6-dioctyldibenzothiophene was performed in the same way as for 4,6-dipentyldibenzothiophene. The amount of alkyl iodide used was 300 mmoles.

The obtained oil was vacuum distilled and the product checked by GC-FID and NMR.

GC-FID measurements showed two main products, one belonging to the monoalkylated product, the other one to the dialkylated product. Small remains of the starting material can be observed as well. The yield of 4,6-dioctyl-DBT was calculated to be 63 % based upon the relative peak areas.

The NMR data represent the mixture of monoalkylated and dialkylated product.

$\delta_H$  (300 MHz,  $CDCl_3$ ;  $Me_4Si$ ): 0.71-0.82 (m,  $CH_3$ ), 1.02-1.43 (m,  $CH_2$ ), 1.61-1.78 (m,  $CH_2$ ), 2.75-2.82 (m,  $CH_2$ ), 7.02-7.18 (d,  $H_{arom}$ ), 7.19-7.38 ppm (m,  $H_{arom}$ ), 7.66-8.05 ppm (m,  $H_{arom}$ )

$\delta_C$  (75 MHz,  $CDCl_3$ ;  $Me_4Si$ ): 14.28 (s,  $CH_3$ ), 22.86 (s,  $CH_2$ ), 29.34 (s,  $CH_2$ ), 29.44 (s,  $CH_2$ ), 29.63 (s,  $CH_2$ ), 32.07 (s,  $CH_2$ ), 35.34 (s,  $CH_2$ ), 77.15 ( $CDCl_3$ ), 119.39 (s,  $C_{arom}$ ), 124.80 (s,  $C_{arom}$ ), 126.05 (s,  $C_{arom}$ ), 136.44 (s,  $C_{arom}$ ), 137.18 (s,  $C_{arom}$ ), 138.98 (s,  $C_{arom}$ ).

#### 10.4 Synthesis of 4,6-didecyl-DBT

The reaction for the synthesis of 4,6-didecyl dibenzothiophene was performed in the same way as for 4,6-dipentyl dibenzothiophene. The amount of alkyl iodide used was 200 mmoles.

The obtained oil was vacuum distilled and the product checked by GC-FID and NMR.

GC-FID measurements showed two main products, one belonging to the monoalkylated product, the other one to the dialkylated product. Small remains of the starting materials can be observed as well. The yield of 4,6-dioctyl-DBT was calculated to be 51 % based upon the relative peak areas.

The NMR data represent the mixture of monoalkylated and dialkylated product.

$\delta_H$  (300 MHz,  $CDCl_3$ ;  $Me_4Si$ ): 0.75-0.84 (m,  $CH_3$ ), 1.10-1.38 (m,  $CH_2$ ), 1.65-1.79 (m,  $CH_2$ ), 2.75-2.86 (m,  $CH_2$ ), 7.08-7.21 (m,  $H_{arom}$ ), 7.23-7.39 ppm (m,  $H_{arom}$ ), 7.52-8.20 ppm (m,  $H_{arom}$ )

$\delta_C$  (75 MHz,  $CDCl_3$ ;  $Me_4Si$ ): 14.17 (s,  $CH_3$ ), 22.74 (s,  $CH_2$ ), 29.15-29.80 (m,  $CH_2$ ), 31.96 (s,  $CH_2$ ), 36.22 (s,  $CH_2$ ), 77.05 ( $CDCl_3$ ), 119.16 (s,  $C_{arom}$ ), 119.28 (s,  $C_{arom}$ ), 121.70 (s,  $C_{arom}$ ), 122.79 (s,  $C_{arom}$ ), 124.29 (s,  $C_{arom}$ ), 124.69 (s,  $C_{arom}$ ), 124.76 (s,  $C_{arom}$ ), 125.95 (s,  $C_{arom}$ ), 122.79 (s,  $C_{arom}$ ), 126.11 (s,  $C_{arom}$ ), 126.55 (s,  $C_{arom}$ ), 136.30 (s,  $C_{arom}$ ), 137.09 (s,  $C_{arom}$ ), 138.86 (s,  $C_{arom}$ ).

#### 10.5 RP-HPLC parameters

HPLC system:	Merck Hitachi D-6000 interface
Pump:	L-6200A intelligent pump
Autosampler:	AS-2000A autosampler
Detector:	L-4500 diode array detector
Column:	4.6 mm×150 mm LiChrosorb RP18 with 7 $\mu m$ particles



Gradient:	75 % aq. acetonitrile for 3 min to 100 % at 8 min
Flow rate:	2 mL/min
Injection volume:	10 µL
Detection wavelength:	254 nm

#### **10.6 GC-FID parameters**

Gas chromatograph:	Agilent 5890 Series II
Autosampler:	Agilent 7673
Injector:	split/splitless (splitless)
Injector temperature:	330 °C
Detector temperature:	350 °C
Capillary column:	Supelco SLB5ms, 30 m x 0,25 mm x 0,25 µm
Temperature program:	60 °C – 1 min – 5 °C/min – 330 °C – 15 min
Carrier gas:	Hydrogen 4.8

#### **10.7 GC-MS parameters**

GC-MS:	Gaschromatograph Finnegan MAT GCQ
Mass spectrometer:	Finnegan MAT GCQ Polaris MS
Injector:	split / splitless (60 s)
Injector temperature:	300 °C
Column:	Supelco SLB5ms, 30 m x 0,25 mm x 0,25 µm
Carrier gas:	Helium 6.0 (BIP), 40 cm/s (constant flow)
Transfer line:	300 °C

Ionization conditions:	EI positive mode, 70 eV, Ion source 200 °C
Mass range:	Full Scan (50-600 amu)
Temperatur program:	60 °C – 1 min – 5 °C/min – 300 °C – 15 min
Solvent delay:	6 min
Injection volume:	1 µL

### **10.8 List of chemicals**

Acetic acid	96 %	Merck
Ammonia solution	25 %	VWR
Benzothiophene	99 %	Aldrich
Butyl lithium	1,6 M in Hexan	Merck
$\beta$ -Cyclodextrin	98 %	Merck
Cyclohexane	99,98 %	Acros
Dibenzothiophene	98 %	Aldrich
Dichloromethane	99,98 %	Acros
1,2-Dichloroethane	99 %	Fisher
4,6-Dimethyl-DBT	95 %	Acros
Diphenyliodonium triflate	97 %	abcr
Hydrochloric acid	37 %	VWR
Hydroxypropyl- $\alpha$ -cyclodextrin	98 %	Aldrich
1-Iododecane	98 %	Acros
1-Iodooctane	98 %	Acros
1-Iodopentane	99 %	Acros

1-Iodopropane	99 %	Acros
Isopropanol	99,8 %	Fluka
3-Mercaptopropyltrimethoxysilane	95%	abcr
Methanol	99,9 %	VWR
Methyl iodide	99 %	Aldrich
Palladium(II) chloride	99,9 %	abcr
Silver tetrafluoroborate	85 %	AlfaAesar
Sodium dodecylsulfate	98 %	Acros
Tetramethylethylenediamine	99,5 %	Aldrich

## **10.9 List of abbreviations**

ACN	Acetonitril
AED	Atomic emission detector
atm	Standard atmosphere (101.325 kPa)
BNT	Benzonaphthothiophene
BT	Benzo[ <i>b</i> ]thiophene
BuLi	Butyl lithium
CD	Cyclodextrin
CE	Capillary electrophoresis
CEC	Capillary electrochromatography
CMC	Critical micelle concentration
CPBr	Cetylpyridinium bromide

CTAB	Cetyltrimethylammonium bromide
DBT	Dibenzo[ <i>b,d</i> ]thiophen
DDS	Direct desulfurization
DHPT	Dihydrophenanthrothiophene
DOSS	Dioctyl sulfosuccinate
e.g.	Exempli gratia, for example
EOF	Electroosmotic flow
EPA	Environmental Protection Agency
ESI	Electrospray ionization
etc.	Et cetera, and so on
FID	Flame ionization detector
FT-ICR MS	Fourier transform ion cyclotron resonance mass spectrometry
GC	Gas chromatography
HDS	Hydrodesulfurization
HGO	Heavy gas oil
HPLC	High-performance liquid chromatography
LEC	Ligand exchange chromatography
LGO	Light gas oil
MEKC	Micellar electrokinetic chromatography
MOA	Mars Organic Analyzer
MS	Mass spectrometry
m/z	Mass-to-charge ratio
PAHs	Polycyclic aromatic hydrocarbons

PASHs	Polycyclic aromatic sulfur heterocycles
ppm	Parts per milion
PSP	Pseudostationary phase
RP-HPLC	Reversed-phase high-performance liquid chromatography
SDBS	Sodium dodecylbenzenesulfonate
SDS	Sodium dodecylsulfate
THAP	Tetrahexylammonium perchlorate
THBNT	Tetrahydrobenzonaphthothiophene
THDBT	Tetrahydrodibenzothiophene
TOF	Time-of-flight
UV-vis	Ultraviolet-visible

## 11 Curriculum Vitae

Name: Thies Nolte  
Geburtsdatum: 26.04.1982  
Geburtsort: Dorsten  
Staatsangehörigkeit: deutsch  
Eltern: Marita Nolte (geb. Harding) und Rainer Nolte

### Schulbildung

08/1988 - 06/1992 Wittenbrinkgrundschule in Dorsten-Wulfen  
08/1992 - 06/2001 Gymnasium Petrinum in Dorsten  
06/2001 Abschluss der Schullaufbahn mit der Allg. Hochschulreife

### Grundwehrdienst

09/2001 - 06/2002 Grundwehrdienst beim Panzerartilleriebataillon 205 in Dülmen

### Studium

10/2002 Beginn Diplomstudium der Chemie an der Westfälischen Wilhelms-Universität Münster  
09/2004 Ablegen der Diplomchemiker Vorprüfung  
04/2006 - 07/2006 Forschungspraktikum im Bereich der Biomedizinischen Chemie an der Universität i Bergen (Norwegen), Institut for Biomedisin  
08/2007 - 02/2008 Diplomarbeit in der Arbeitsgruppe Andersson am Institut für Anorganische und Analytische Chemie:  
„Kapillarelektrophoretische Trennung derivatisierter polyaromatischer Schwefelheterocyclen“  
02/2008 Abschluss des Studiums zum Diplom-Chemiker

### Promotionsstudium

seit 07/2008 Beginn der Dissertation am Institut für Anorganische und Analytische Chemie unter Betreuung von Prof. Jan T. Andersson

### Tätigkeiten

seit 07/2008

wissenschaftlicher Mitarbeiter am Institut für Anorganische und Analytische Chemie der Westfälischen Wilhelm-Universität Münster

Münster, den